NACA TN 3502 9785

TECH LIBRARY KAFB, NM
0066618

NATIONAL ADVISORY COMMITTEE FOR AERONAUTICS

TECHNICAL NOTE 3502

THE TRANSONIC CHARACTERISTICS OF 38 CAMBERED RECTANGULAR WINGS OF VARYING ASPECT RATIO AND THICKNESS AS DETERMINED BY THE TRANSONIC-BUMP TECHNIQUE

By Warren H. Nelson and Walter J. Krumm

Ames Aeronautical Laboratory
Moffett Field, Calif.

Washington
June 1955

AFMDC
TECHNICAL LIBRARY
AFL 2811

1N

TECH LIBRARY KAFB, NM

0066618

NATIONAL ADVISORY COMMITTEE FOR AERONAUTIC

TECHNICAL NOTE 3502

THE TRANSONIC CHARACTERISTICS OF 38 CAMBERED RECTANGULAR WINGS OF VARYING ASPECT RATIO AND THICKNESS AS DETERMINED BY THE TRANSONIC-BUMP TECHNIQUE[1]

By Warren H. Nelson and Walter J. Krumm

SUMMARY

An investigation to determine the effects of camber on the aerodynamic characteristics of a series of rectangular wings having various aspect ratios and thickness-to-chord ratios was conducted in the Ames 16-foot high-speed wind tunnel, utilizing the transonic-bump method. The Mach number range of the investigation was from 0.6 to 1.12, with a corresponding Reynolds number range of 1.7 to 2.2 million. The lift, drag, and pitching-moment data are presented for wings having aspect ratios of 4, 3, 2, 1.5, and 1, and NACA 63A2XX and 63A4XX sections with thickness-to-chord ratios of 10, 8, 6, 4, and 2 percent.

INTRODUCTION

An investigation was initiated in the Ames 16-foot high-speed wind tunnel to provide comprehensive data as to the effects of aspect ratio, thickness, and camber on the aerodynamic characteristics of a series of rectangular wings throughout the transonic speed range. The first part of the investigation, which was concerned with the uncambered wings, has been reported in reference 1.

The purpose of this report is to present the part of the investigation dealing with the wings having sections cambered for design lift coefficients of 0.2 and 0.4.

Thirty-eight wings with aspect ratios of 4, 3, 2, 1.5, and 1 were investigated. The profiles were NACA 63A2XX and 63A4XX sections having thickness-to-chord ratios of 10, 8, 6, 4, and 2 percent.

[1]Supersedes recently declassified NACA RM A52D11 by Warren H. Nelson and Walter J. Krumm, 1952.

NOTATION

C_D drag coefficient, $\frac{\text{twice semispan drag}}{qS}$

C_L lift coefficient, $\frac{\text{twice semispan lift}}{qS}$

C_m pitching-moment coefficient, referred to $0.25\bar{c}$, $\frac{\text{twice semispan pitching moment}}{qS\bar{c}}$

A aspect ratio, $\frac{b^2}{S}$

$\frac{L}{D}$ lift-drag ratio

M average Mach number over the wing

M_L local Mach number

S total wing area (twice wing area of semispan model), sq ft

V velocity, ft/sec

b twice span of semispan model, ft

c local wing chord, ft

$\bar{c}$ mean aerodynamic chord, $\frac{\int_0^{b/2} c^2 dy}{\int_0^{b/2} c\, dy}$, ft

q dynamic pressure, $\frac{1}{2}\rho V^2$, lb/sq ft

$\frac{t}{c}$ thickness-to-chord ratio

y spanwise distance from plane of symmetry, ft

α angle of attack, deg

ρ air density, slugs/cu ft

$\frac{dC_L}{d\alpha}$ slope of lift curve measured at the design lift coefficient, per deg

APPARATUS AND MODELS

The tests were conducted in the Ames 16-foot high-speed wind tunnel, employing a transonic bump which is described in detail in reference 2. The aerodynamic forces and moments were measured by means of a strain-gage balance housed inside the bump.

Photographs illustrating the mounting of the wings on the bump are shown in figure 1. The principal dimensions and plan forms of the wings are shown in figure 2. The profiles of the wings were NACA 63A-series sections with thickness-to-chord ratios of 10, 8, 6, 4, and 2 percent, cambered for design lift coefficients of 0.2 and 0.4 with a modified a=0.8 mean line (fig. 3). The modification to the mean line was made to maintain the straight portions of the NACA 6A-series profiles over approximately the last 15 percent of the chord. (See reference 3.)

Ten aspect-ratio-4 wings of the two profiles and various thicknesses used were constructed and the aspect ratios of 3, 2, 1.5, and 1 were obtained by successively cutting off the tips. The aspect ratios and thickness ratios tested for each profile are shown in the following table:

Aspect ratio	Thickness-to-chord ratio				
	0.10	0.08	0.06	0.04	0.02
4	x	x	x	x	- - -
3	- - -	- - -	x	x	- - -
2	x	x	x	x	x
1.5	- - -	- - -	x	x	x
1	x	x	x	x	x

The wings with thickness-to-chord ratios of 0.10, 0.08, and 0.06 were constructed of aluminum and the wings having thickness-to-chord ratios of 0.04 and 0.02 were made of steel. The radius tips of the wings were constructed by using one half of the thickness at each chord station as the radius.

A fence located three-sixteenth inch from the bump surface was used to prevent the flow through the gap between the wing and bump surface from affecting the flow over the wing.

TESTS AND PROCEDURE

The lift, drag, and pitching-moment characteristics of the wings were determined for a Mach number range from 0.60 to 1.12. The corresponding variation of Reynolds number with Mach number for the tests is shown in figure 4. In general, the angle-of-attack range for these tests was -6° to stall; however, in some cases the maximum angle was limited by the bending stress at the wing root. No data were obtained for the 2-percent-thick wings of aspect ratios 4 and 3 because of structural weakness and flutter at high subsonic speeds.

The test data have been reduced to standard NACA coefficient form. A tare correction to the drag of the wings was made to account for the drag of the fence and support. This drag tare was evaluated by cutting the wing off flush with the fence and measuring the forces on the fence and support. Since the measured tare-drag coefficient did not vary appreciably with changes in Mach number or angle of attack, a constant value was used throughout to correct the drag data. The magnitude of the tare-drag coefficient, which depended on the areas of the wings, was 0.0066 for the aspect-ratio-1 wings and 0.0016 for the aspect-ratio-4 wings. The interference effects of the fence on the wings and the effects of leakage around the fence are unknown.

A Mach number gradient exists in the bump flow field where the models are mounted. Typical contours of local Mach number in the flow field are shown in figure 5. Outlines of the wings have been superimposed on these diagrams to indicate the Mach number gradients which existed across the wings during the tests. No attempt has been made to evaluate the effects of these gradients. The test Mach numbers presented in this report are the average Mach numbers over the wings.

RESULTS

The drag data presented herein should be used with caution, particularly that for the lower Mach numbers or aspect ratios where the measured forces were small compared to the capacity of the balance. Other factors which contribute to the uncertainty of the drag data are the large drag tares (for the lower aspect ratios), and the Mach number gradients existing throughout the flow field of the bump. However, it is believed that the trends shown throughout the transonic speed range are qualitatively correct.

The basic lift, drag, and pitching-moment data are presented for the wings in figures 6 through 11. Summary curves as a function of Mach number are presented for the lift and drag in figures 12 through 15. The lift-curve slopes shown in the summary figures are taken through the design lift coefficient.

The lift-drag ratios as a function of lift coefficient are shown in figures 16 and 17. In view of the aforementioned uncertainty in drag, some of the maximum lift-drag values may be in error. This would be true only at the lower Mach numbers and where the maximum lift-drag ratios occur at low lift coefficients, causing small differences in drag to greatly affect the maximum lift-drag ratios. At the lower Mach numbers, however, the lift-drag ratios for lift coefficients above that for maximum lift-drag ratio are probably correct.

The data presented in this report have been analyzed in reference 4, utilizing the transonic similarity rules.

Ames Aeronautical Laboratory
National Advisory Committee for Aeronautics
Moffett Field, Calif., Apr. 11, 1952

REFERENCES

1. Nelson, Warren H., and McDevitt, John B.: The Transonic Characteristics of 22 Rectangular, Symmetrical Wing Models of Varying Aspect Ratio and Thickness. NACA TN 3501, 1955. (Formerly NACA RM A51A12)

2. Axelson, John A., and Taylor, Robert A.: Preliminary Investigation of the Transonic Characteristics of an NACA Submerged Inlet. NACA RM A50C13, 1950.

3. Loftin, Laurence K., Jr.: Theoretical and Experimental Data for a Number of NACA 6A-Series Airfoil Sections. NACA Rep. 903, 1948. (Formerly NACA RM L6J01 and NACA TN 1368)

4. McDevitt, John B.: A Correlation by Means of Transonic Similarity Rules of the Experimentally Determined Characteristics of 18 Cambered Wings of Rectangular Plan Form. NACA RM A53G31, 1953.

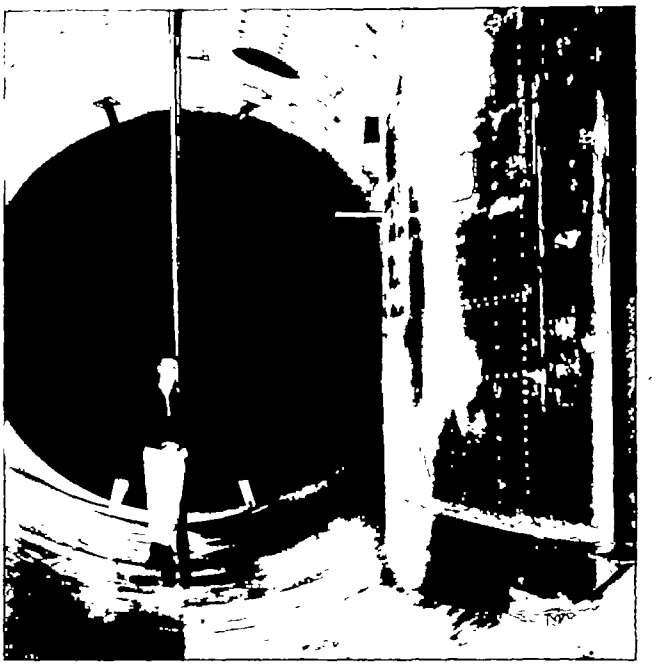

(a) Aspect-ratio-4 wing.

(b) Aspect-ratio-2 wing.

Figure 1.- Wing mounted on the transonic bump in the Ames 16-foot high-speed wind tunnel.

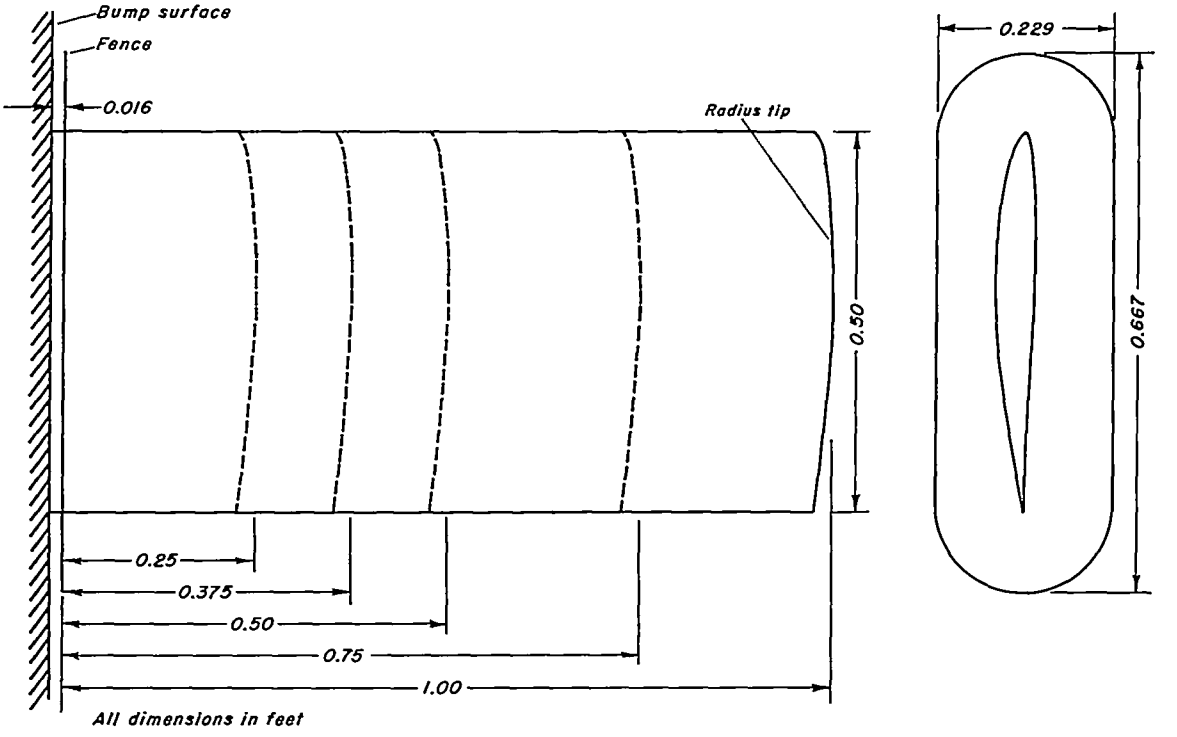

Aspect ratio	Semispan, ft.	Area of semispan, sq. ft.
1	0.25	0.125
1.5	.375	.1875
2	.50	.250
3	.75	.375
4	1.00	.500

Figure 2.—Dimensions and plan forms of the wings.

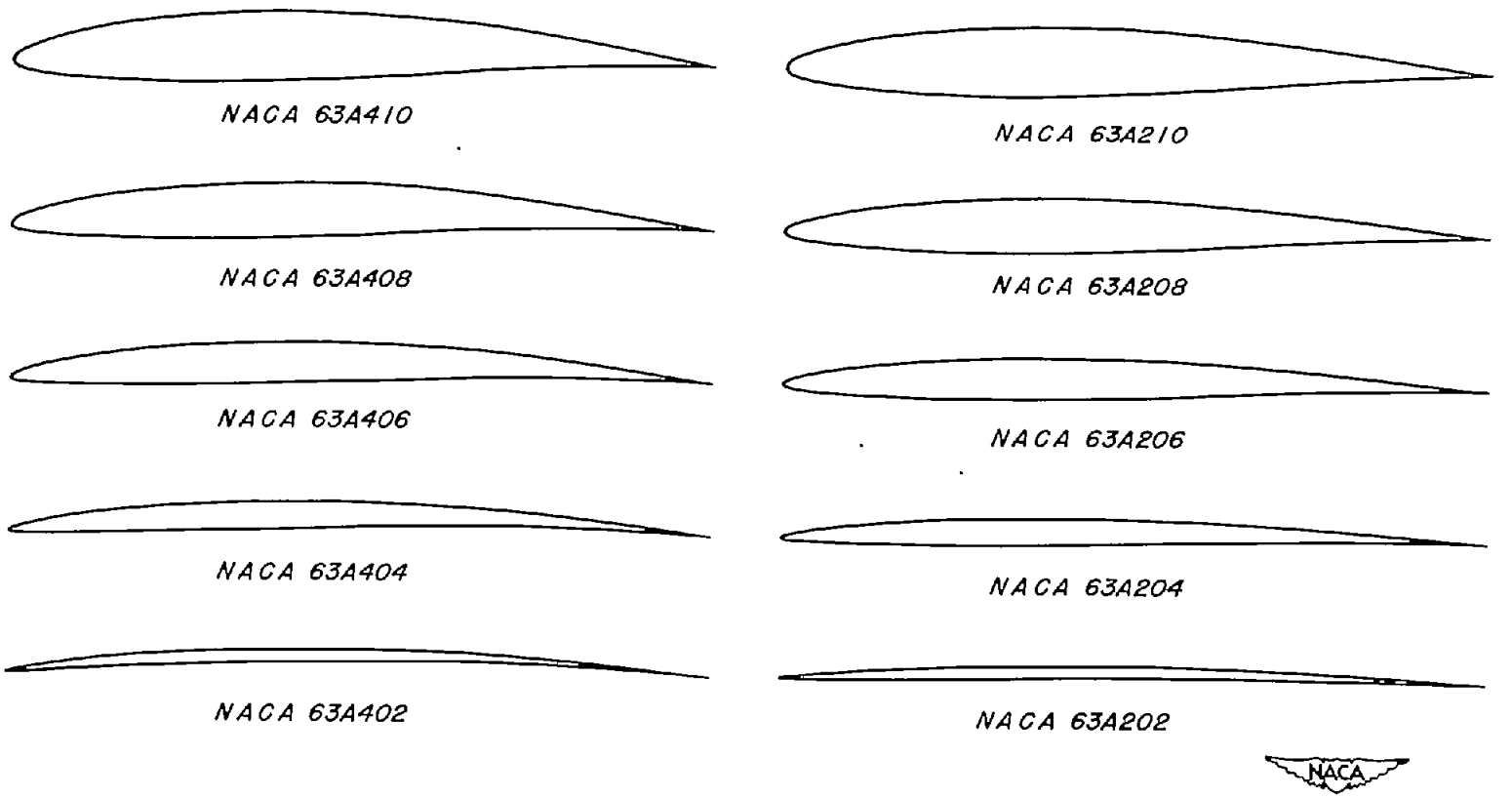

Figure 3.—Profiles of the NACA 63A-series sections investigated.

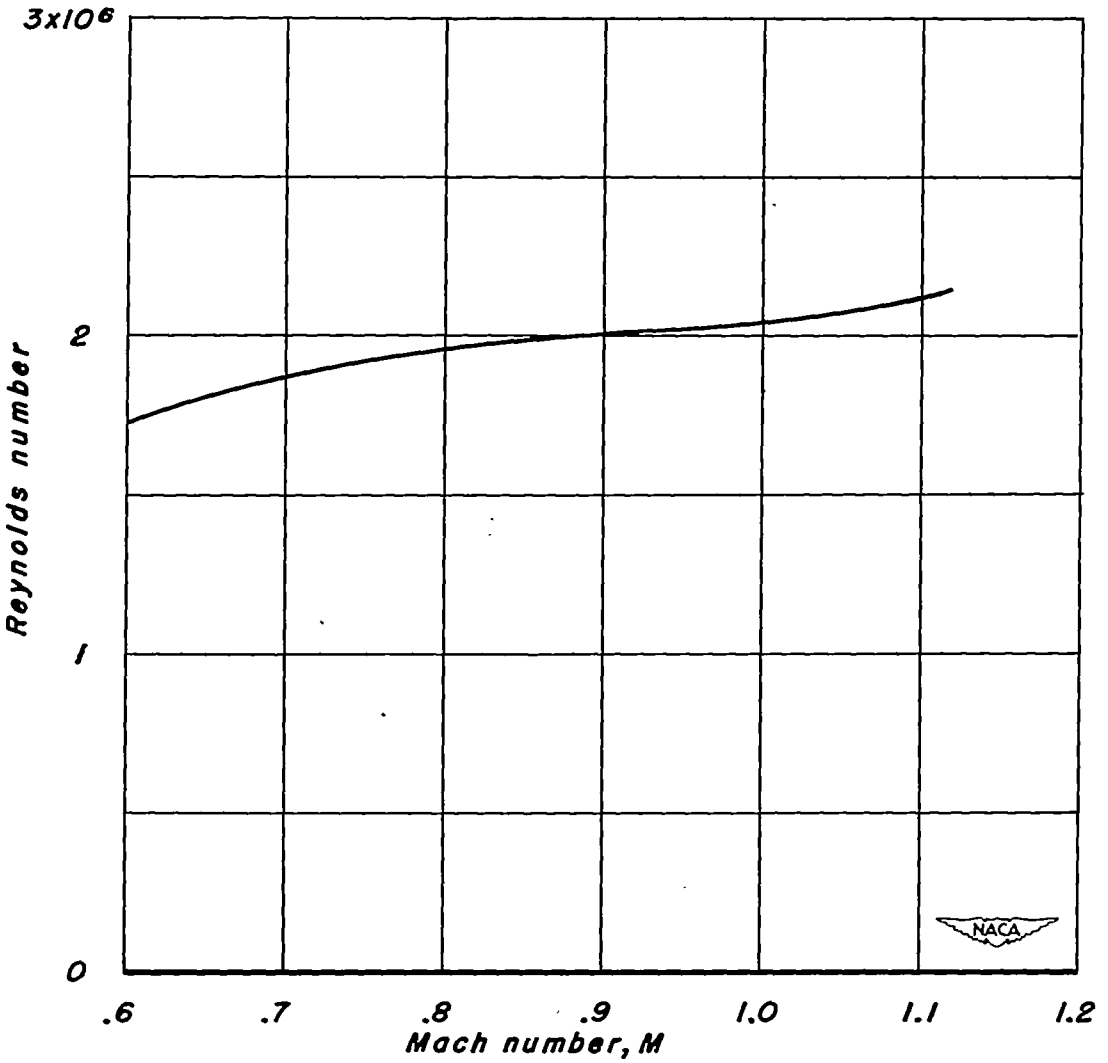

Figure 4.– The variation of Reynolds number with Mach number.

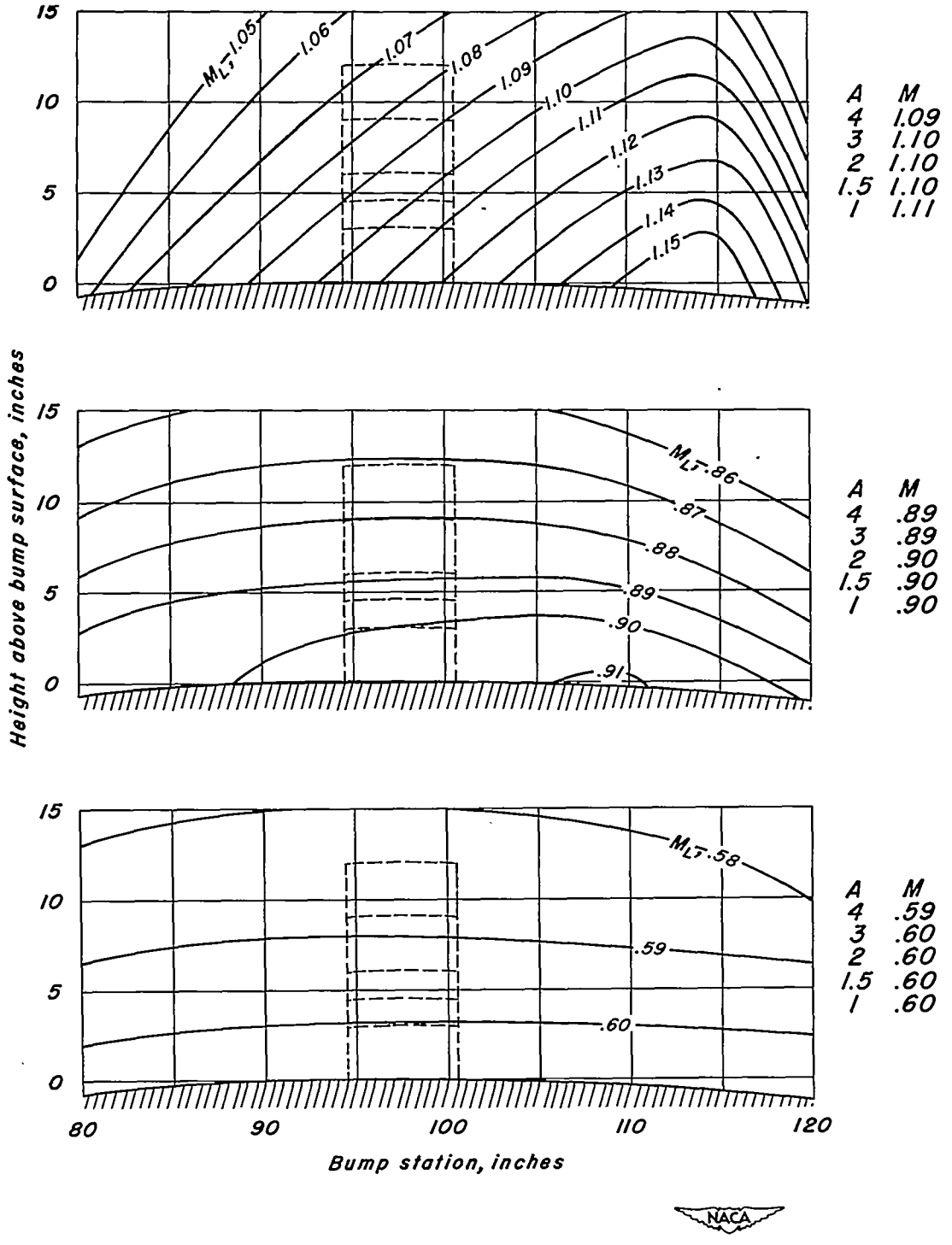

Figure 5.-Typical Mach number contours over the transonic bump in the Ames 16-foot high-speed wind tunnel.

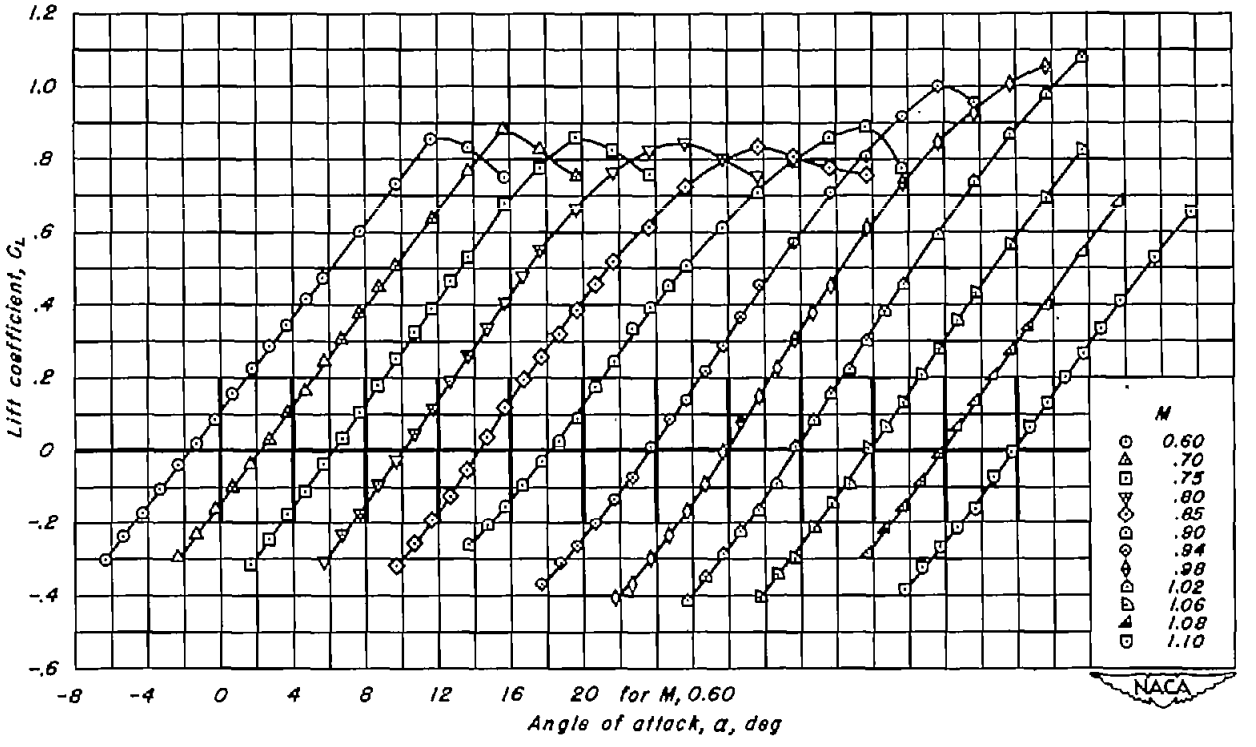

(a) A, 4; t/c, 0.10

Figure 6.–The variation of lift coefficient with angle of attack for the wings with NACA 63A2XX sections.

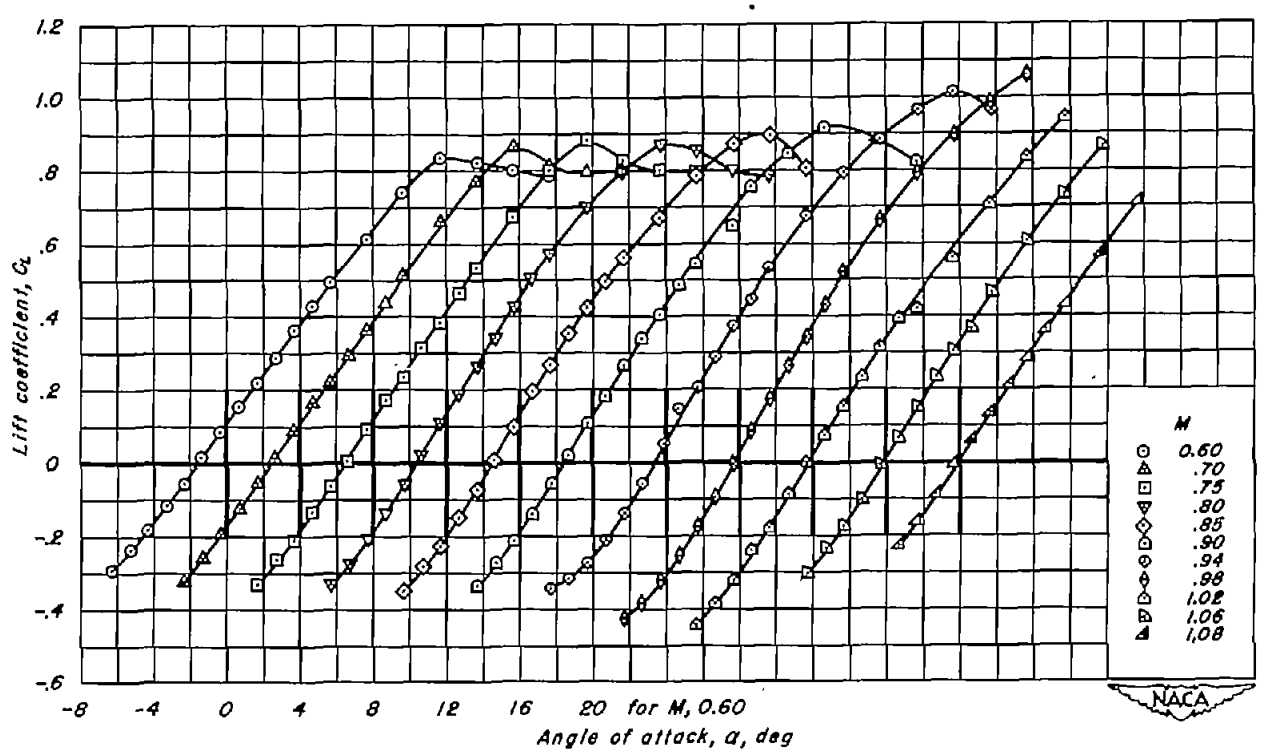

(b) A, 4; t/c, 0.08

Figure 6.- Continued.

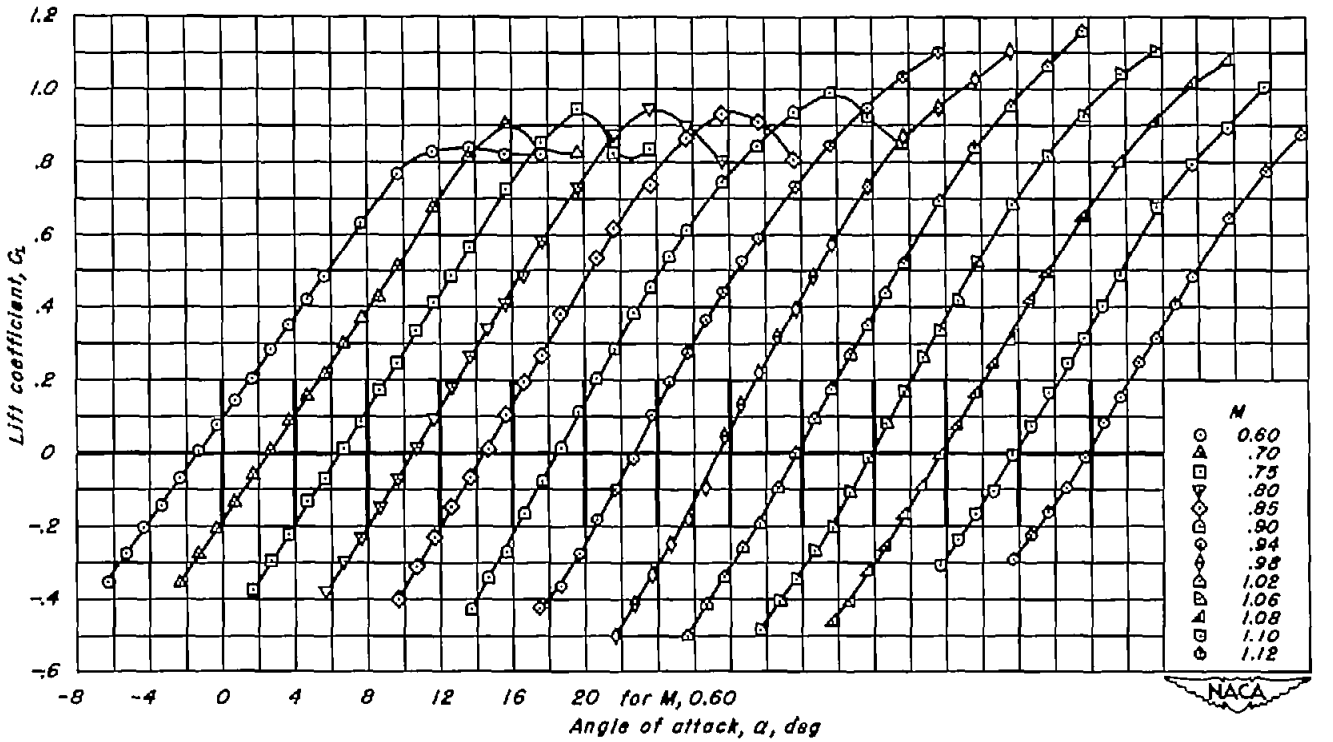

(c) A, 4; t/c, 0.06

Figure 6.- Continued.

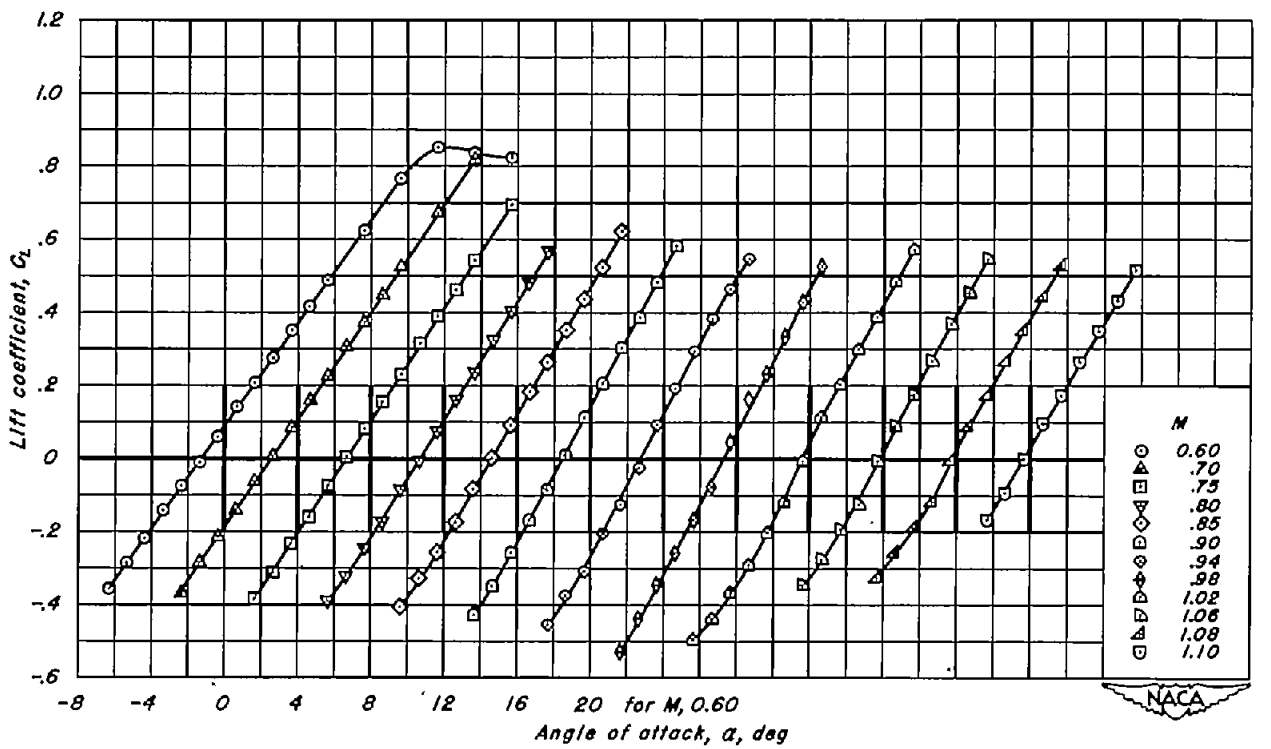

(d) A, 4; t/c, 0.04

Figure 6.- Continued.

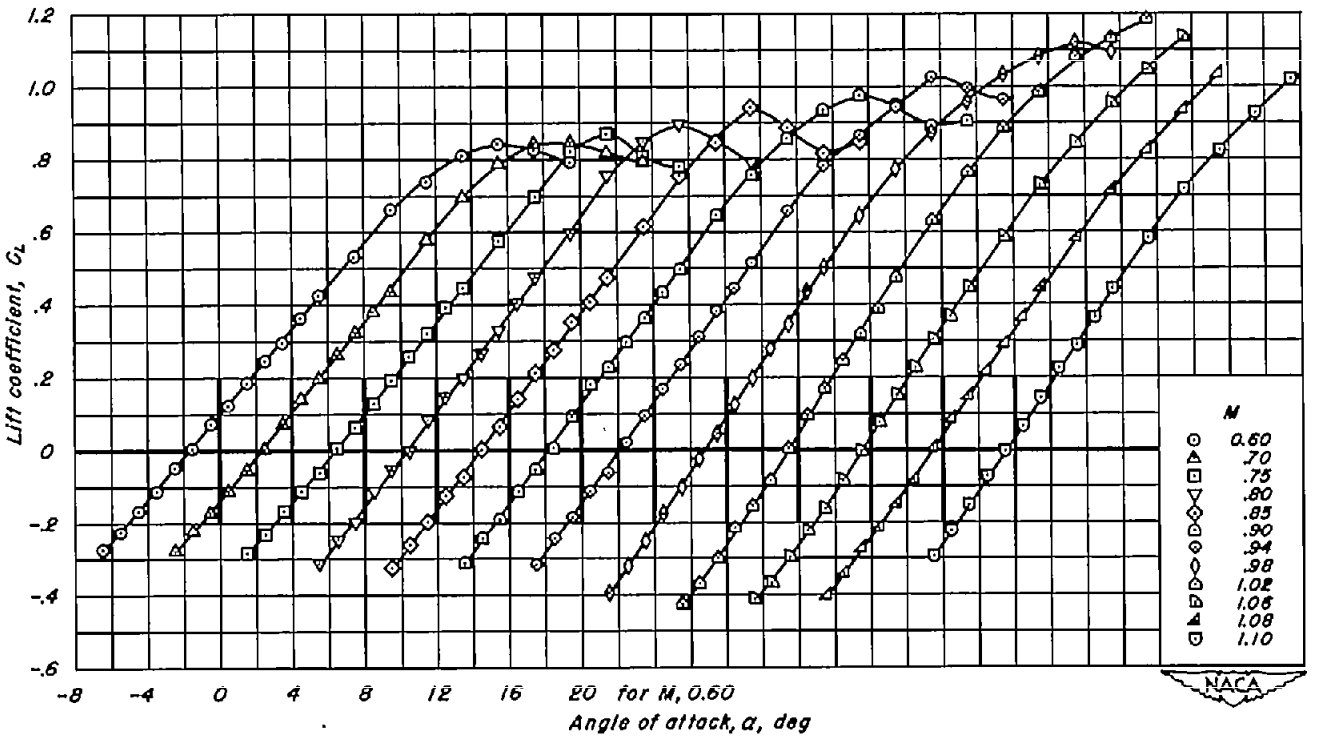

(e) A, 3; t/c, 0.06

Figure 6.- Continued.

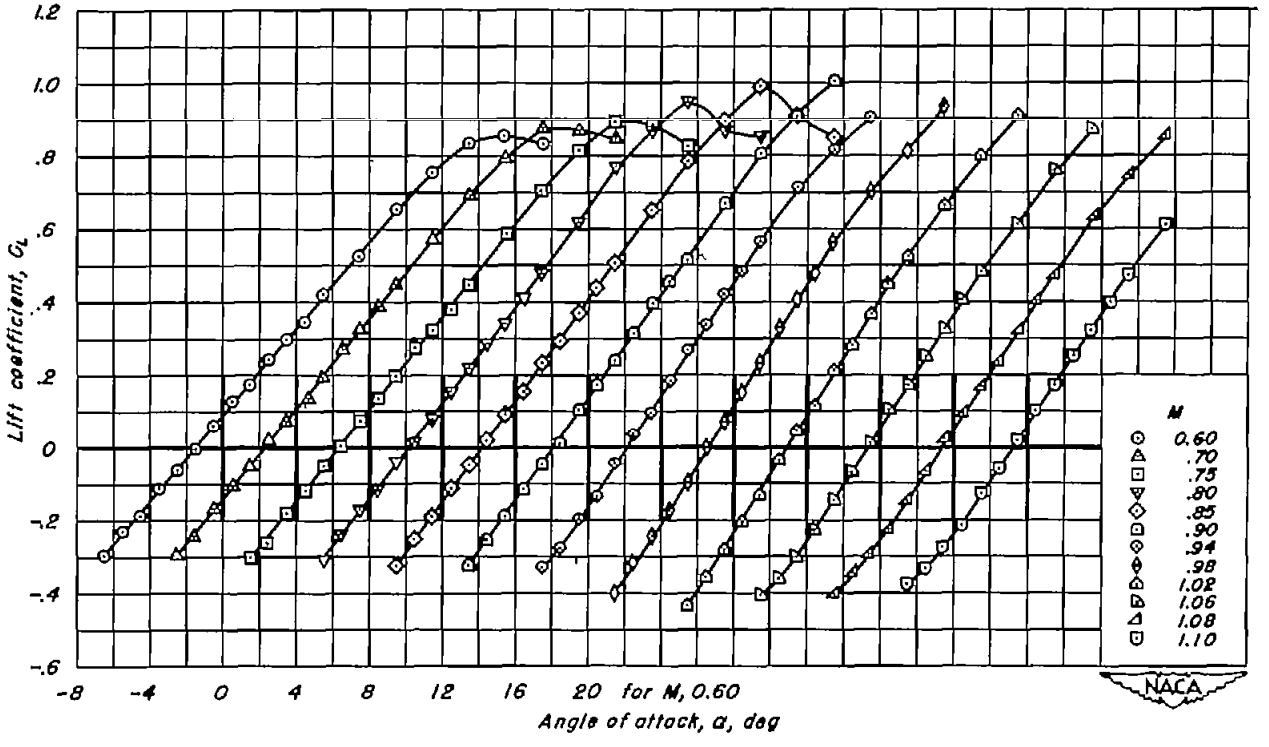

(f) A, 3; t/c, 0.04

Figure 6.- Continued.

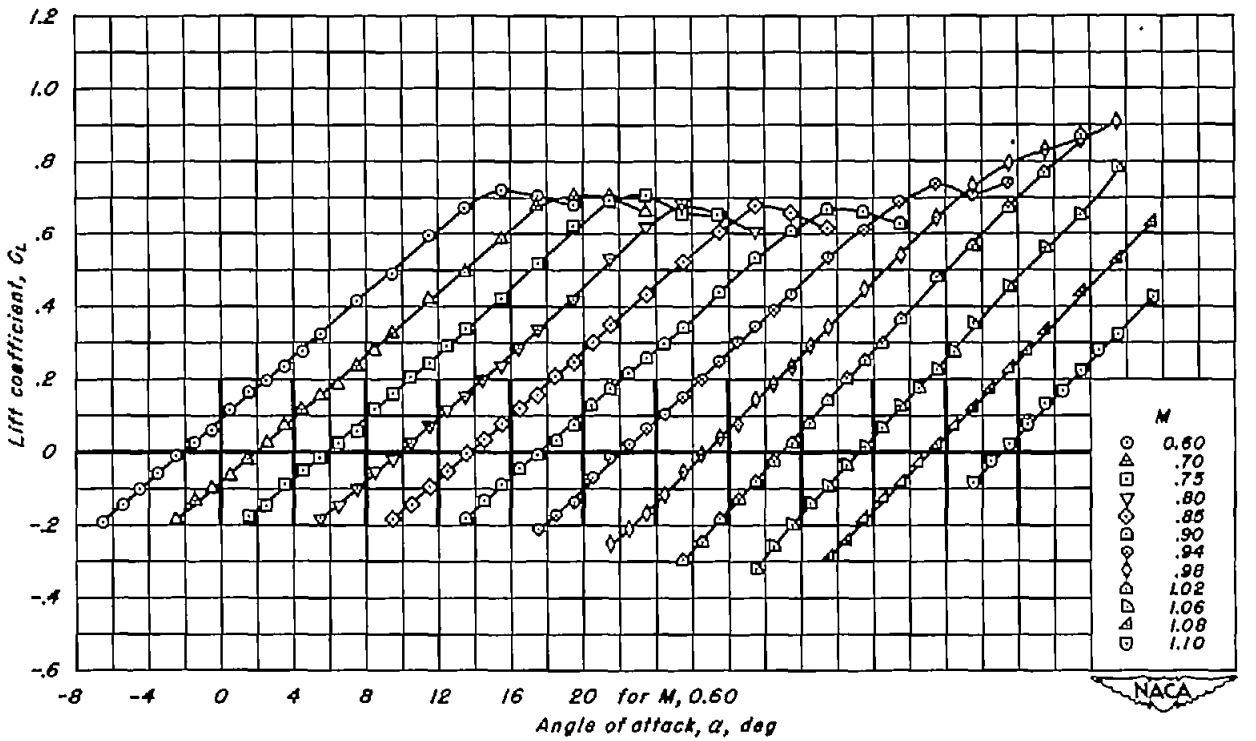

(g) A, 2; t/c, 0.10

Figure 6.- Continued.

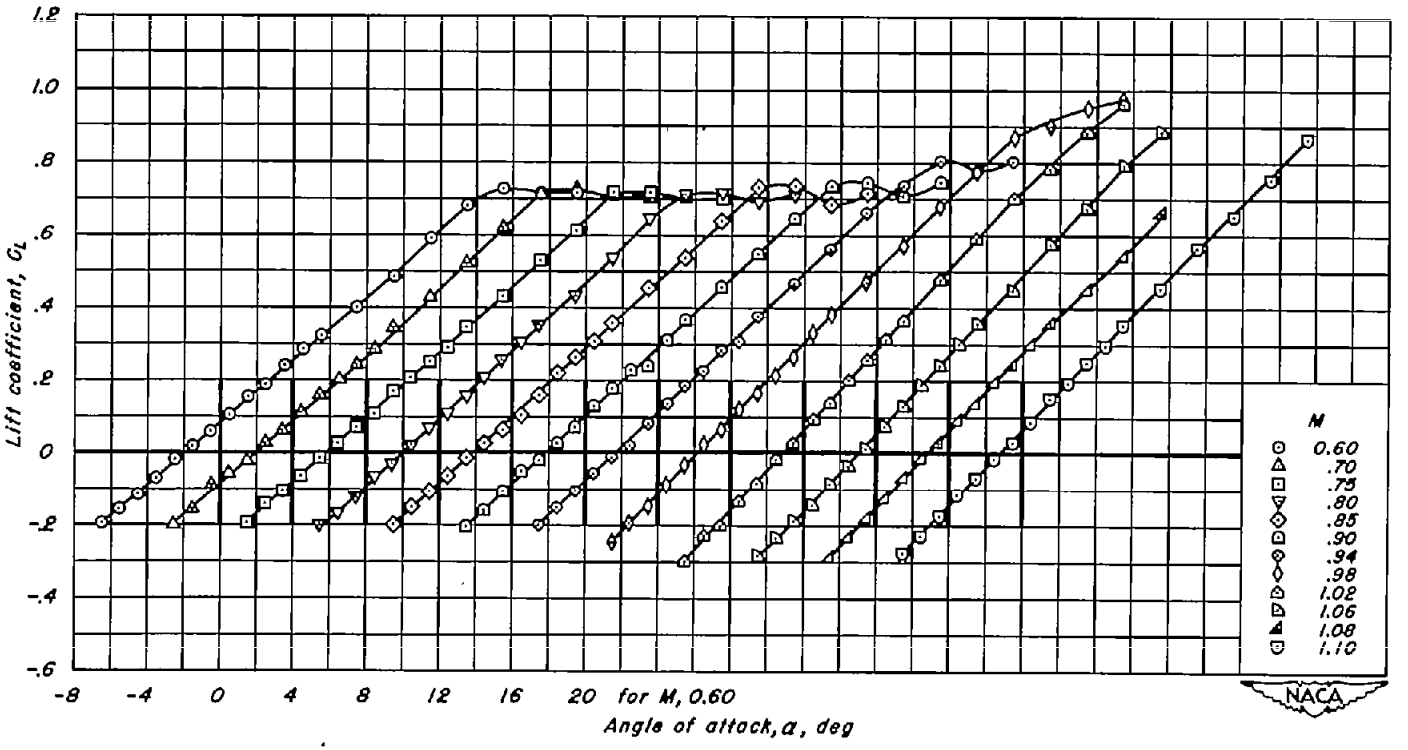

(h) A, 2; t/c, 0.08

Figure 6.- Continued.

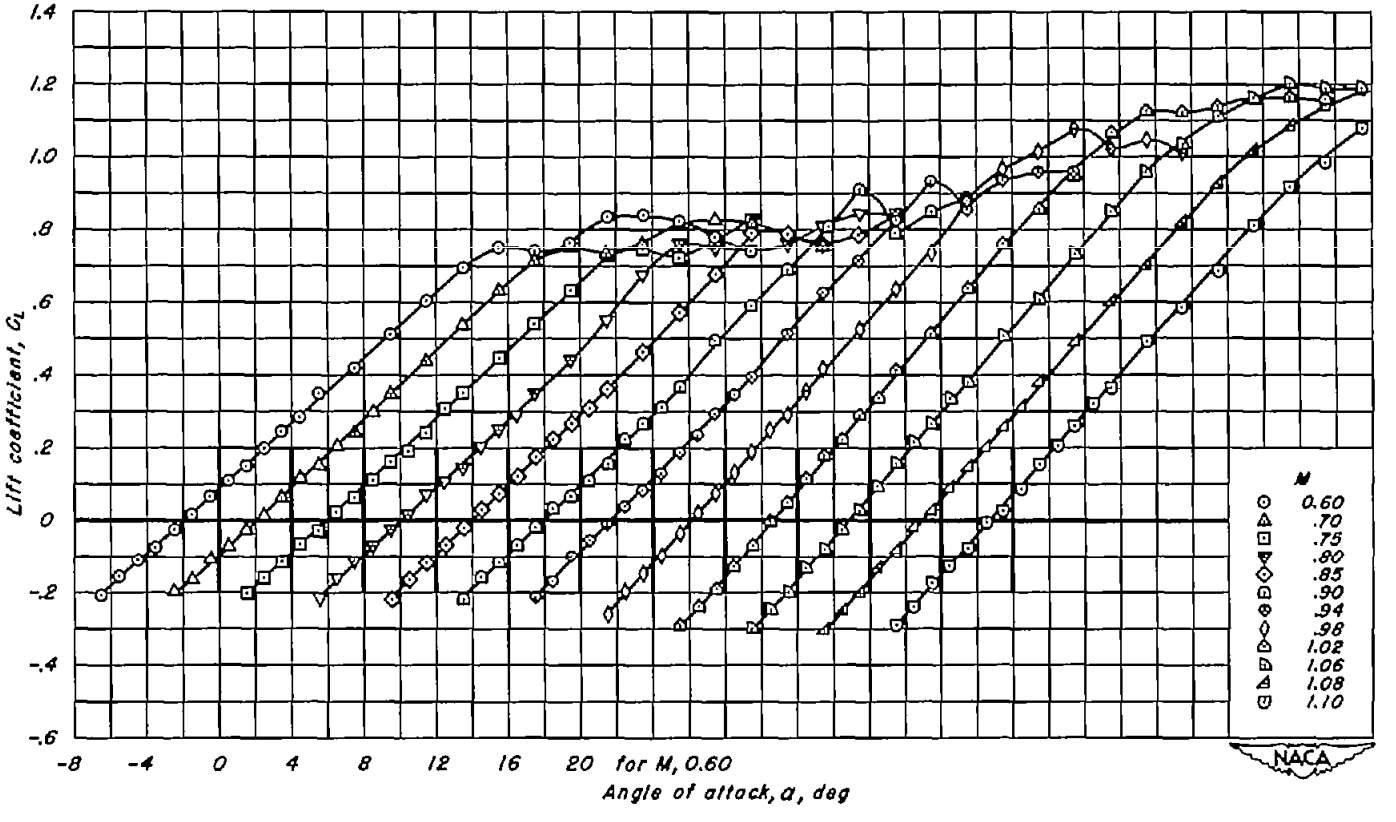

(i) A, 2, t/c, 0.06

Figure 6.- Continued.

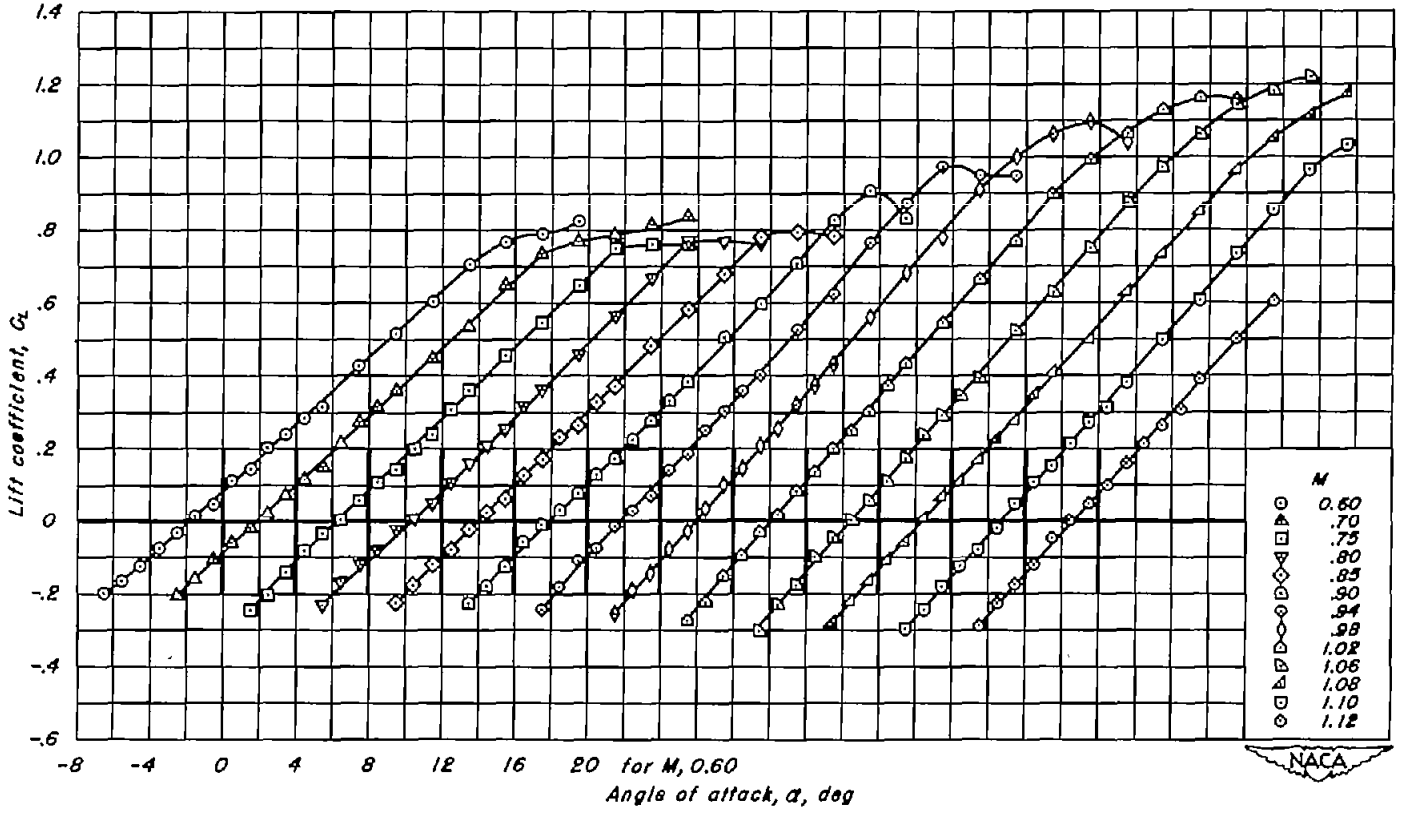

(j) A, 2, t/c, 0.04

Figure 6.- Continued.

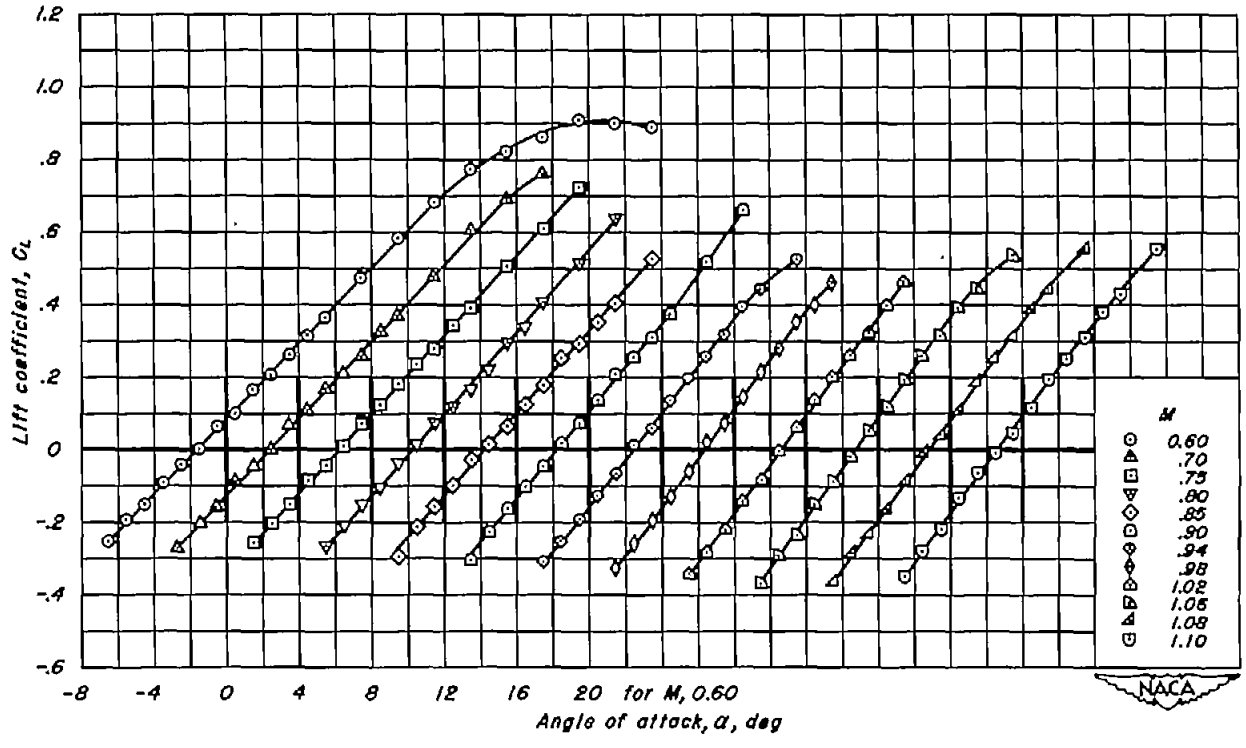

(k) A, 2, t/c, 0.02

Figure 6 .- Continued.

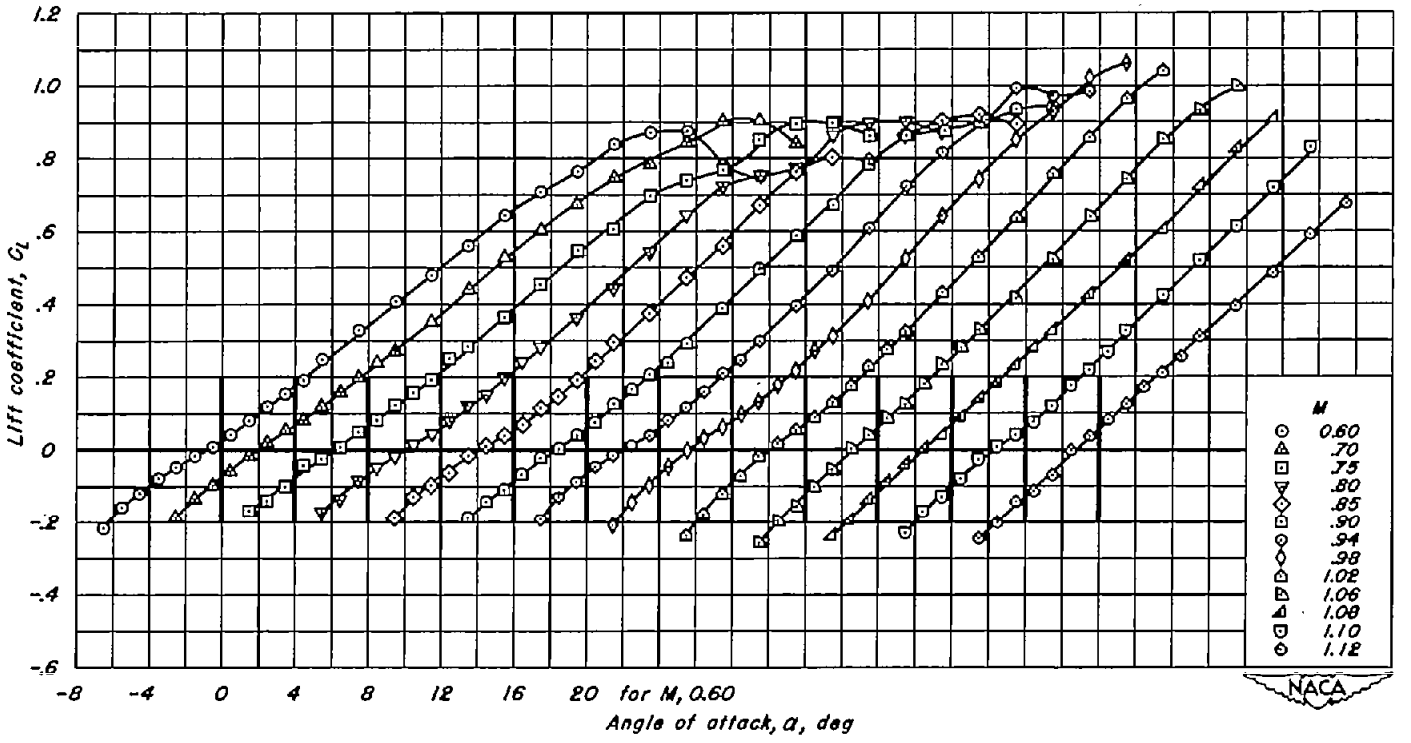

(l) A,1.5; t/c, 0.06

Figure 6.- Continued.

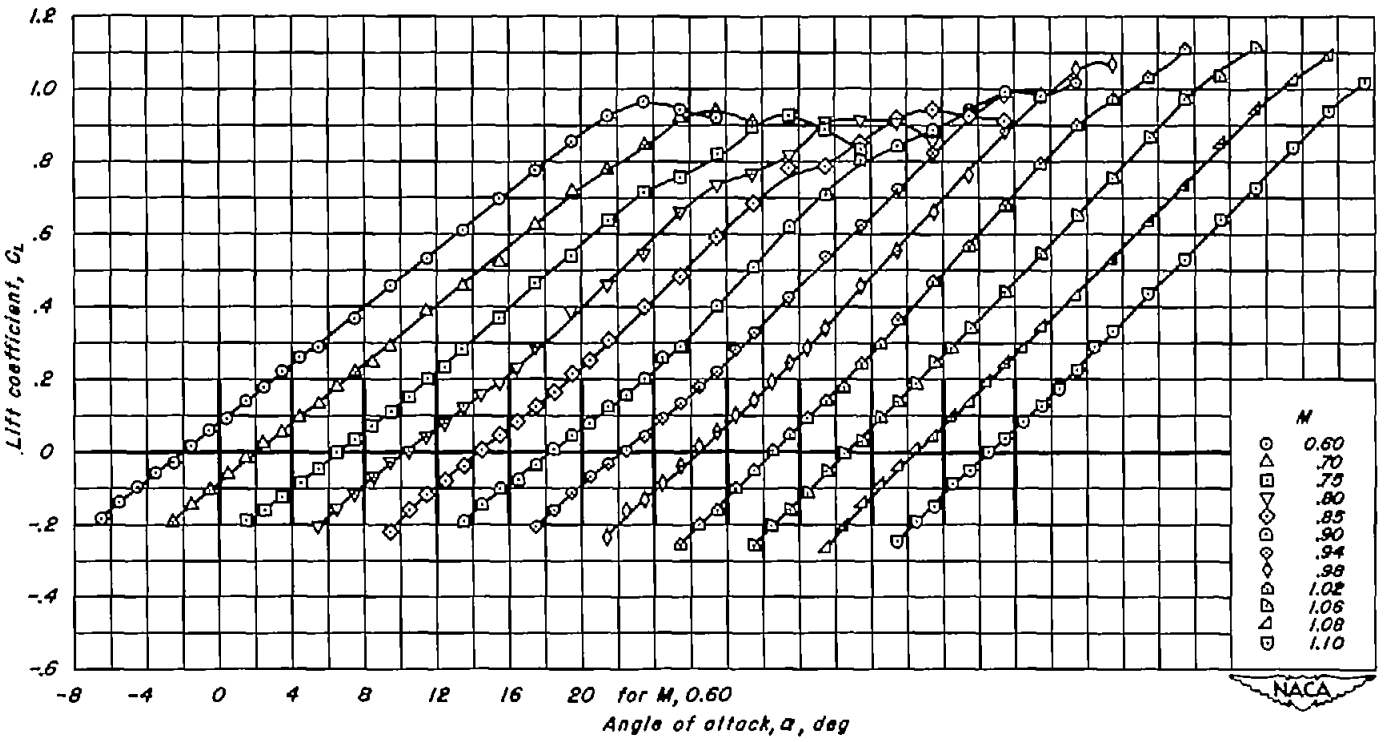

(m) A,1.5; t/c, 0.04

Figure 6 .- Continued.

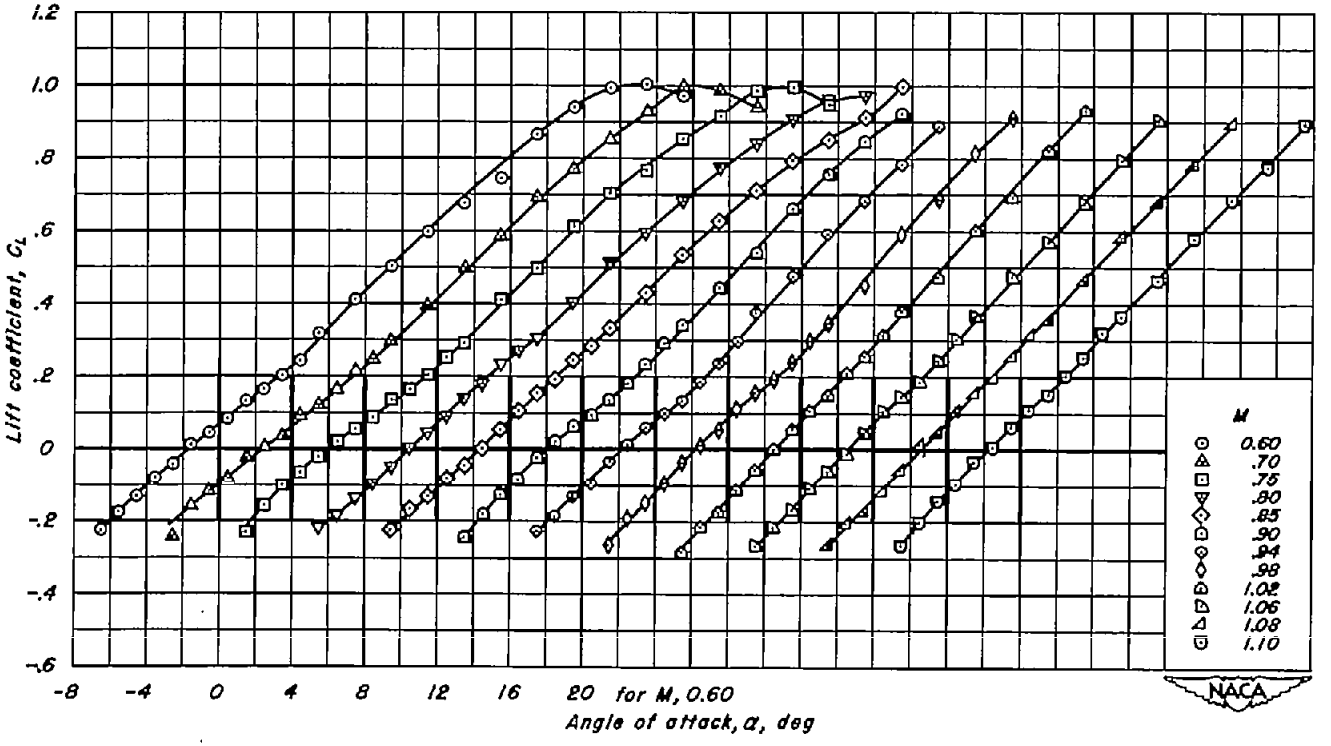

(n) A, 1.5; t/c, 0.02

Figure 6.- Continued.

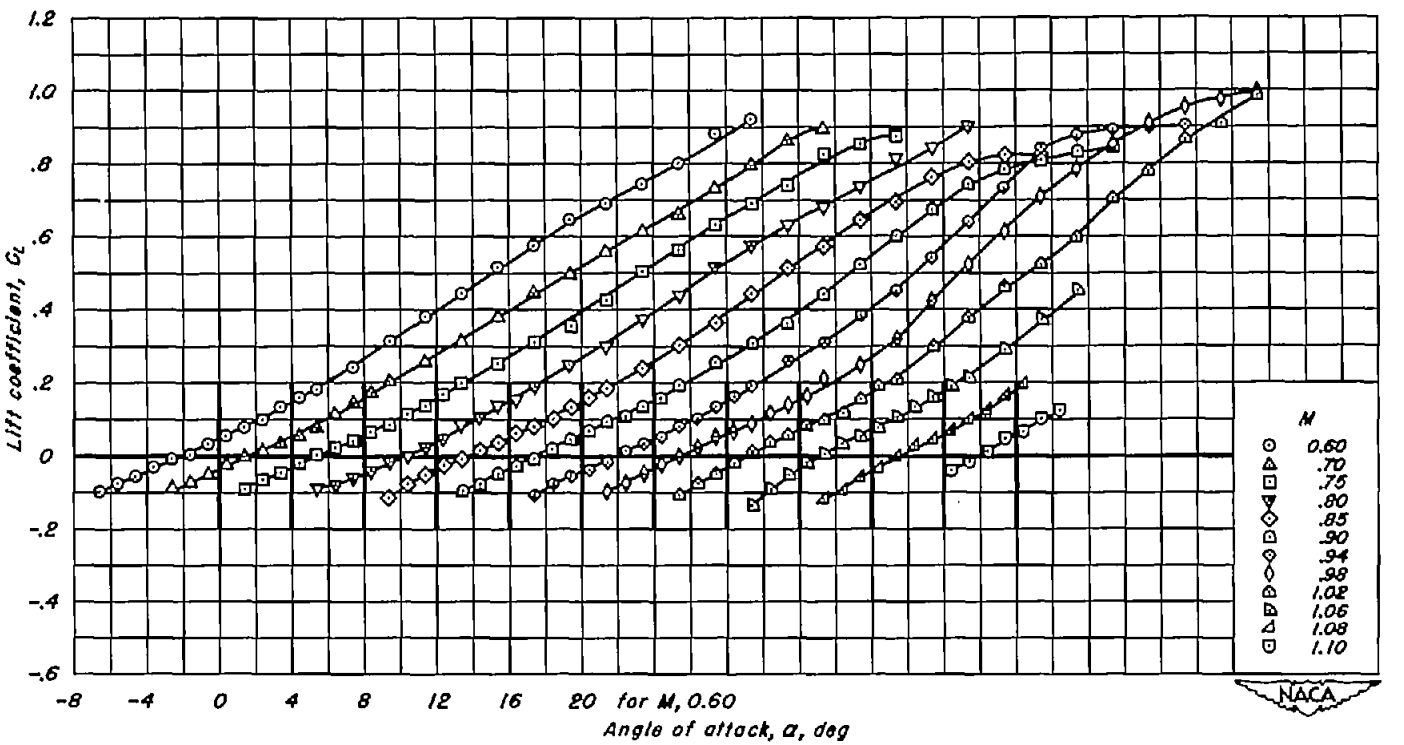

(o) A, 1, t/c, 0.10

Figure 6.- Continued.

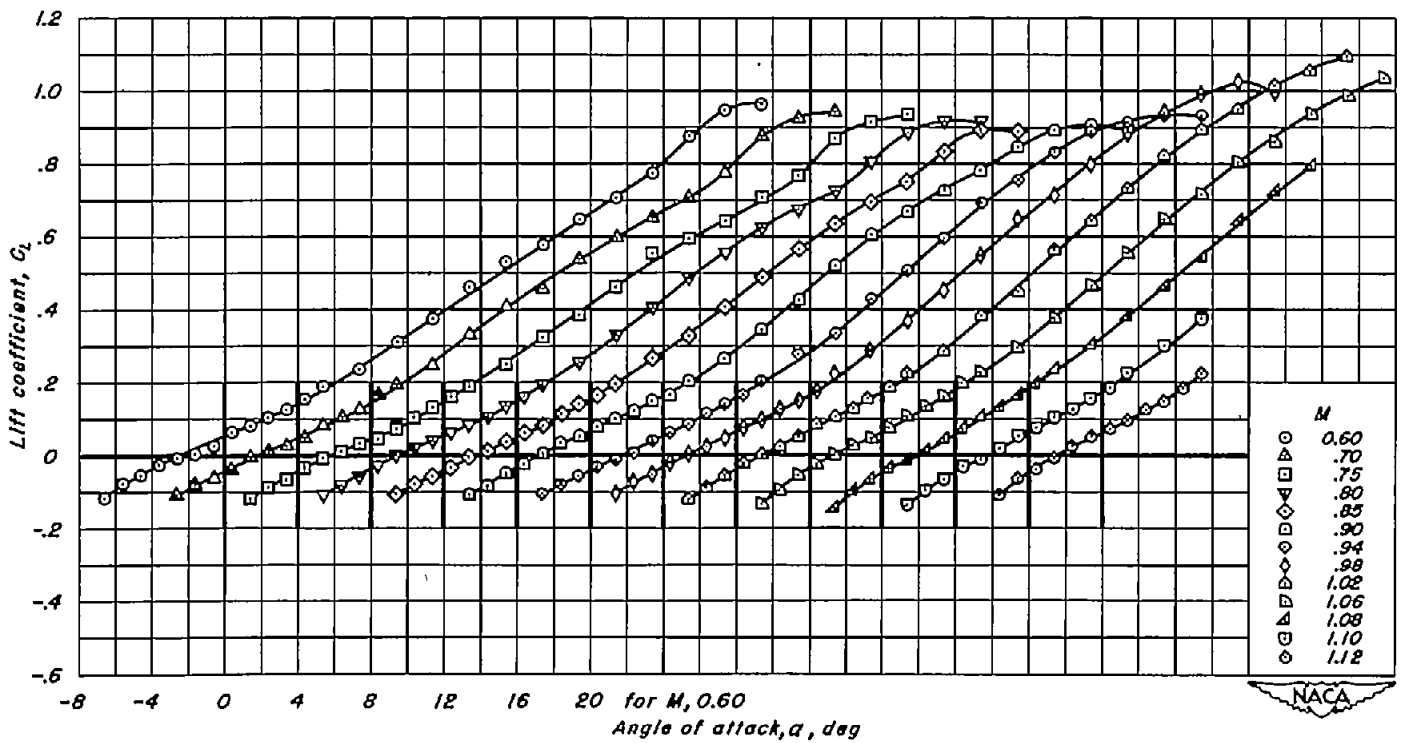

(p) A, 1; t/c, 0.08

Figure 6.- Continued.

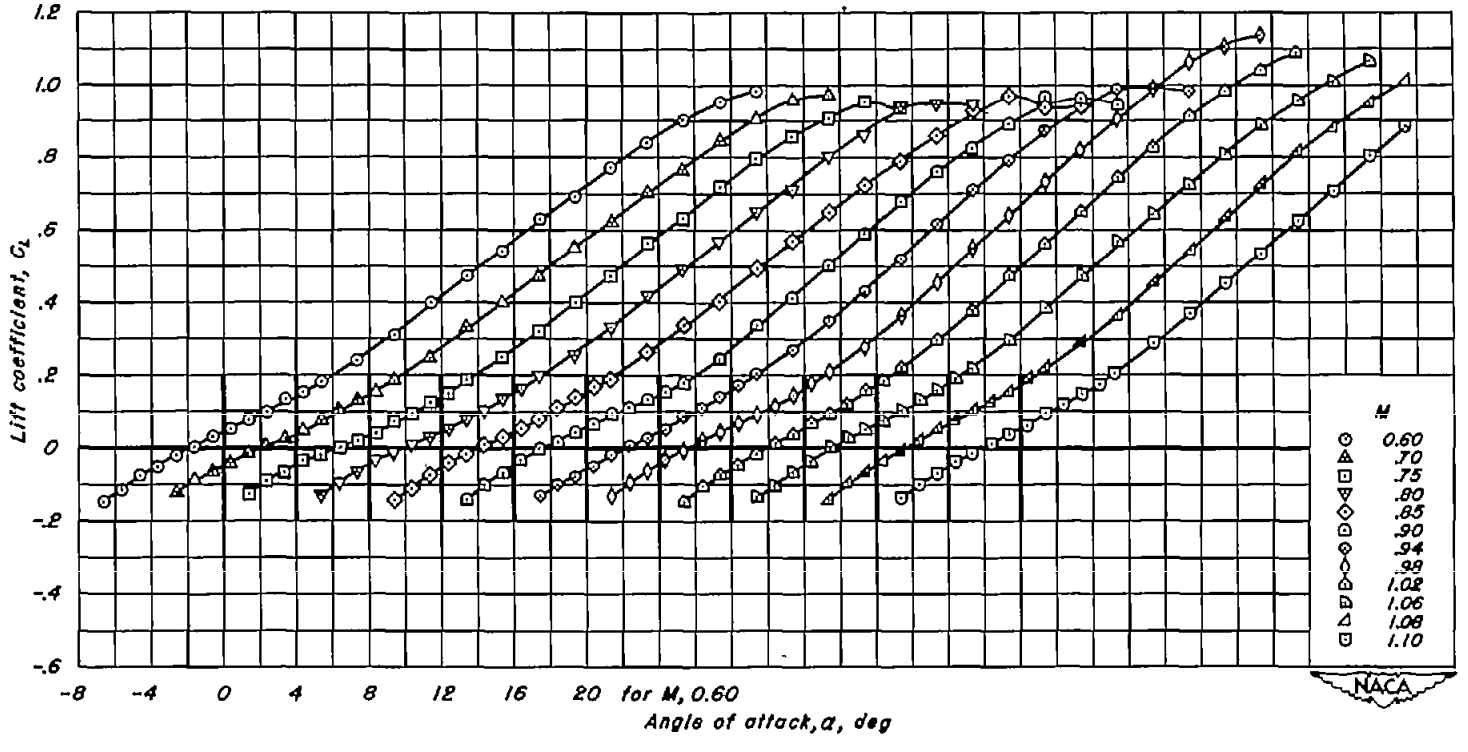

(q) A, 1; t/c, 0.06

Figure 6.- Continued.

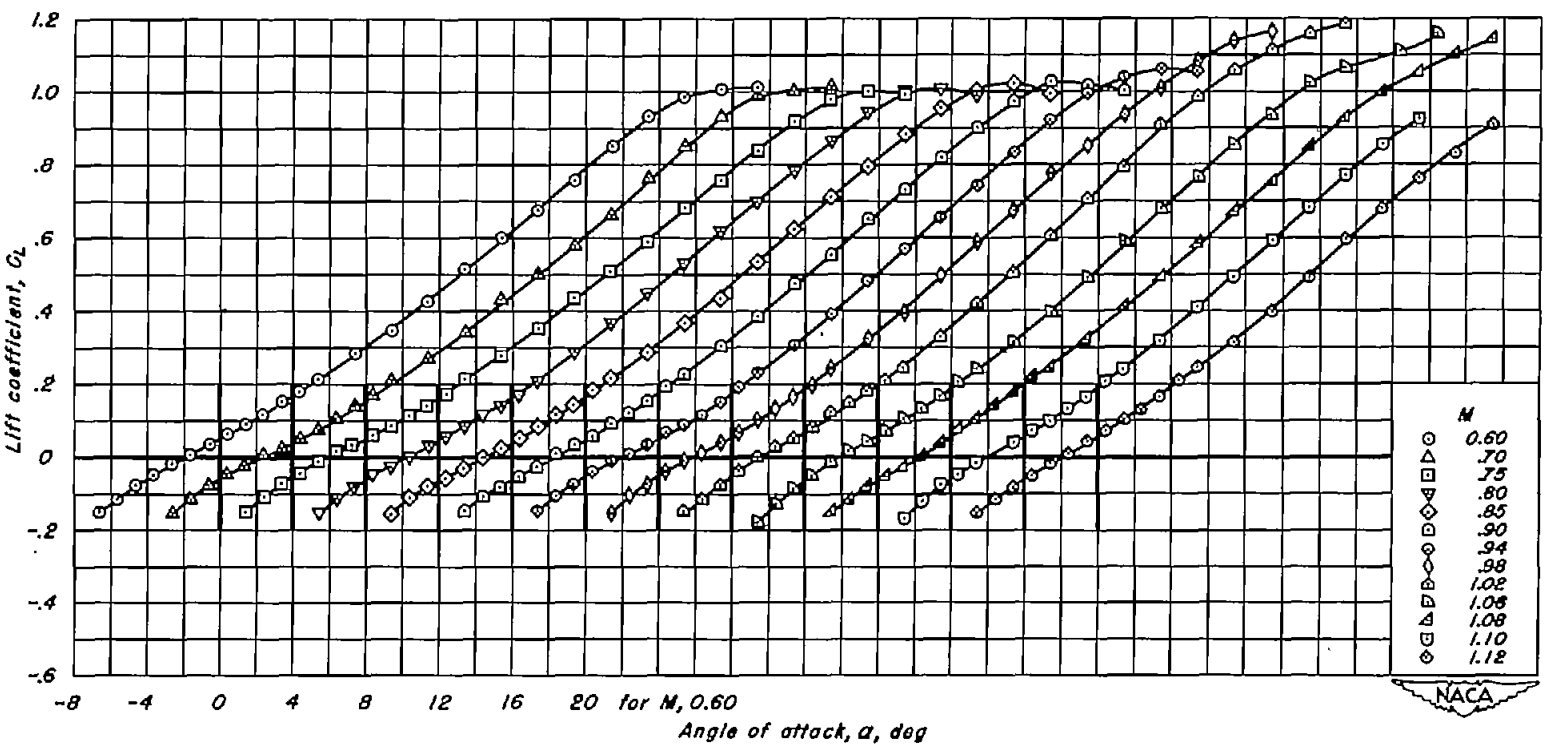

(r) A, 1; t/c, 0.04

Figure 6.- Continued.

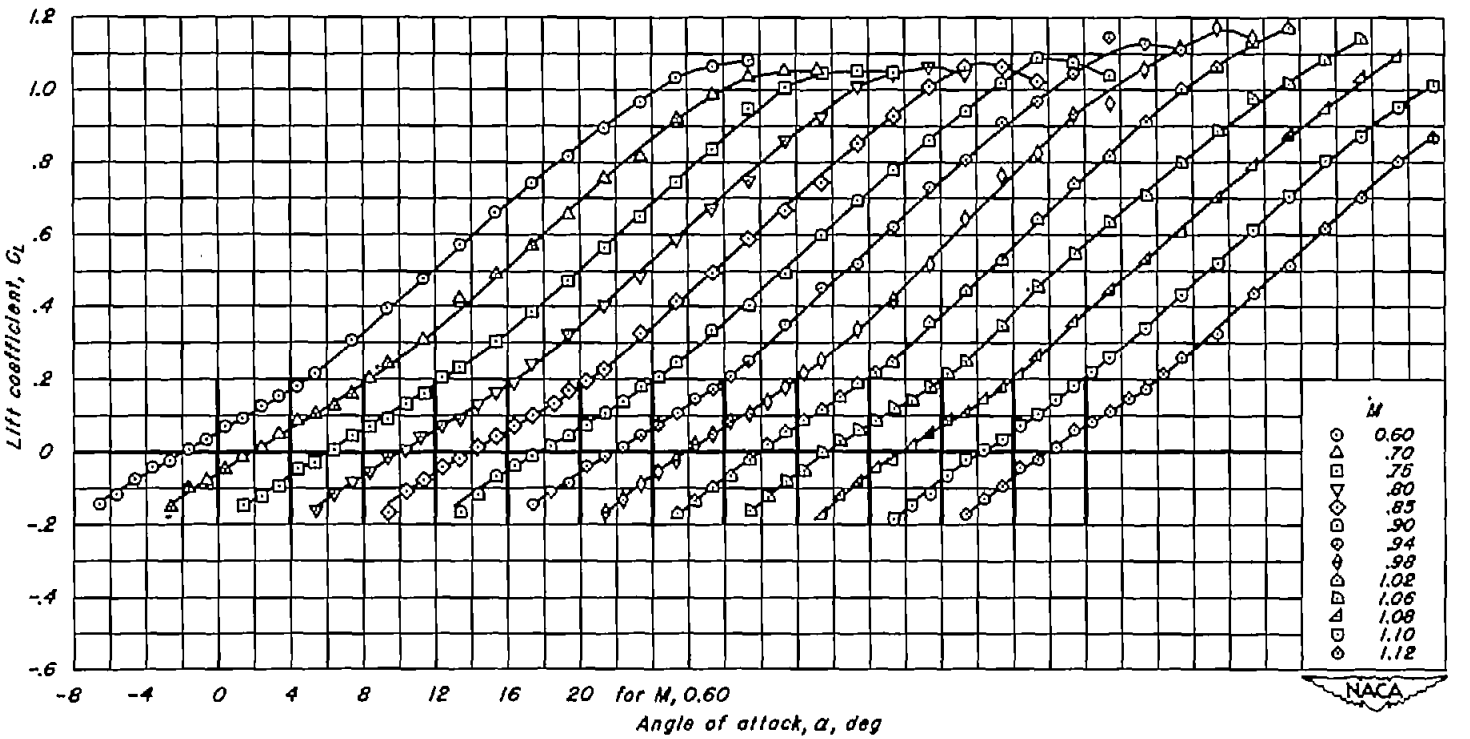

(s) A, 1; t/c, 0.02

Figure 6.- Concluded.

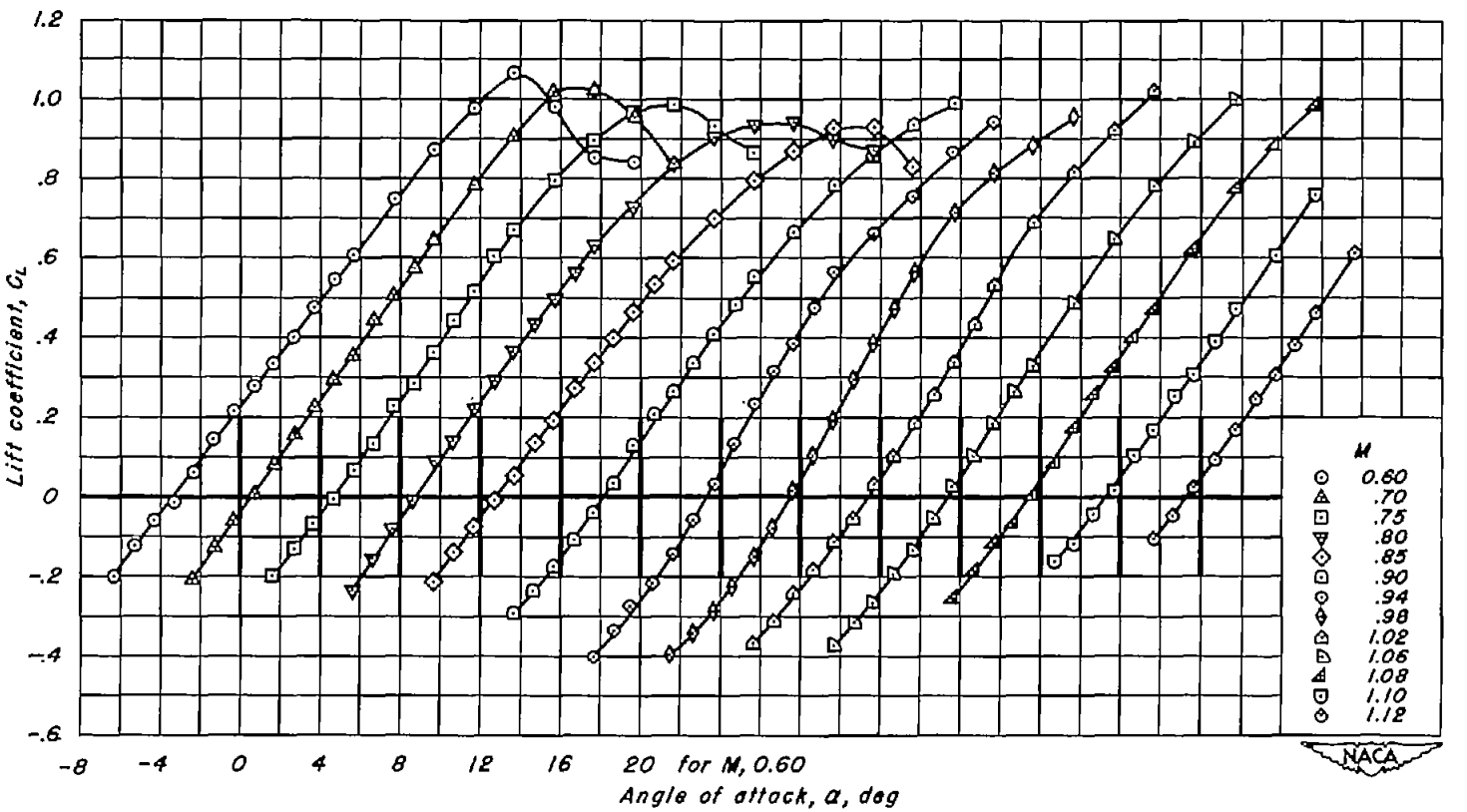

(a) A, 4; t/c, 0.10

Figure 7.–The variation of lift coefficient with angle of attack for the wings with NACA 63A4XX sections.

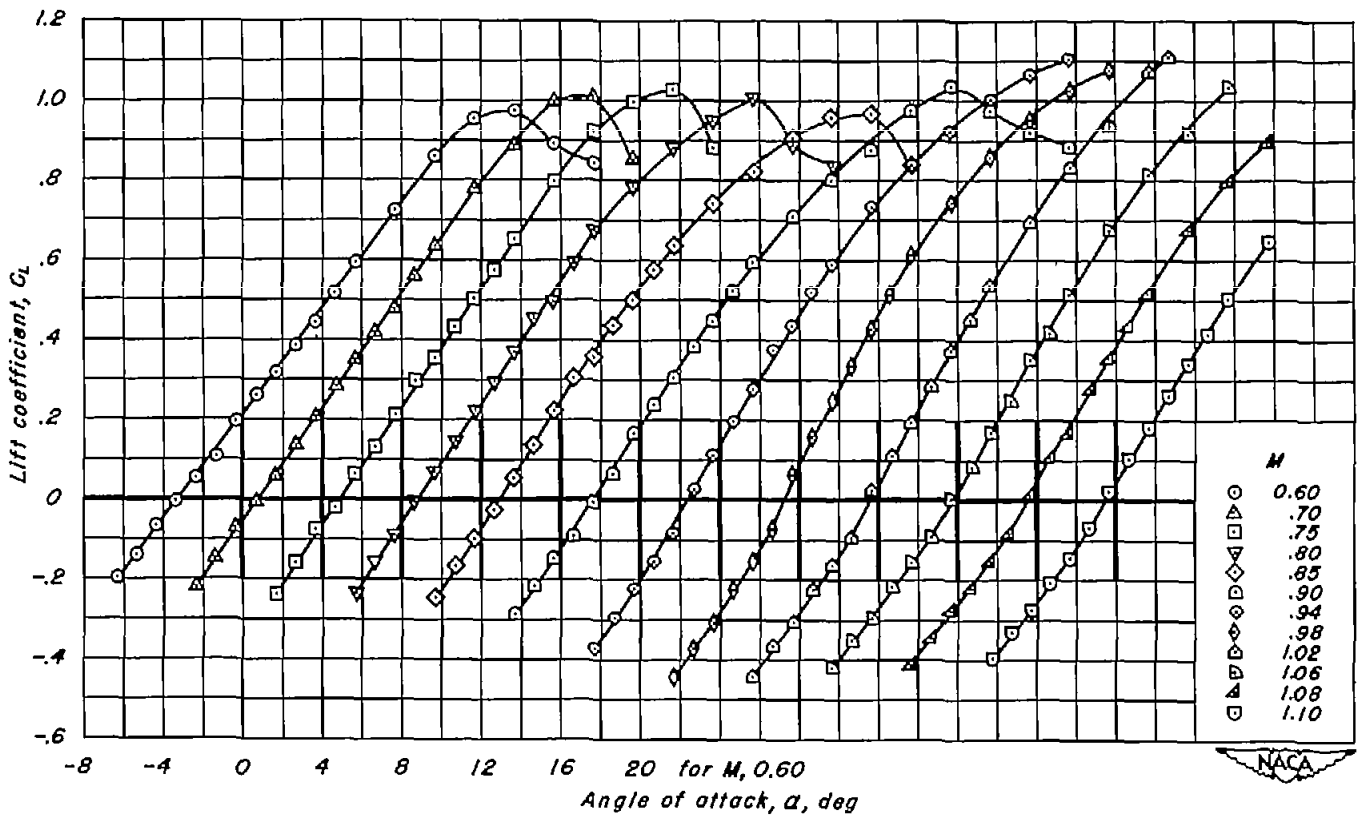

(b) A, 4; t/c, 0.08

Figure 7.- Continued.

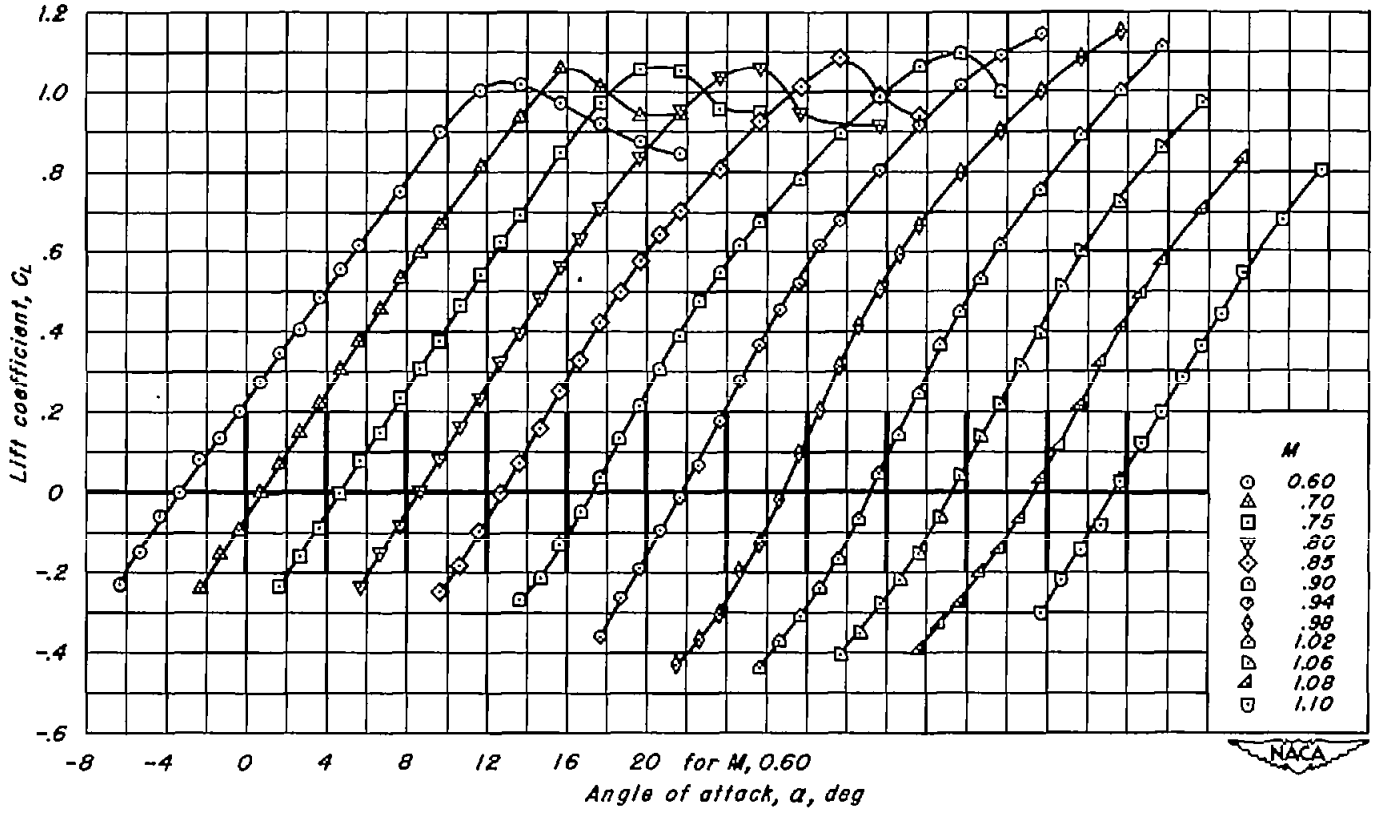

(c) A, 4; t/c, 0.06

Figure 7.- Continued.

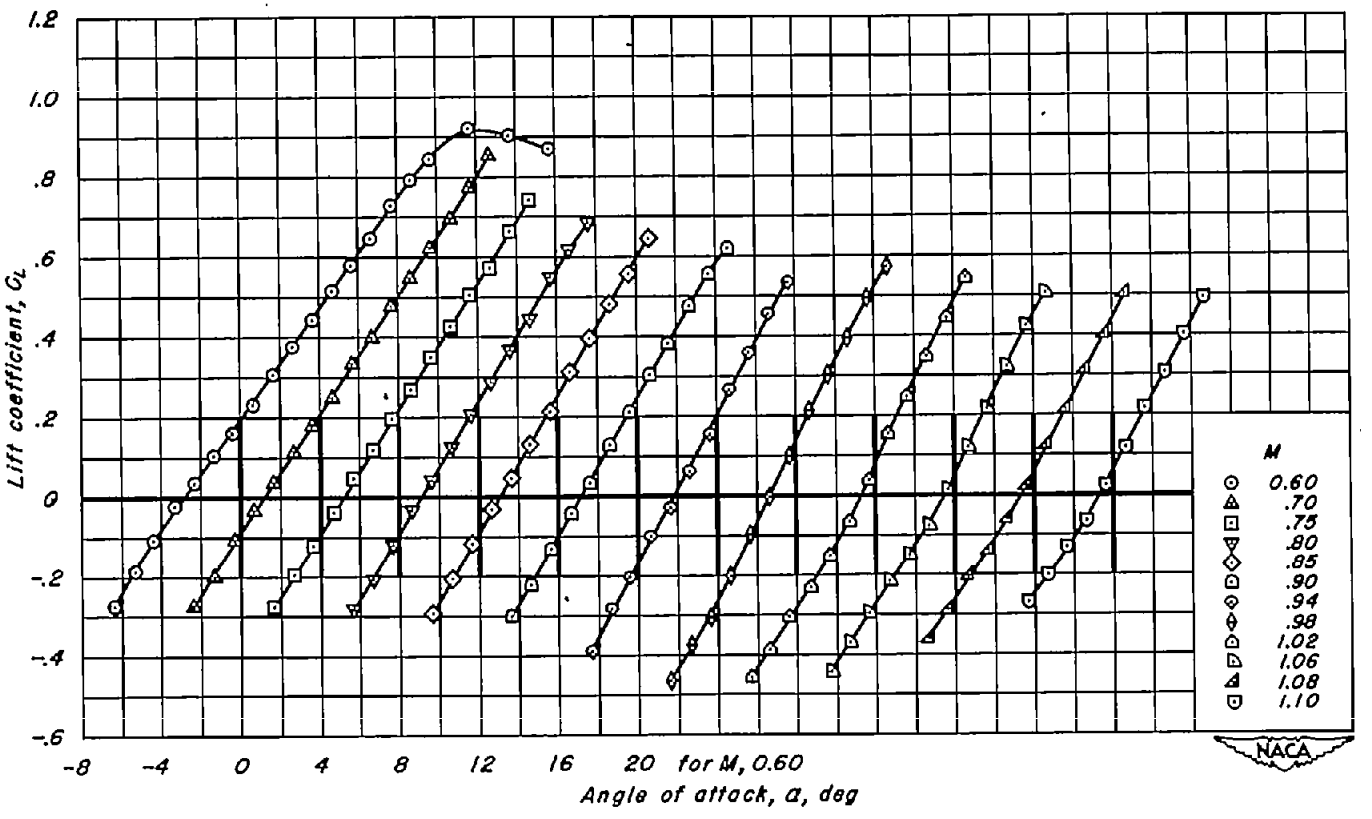

(d) A, 4; t/c, 0.04

Figure 7.- Continued.

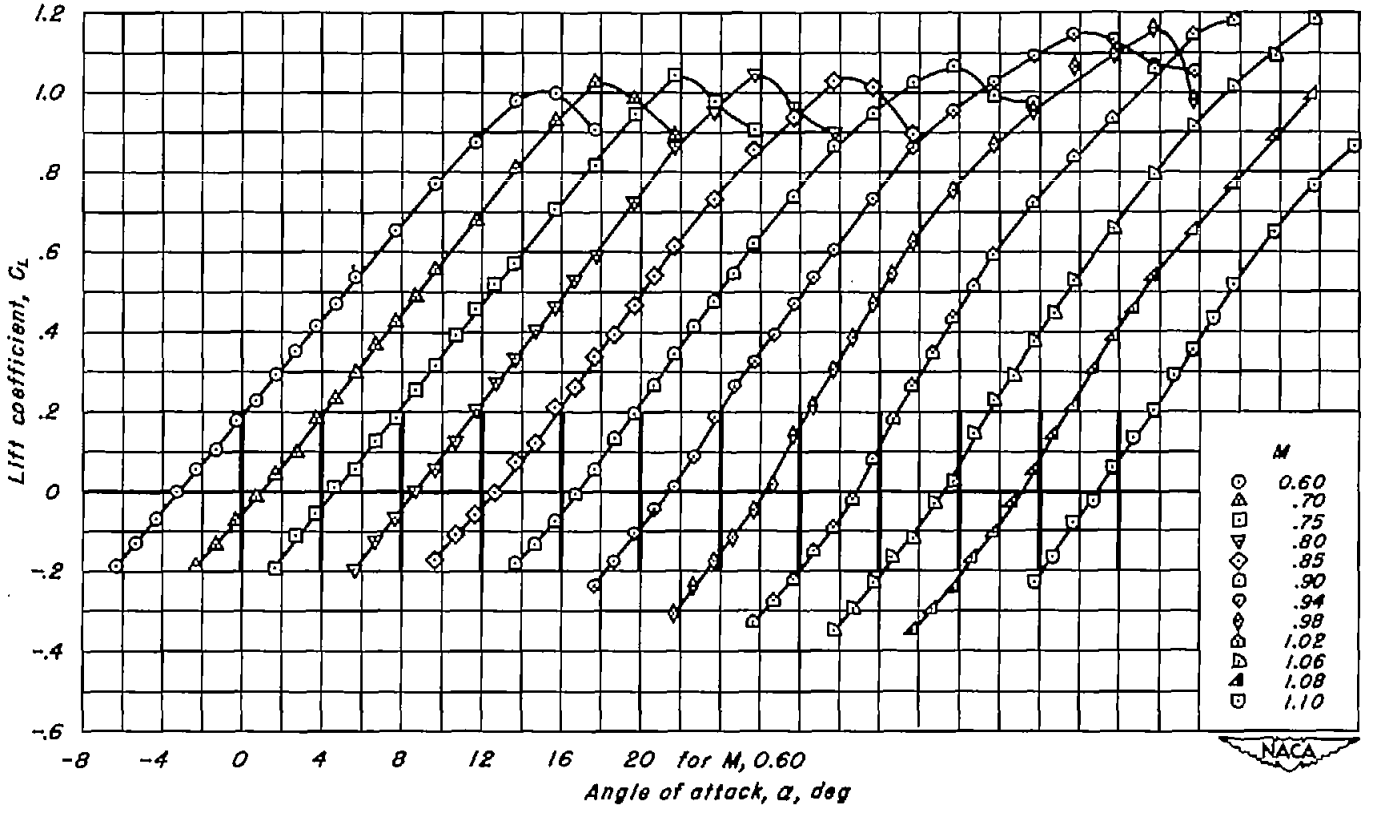

(e) A, 3; t/c, 0.06

Figure 7.- Continued.

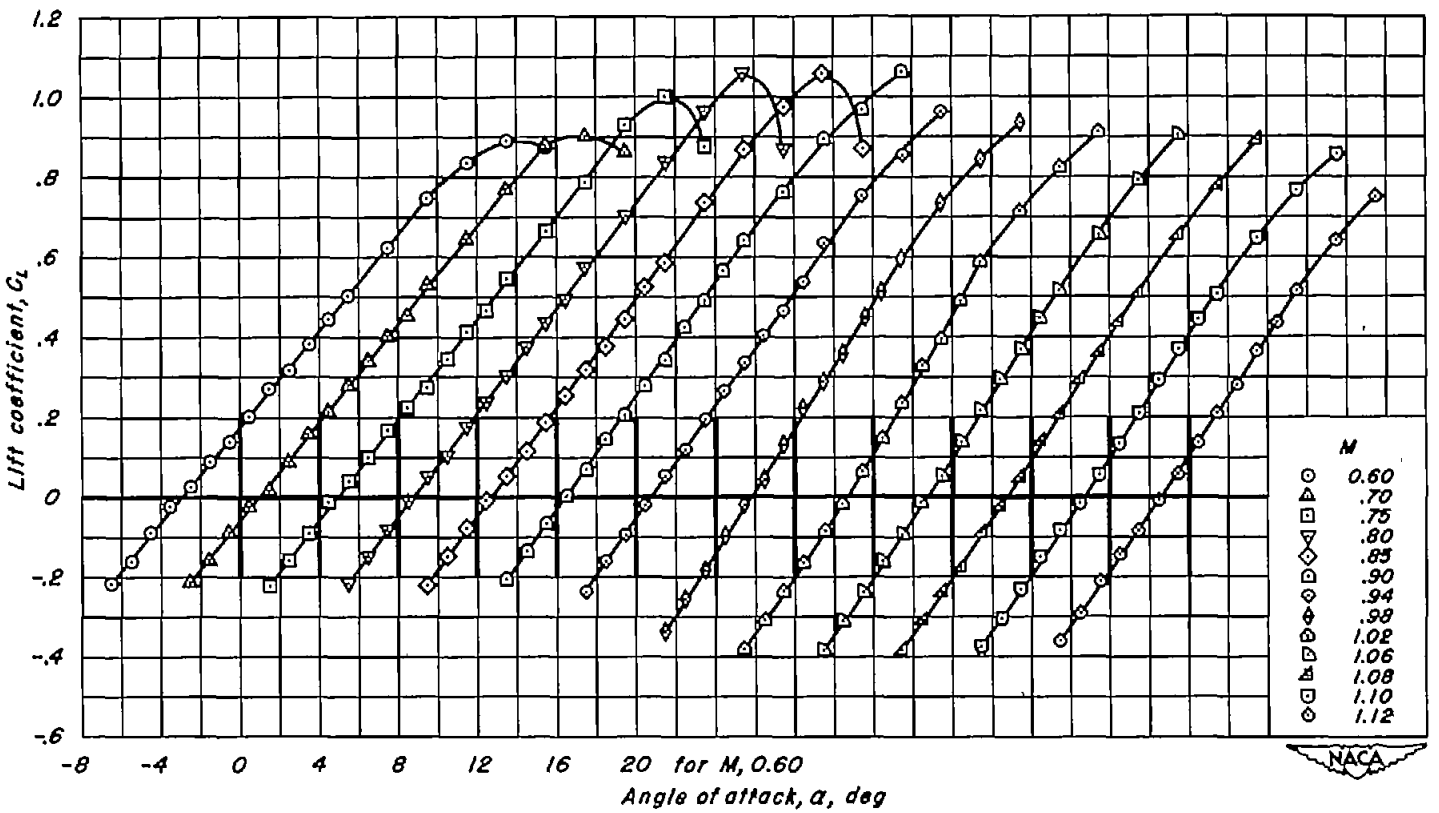

(f) A, 3; t/c, 0.04

Figure 7.- Continued.

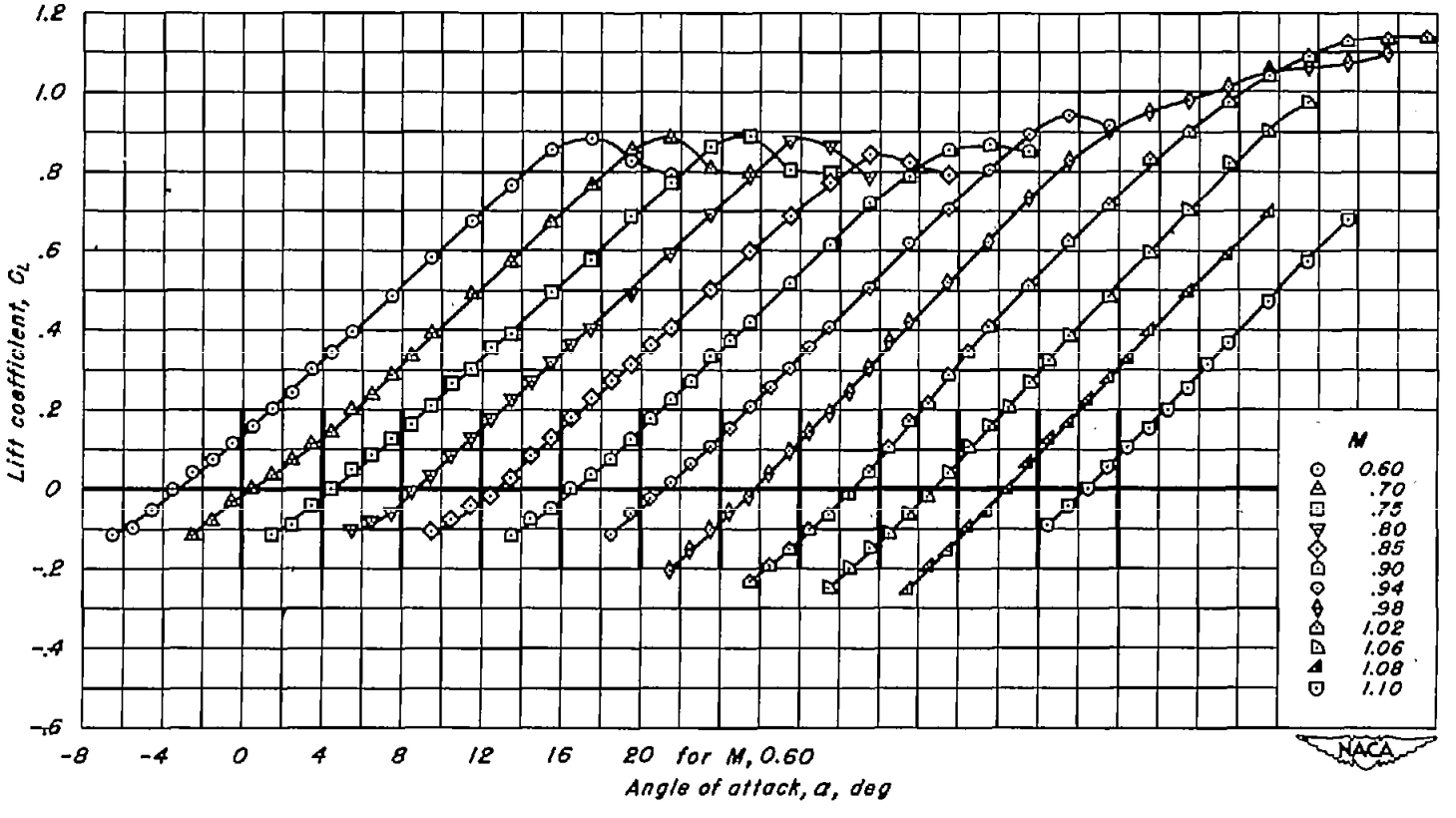

(g) A, 2; t/c, 0.10

Figure 7.- Continued.

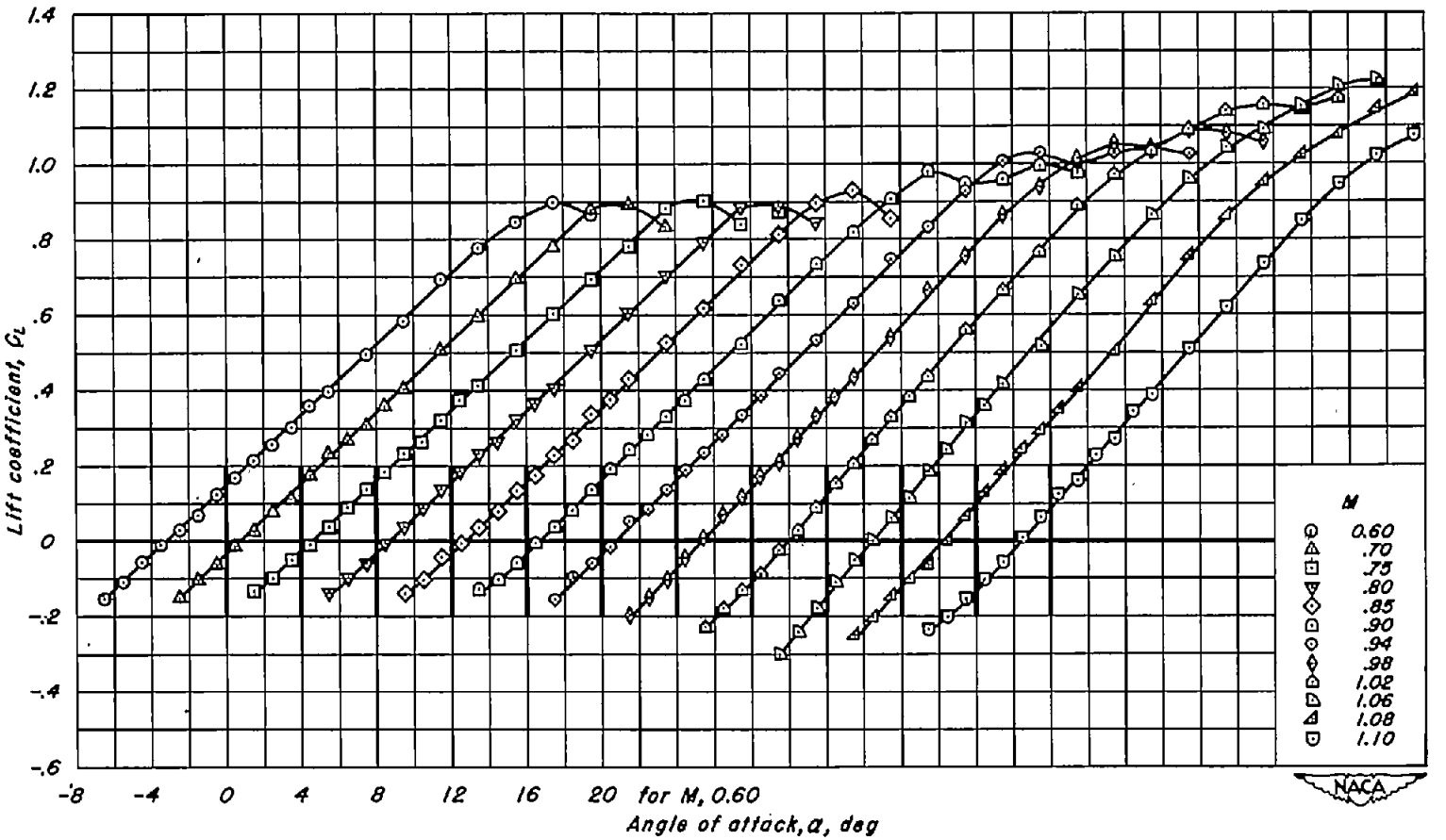

(h) A, 2; t/c, 0.08

Figure 7.- Continued.

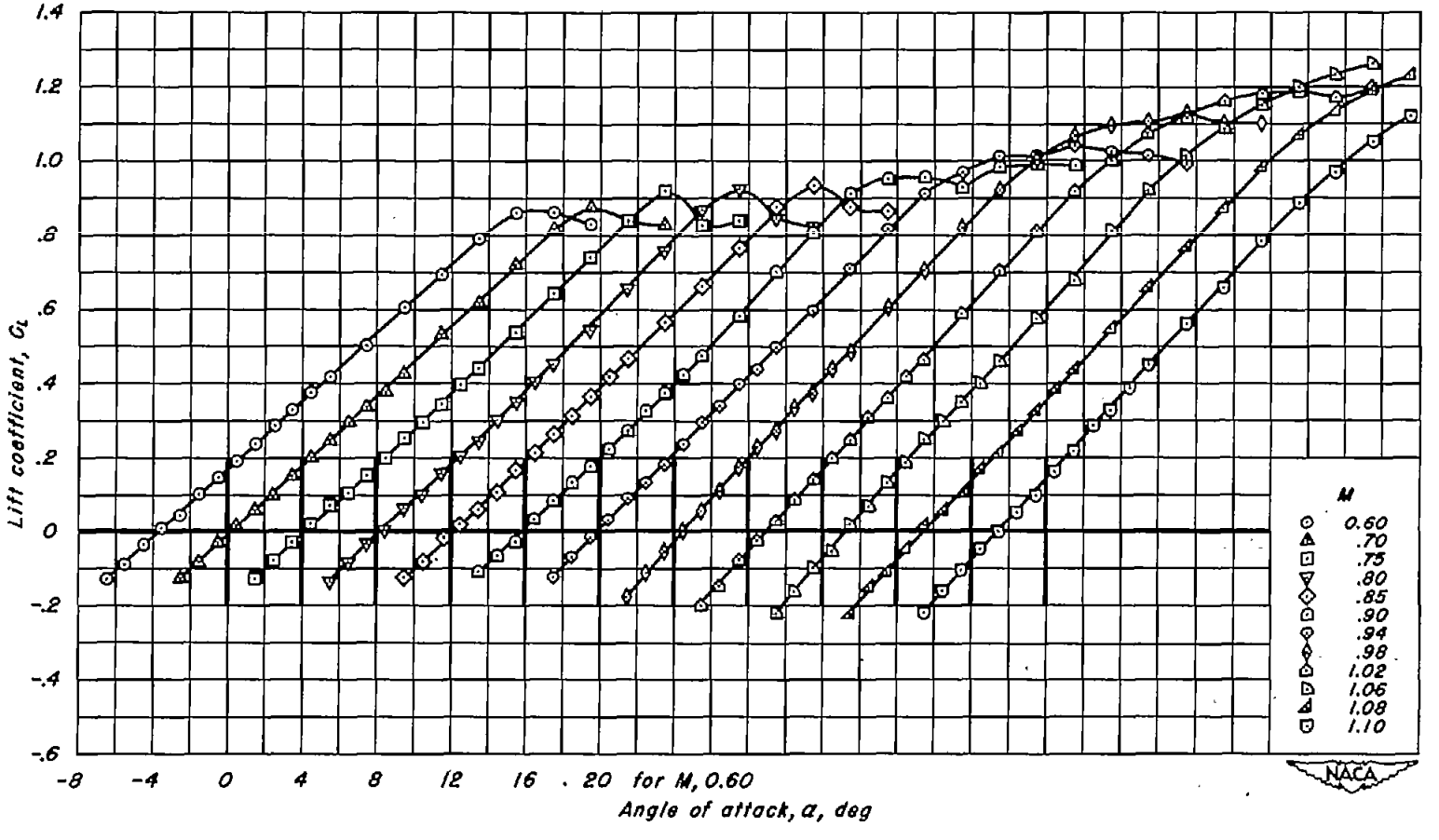

(i) A, 2; t/c, 0.06

Figure 7.- Continued.

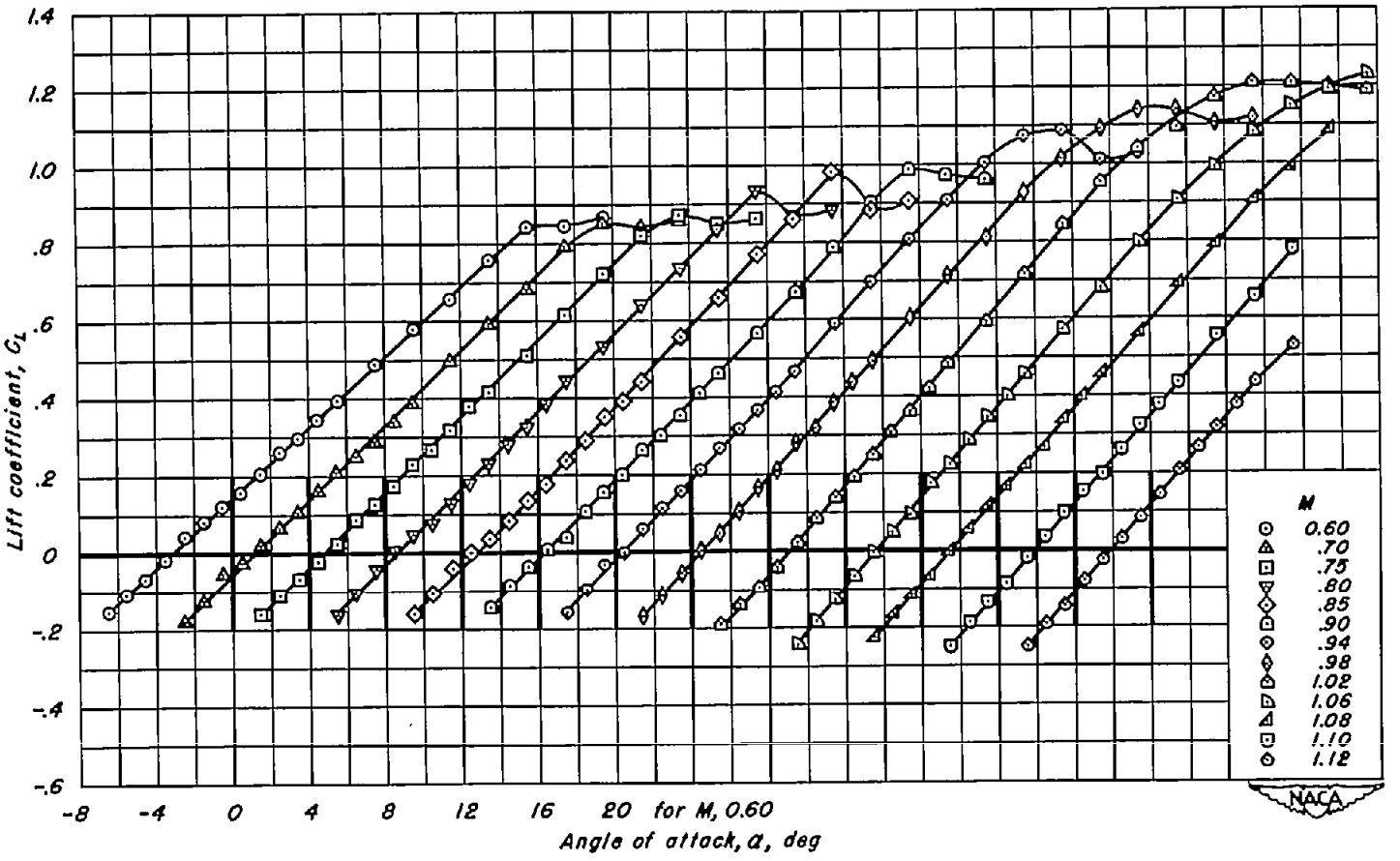

(j) A, 2; t/c, 0.04

Figure 7.- Continued.

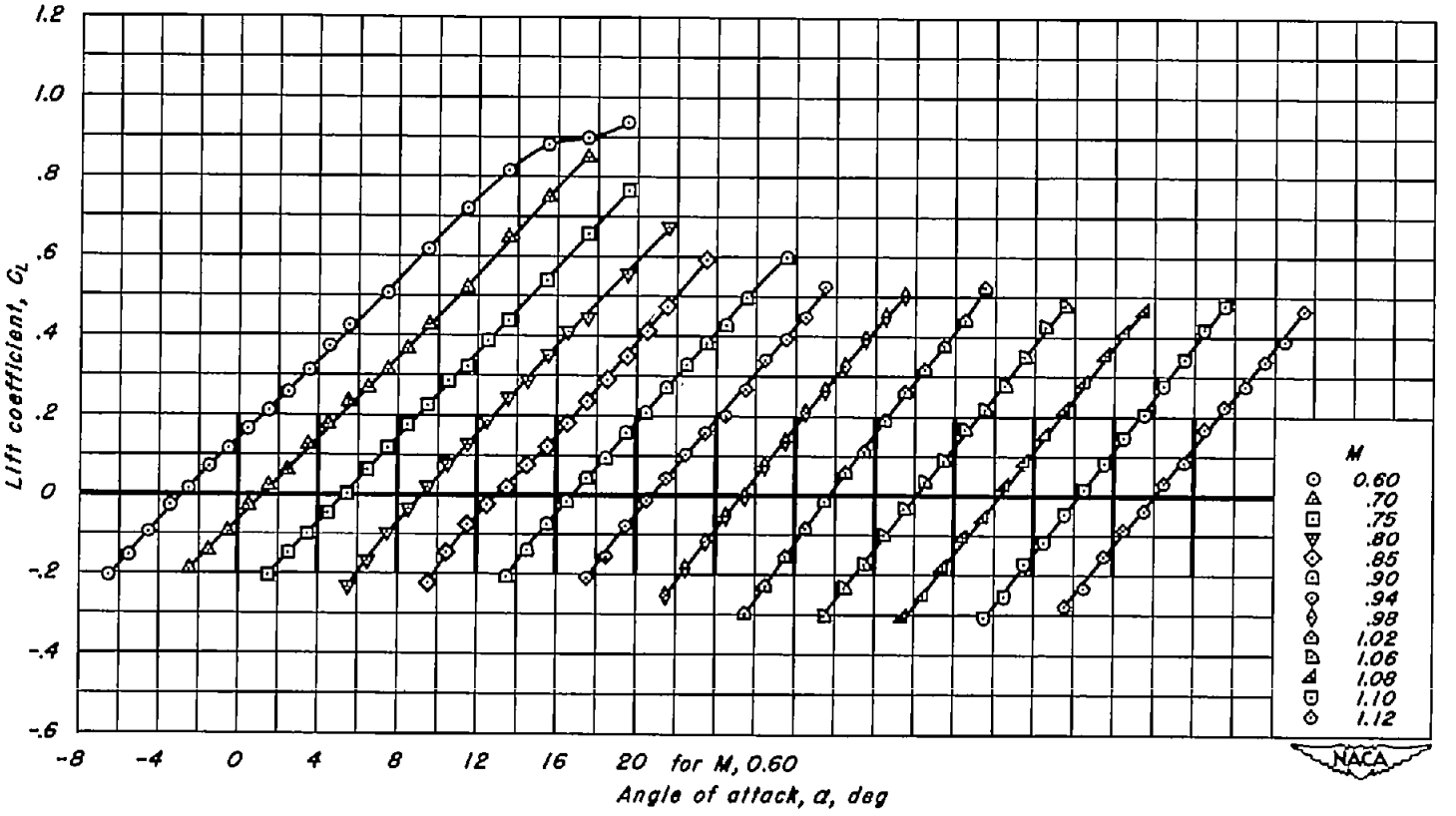

(k) A, 2; t/c, 0.02

Figure 7.- Continued.

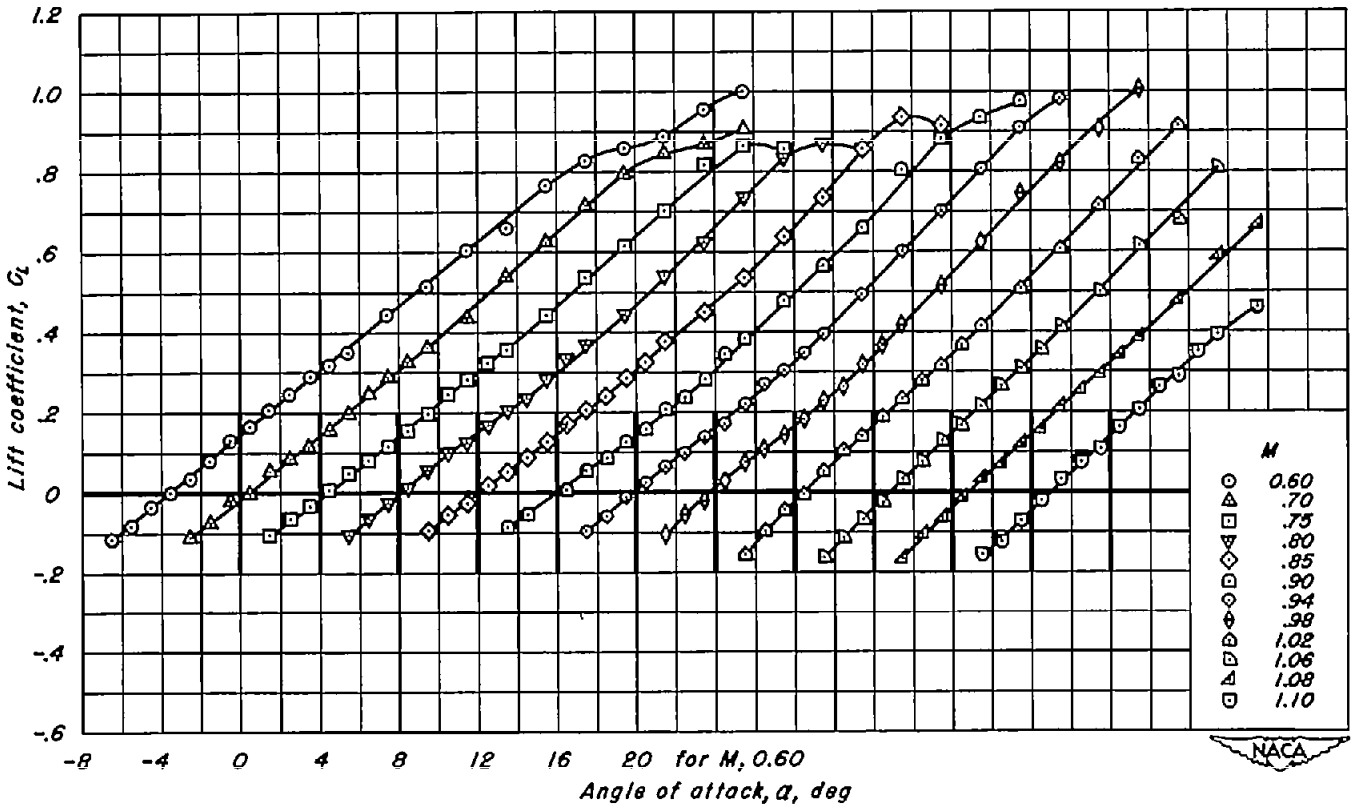

(1) A,1.5; t/c, 0.06

Figure 7.- Continued.

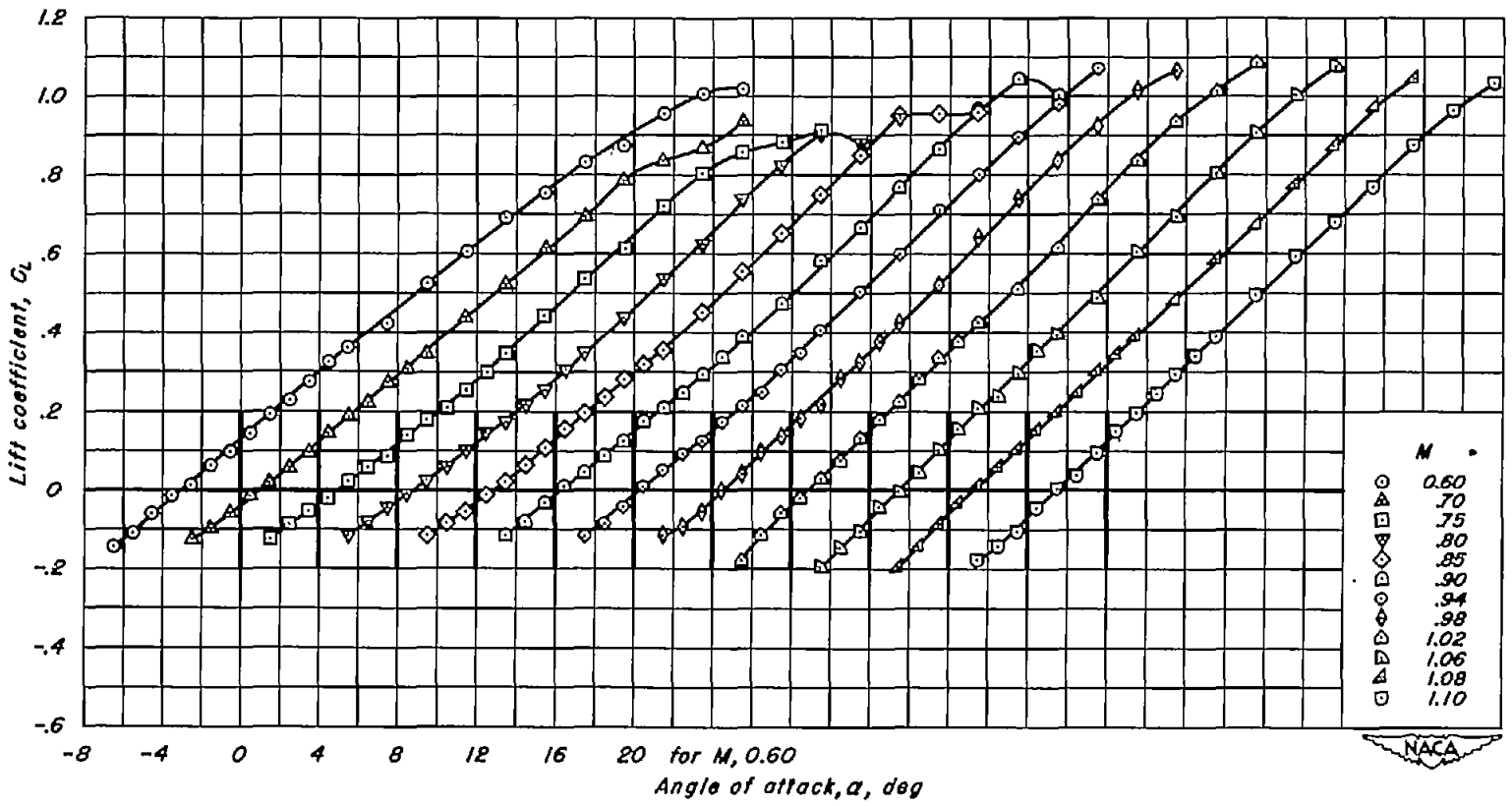

(m) A, 1.5; t/c, 0.04

Figure 7.- Continued.

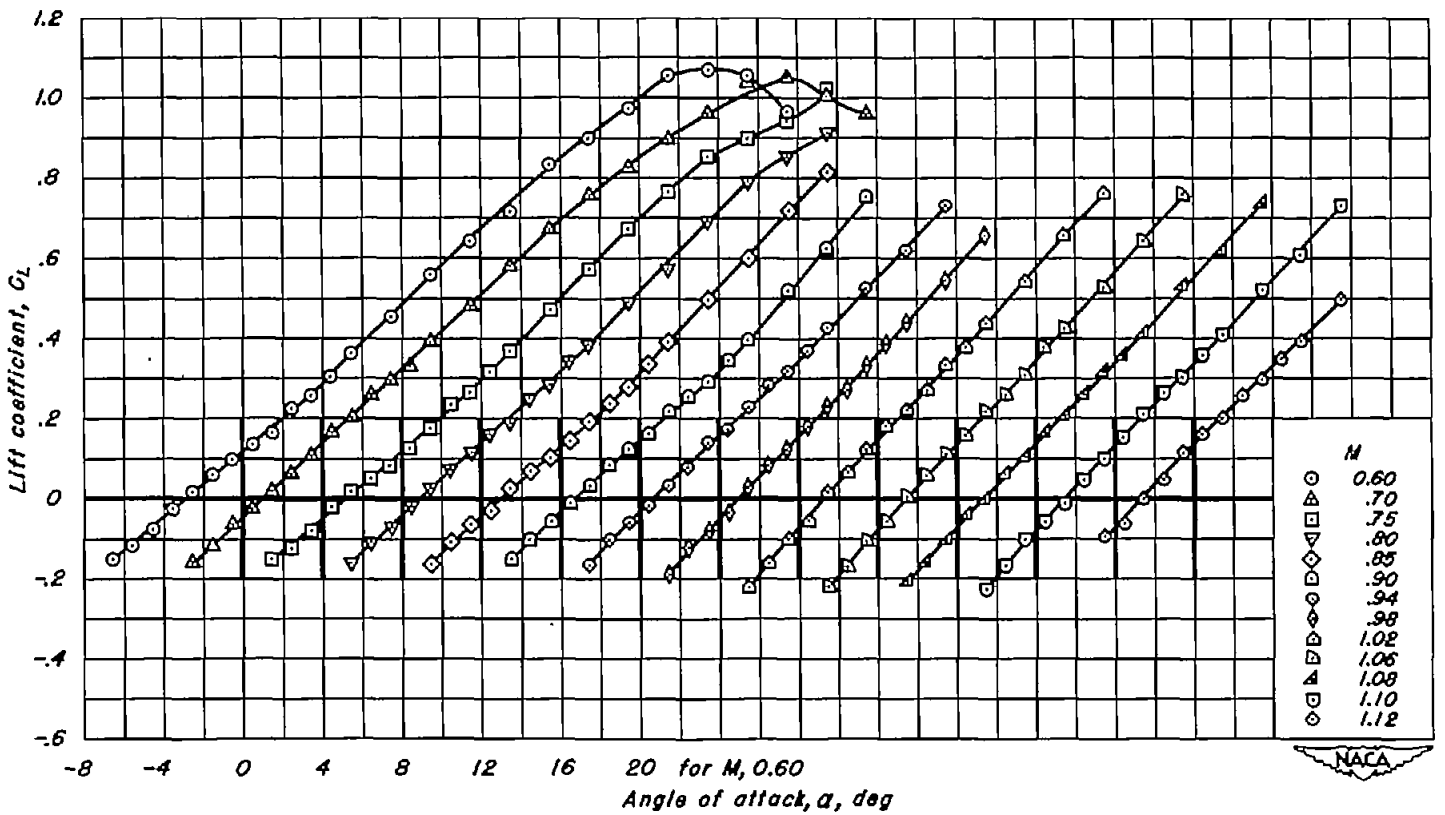

(n) A,1.5; t/c, 0.02

Figure 7.- Continued.

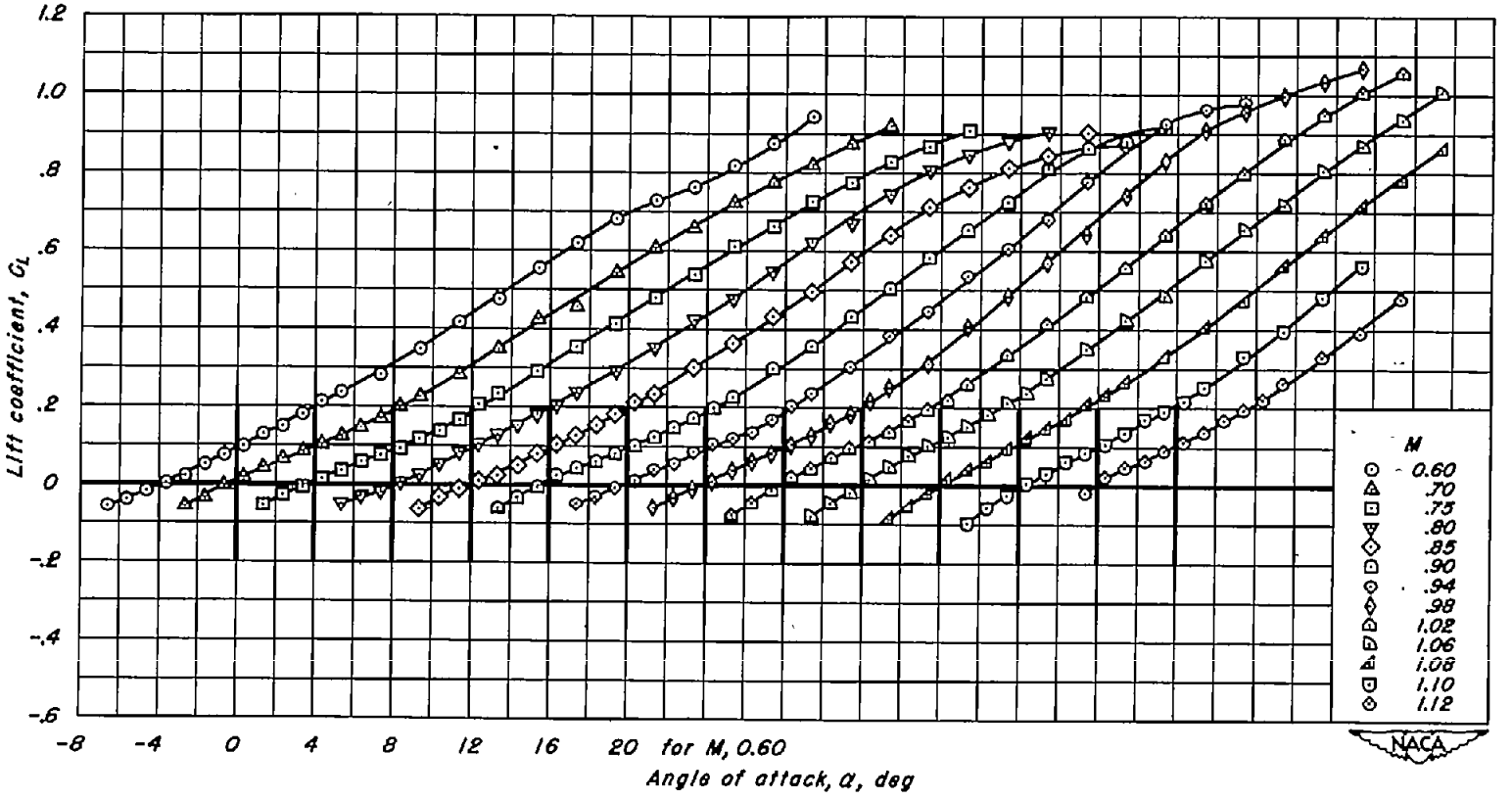

(o) A, 1; t/c, 0.10

Figure 7.- Continued.

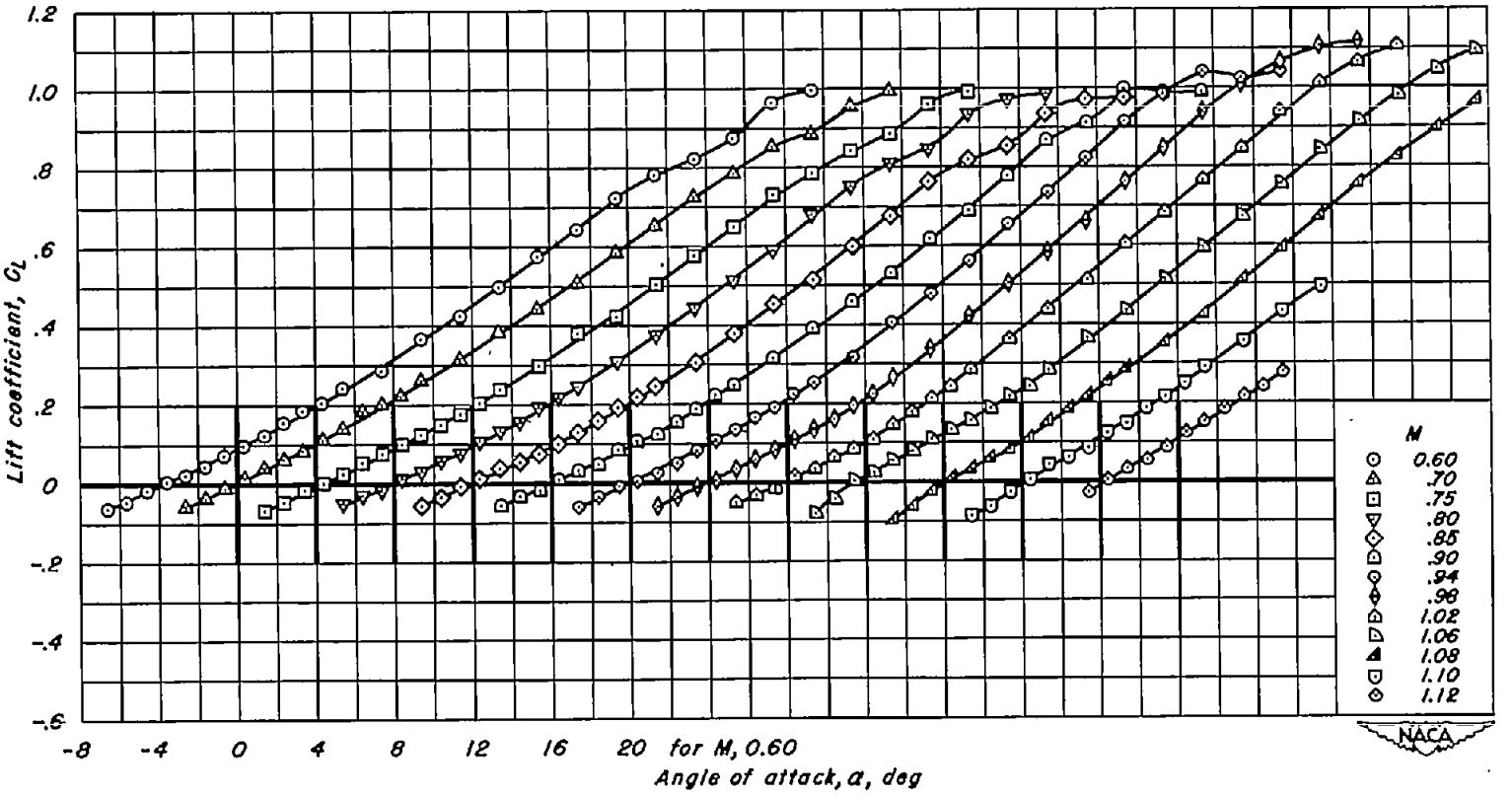

(p) A, 1; t/c, 0.08

Figure 7.- Continued.

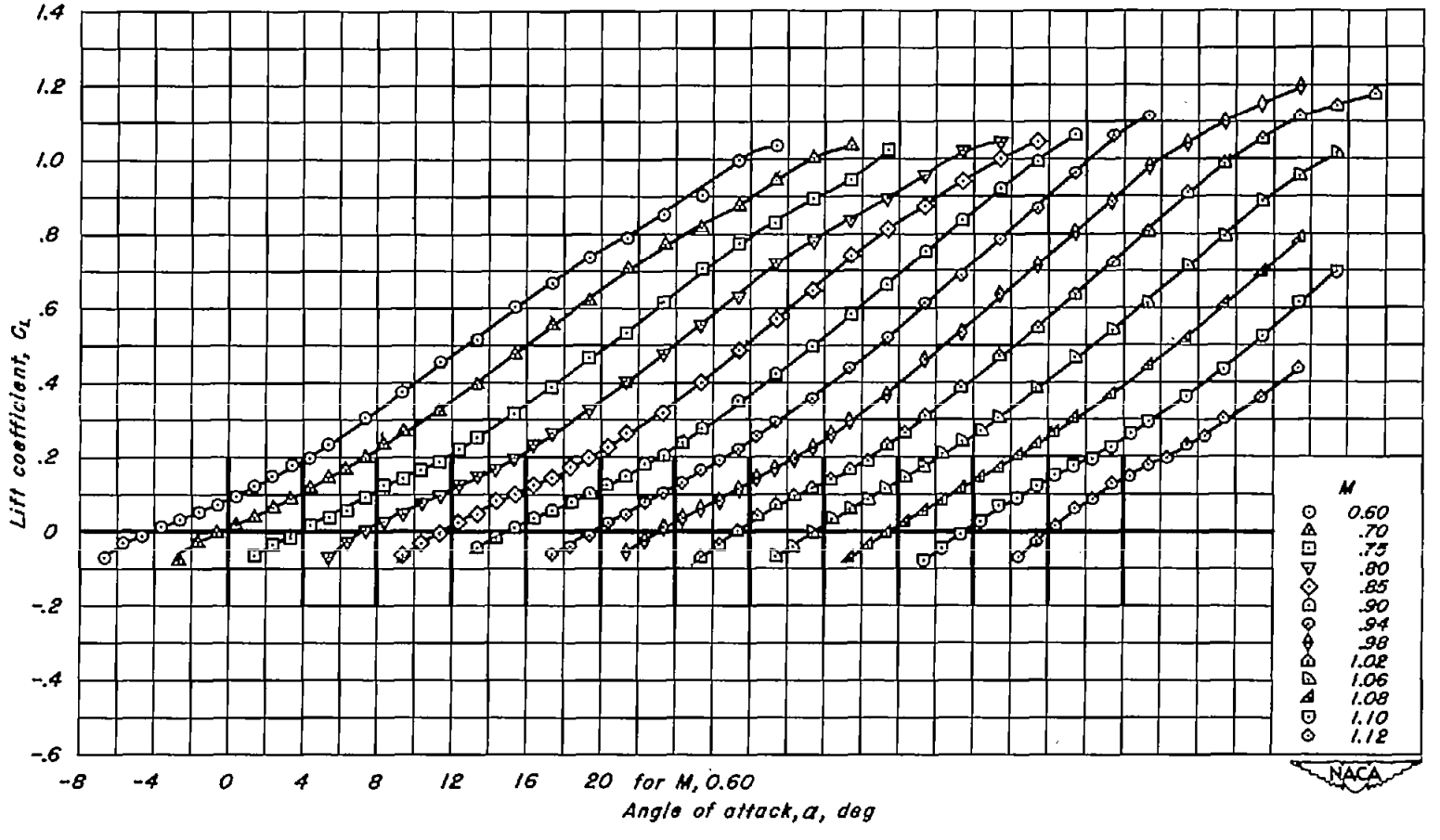

(q) A, I, t/c, 0.06

Figure 7.- Continued.

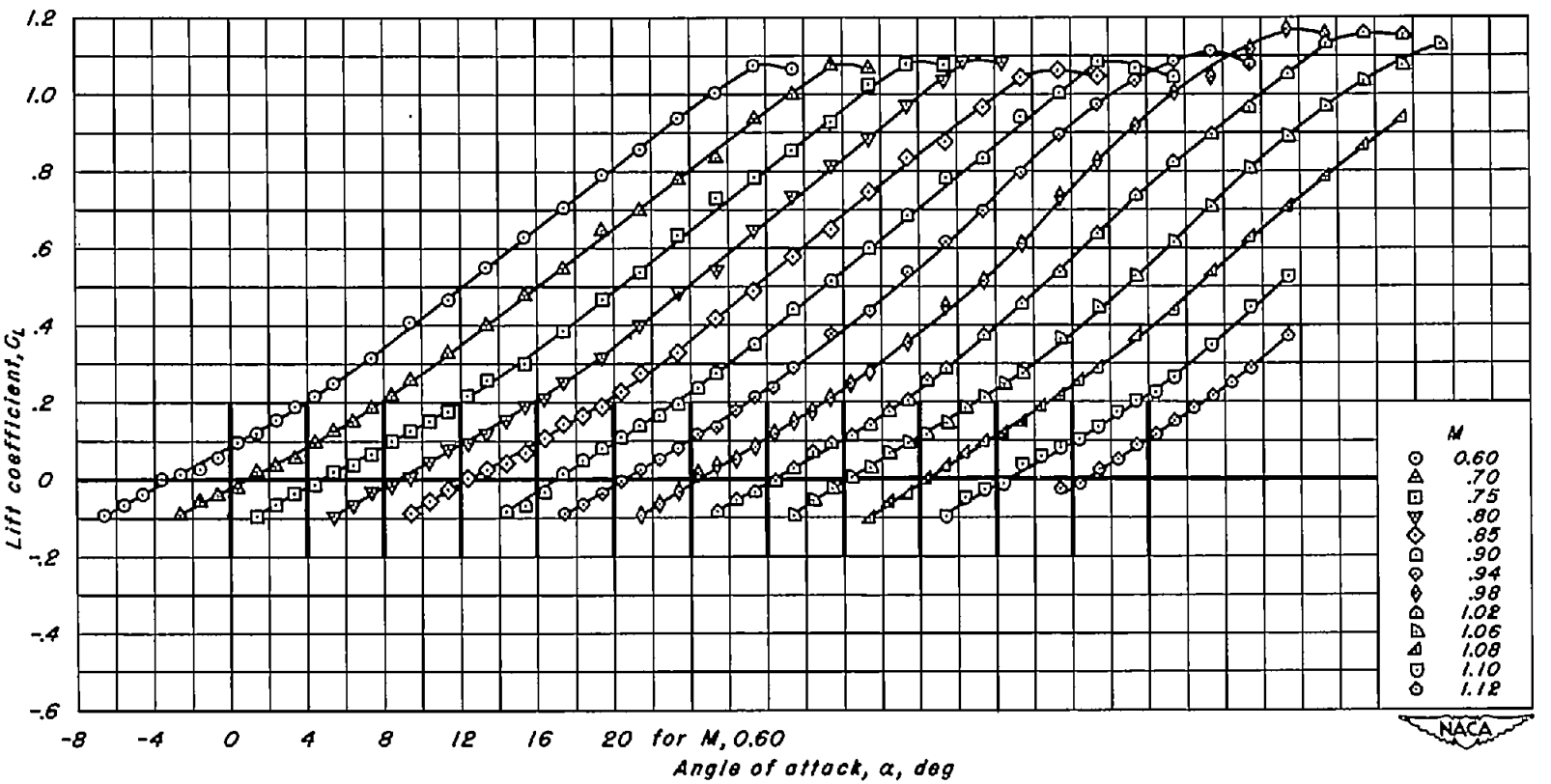

(r) A, 1; t/c, 0.04

Figure 7.- Continued.

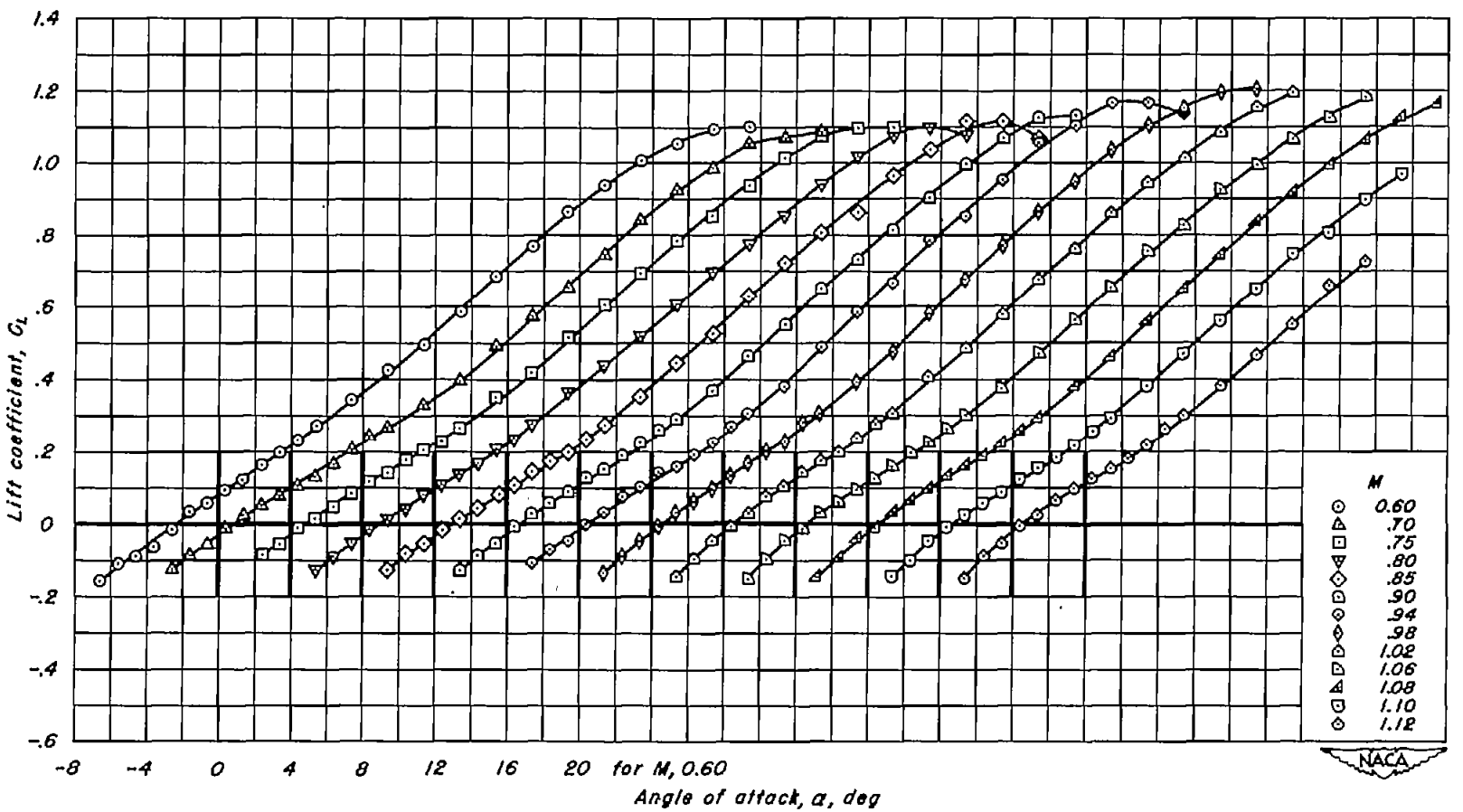

(s) A, 1; t/c, 0.02

Figure 7.- Concluded.

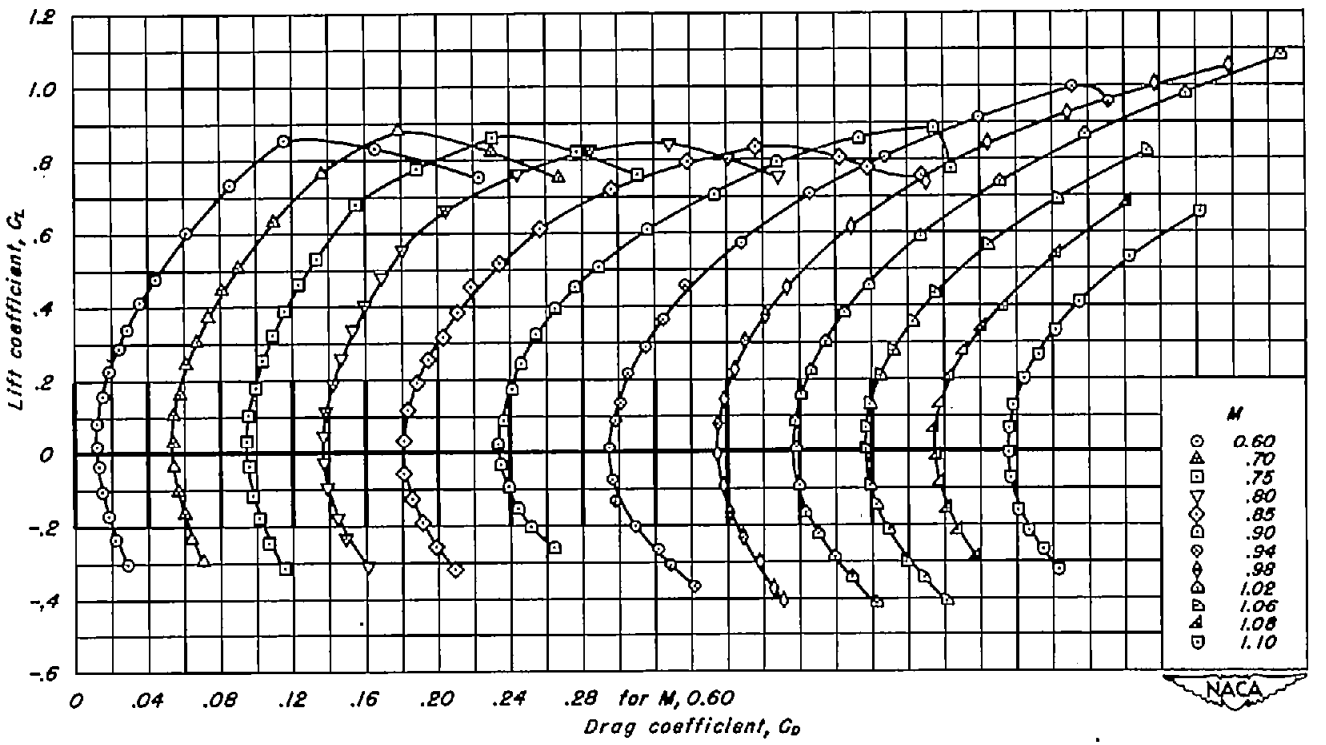

(a) A, 4; t/c, 0.10

Figure 8.—The variation of drag coefficient with lift coefficient for the wings with NACA 63A2XX sections.

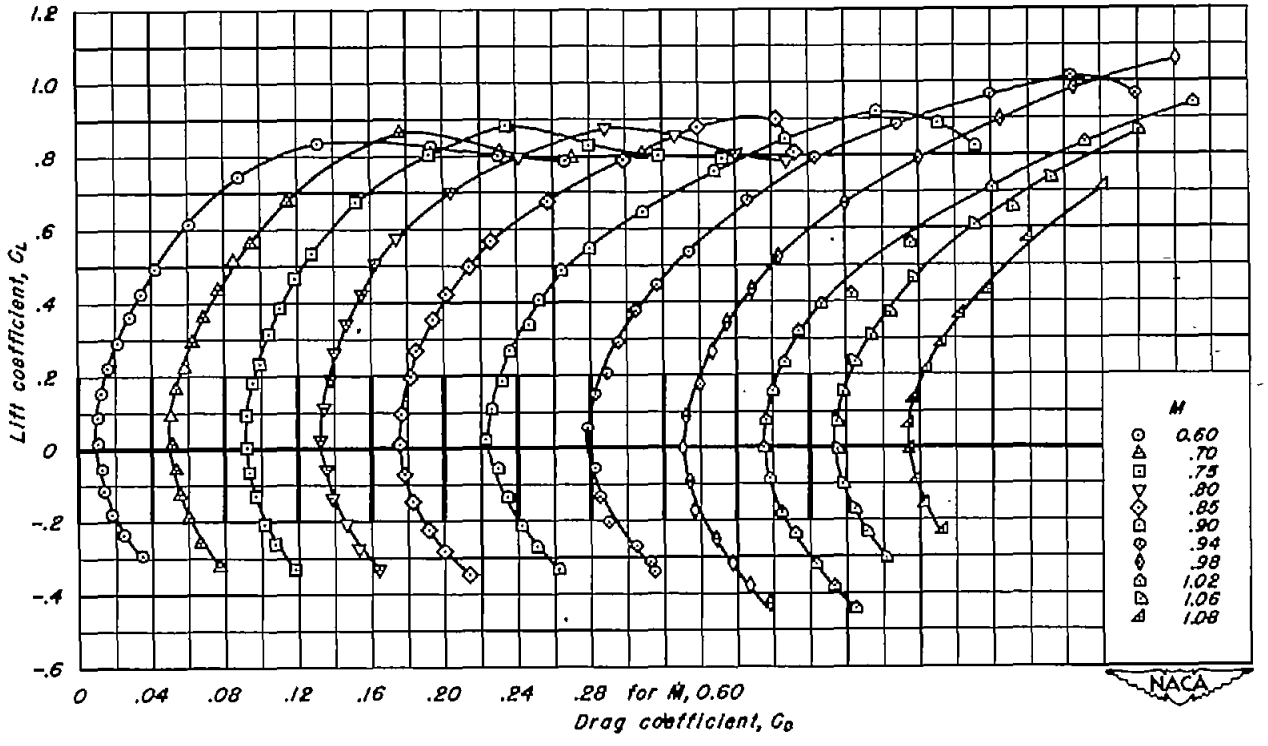

(b) A, 4; t/c, 0.08

Figure 8.- Continued.

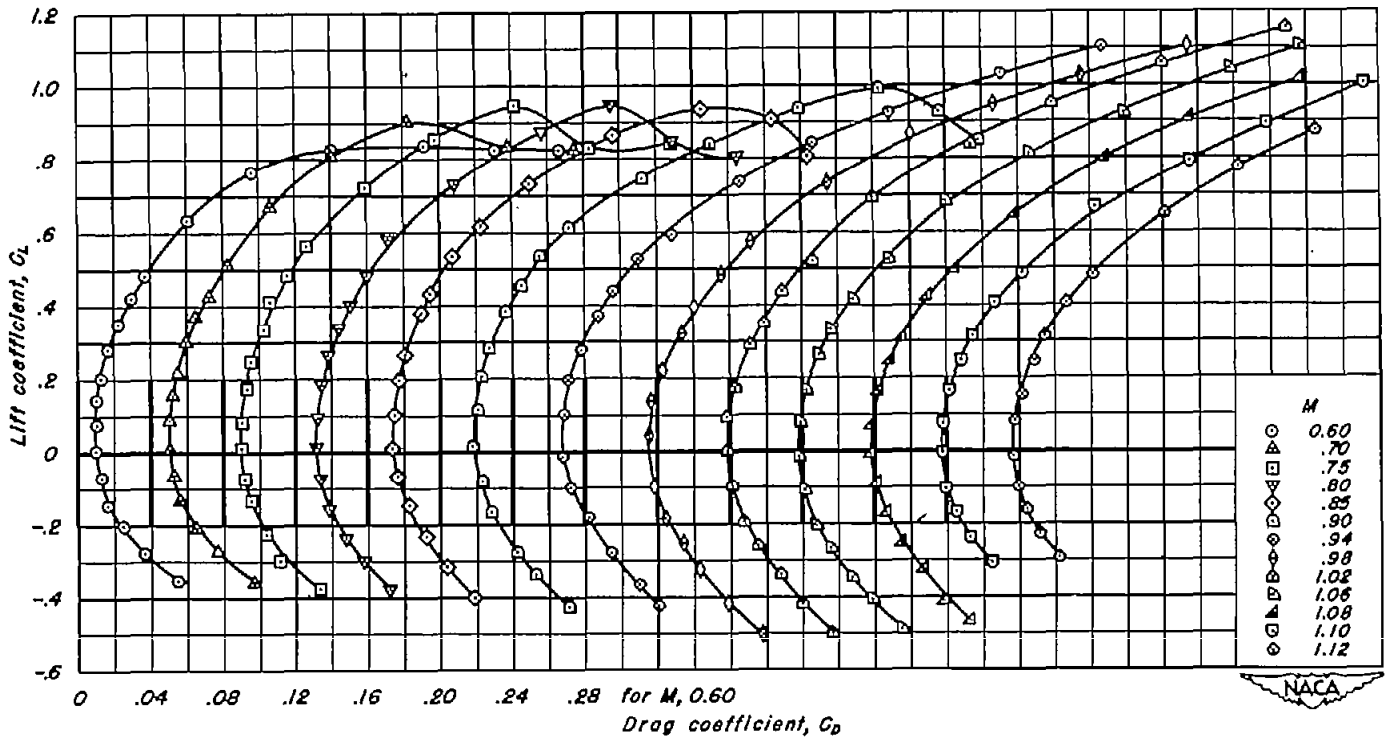

(c) A, 4; t/c, 0.06

Figure 8.- Continued.

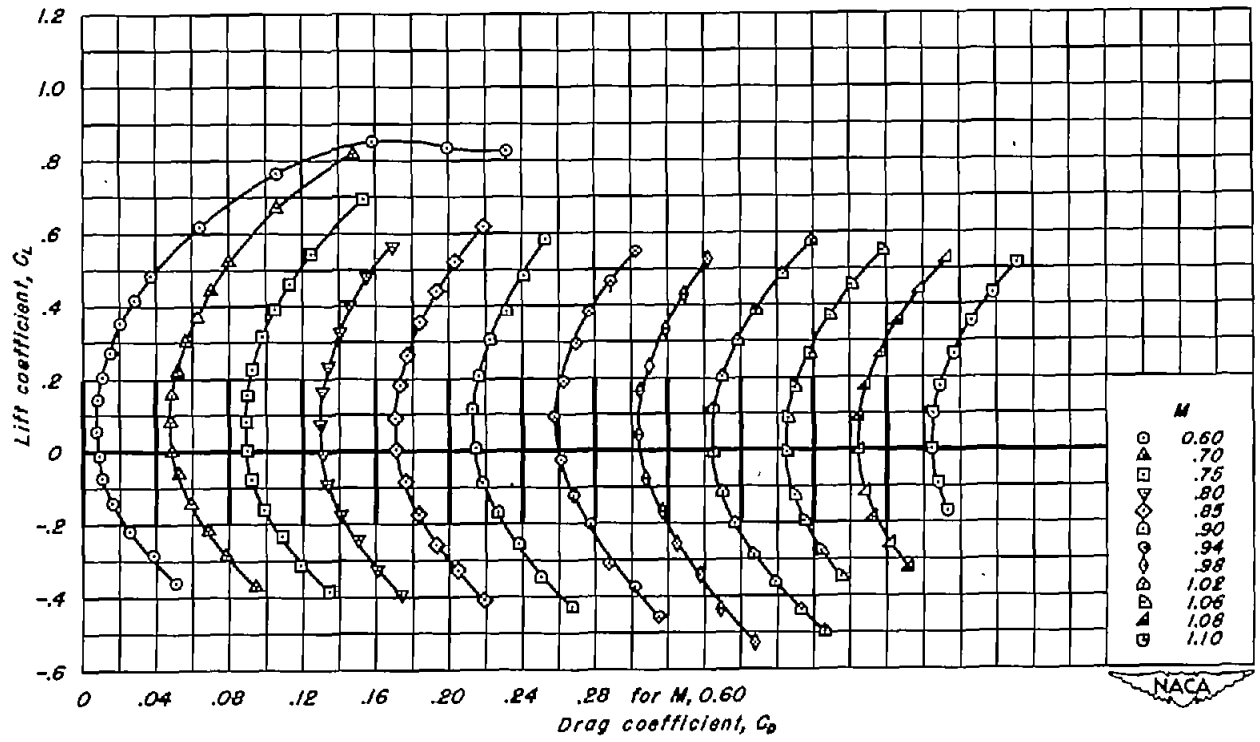

(d) A, 4; t/c, 0.04

Figure 8.- Continued.

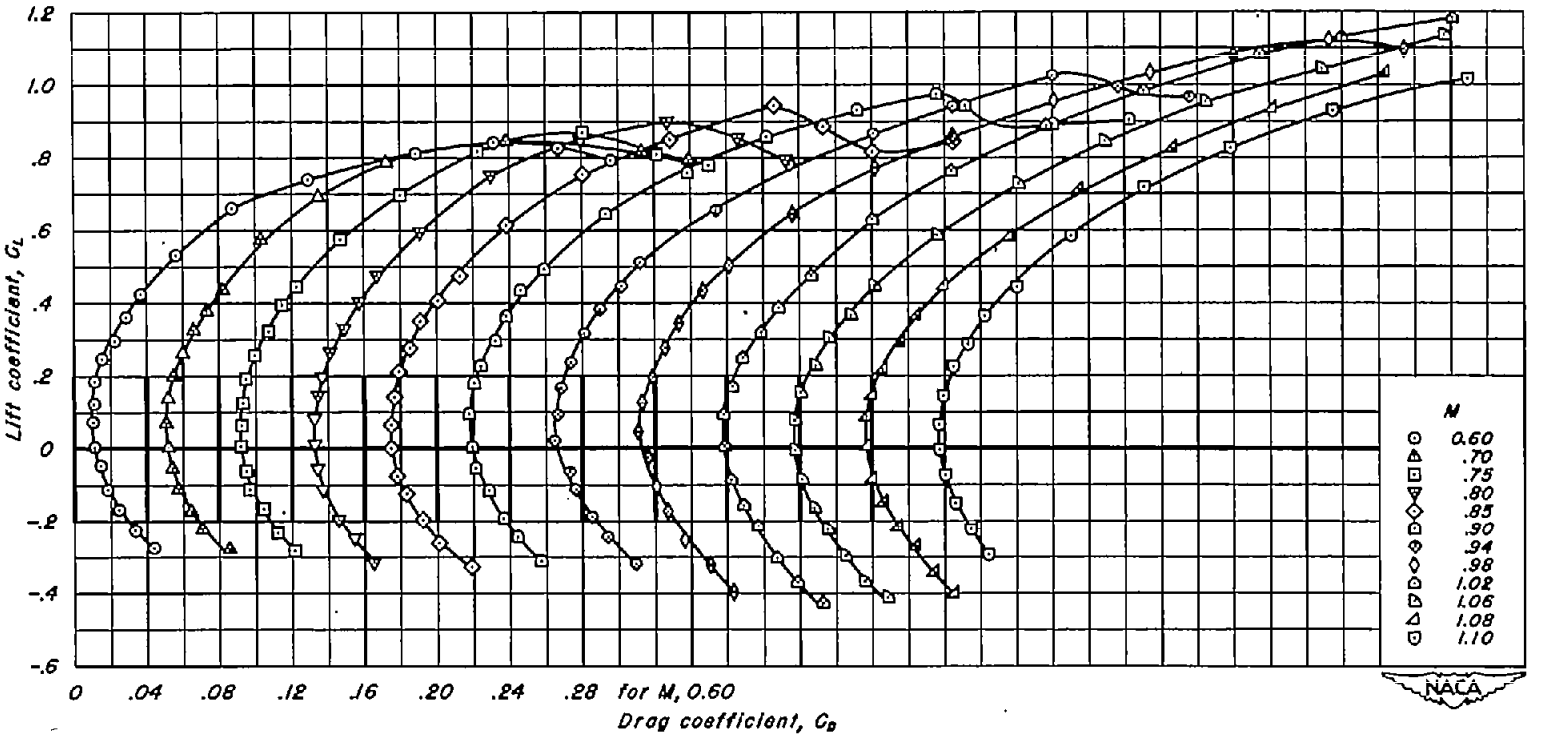

(e) A, 3; t/c, 0.06

Figure 8.- Continued.

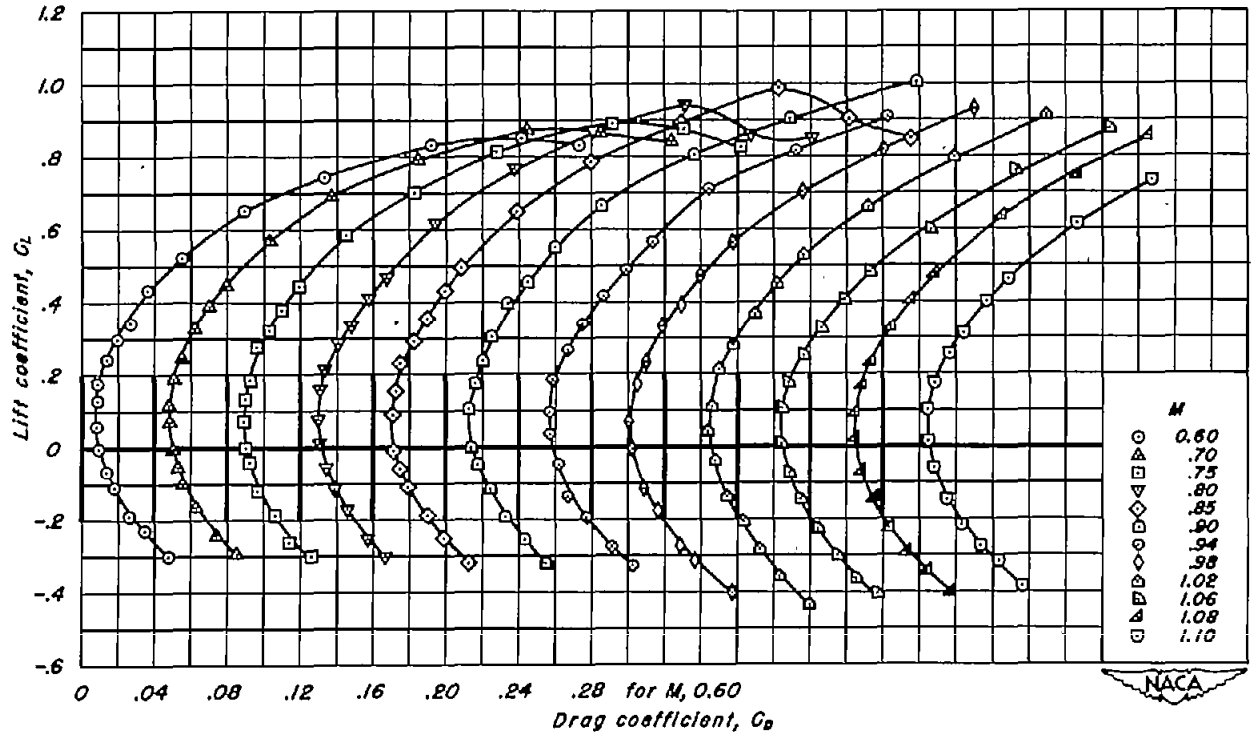

(f) A, 3; t/c, 0.04

Figure 8.- Continued.

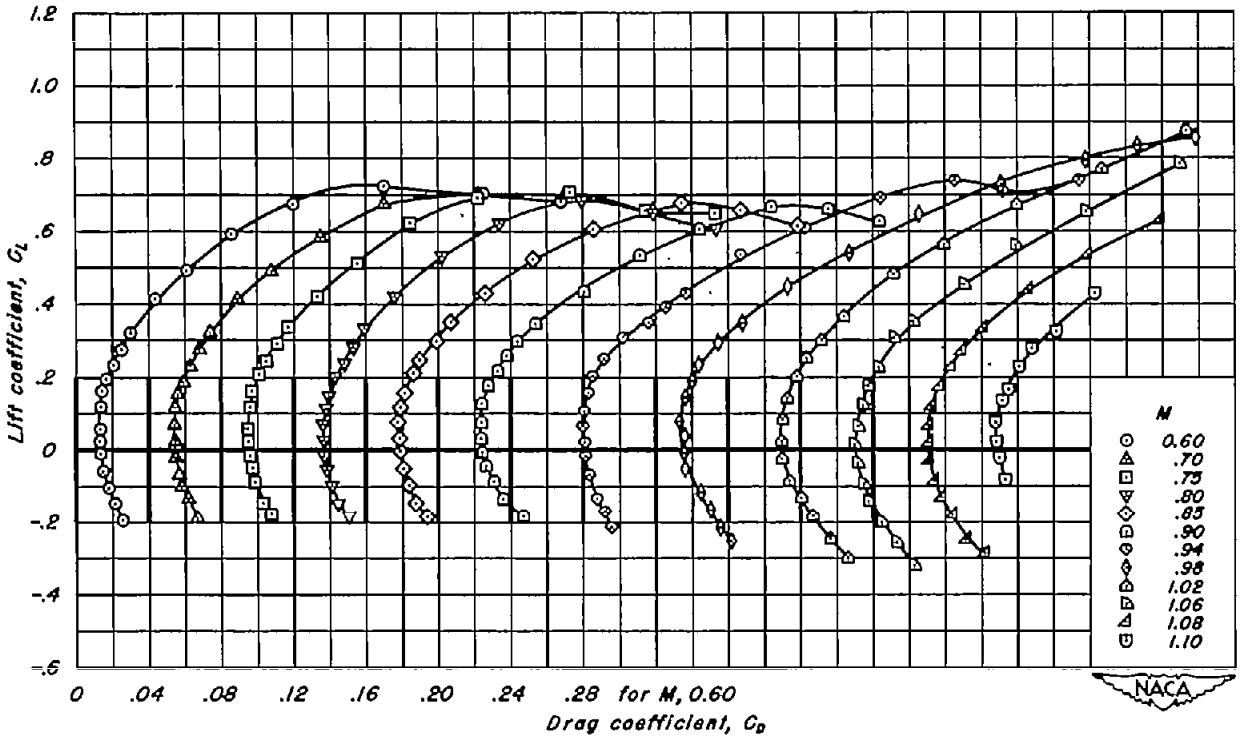

(g) A, 2; t/c, 0.10

Figure 8.- Continued.

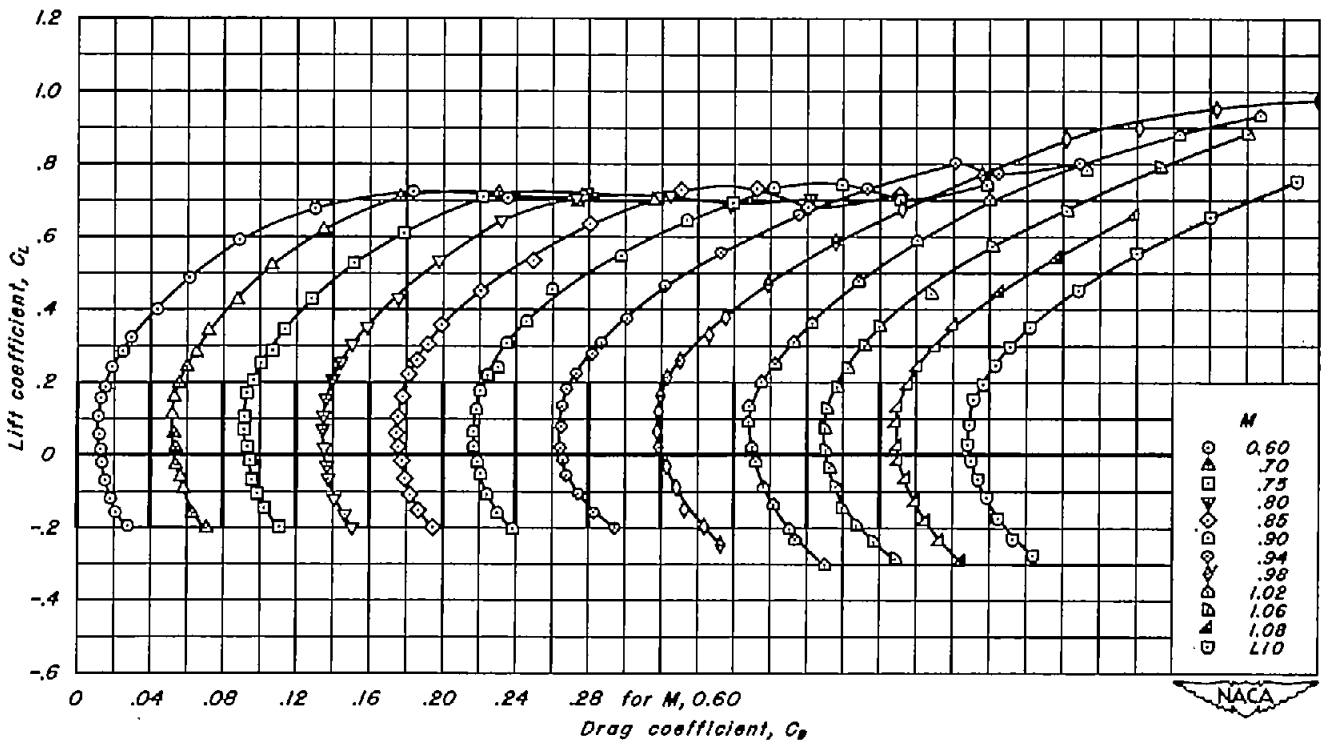

(h) A, 2; t/c, 0.08

Figure 8.- Continued.

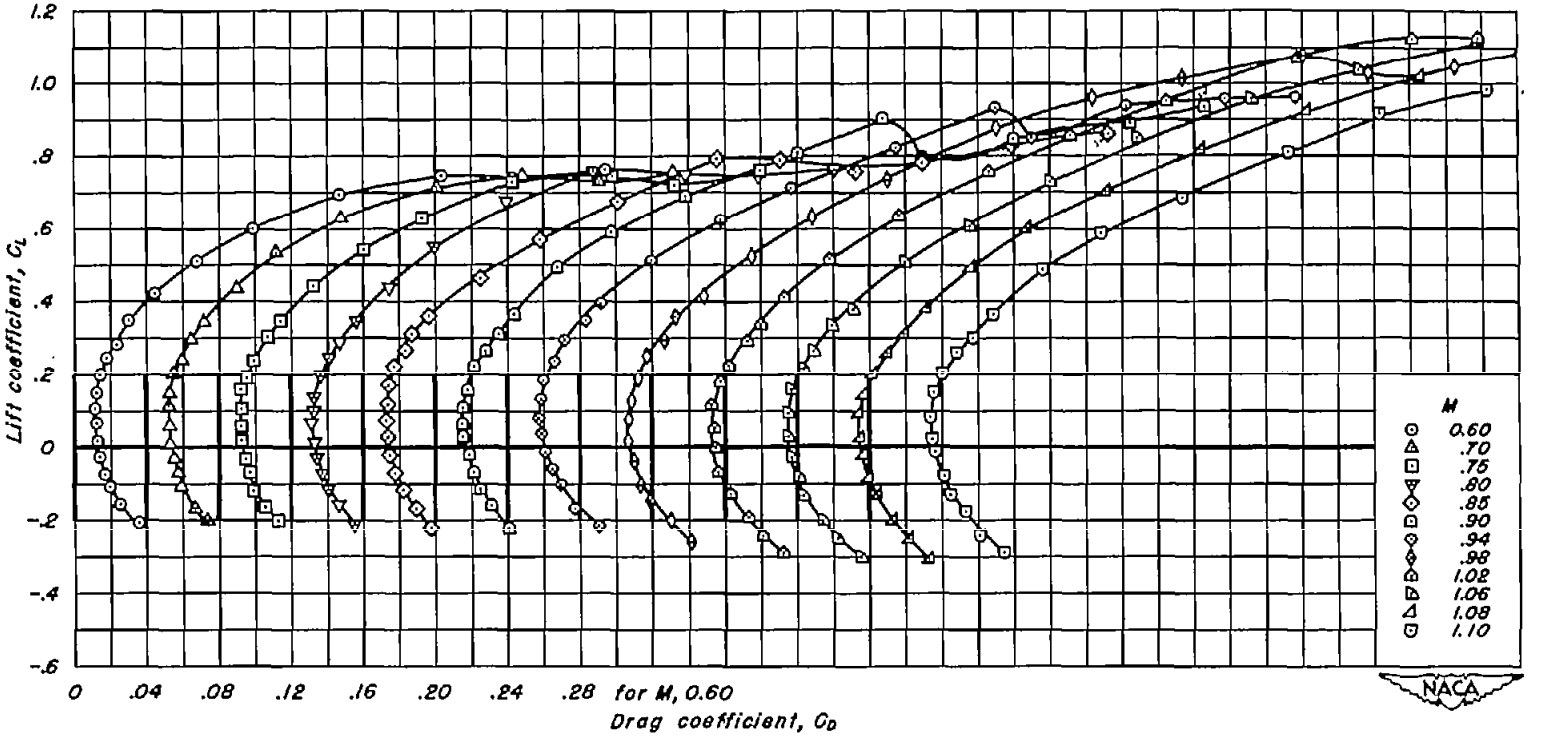

(i) A, 2; t/c, 0.06

Figure 8.- Continued.

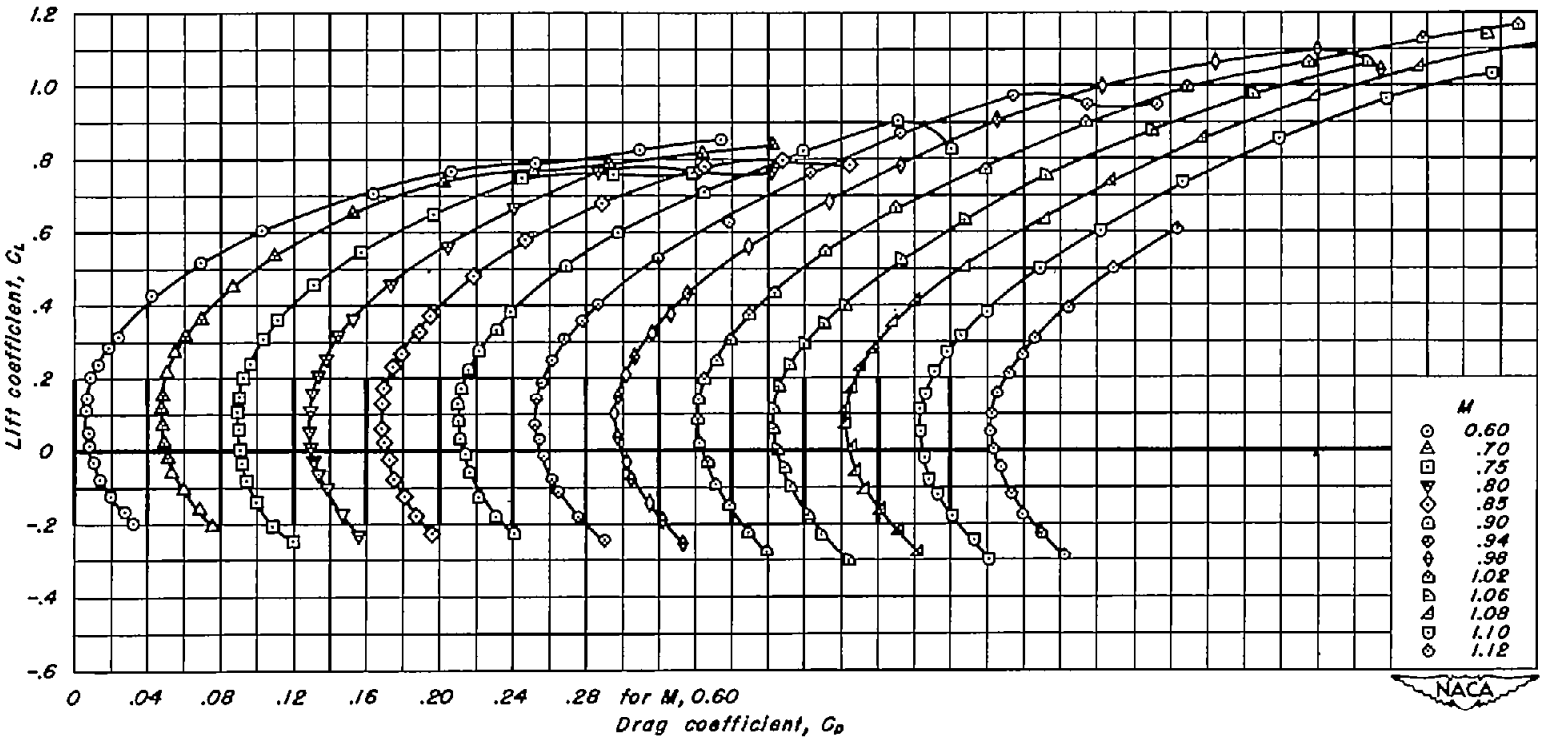

(j) A, 2; t/c, 0.04

Figure 8.- Continued.

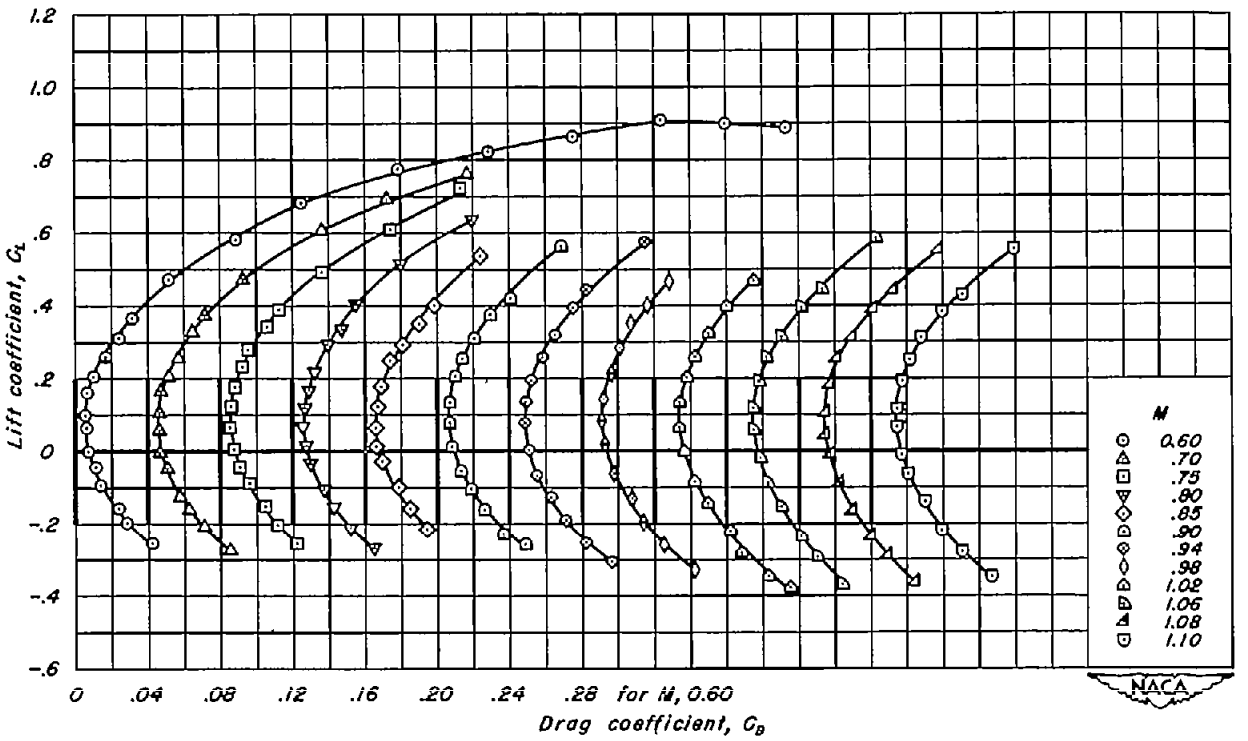

(k) A, 2; t/c, 0.02

Figure 8.- Continued.

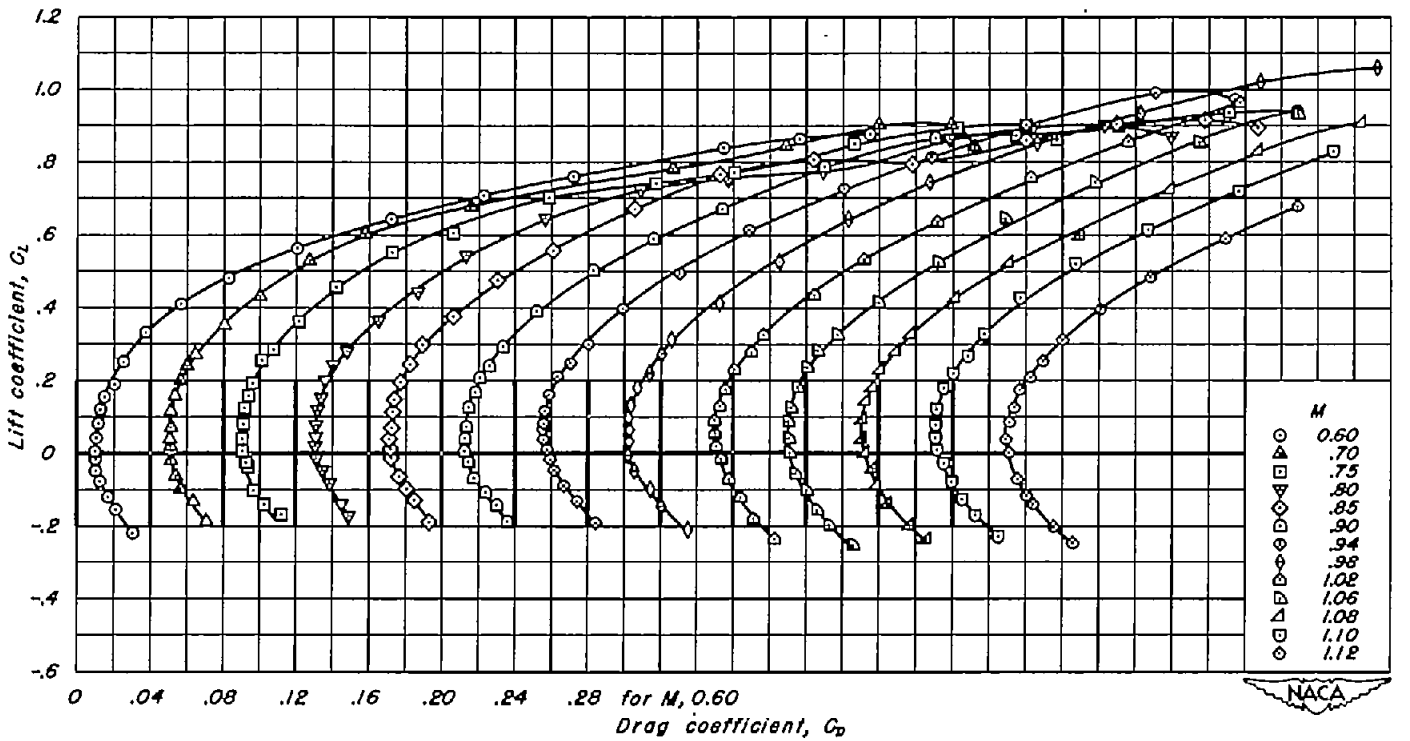

(1) A,1.5; t/c, 0.06

Figure 8.- Continued.

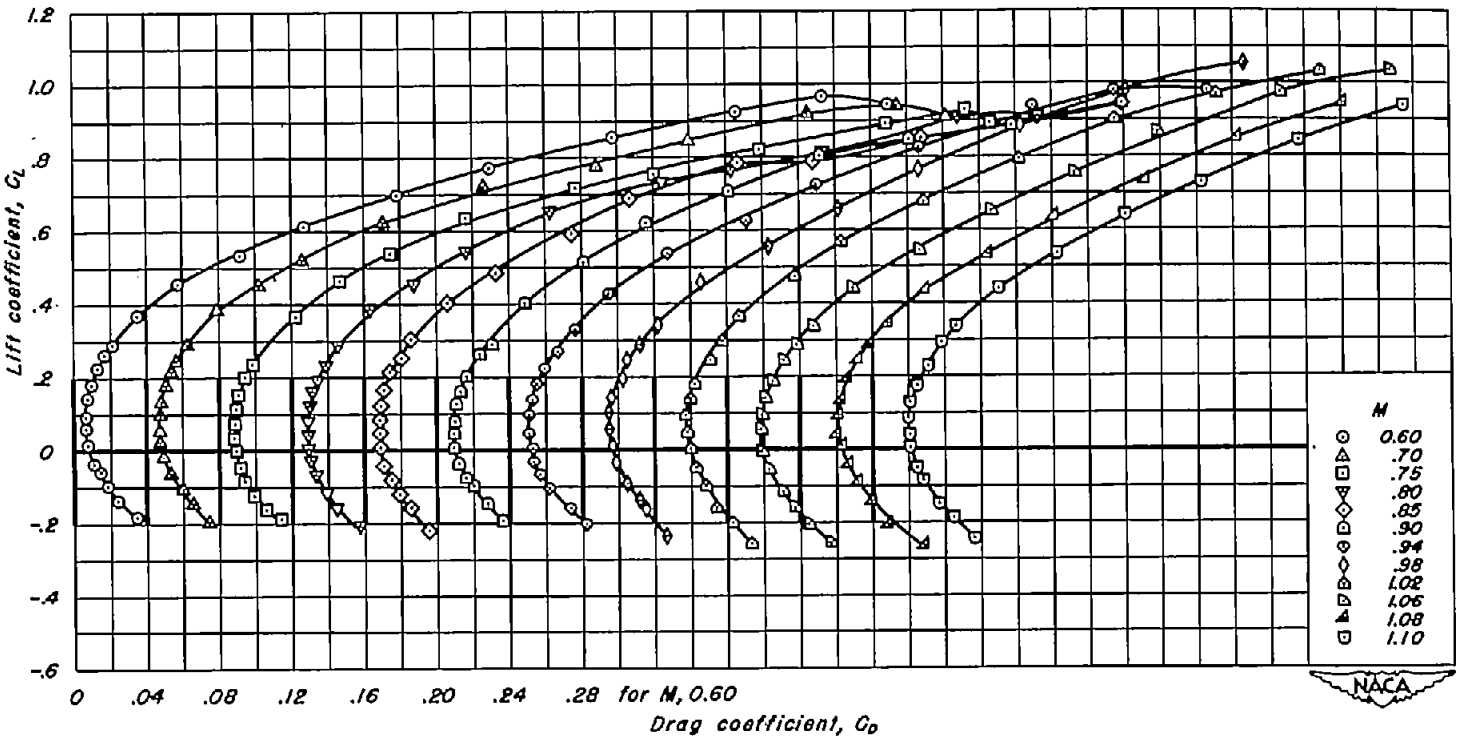

(m) A,1.5; t/c, 0.04

Figure 8.- Continued.

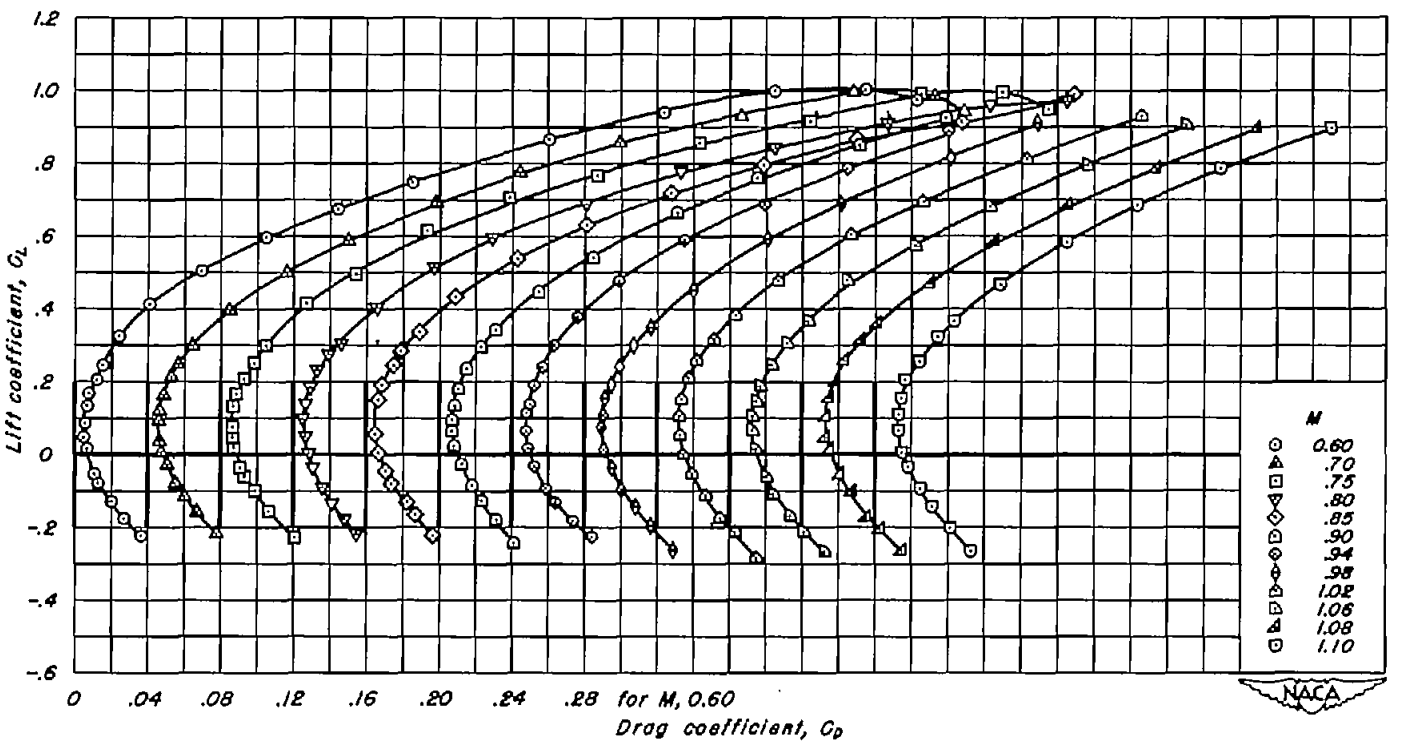

(n) A,1.5; t/c, 0.02

Figure 8.- Continued.

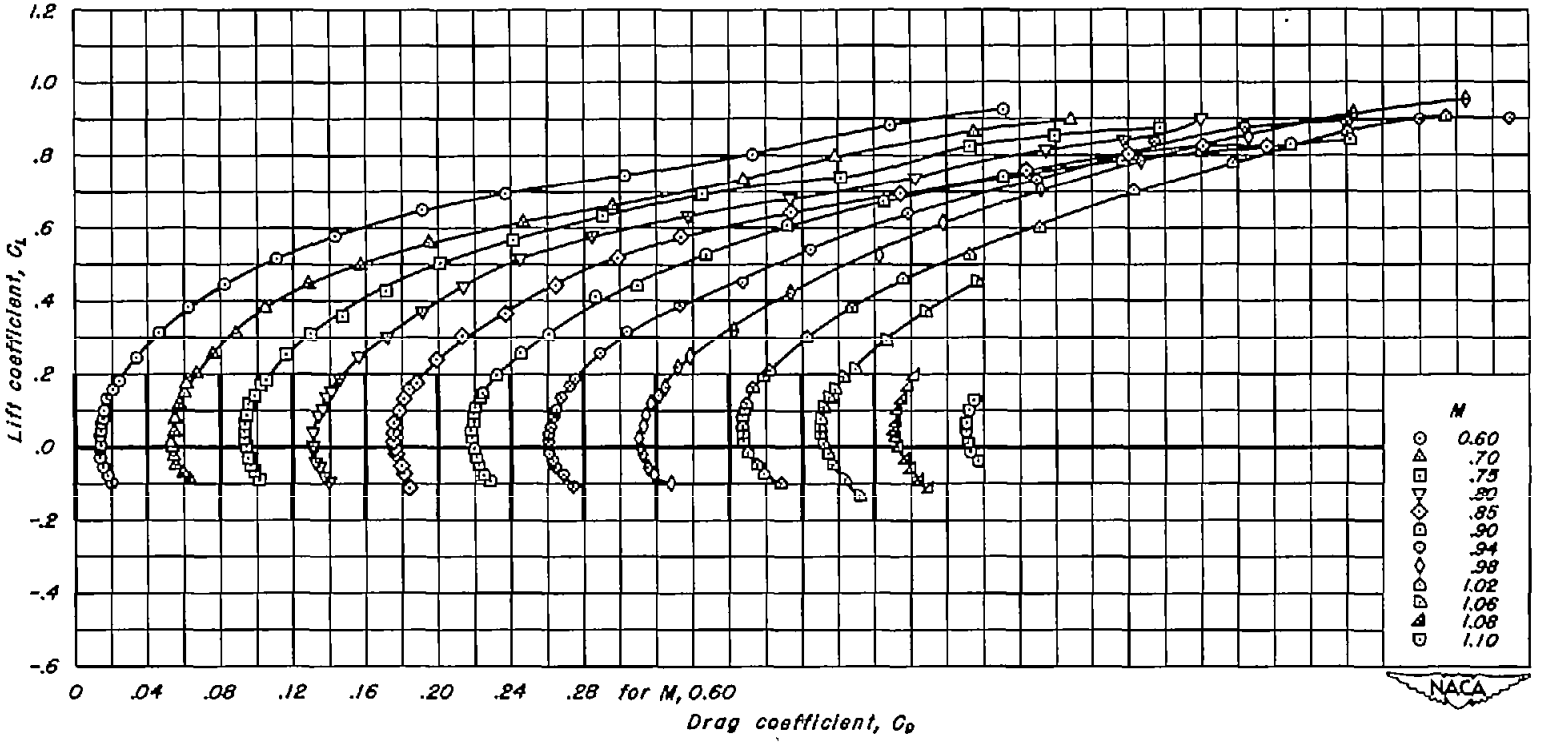

(a) A, 1; t/c, 0.10.

Figure 8.- Continued.

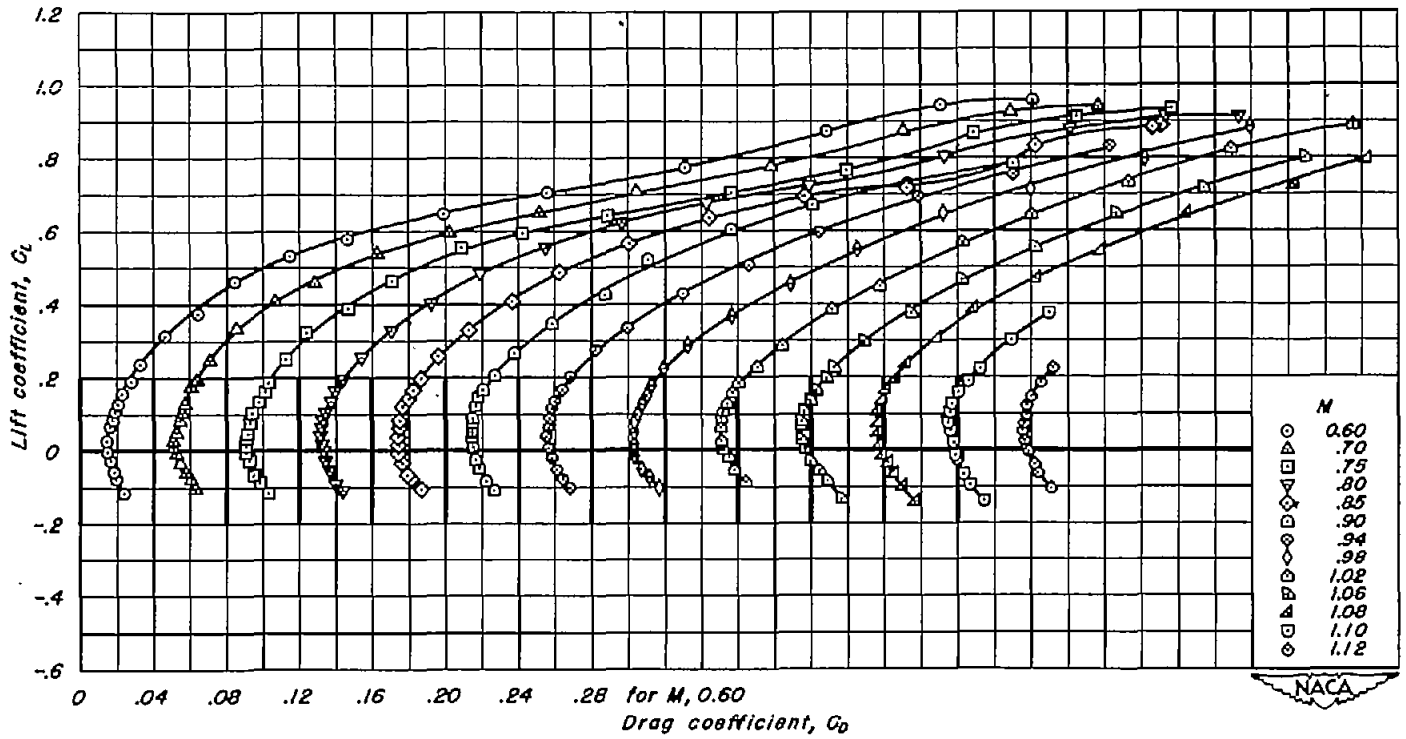

(p) A, 1; t/c, 0.08

Figure 8.- Continued.

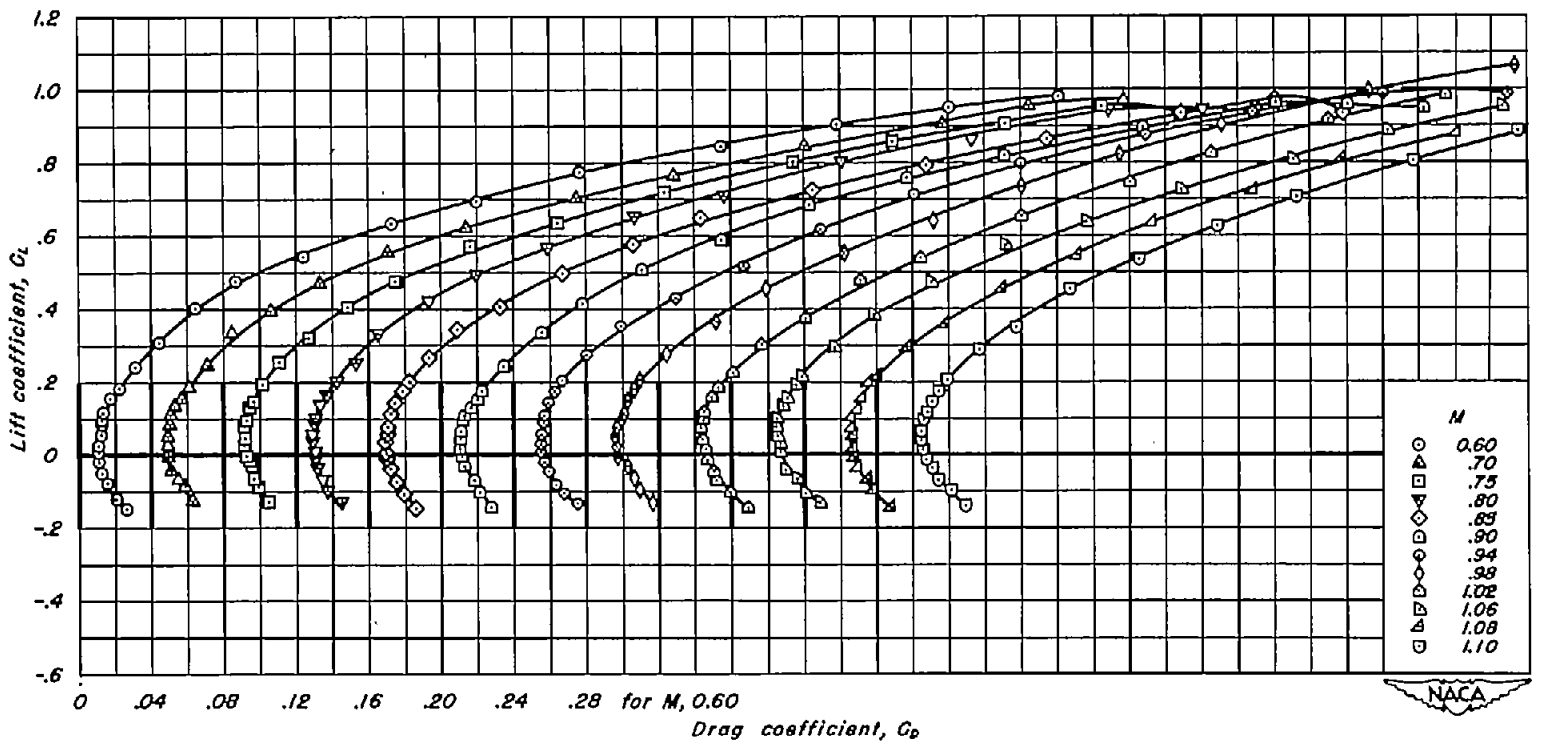

(q) A, l_1 t/c, 0.06

Figure 8.- Continued.

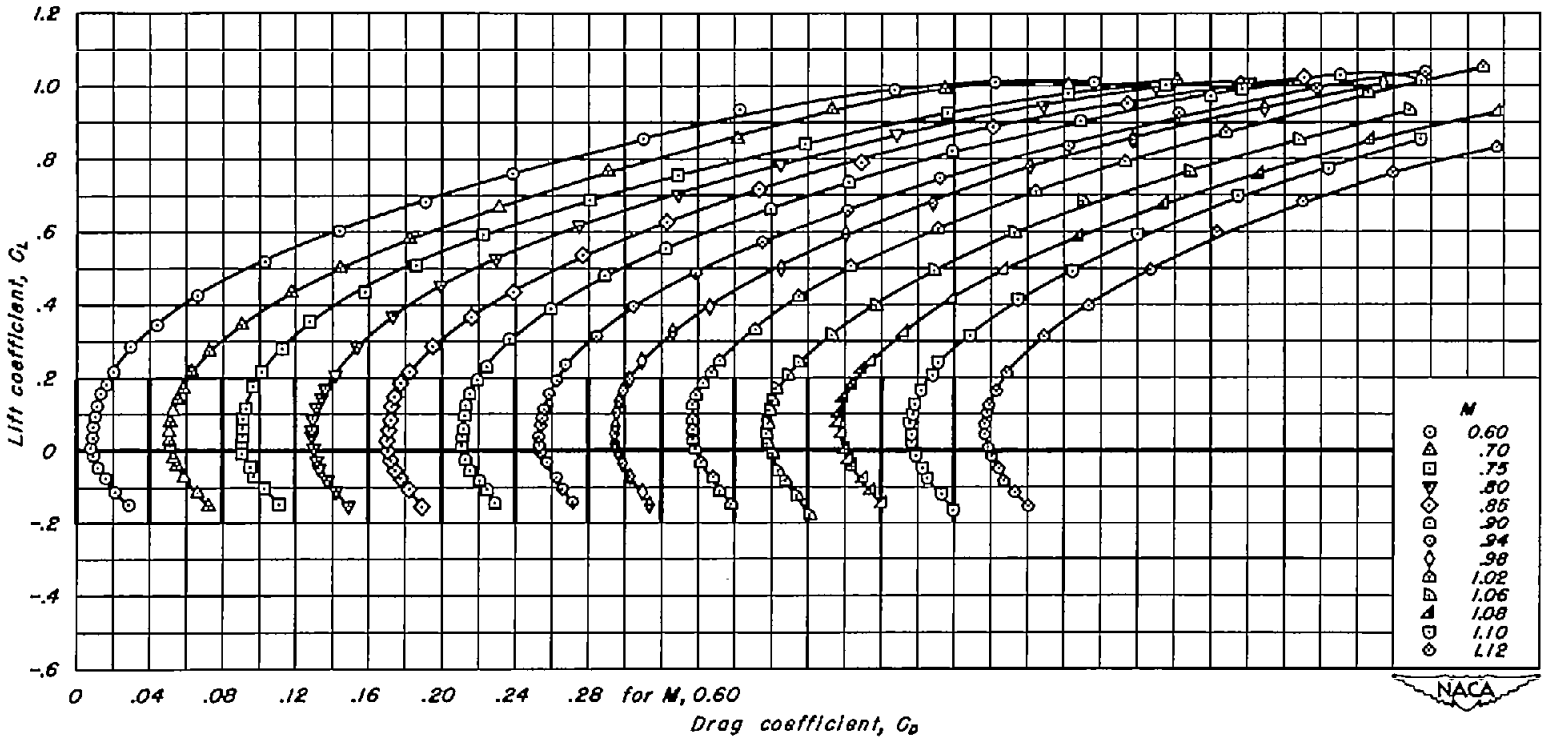

(r) A, I; t/c, 0.04

Figure 8.- Continued.

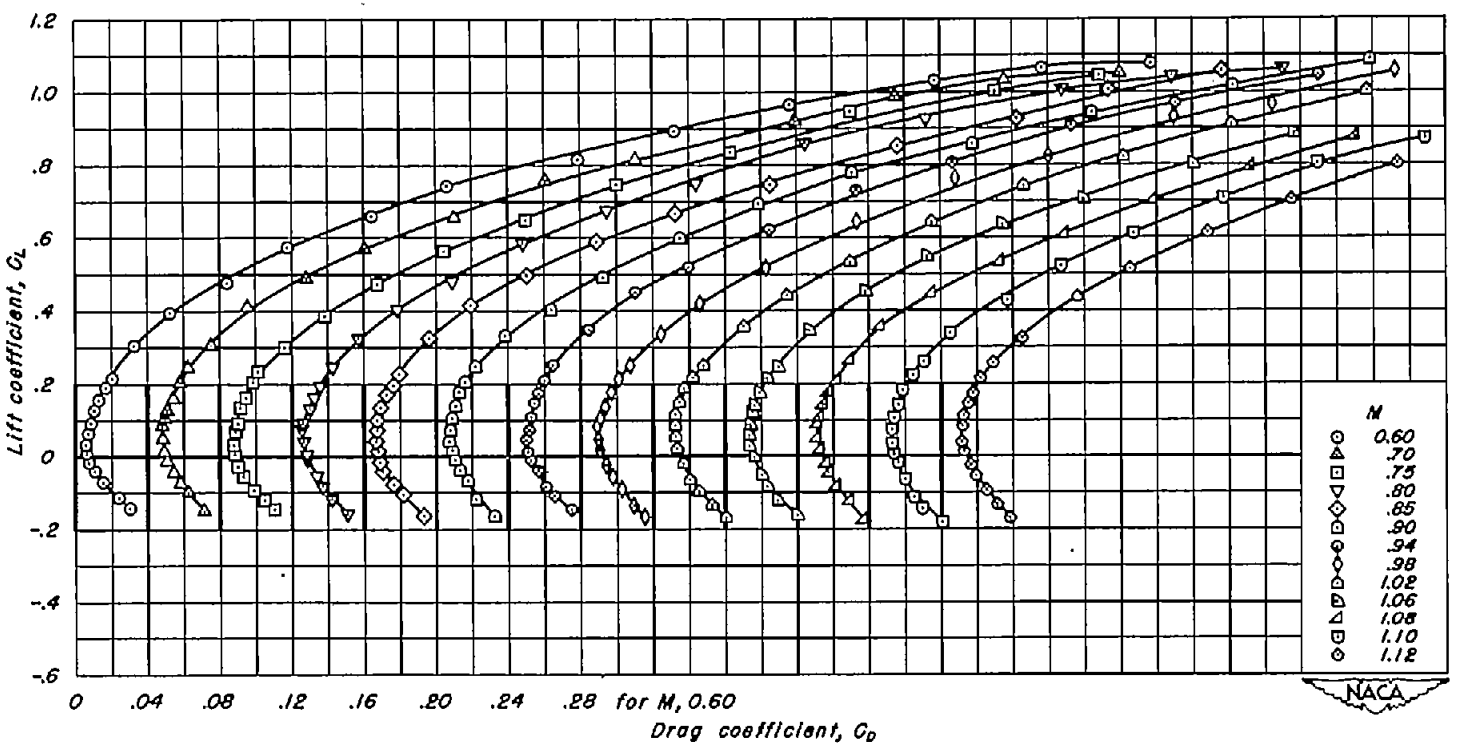

(s) A, 1; t/c, 0.02

Figure 8.- Concluded.

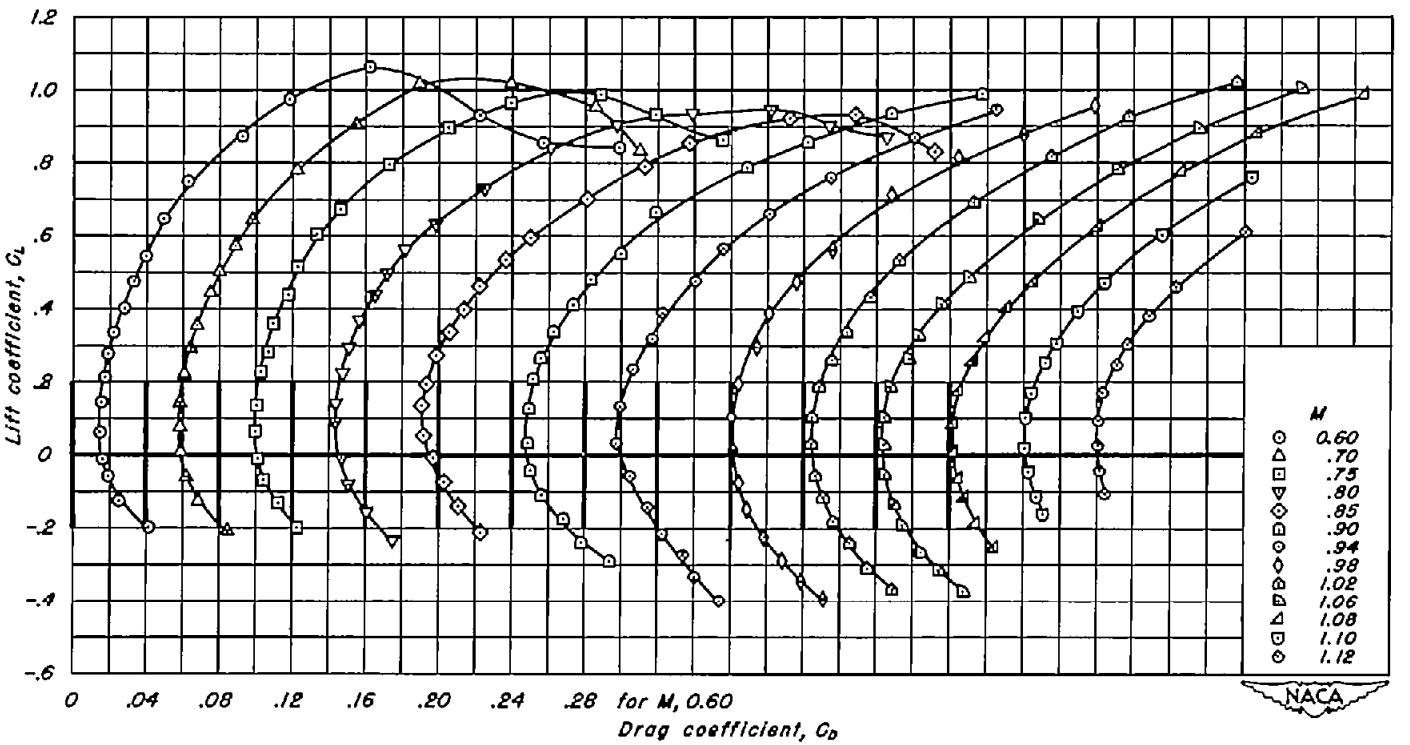

(a) A, 4; t/c, 0.10

Figure 9.—The variation of drag coefficient with lift coefficient for the wings with NACA 63A4xx sections.

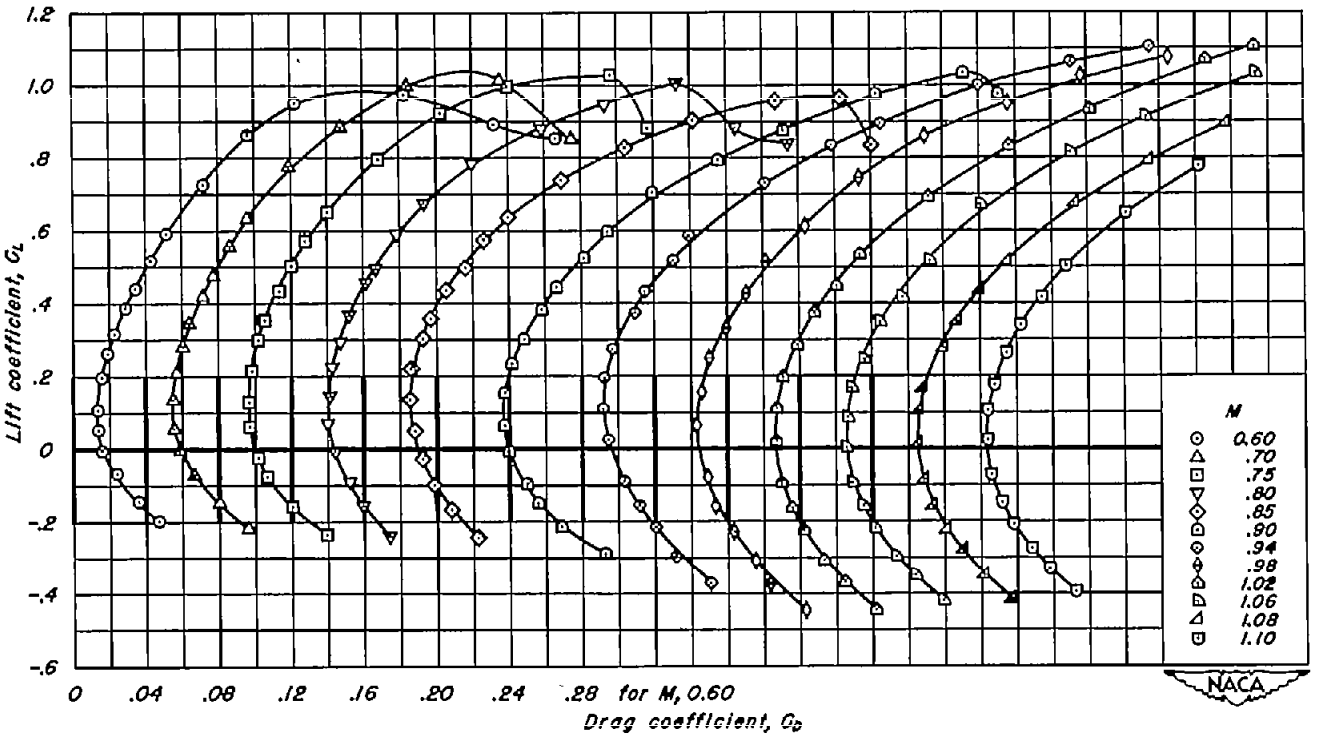

(b) A, 4; t/c, 0.08

Figure 9.- Continued.

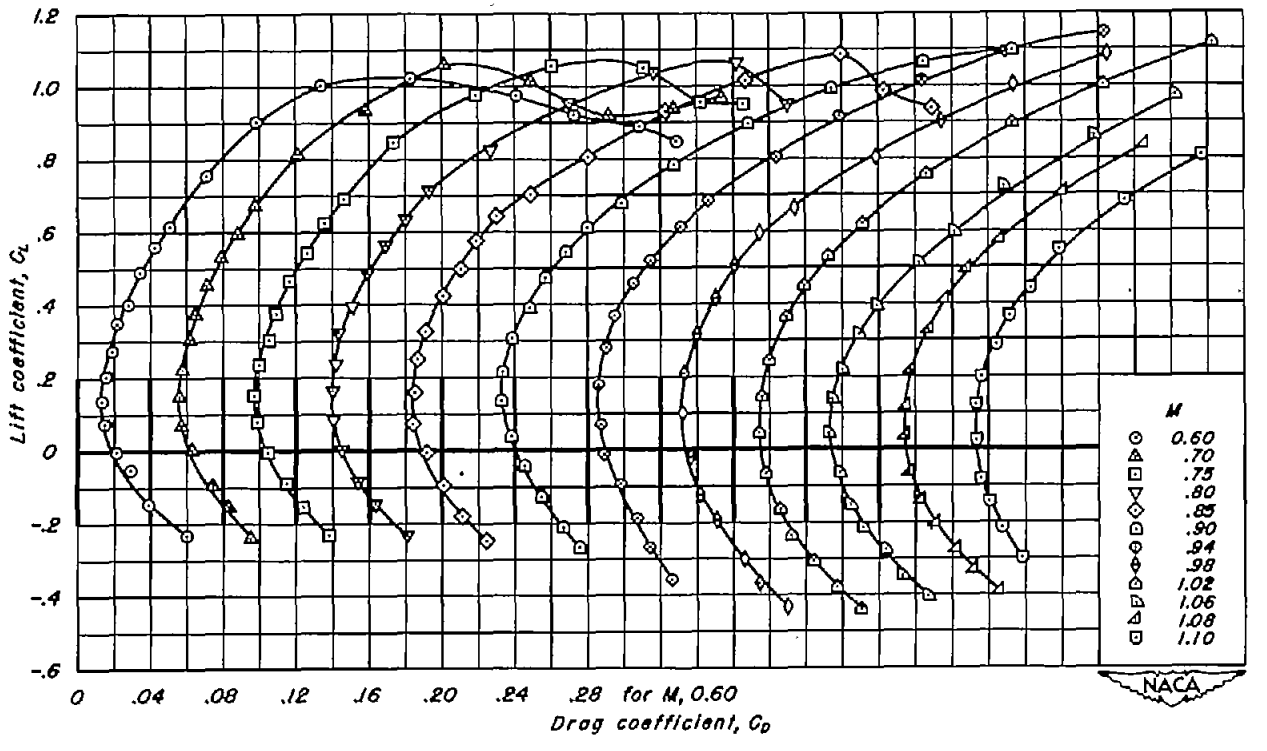

(c) A, 4; t/c, 0.06

Figure 9.- Continued.

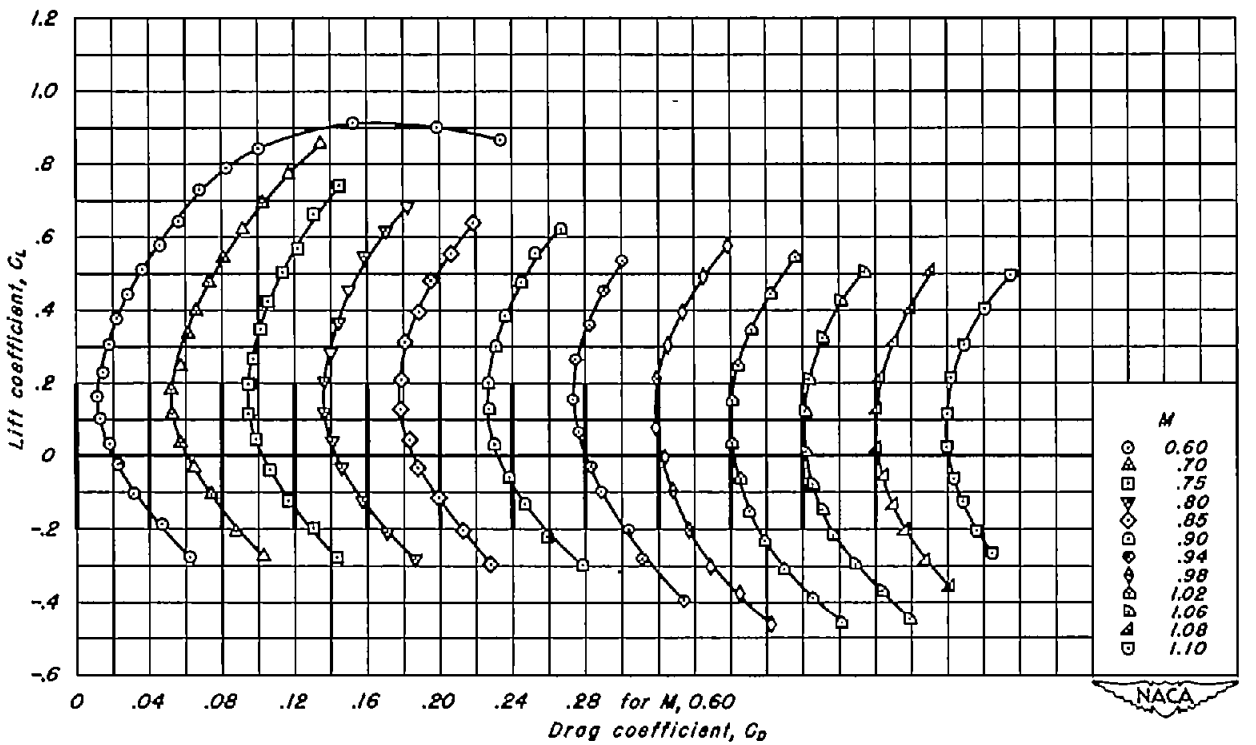

(d) A, 4; t/c, 0.04

Figure 9.- Continued.

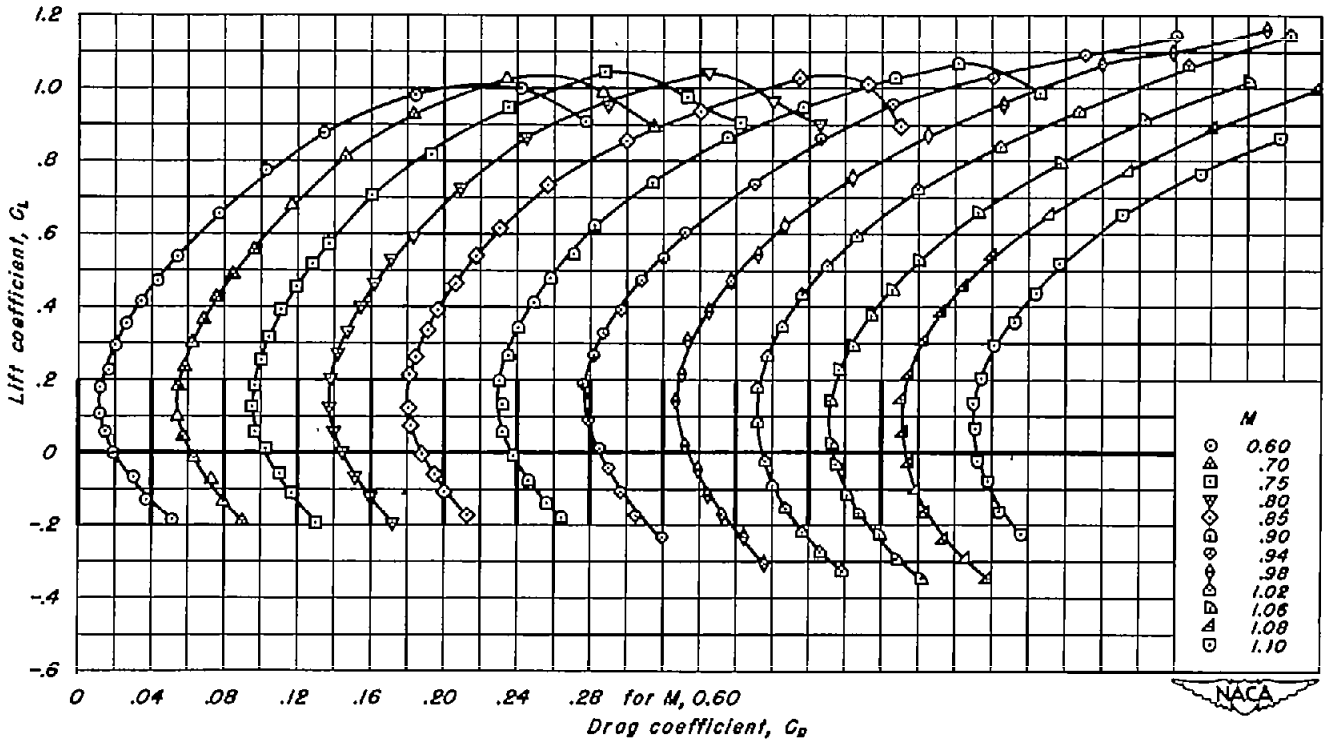

(e) A, 3; t/c, 0.06

Figure 9.- Continued.

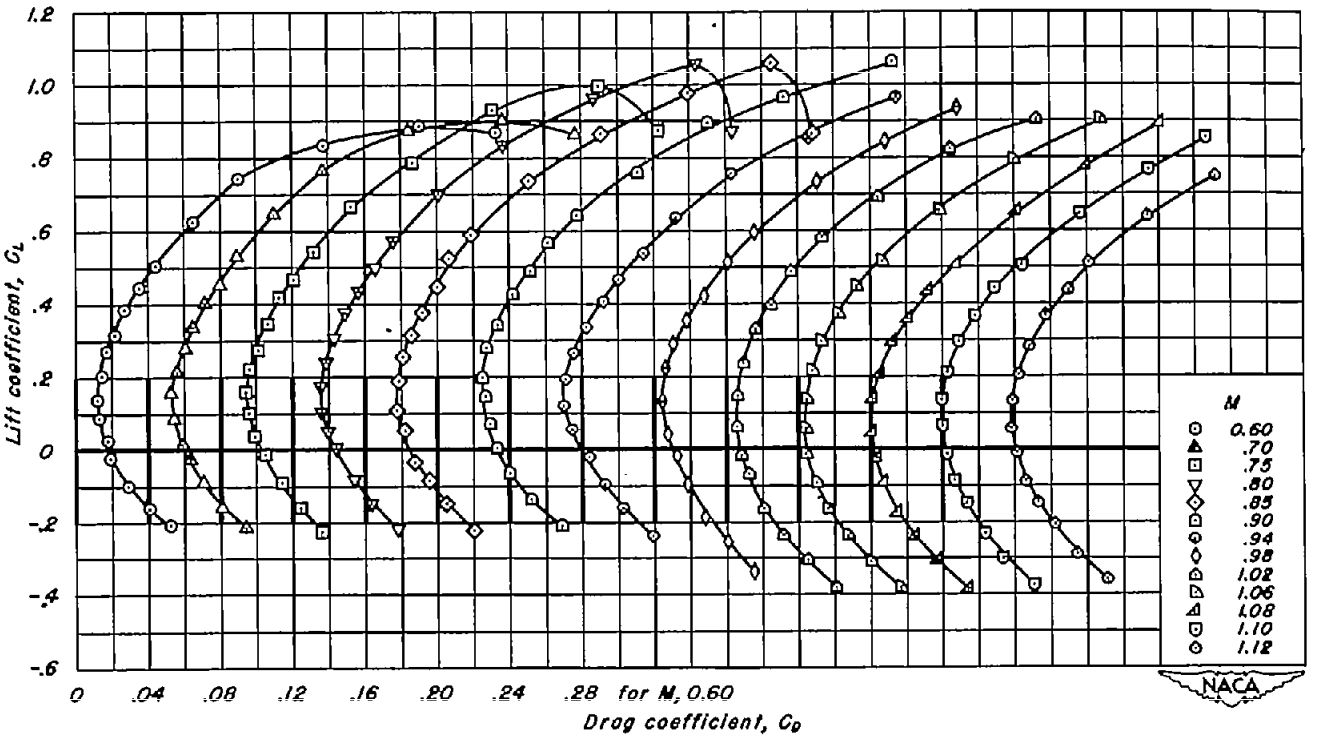

(f) A, 3; t/c, 0.04

Figure 9.- Continued.

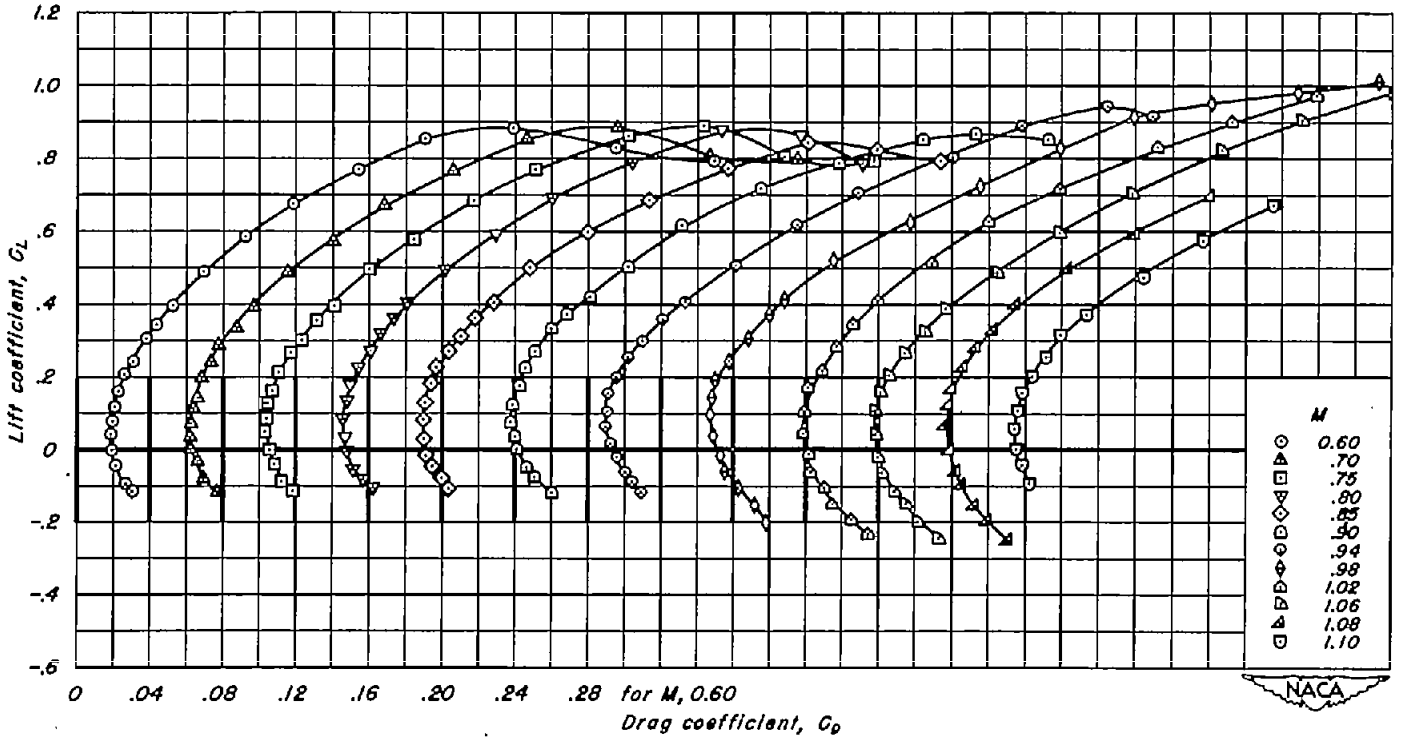

(g) A, 2; t/c, 0.10

Figure 9.- Continued.

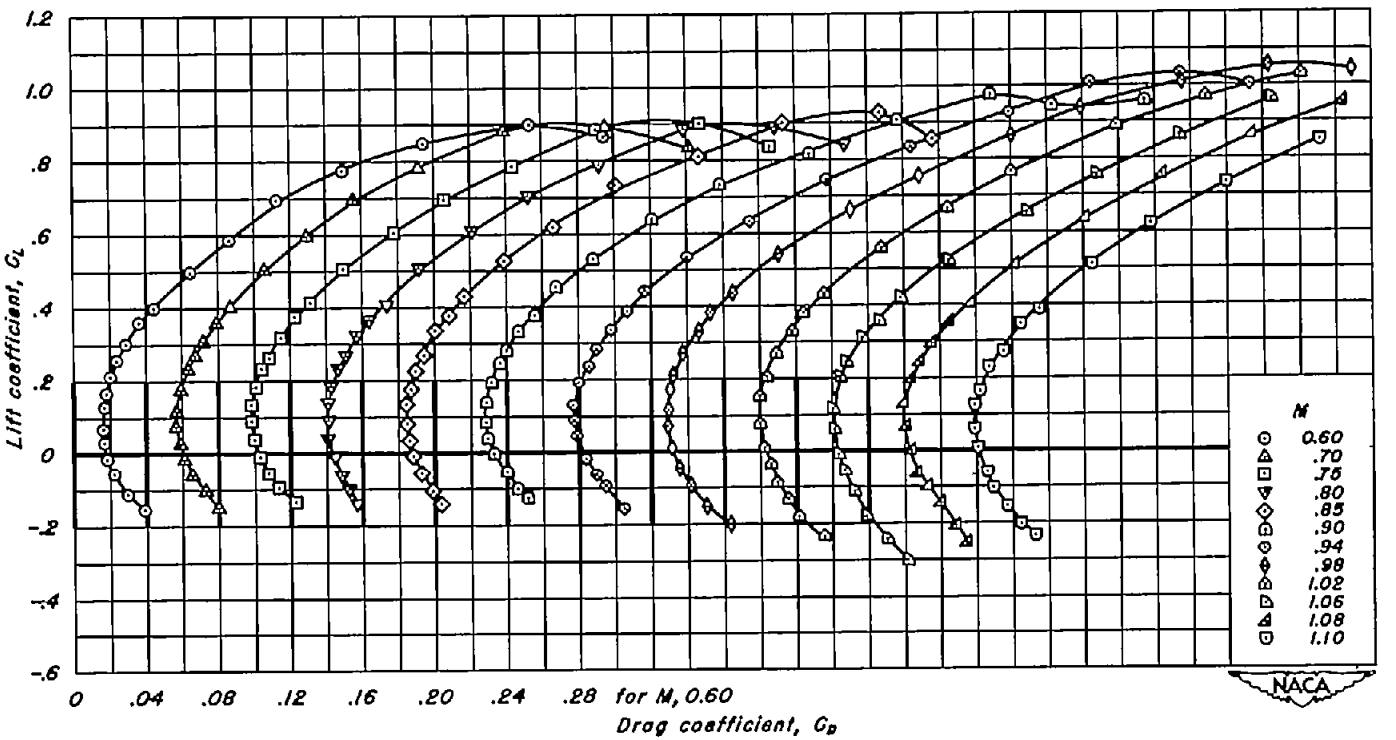

(h) A, 2; t/c, 0.08

Figure 9.- Continued.

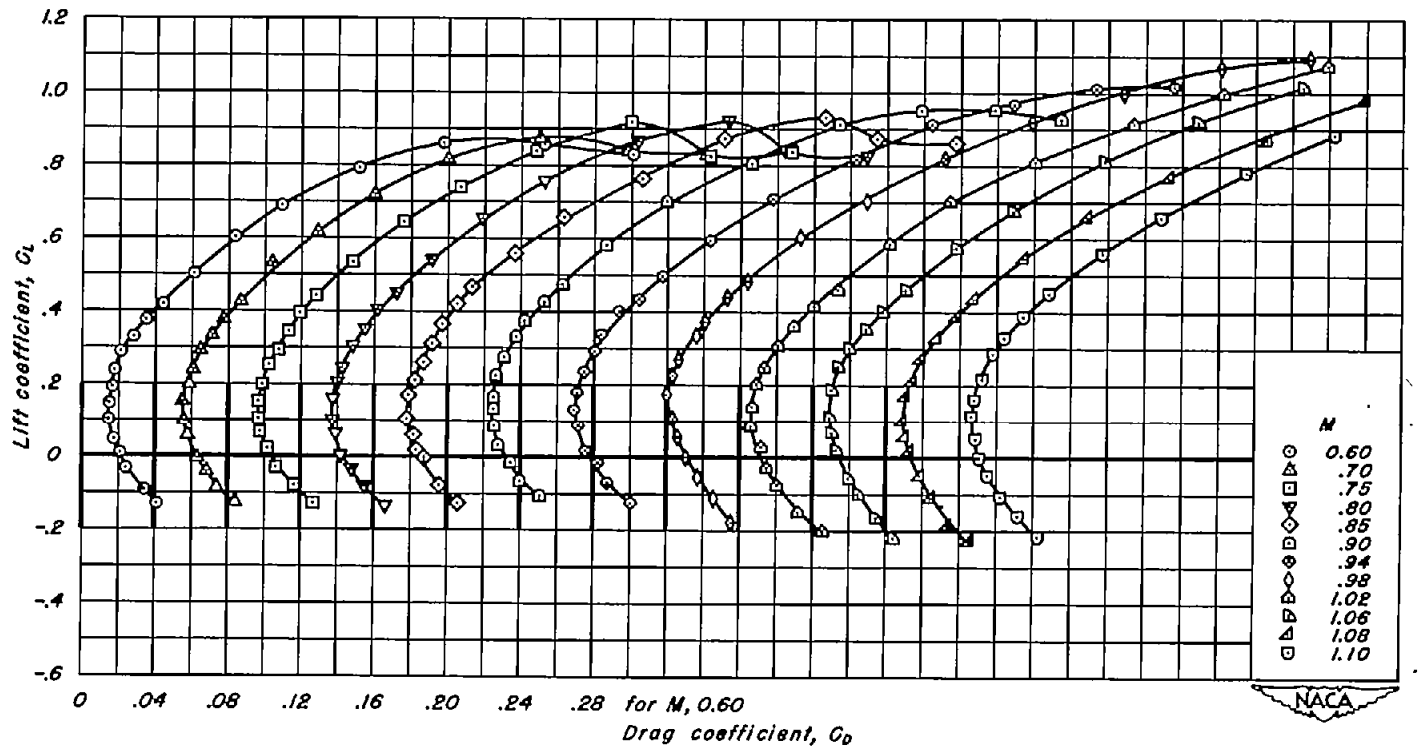

(i) A, 2; t/c, 0.06

Figure 9.- Continued.

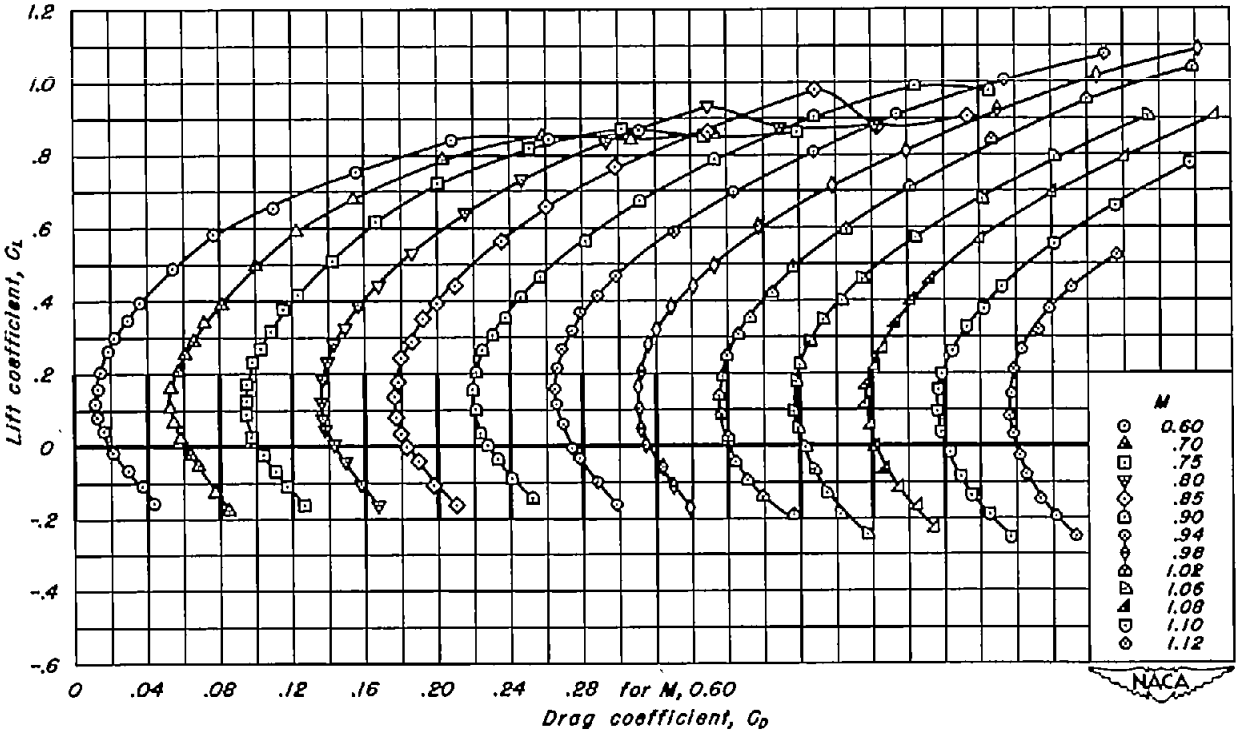

(j) A, 2; t/c, 0.04

Figure 9.- Continued.

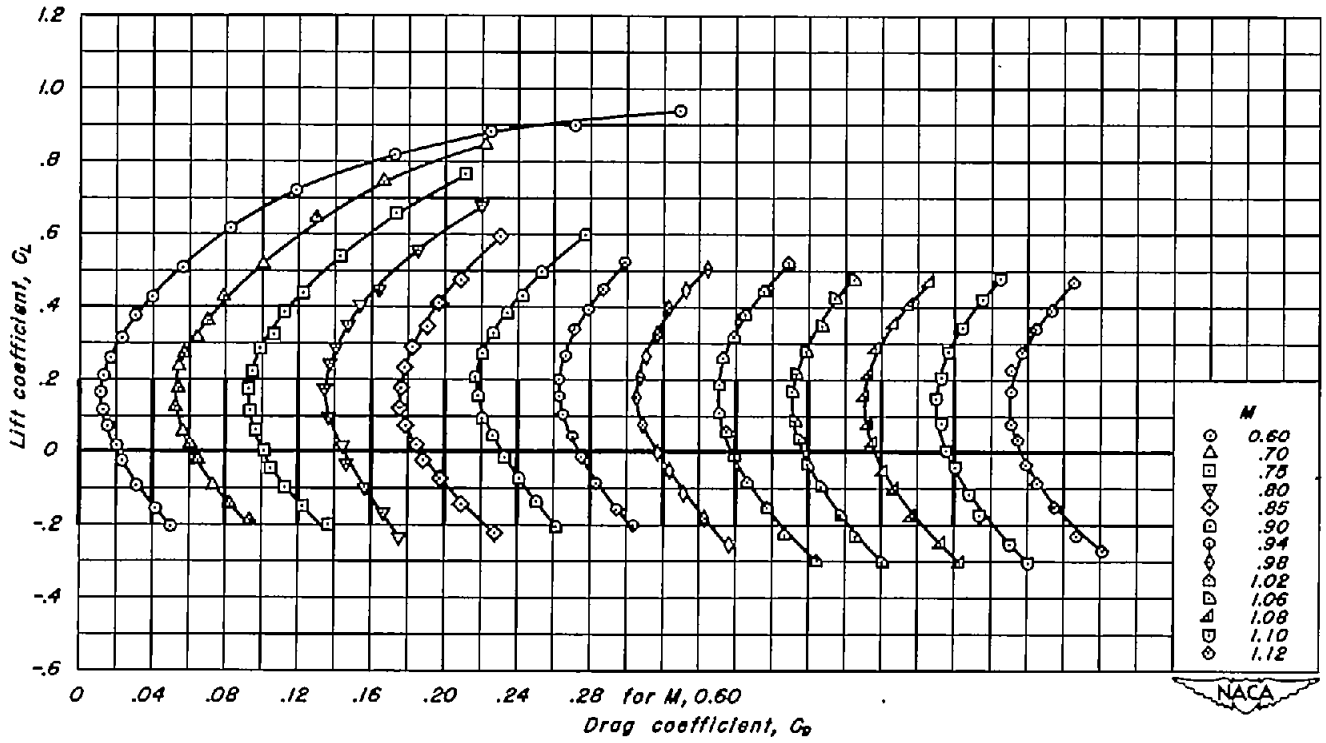

(k) A, 2; t/c, 0.02

Figure 9.- Continued.

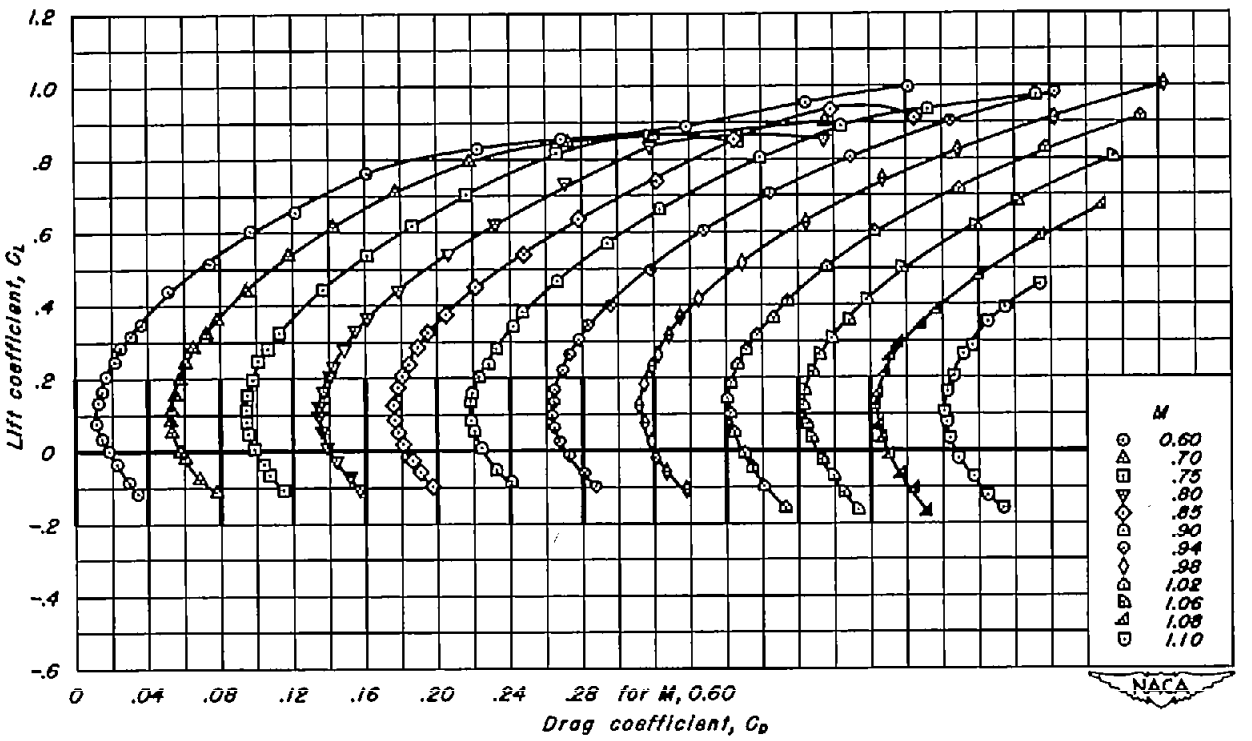

(l) A,1.5; t/c, 0.06

Figure 9.- Continued.

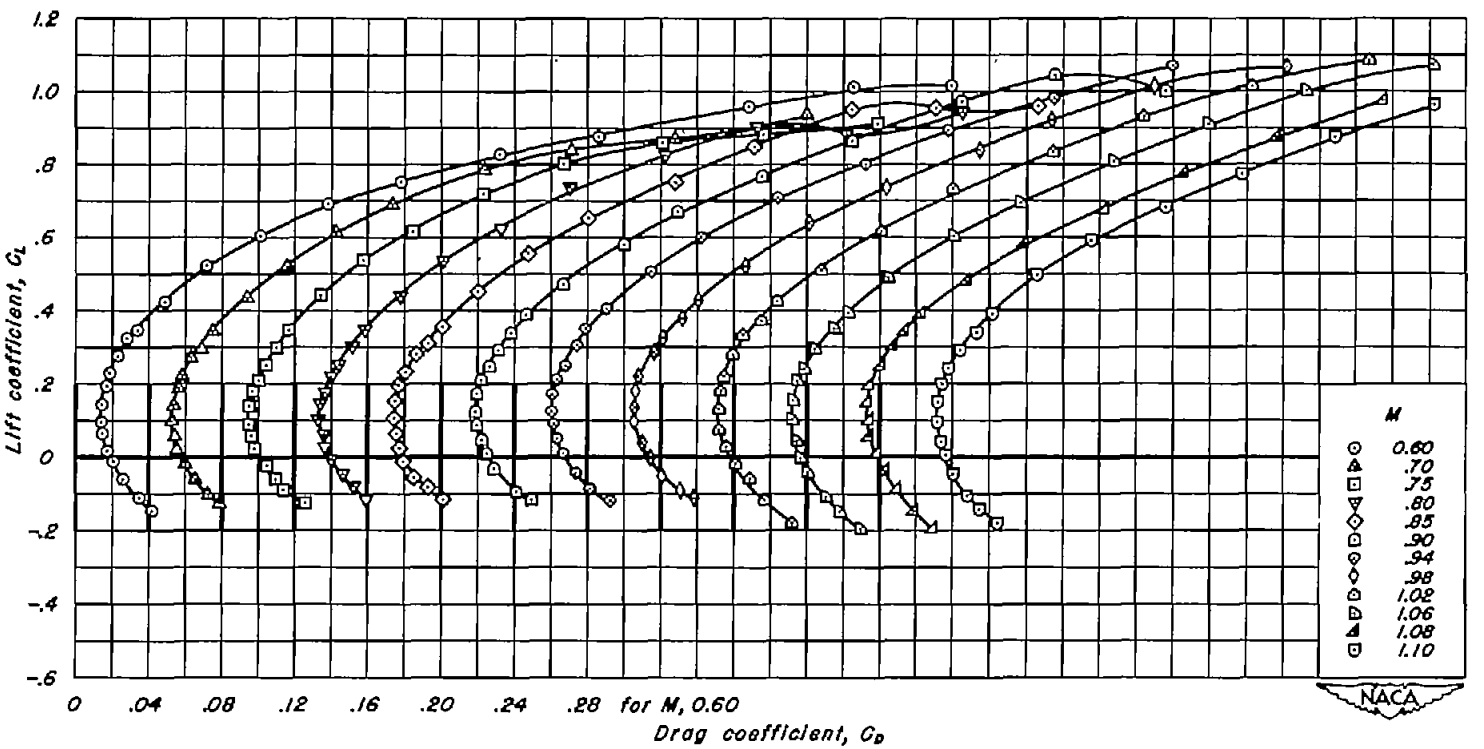

(m) A,1.5; t/c, 0.04

Figure 9.- Continued.

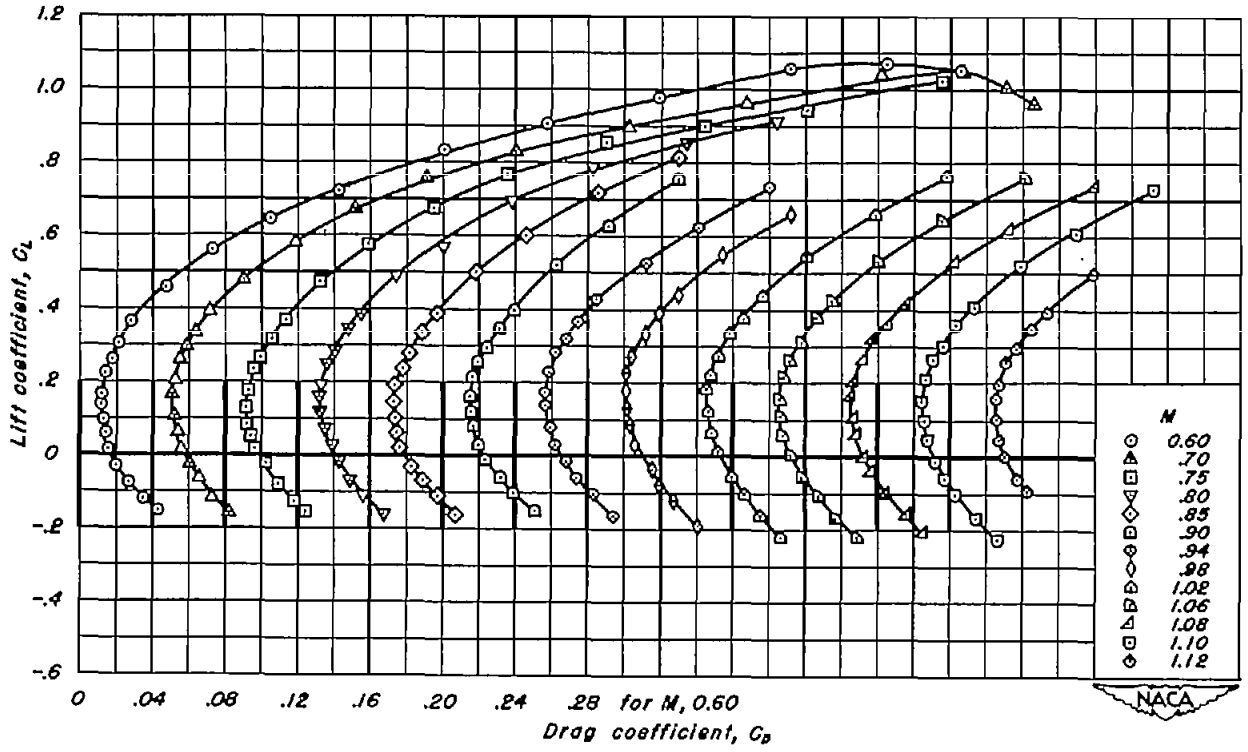

(n) A, 1.5; t/c, 0.02

Figure 9.- Continued.

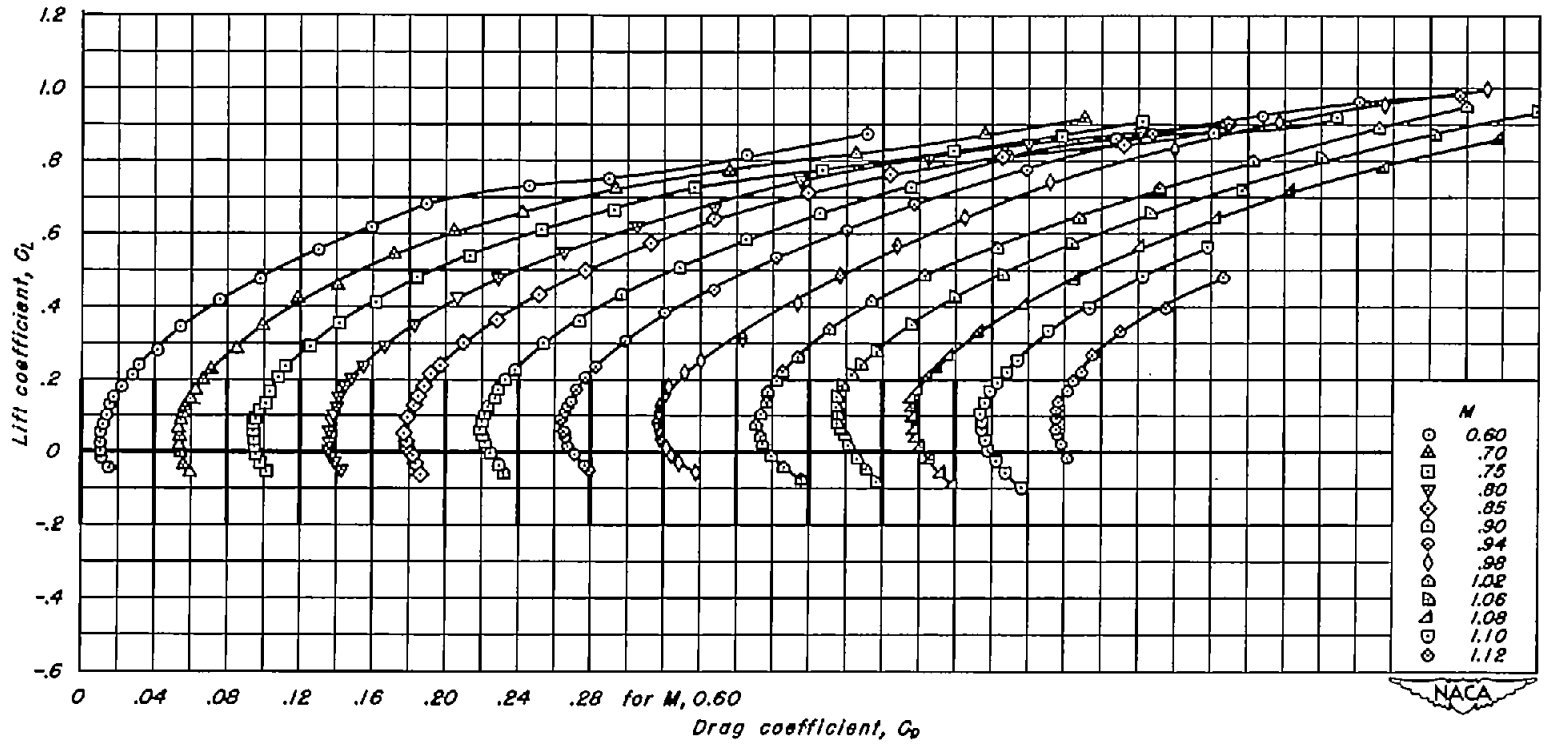

(o) A, 1; t/c, 0.10

Figure 9.- Continued.

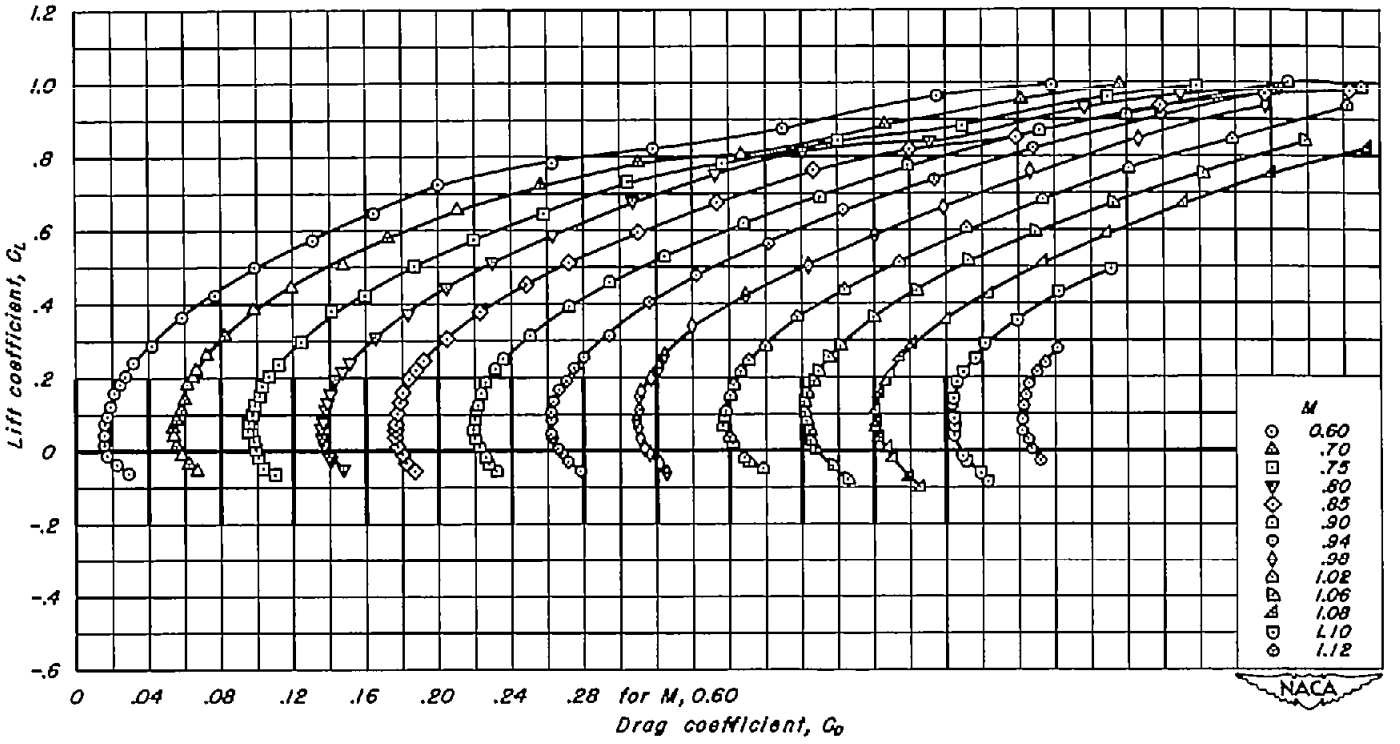

(p) A, 1; t/c, 0.08

Figure 9.- Continued.

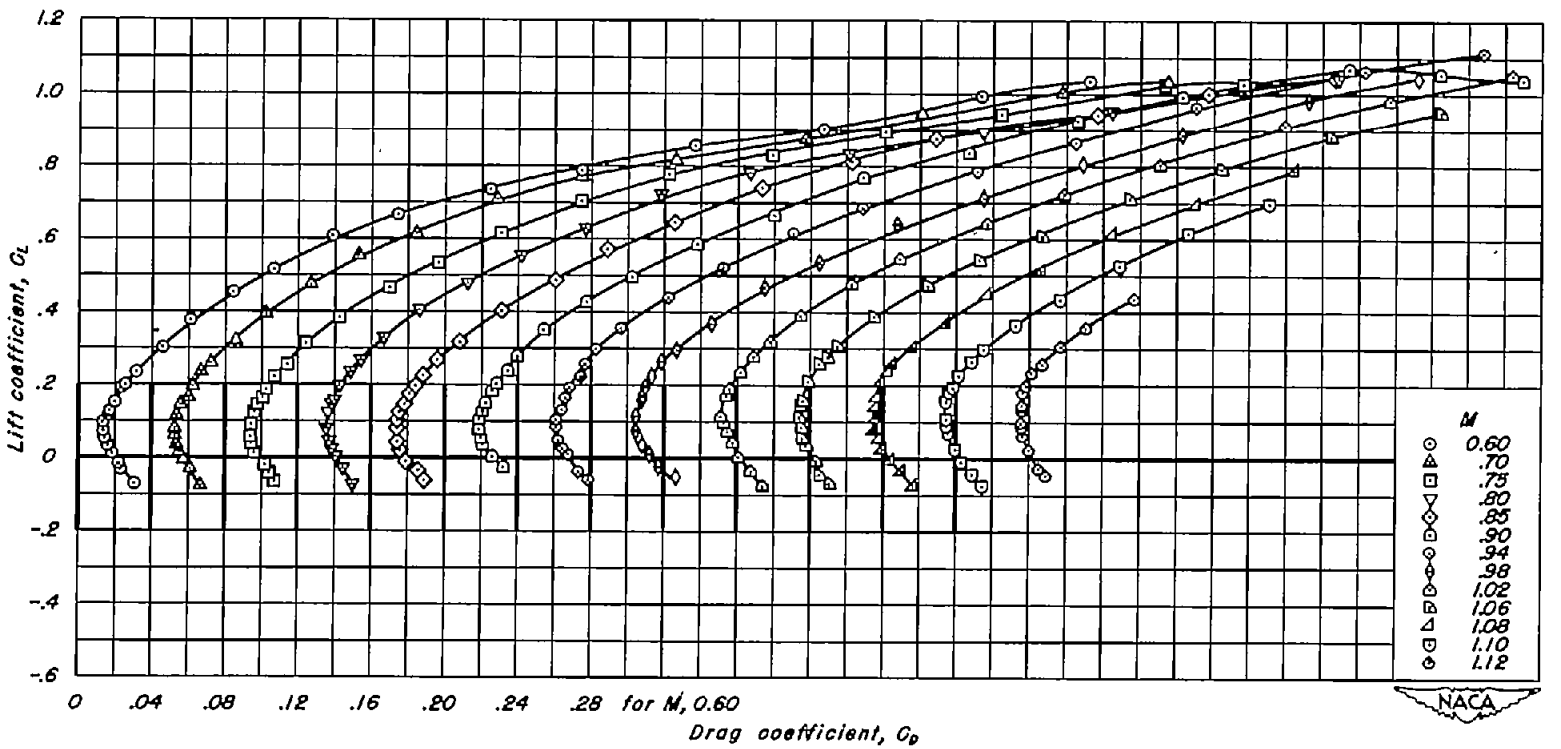

(q) A, 1; t/c, 0.06

Figure 9.- Continued.

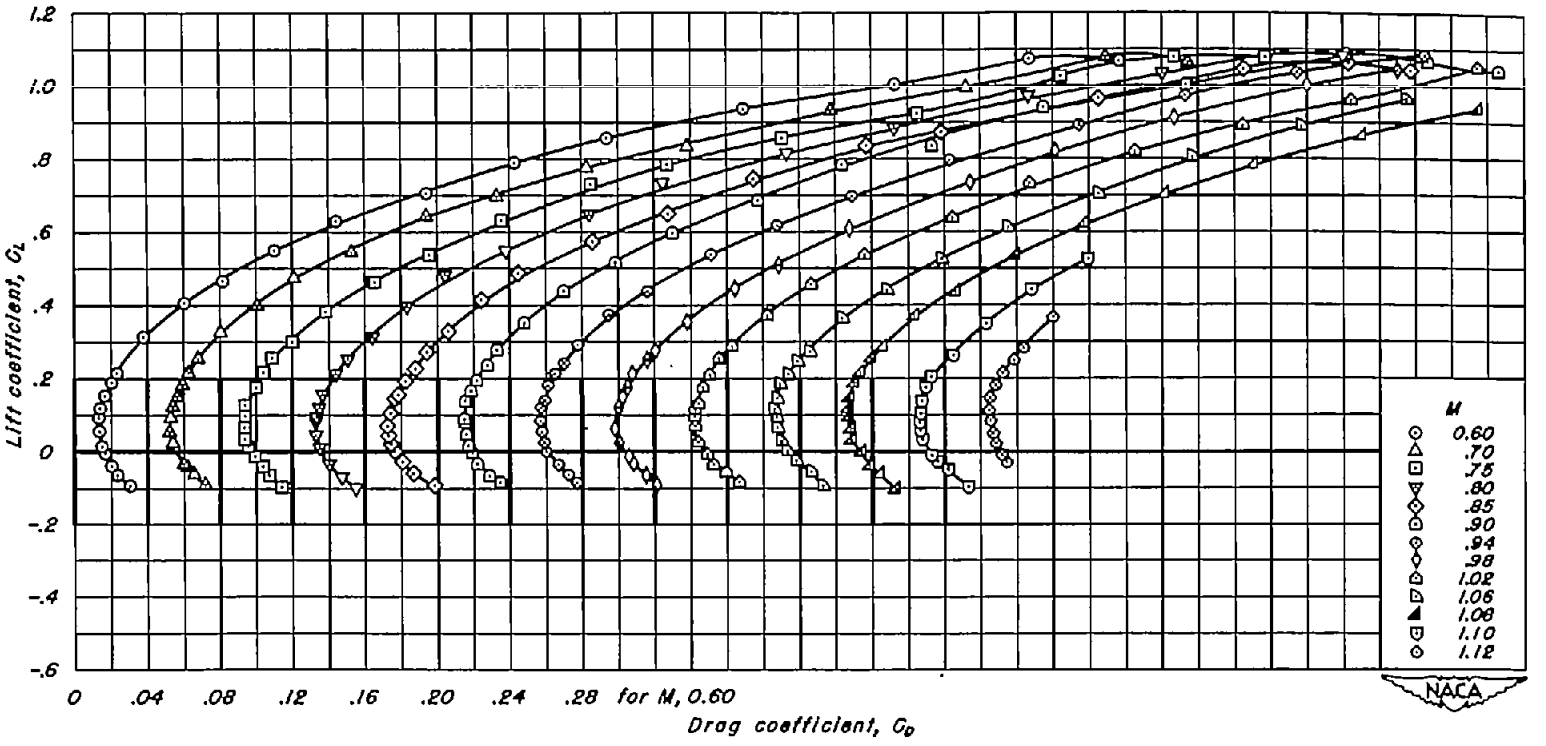

(r) A, I; t/c, 0.04

Figure 9.- Continued.

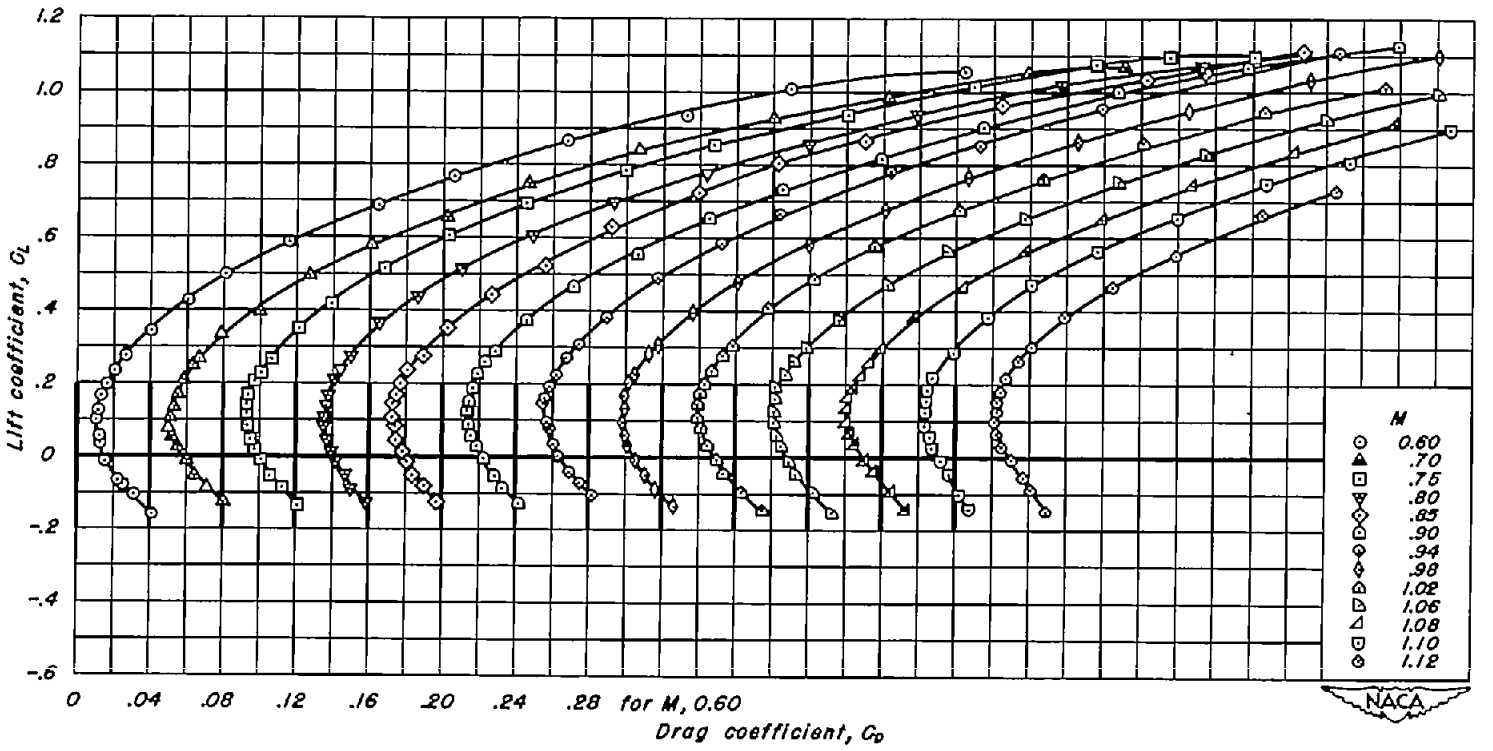

(s) A, 1; t/c, 0.02

Figure 9.- Concluded.

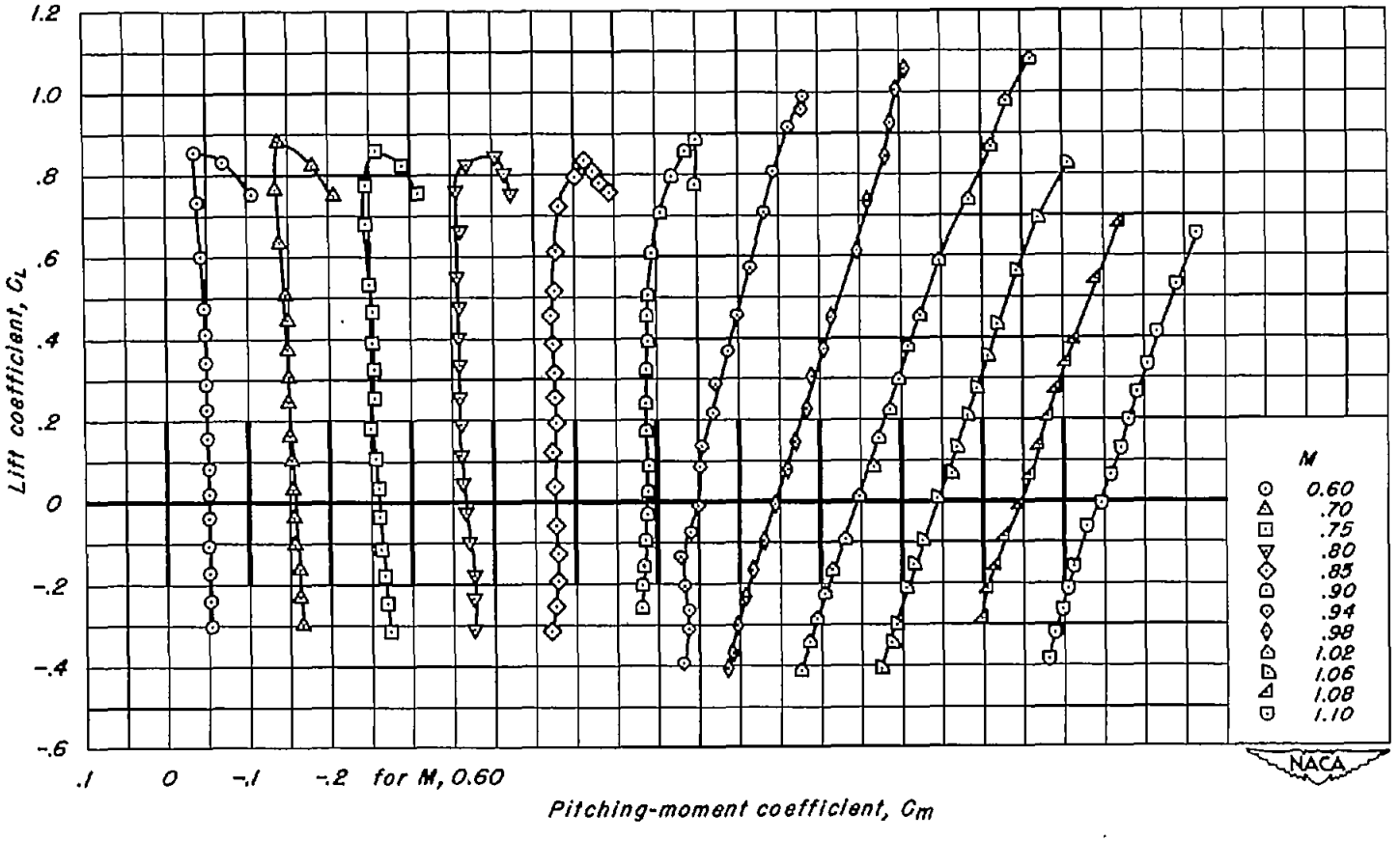

(a) A, 4; t/c, 0.10

Figure 10.—The variation of pitching-moment coefficient with lift coefficient for the wings with NACA 63A2XX sections.

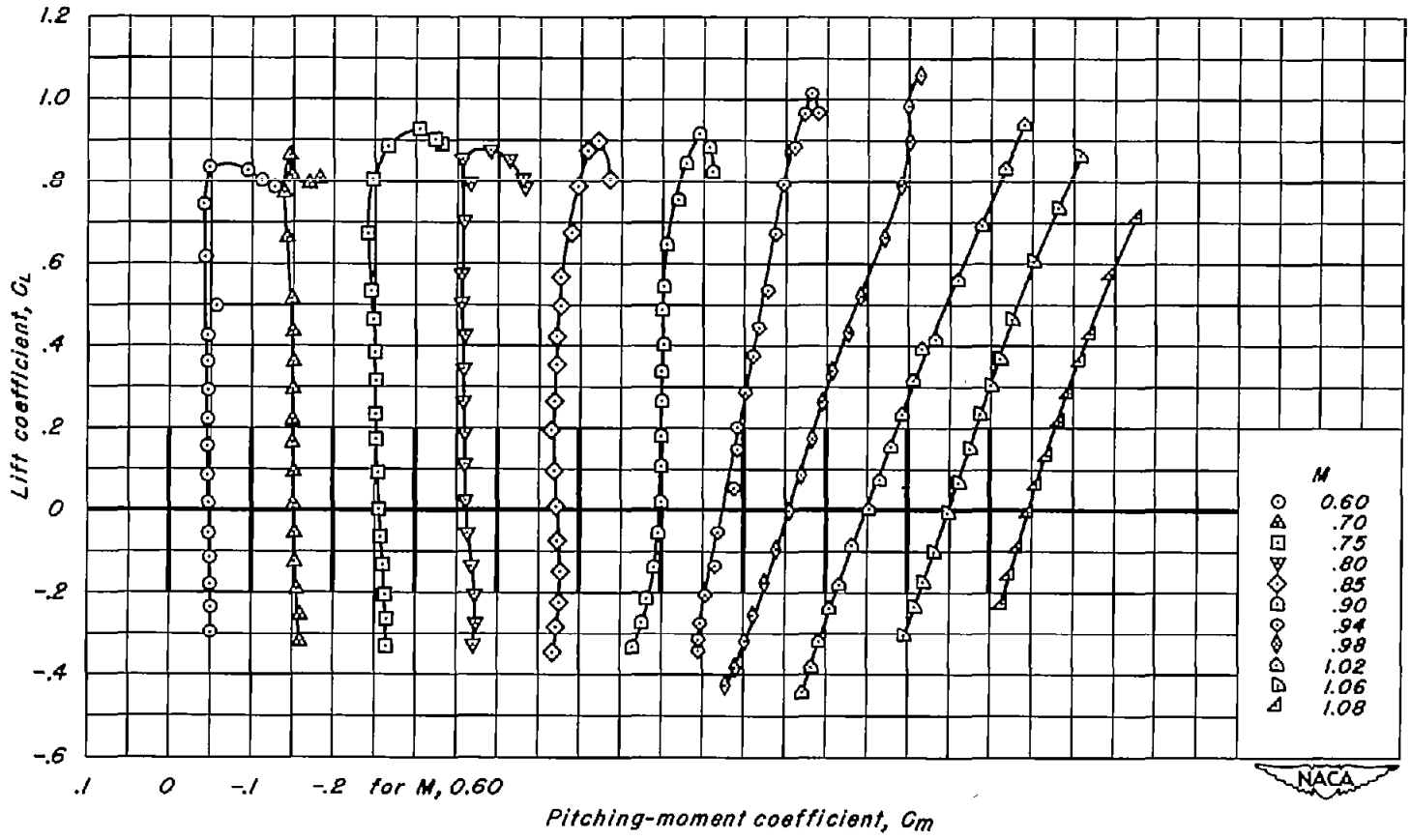

(b) A, 4; t/c, 0.08

Figure 10.- Continued.

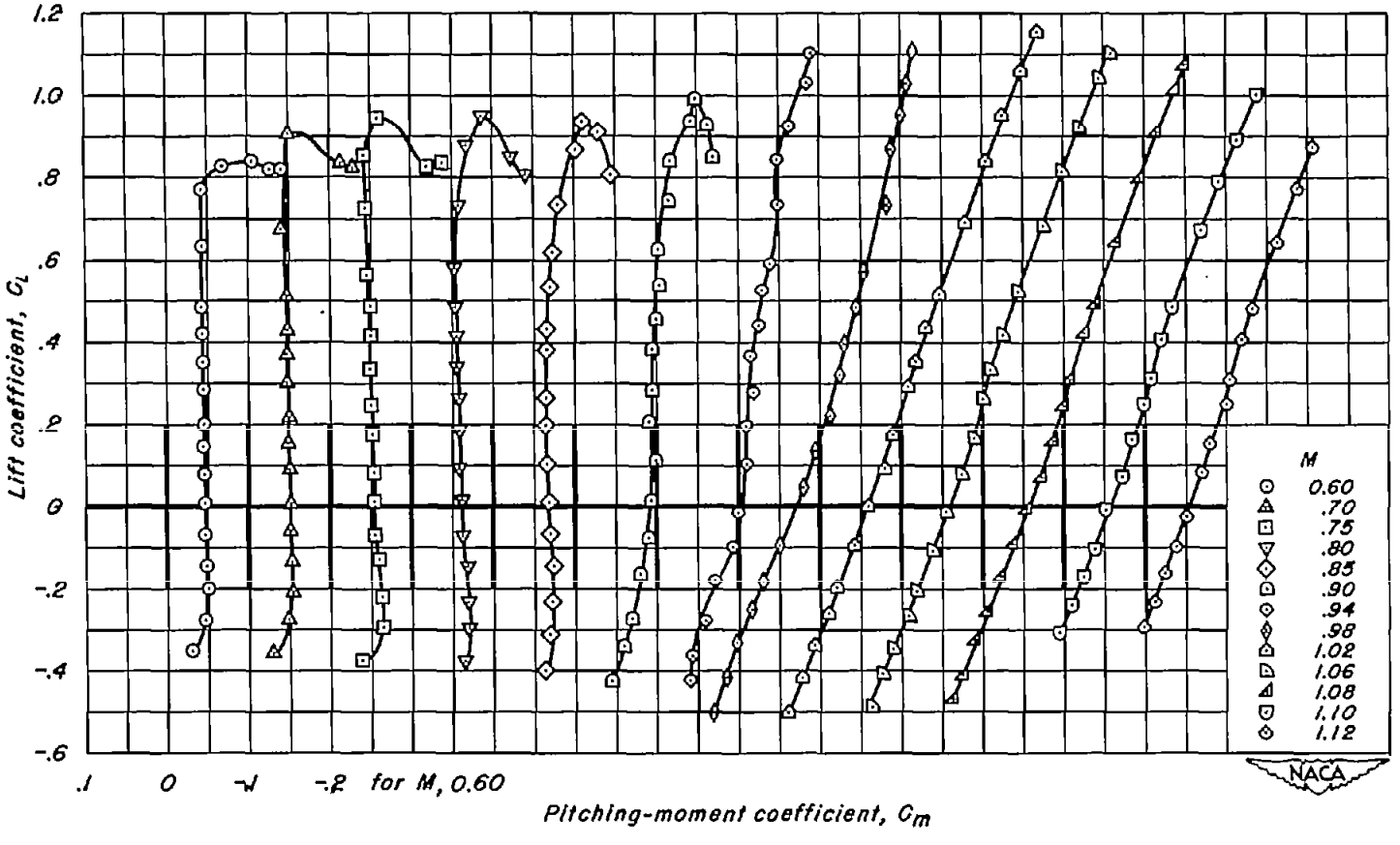

(c) A, 4; t/c, 0.06

Figure 10.- Continued.

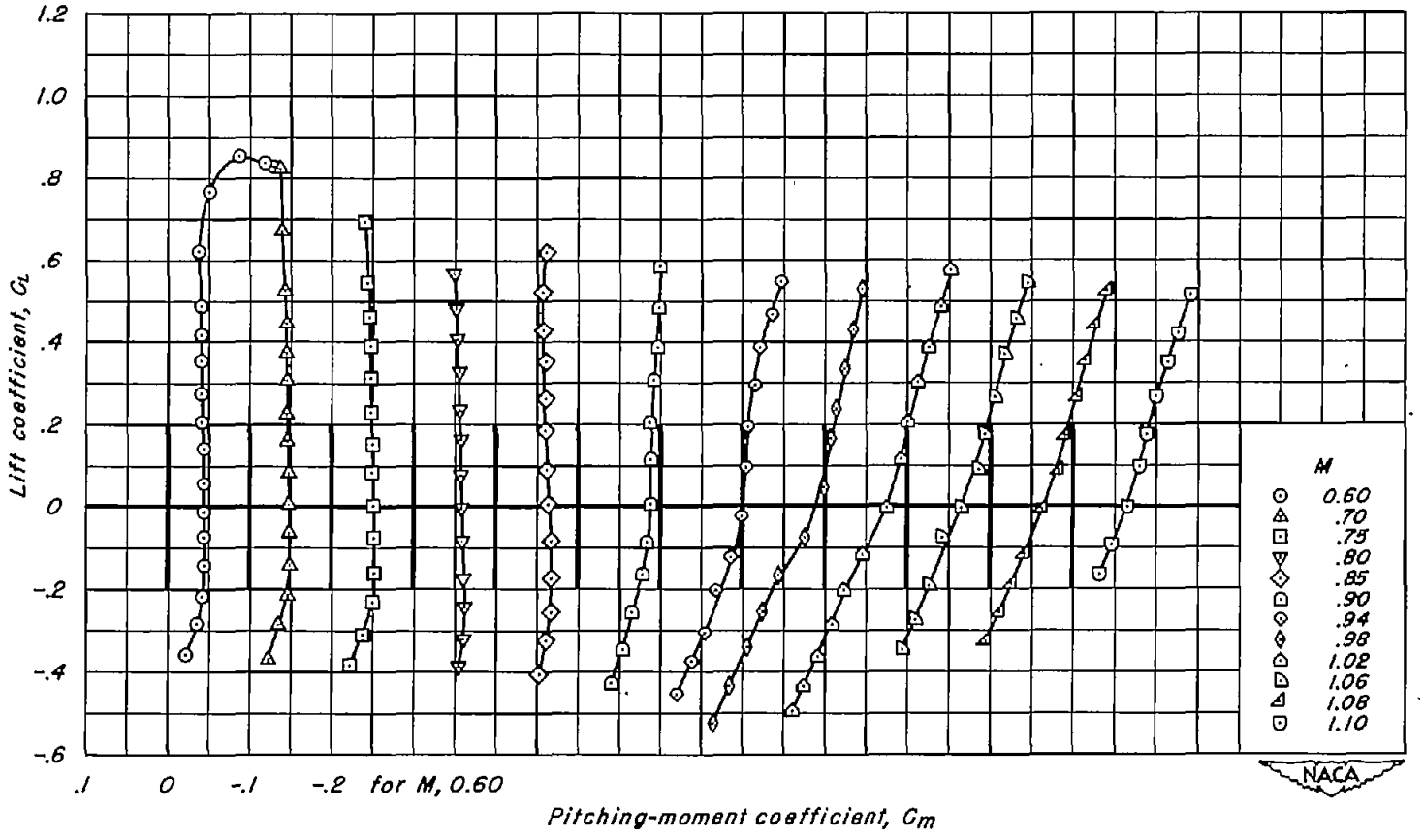

(d) A, 4, t/c, 0.04

Figure 10.- Continued.

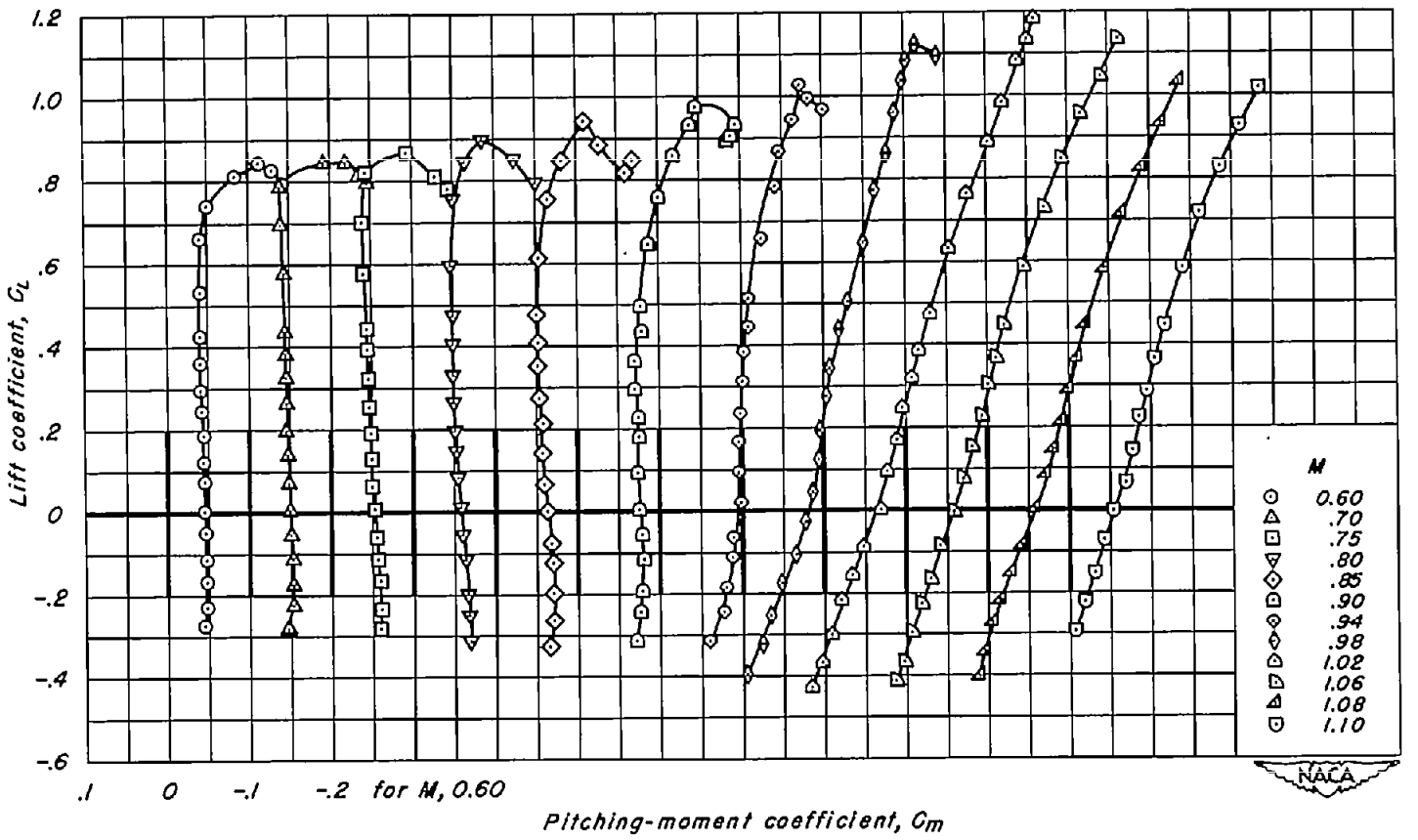

(e) A, 3; t/c, 0.06

Figure 10.- Continued.

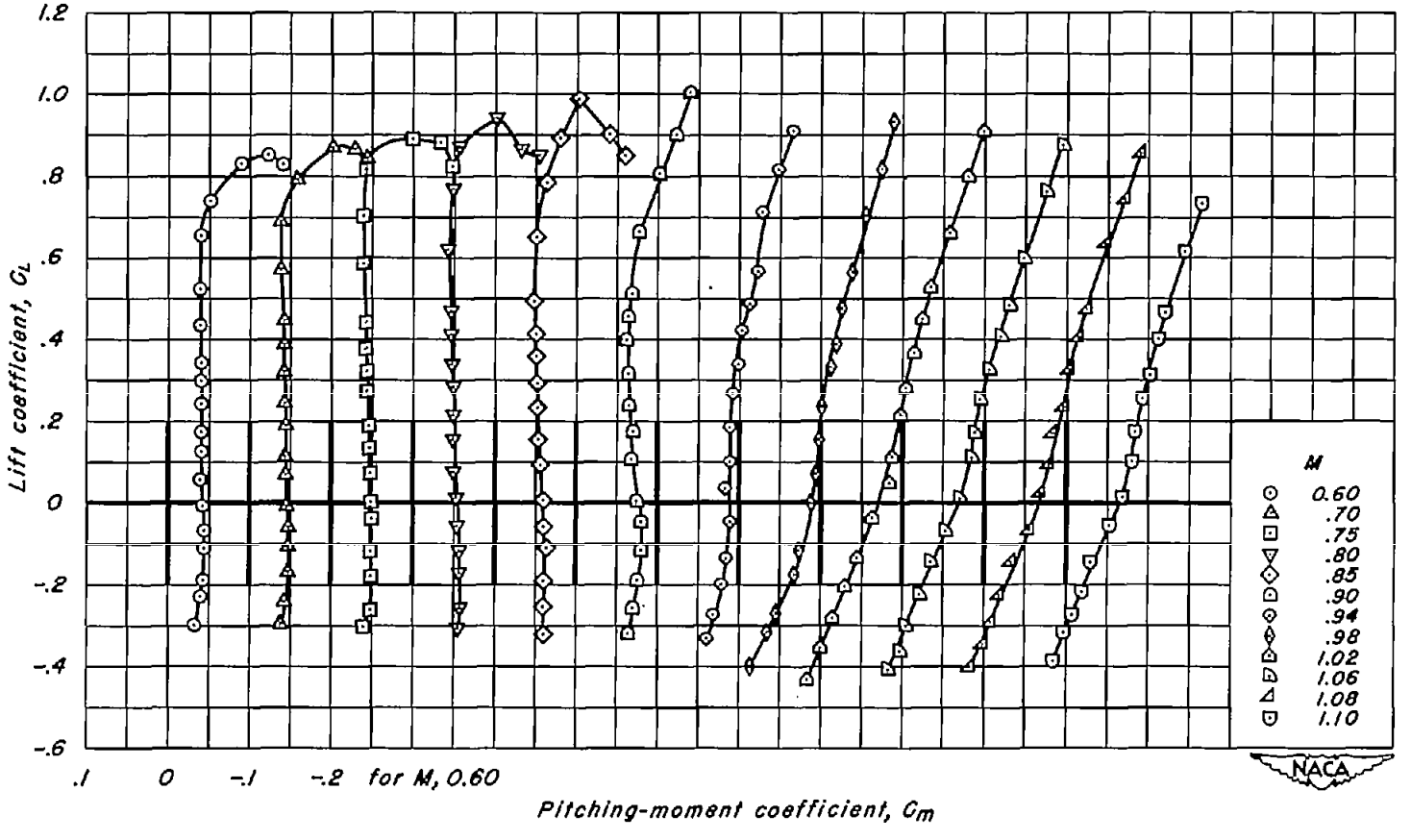

(f) A, 3; t/c, 0.04

Figure 10.- Continued.

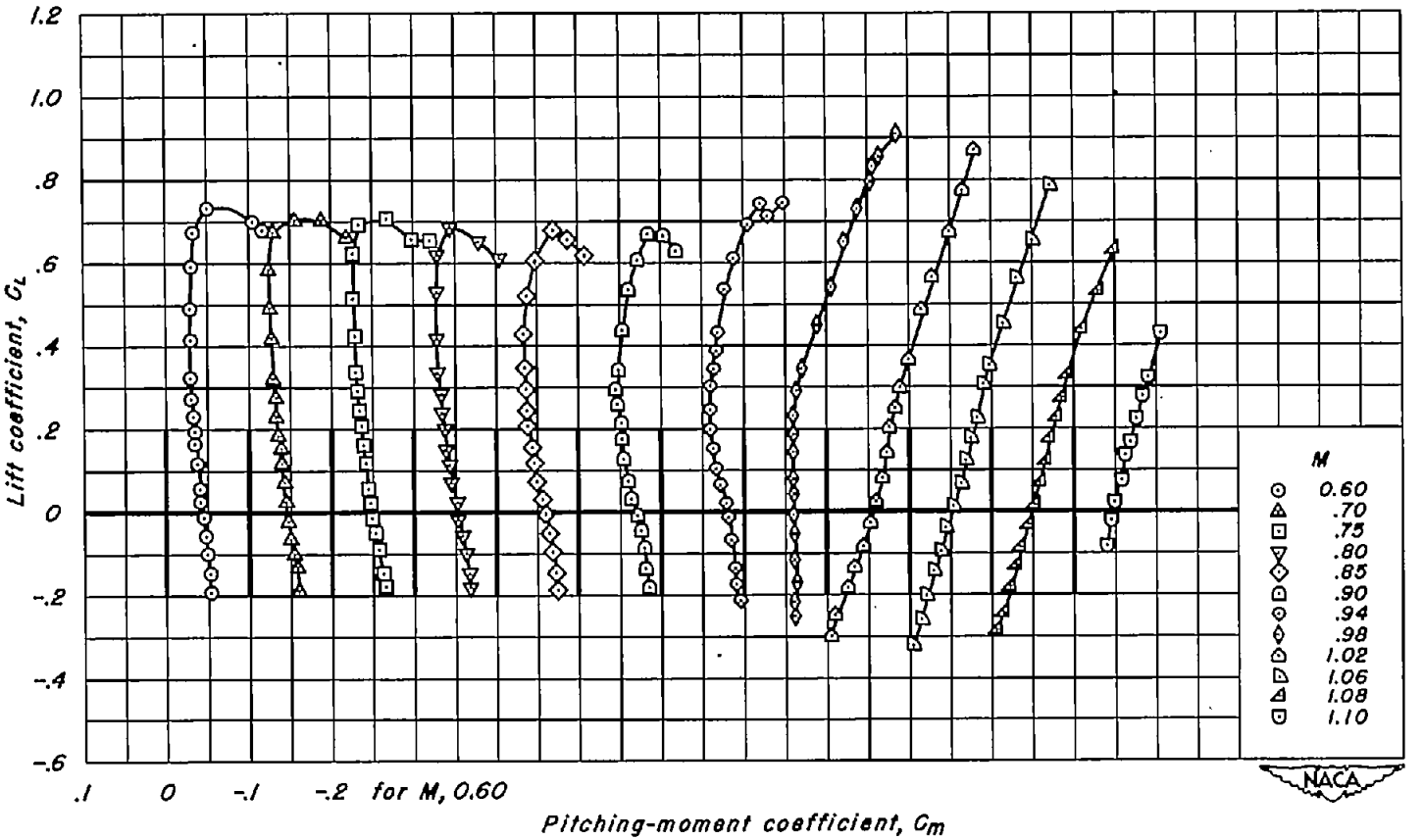

(g) A, 2; t/c, 0.10

Figure 10.- Continued.

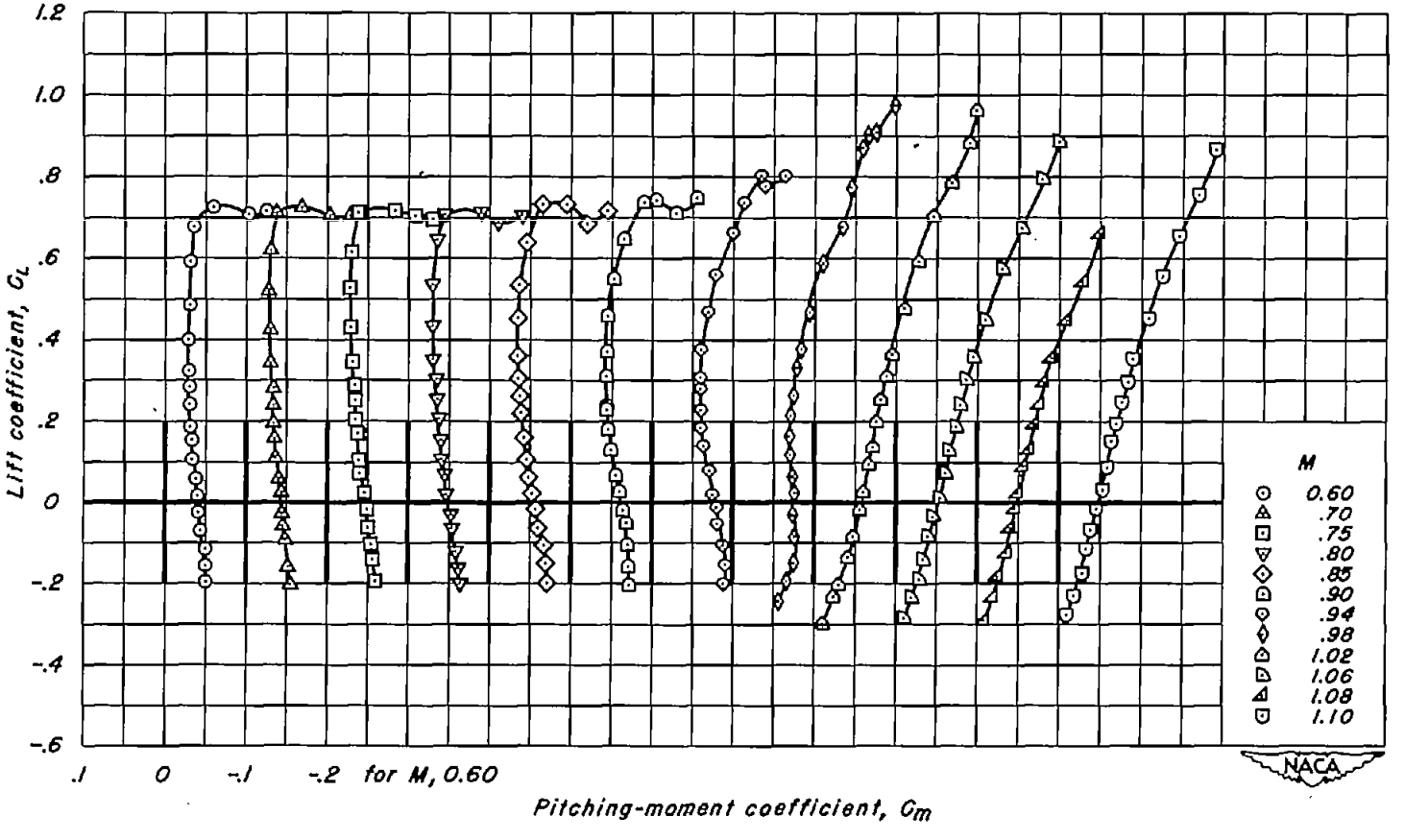

(h) A, 2; t/c, 0.08

Figure 10.- Continued.

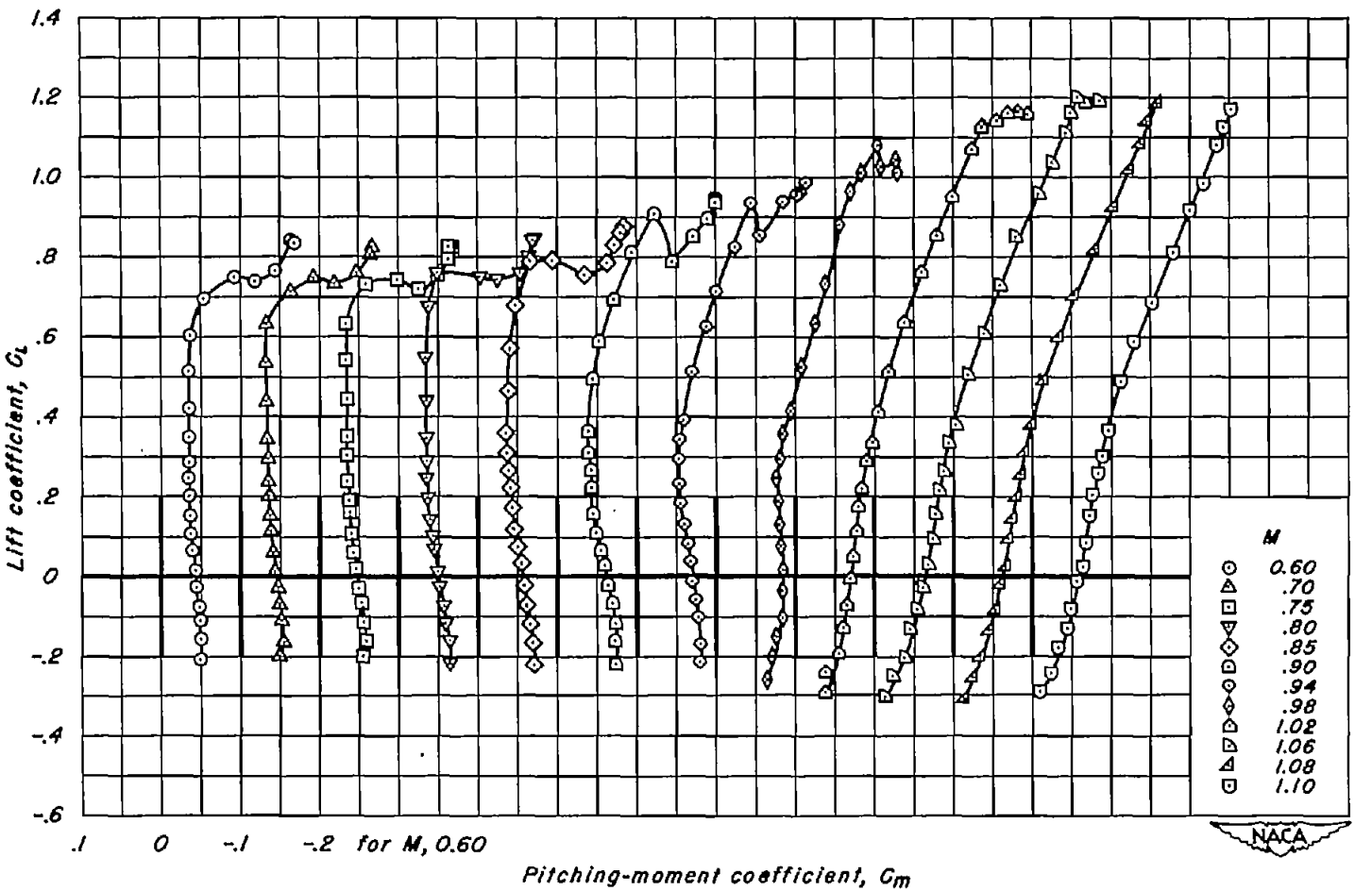

(i) A, 2; t/c, 0.06

Figure 10.- Continued.

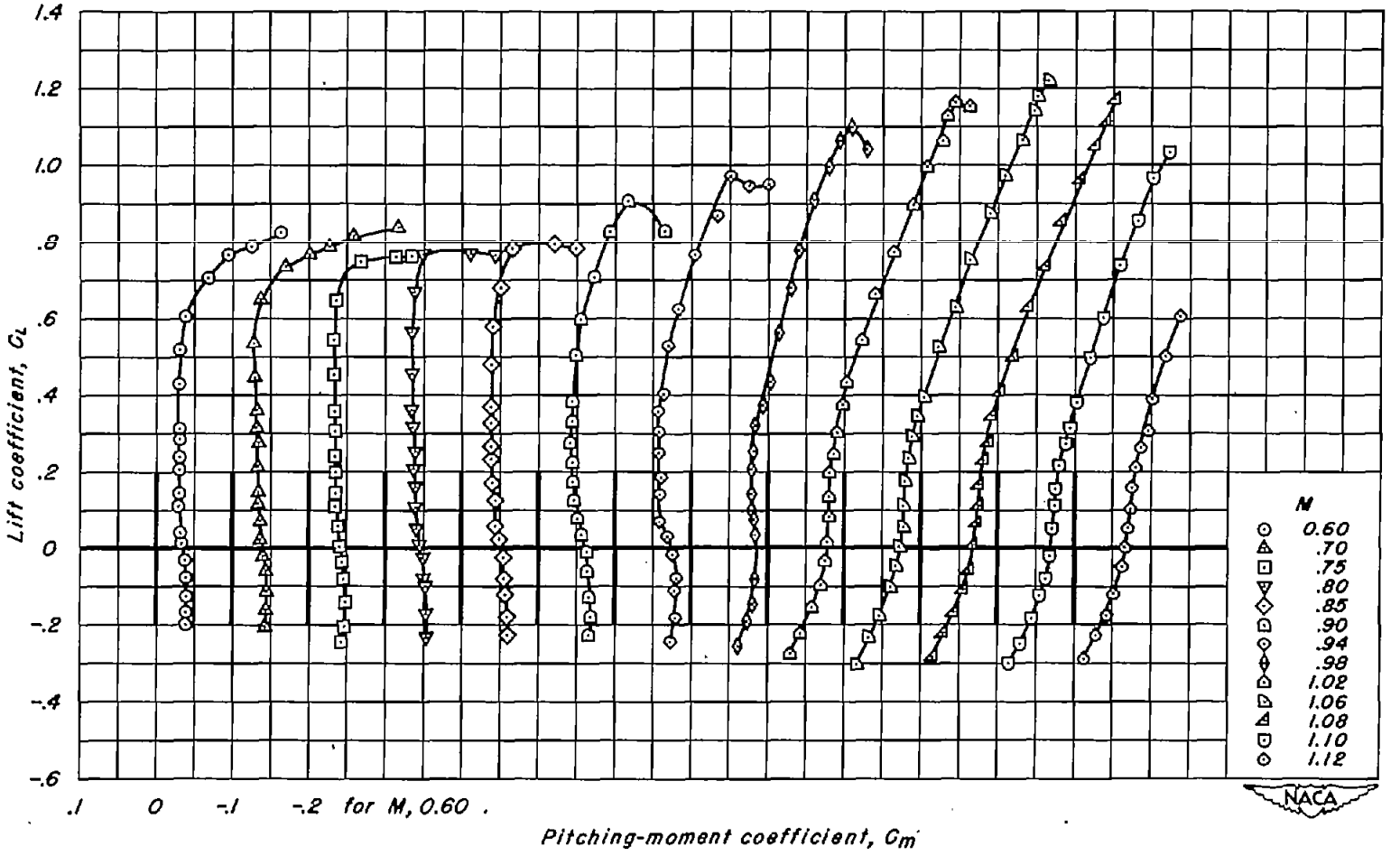

(j) A, 2; t/c, 0.04

Figure 10.- Continued.

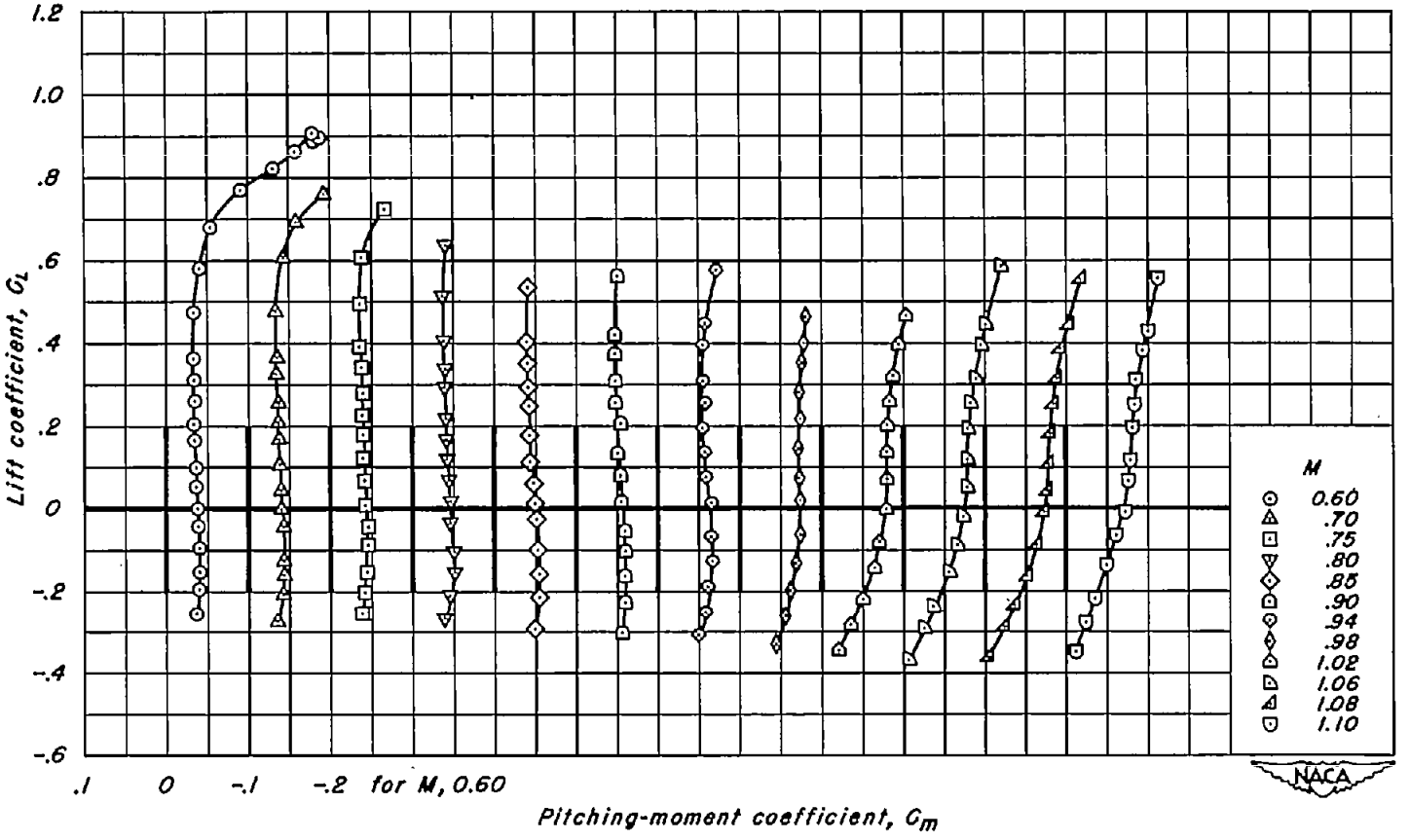

(k) A, 2; t/c, 0.02

Figure 10.- Continued.

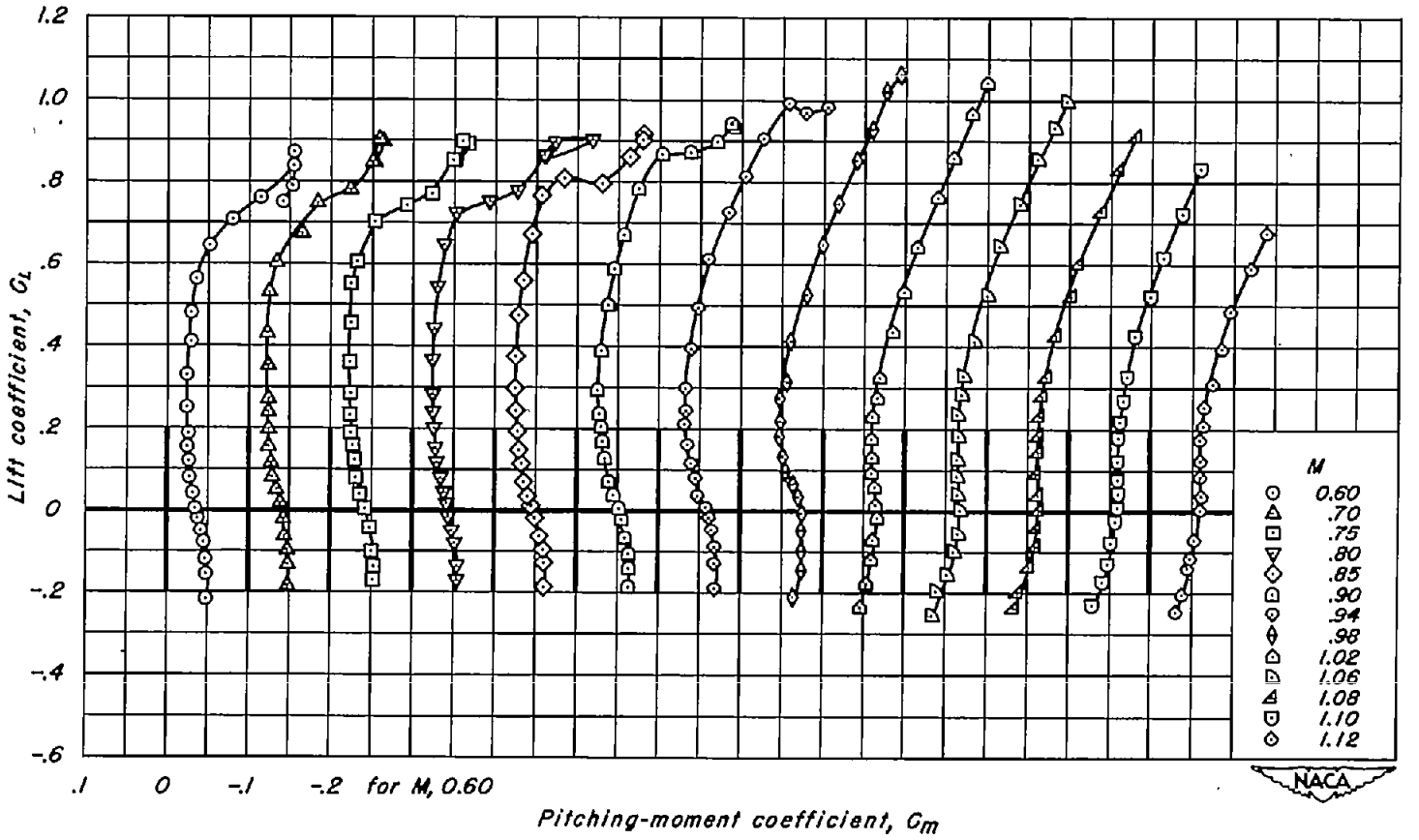

(l) A,1.5; t/c, 0.06

Figure 10.- Continued.

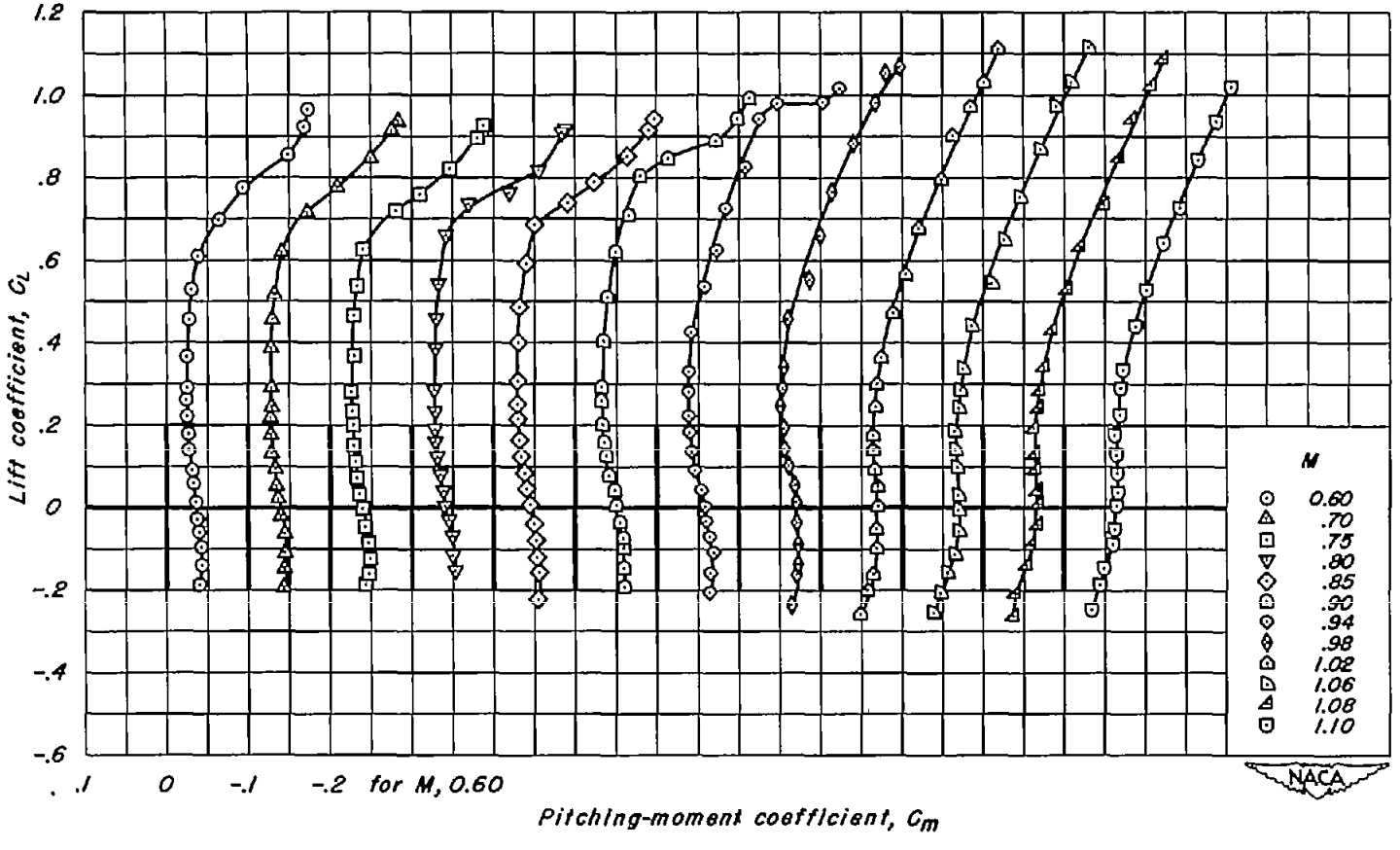

(m) A,1.5;t/c, 0.04

Figure 10.- Continued.

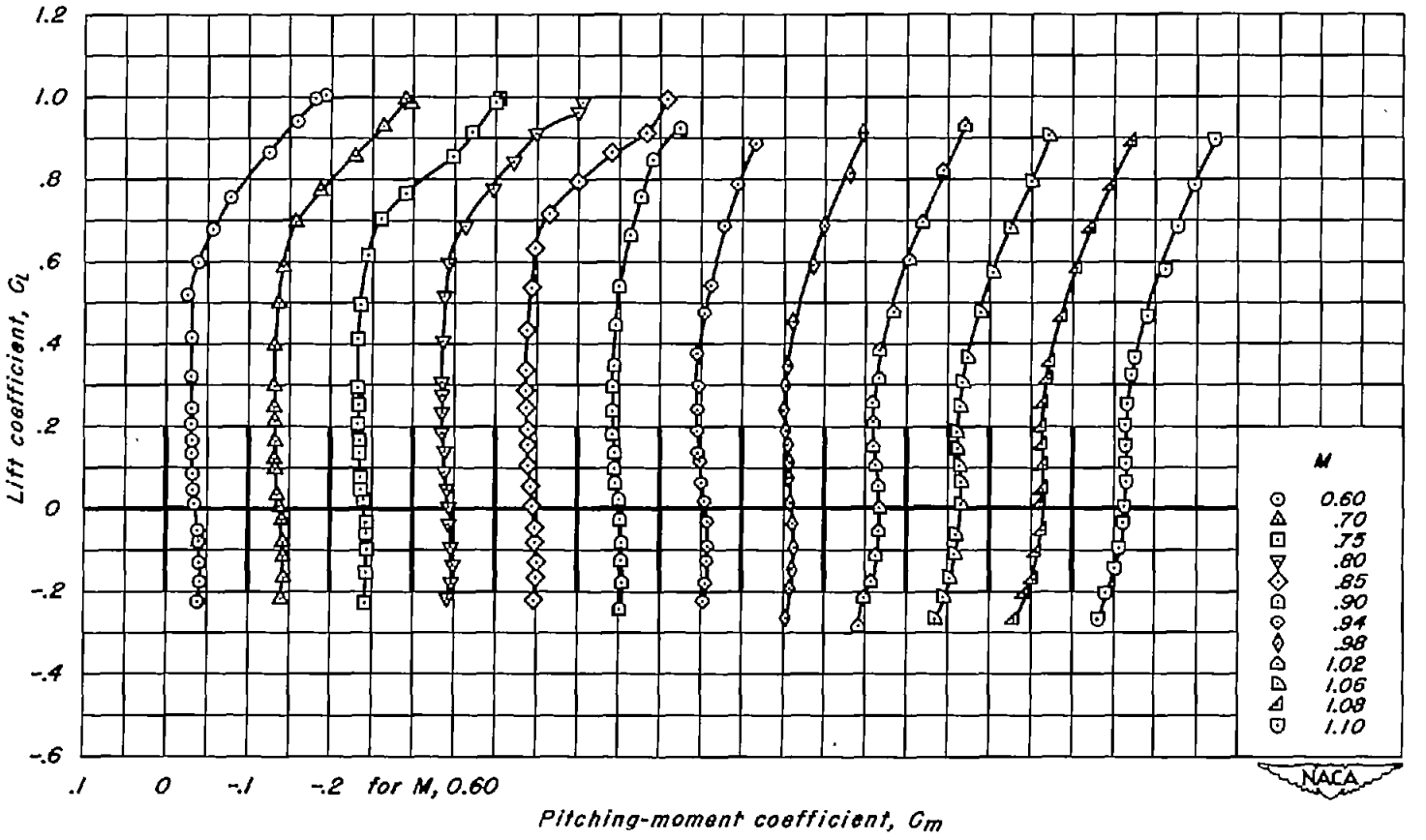

(n) A,1.5; t/c, 0.02

Figure 10.- Continued.

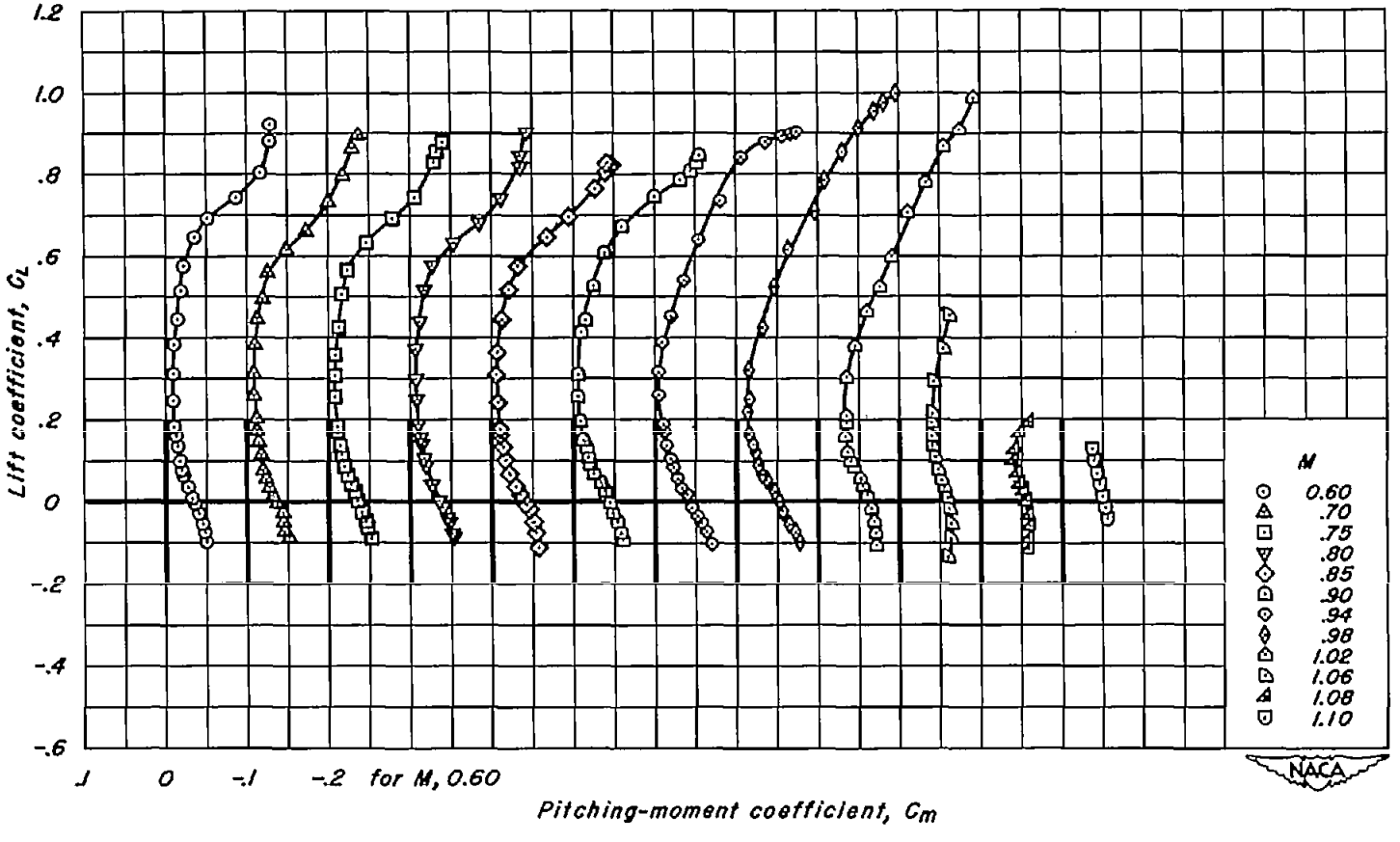

(o) A, 1; t/c, 0.10

Figure 10.- Continued.

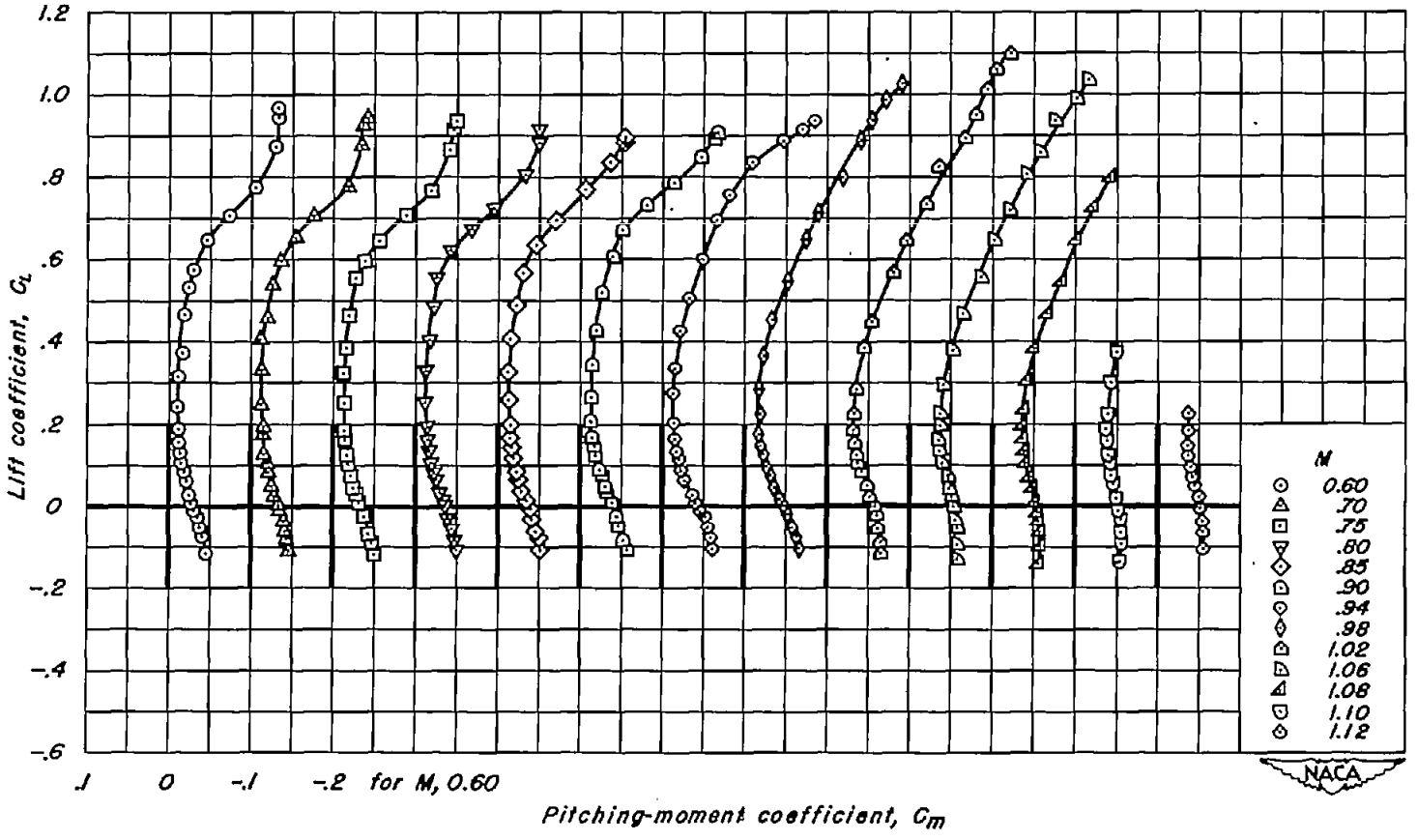

(p) A, 1; t/c, 0.08

Figure 10.- Continued.

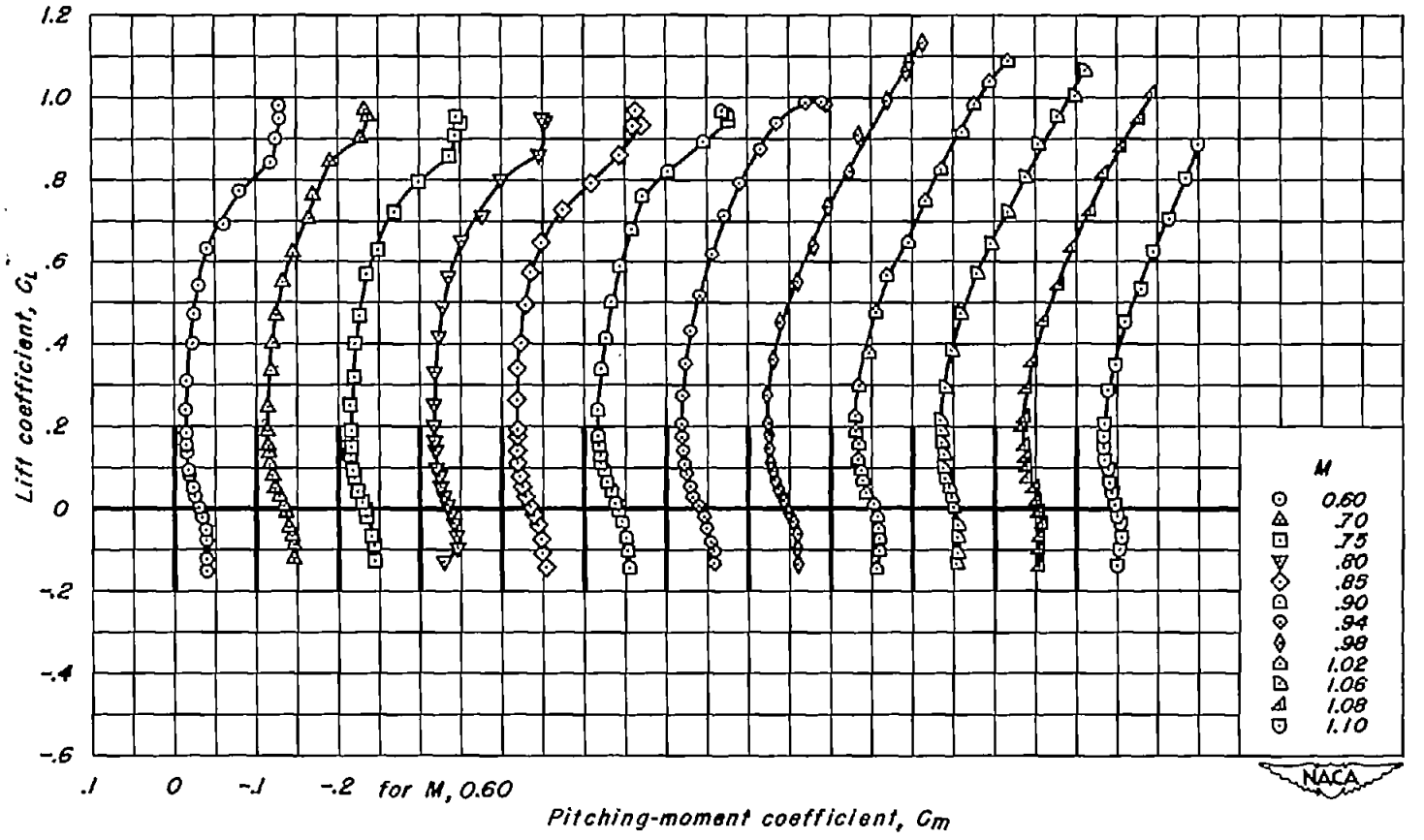

(q) A, 1; t/c, 0.06

Figure 10.- Continued.

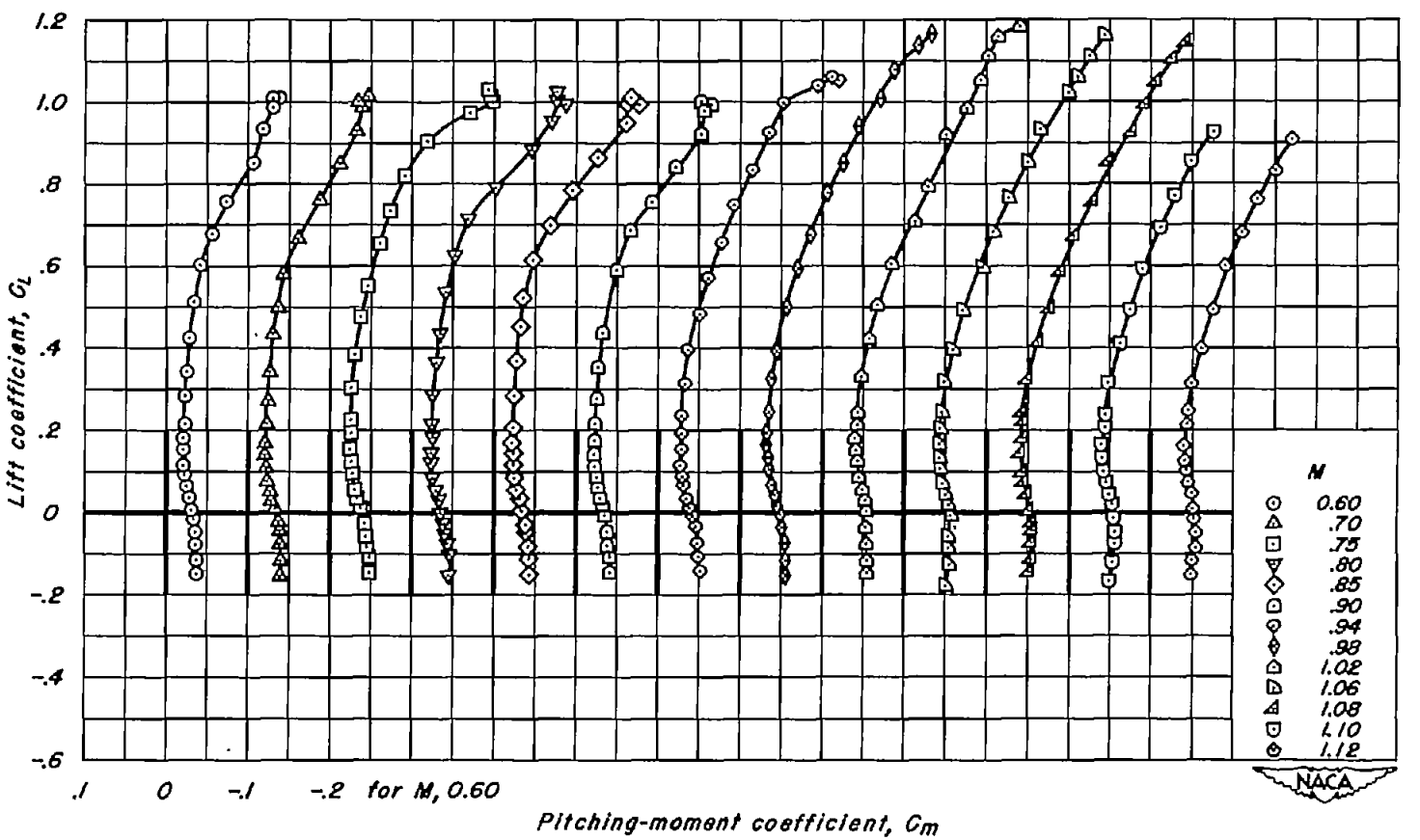

(r) A, 1; t/c, 0.04

Figure 10.- Continued.

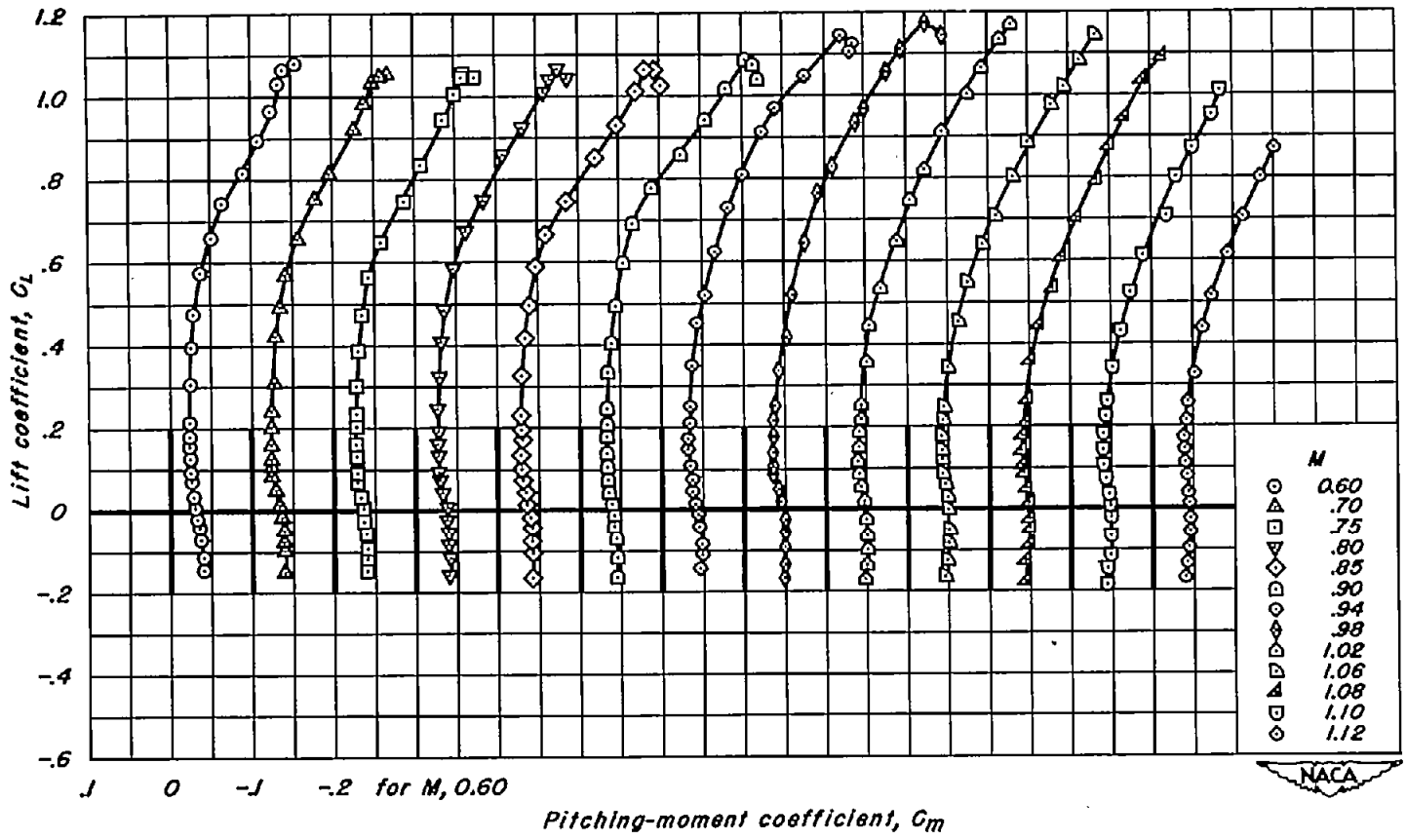

(s) A, 1; t/c, 0.02

Figure 10.- Concluded.

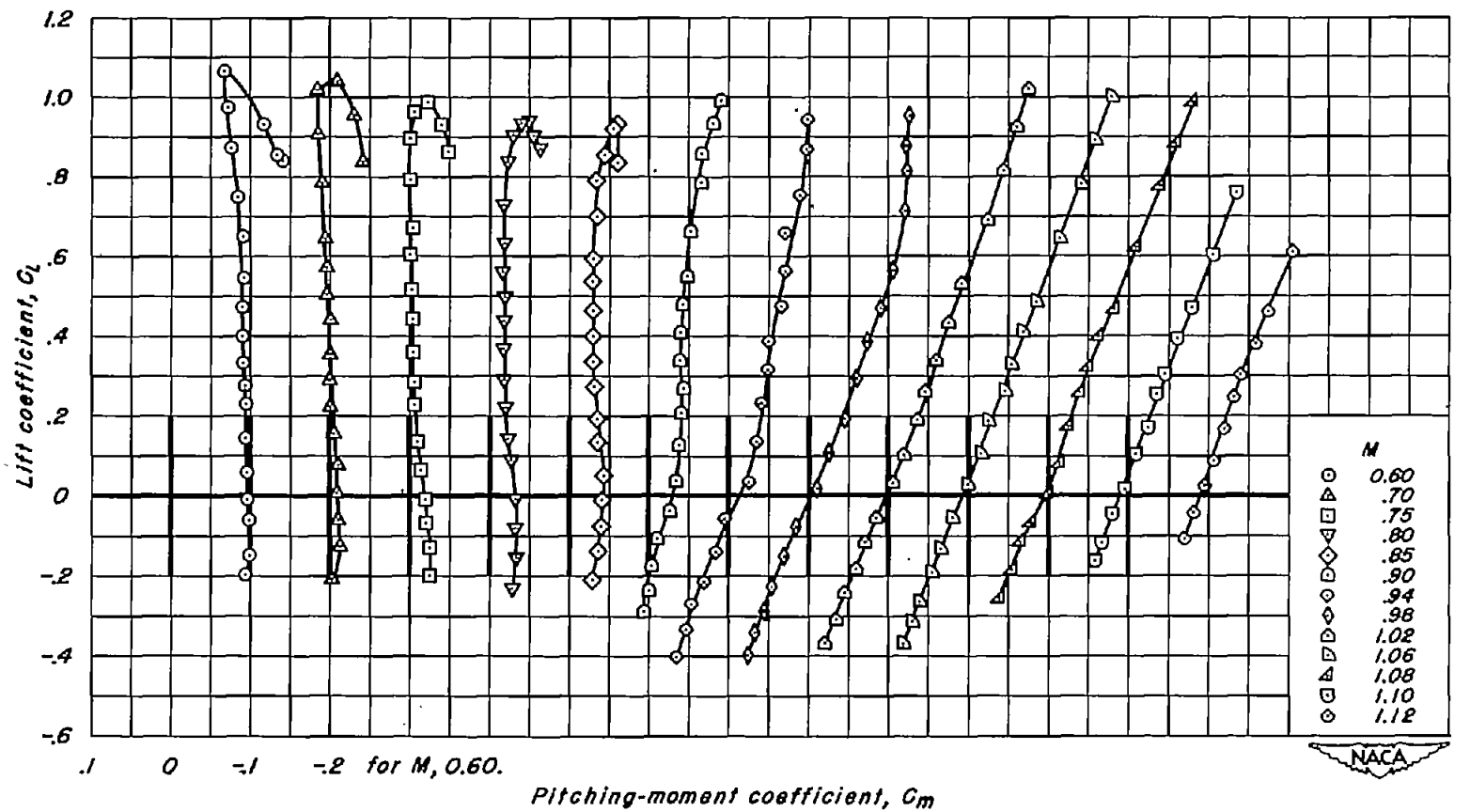

(a) A, 4; t/c, 0.10

Figure 11.–The variation of pitching-moment coefficient with lift coefficient for the wings with NACA 63A4XX sections.

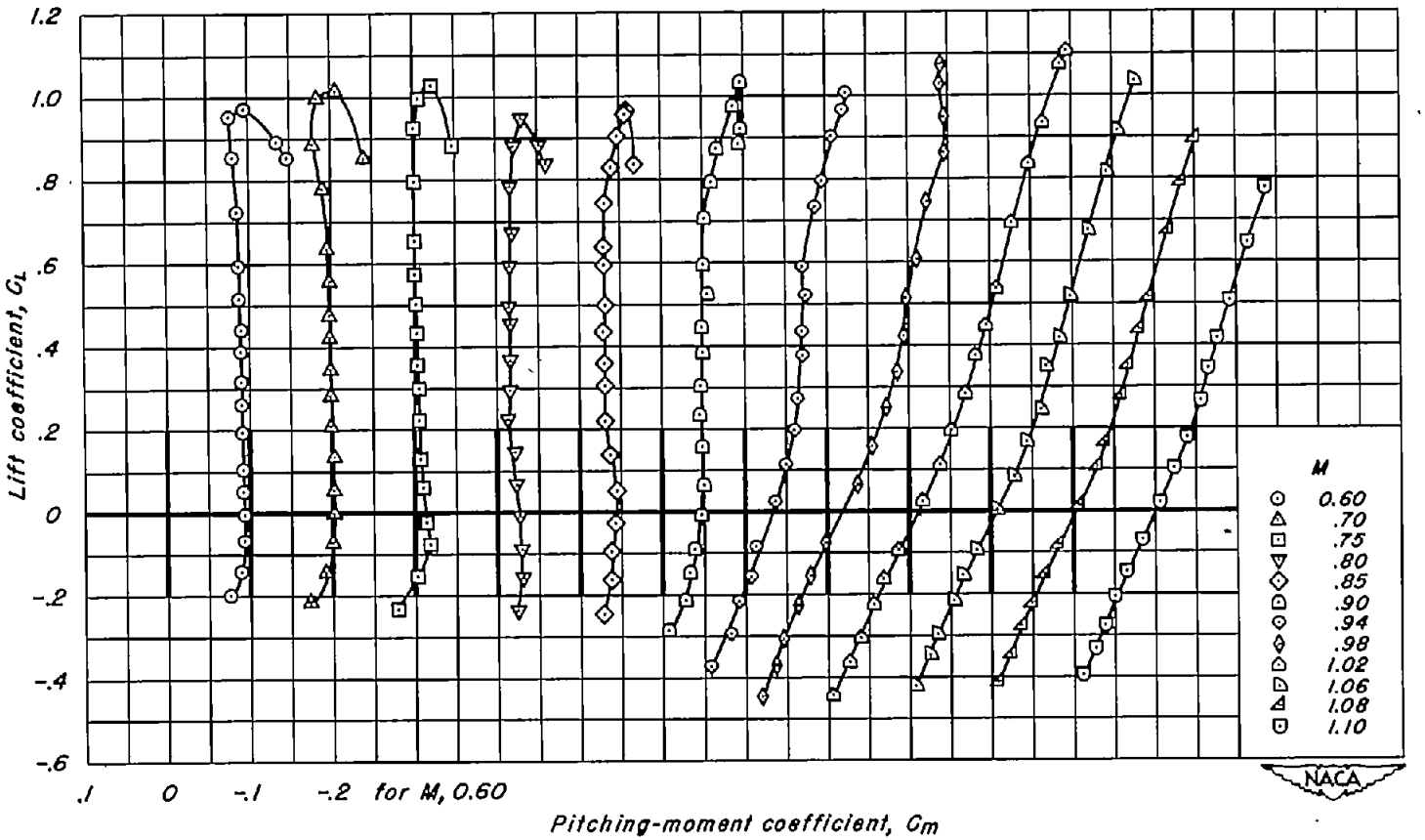

(b) A, 4; t/c, 0.08

Figure 11.- Continued.

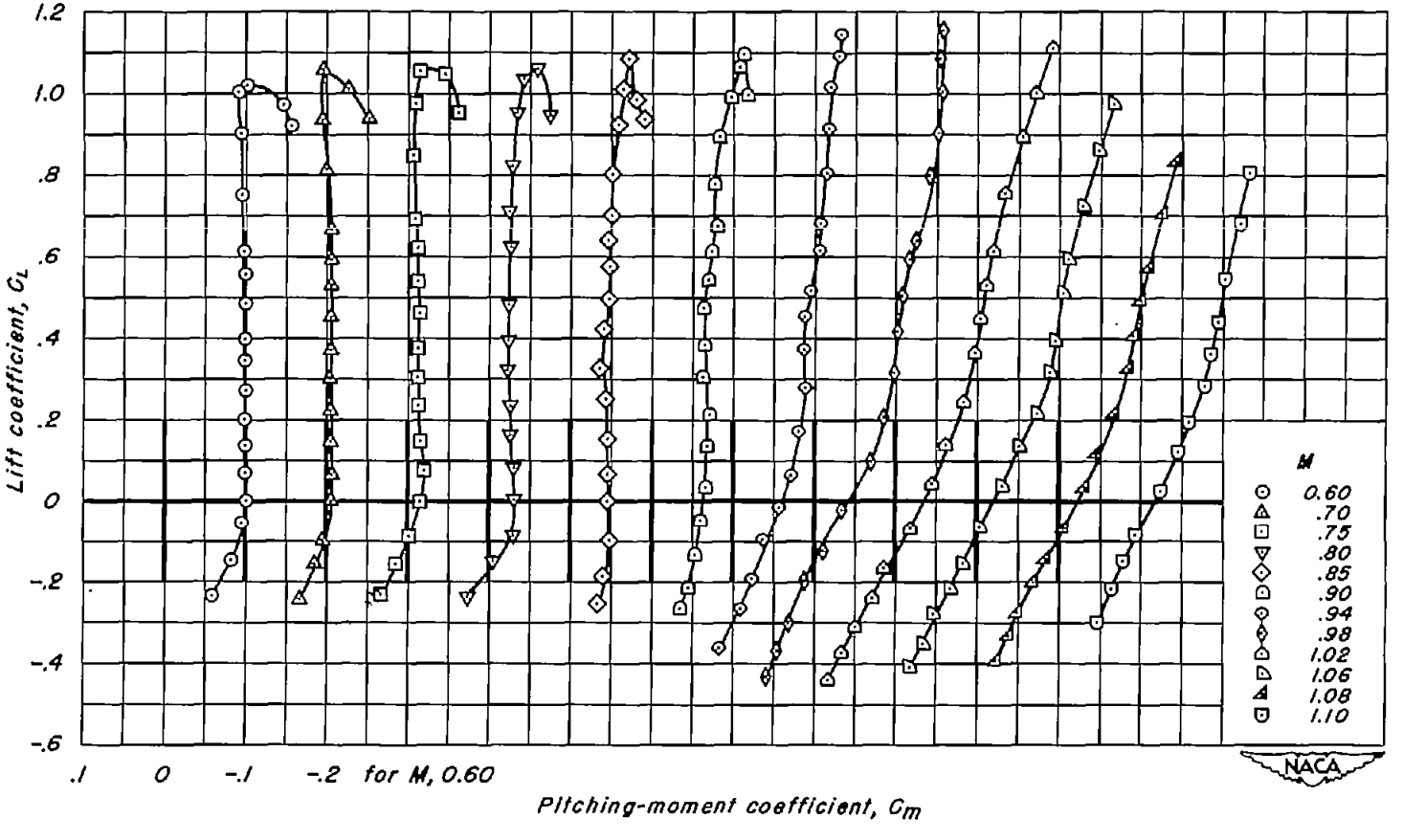

(c) A, 4; t/c, 0.06

Figure 11.- Continued.

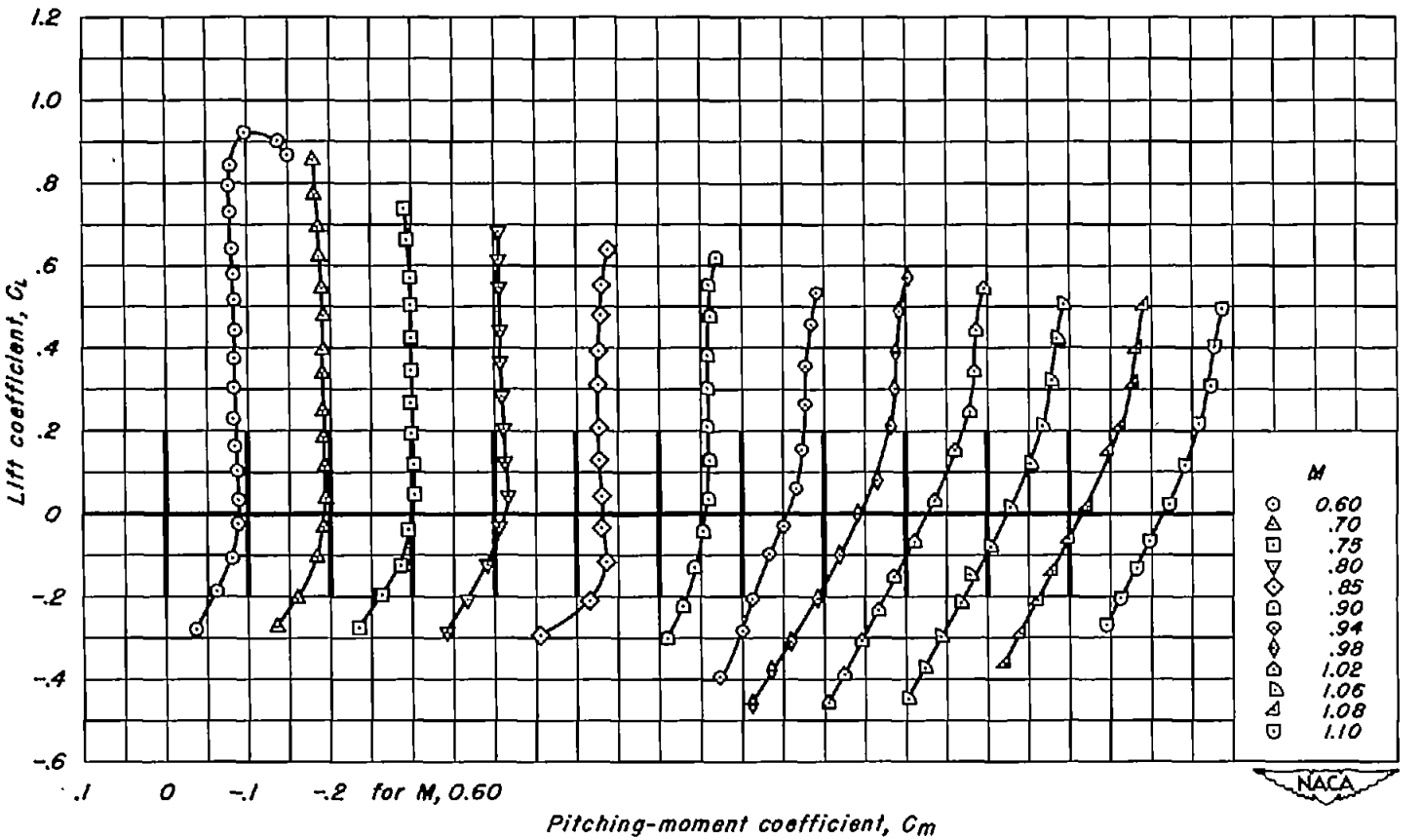

(d) A, 4; t/c, 0.04

Figure 11.- Continued.

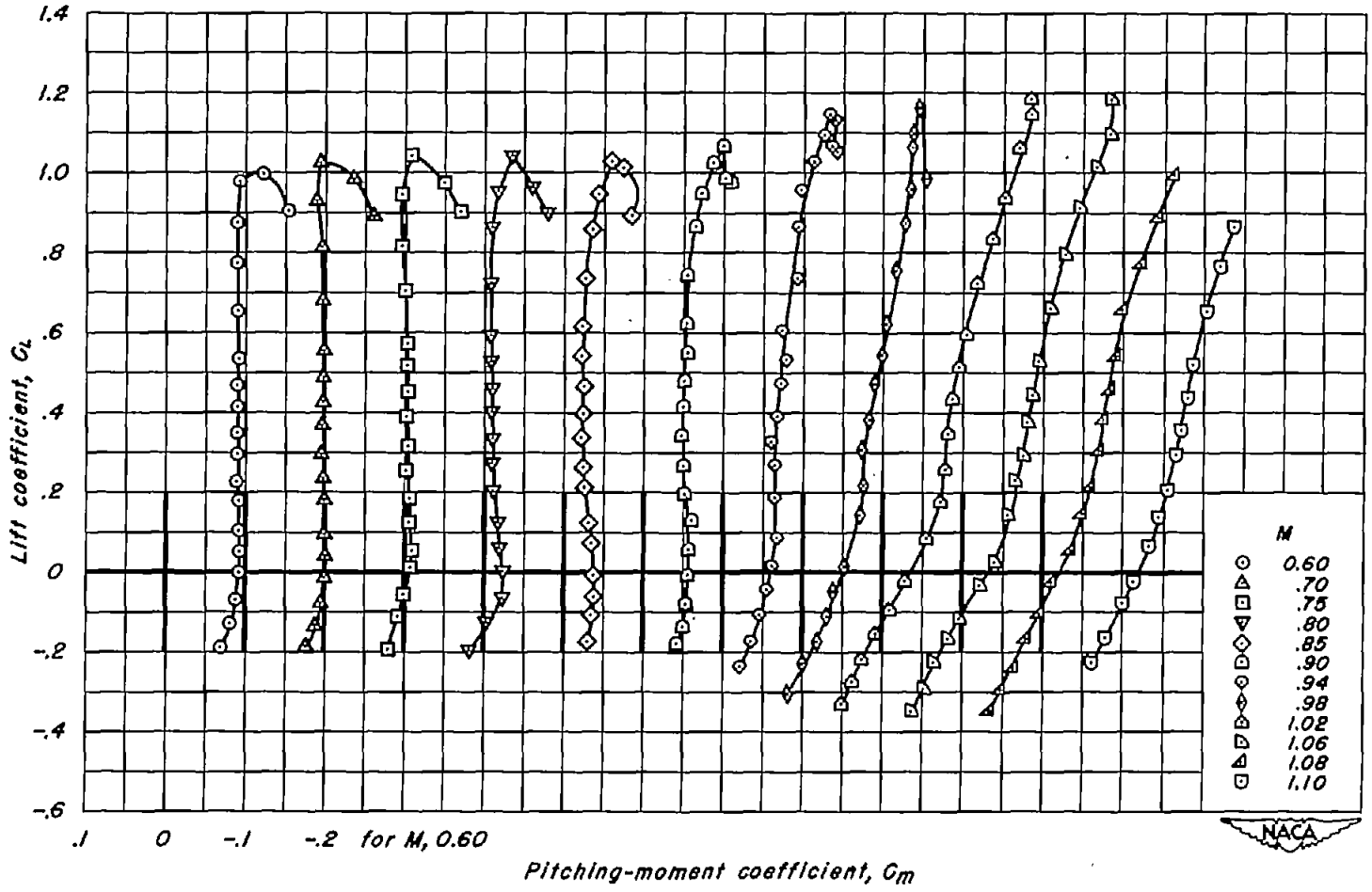

(e) A, 3; t/c, 0.06

Figure 11.- Continued.

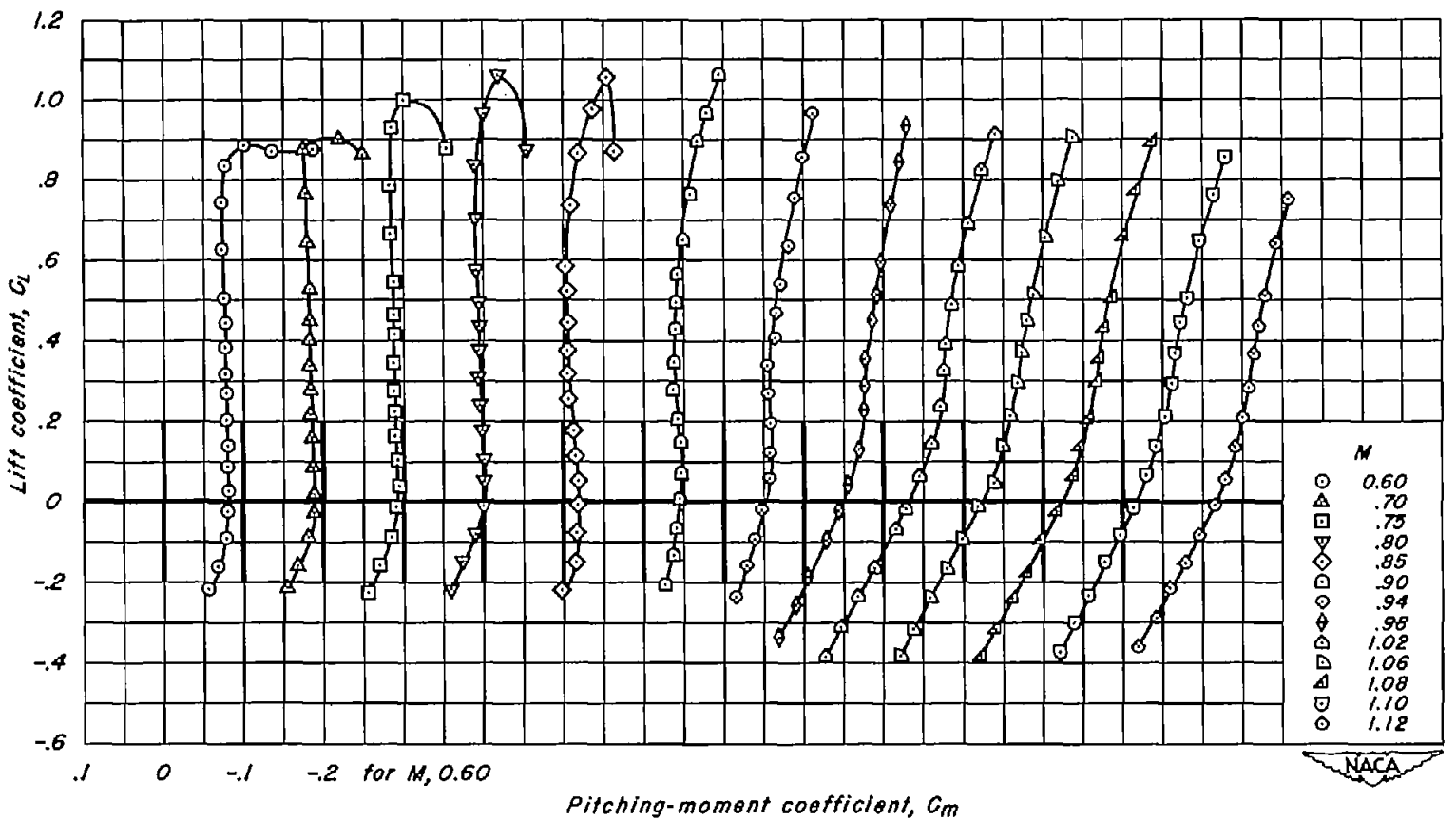

(f) A, 3; t/c, 0.04

Figure 11.- Continued.

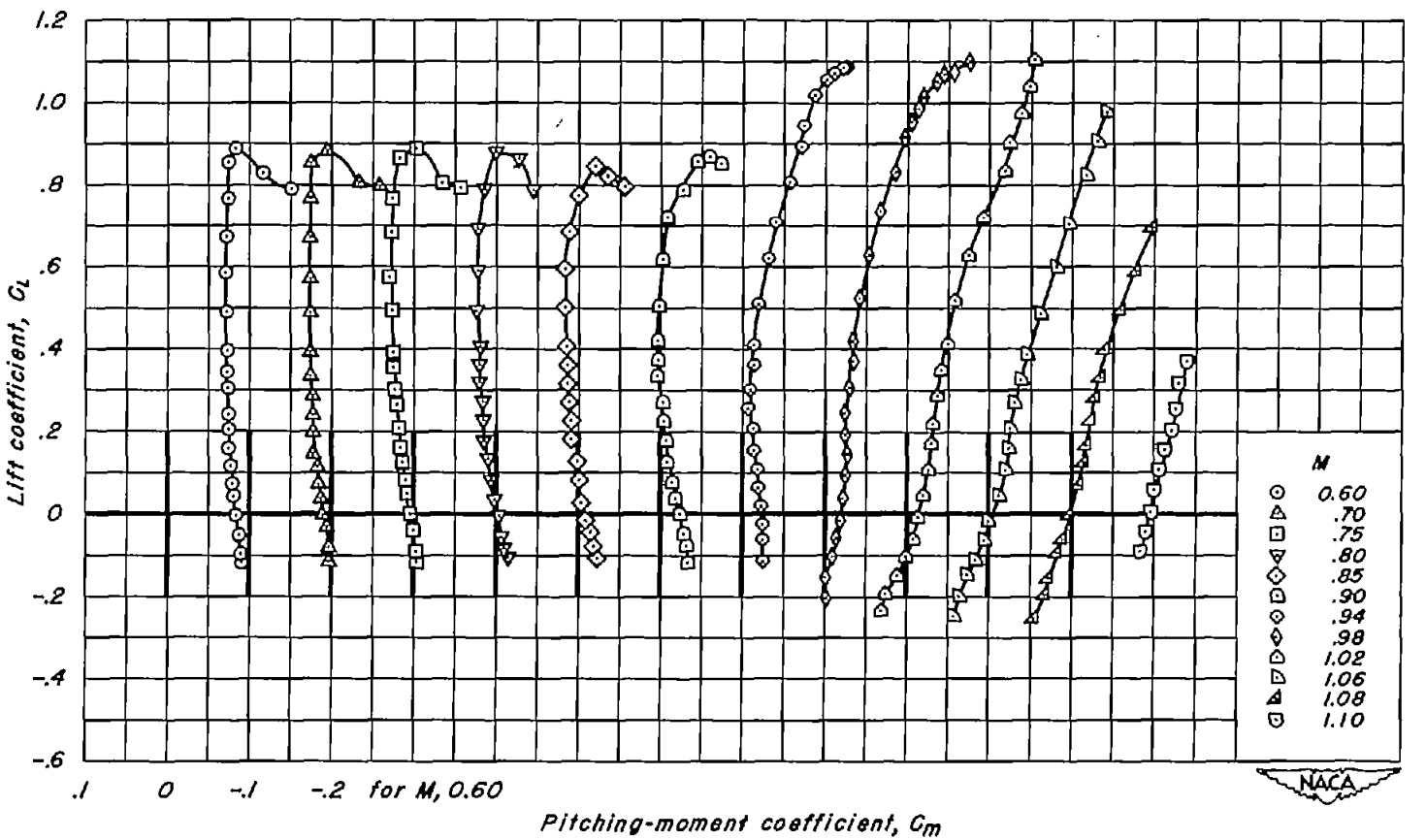

(g) A, 2; t/c, 0.10

Figure 11.- Continued.

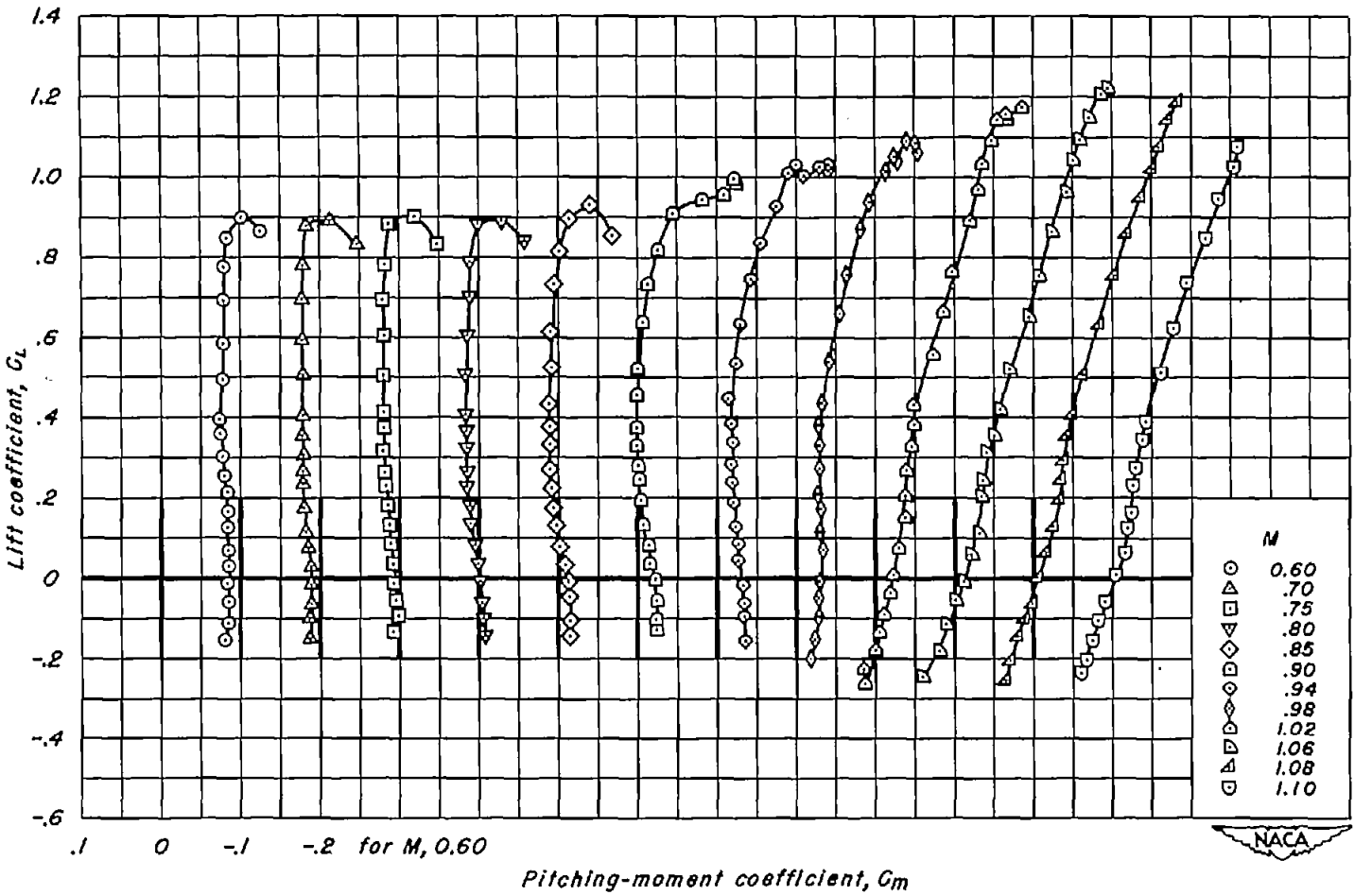

(h) A, 2; t/c, 0.08

Figure 11.- Continued.

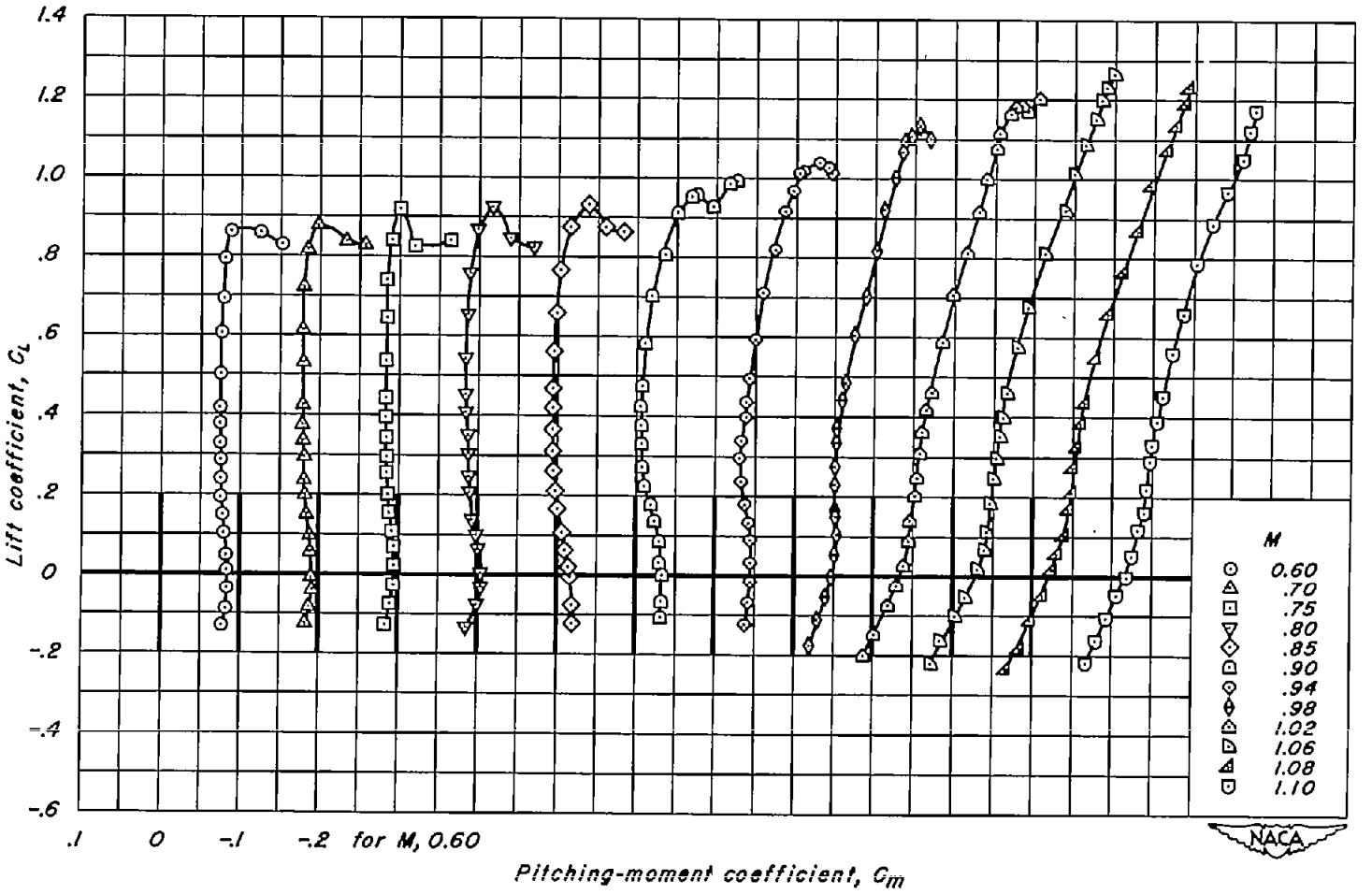

(i) A, 2; t/c, 0.06

Figure 11.- Continued.

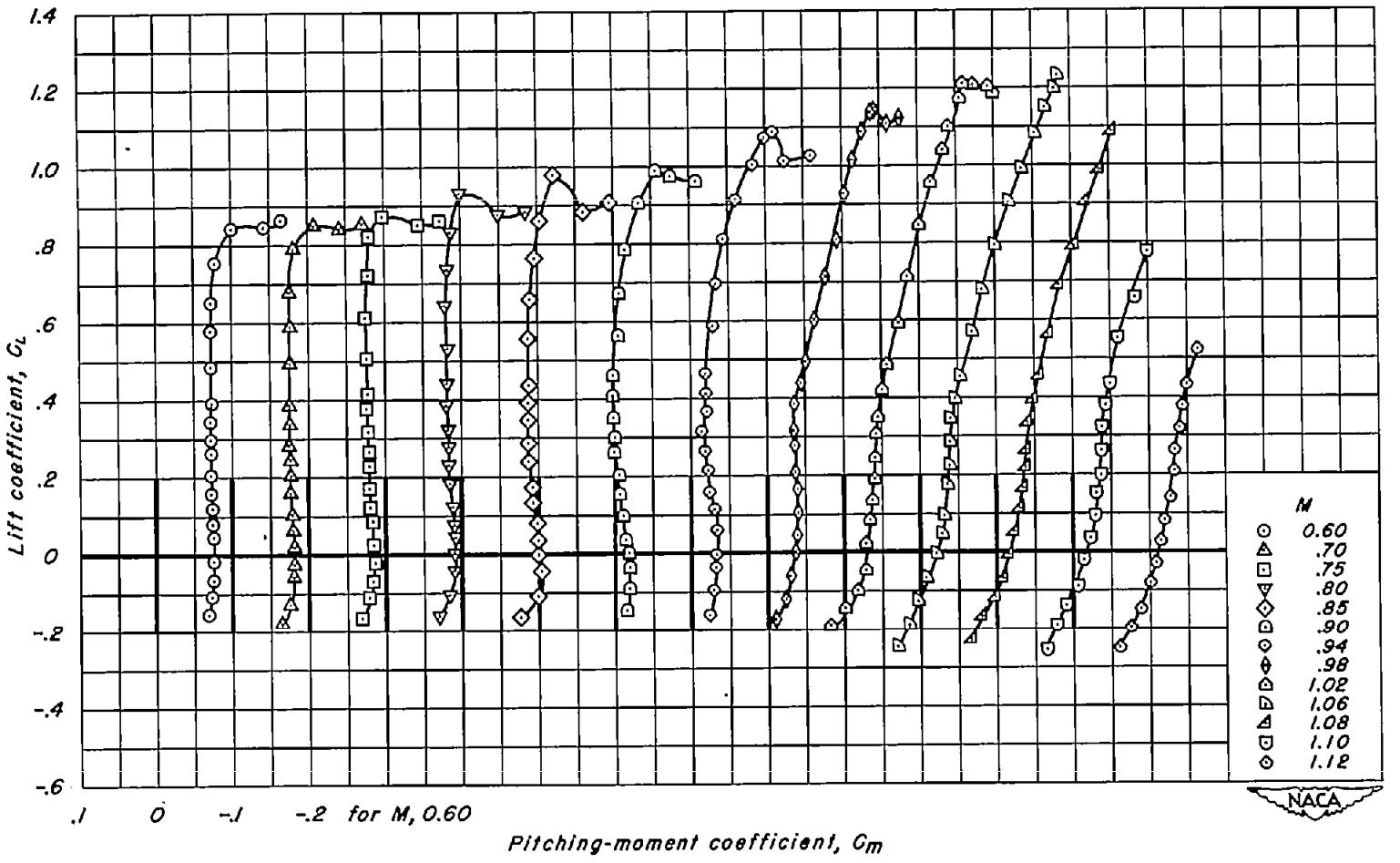

(j) A, 2, t/c, 0.04

Figure 11.- Continued.

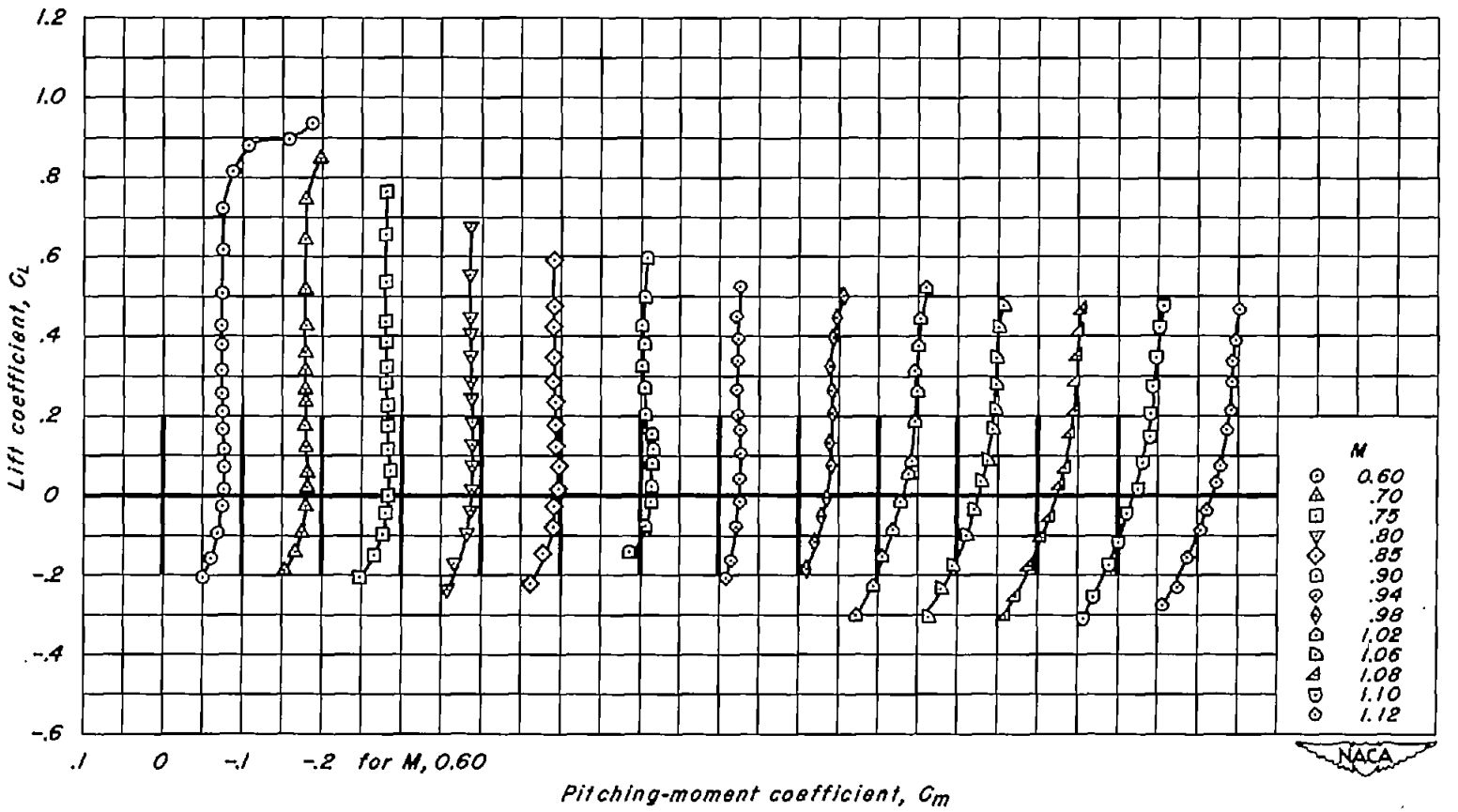

(k) A, 2; t/c, 0.02

Figure 11.- Continued.

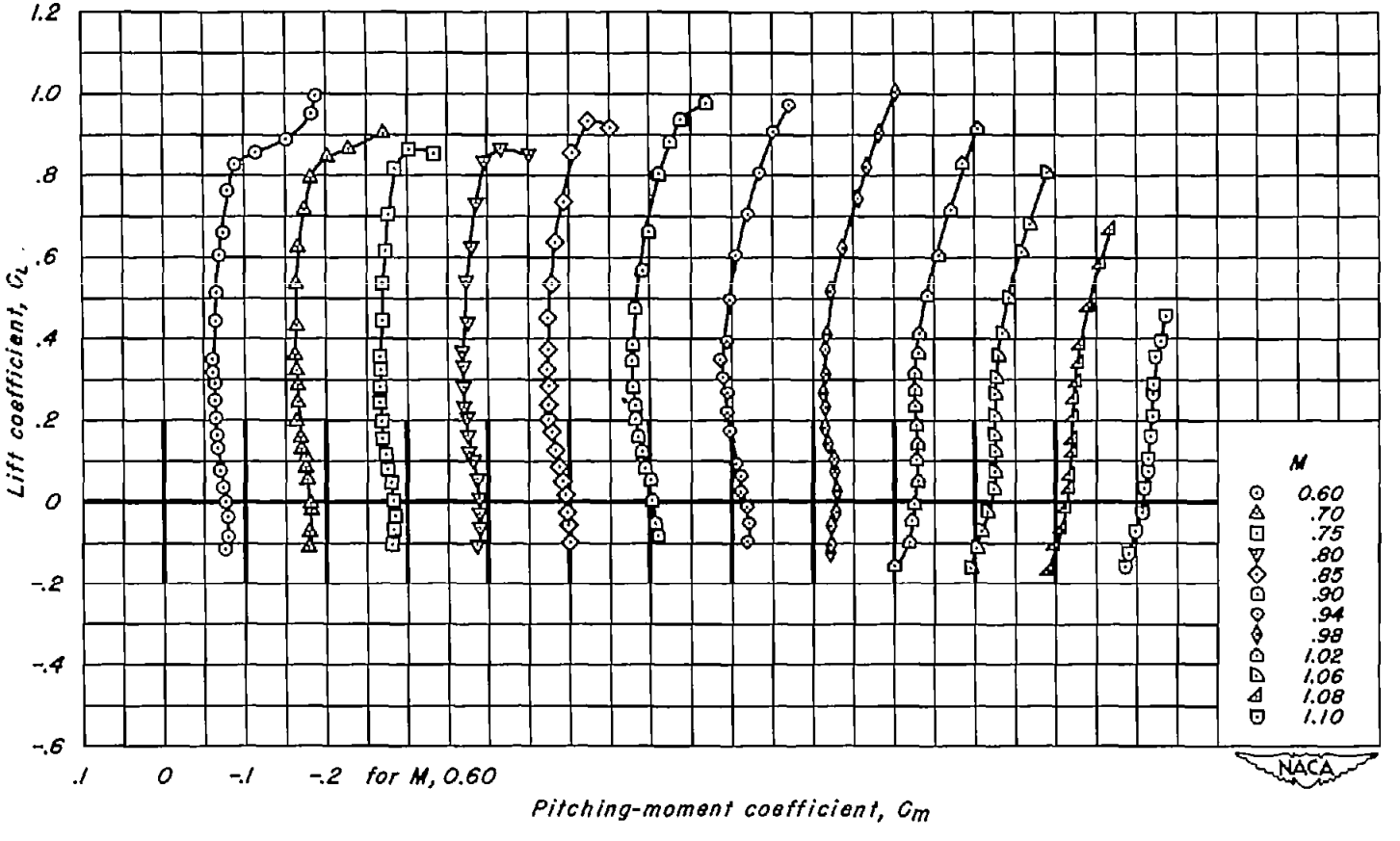

(l) A,1.5; t/c, 0.06

Figure 11.- Continued.

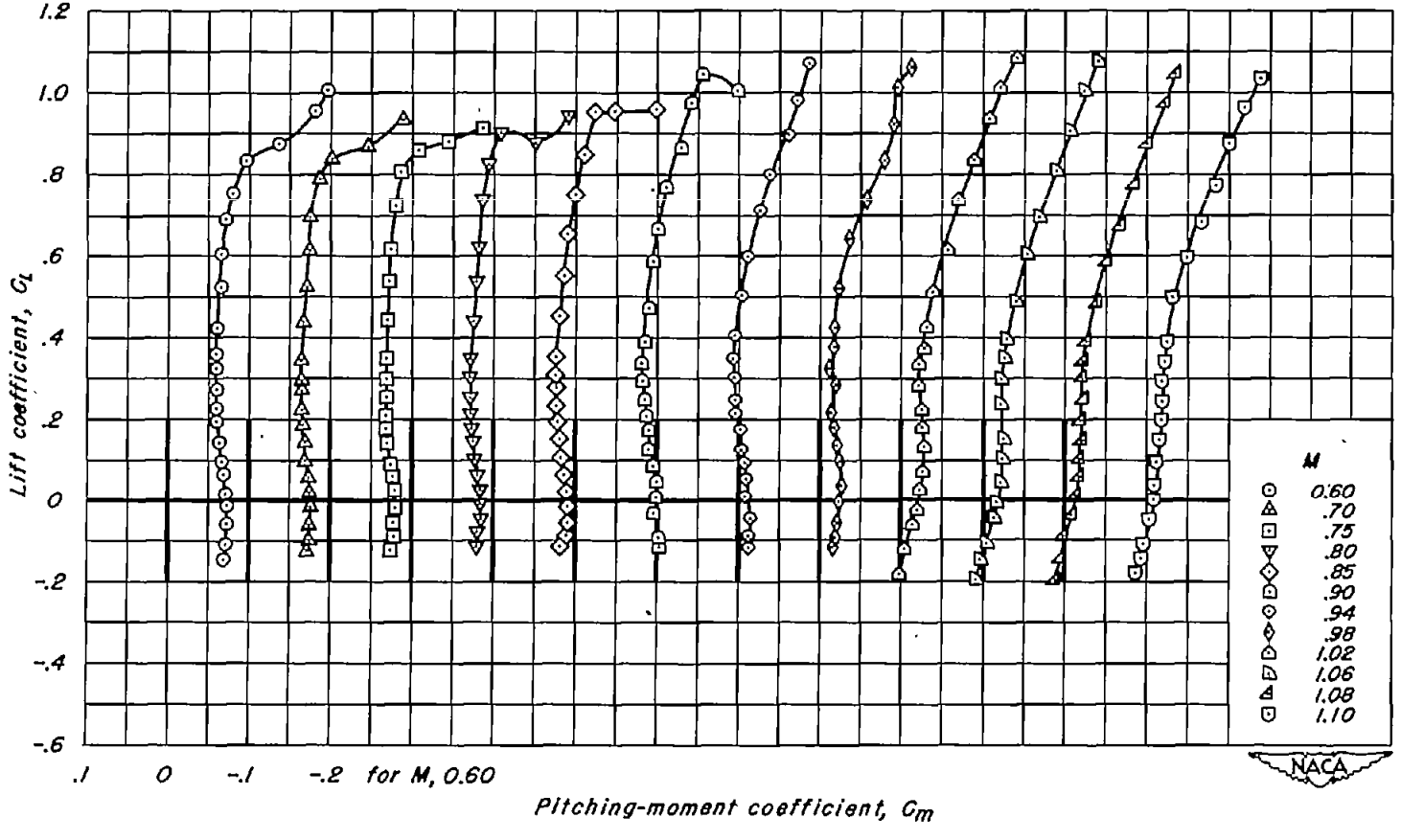

(m) A,1.5; t/c, 0.04

Figure 11.- Continued.

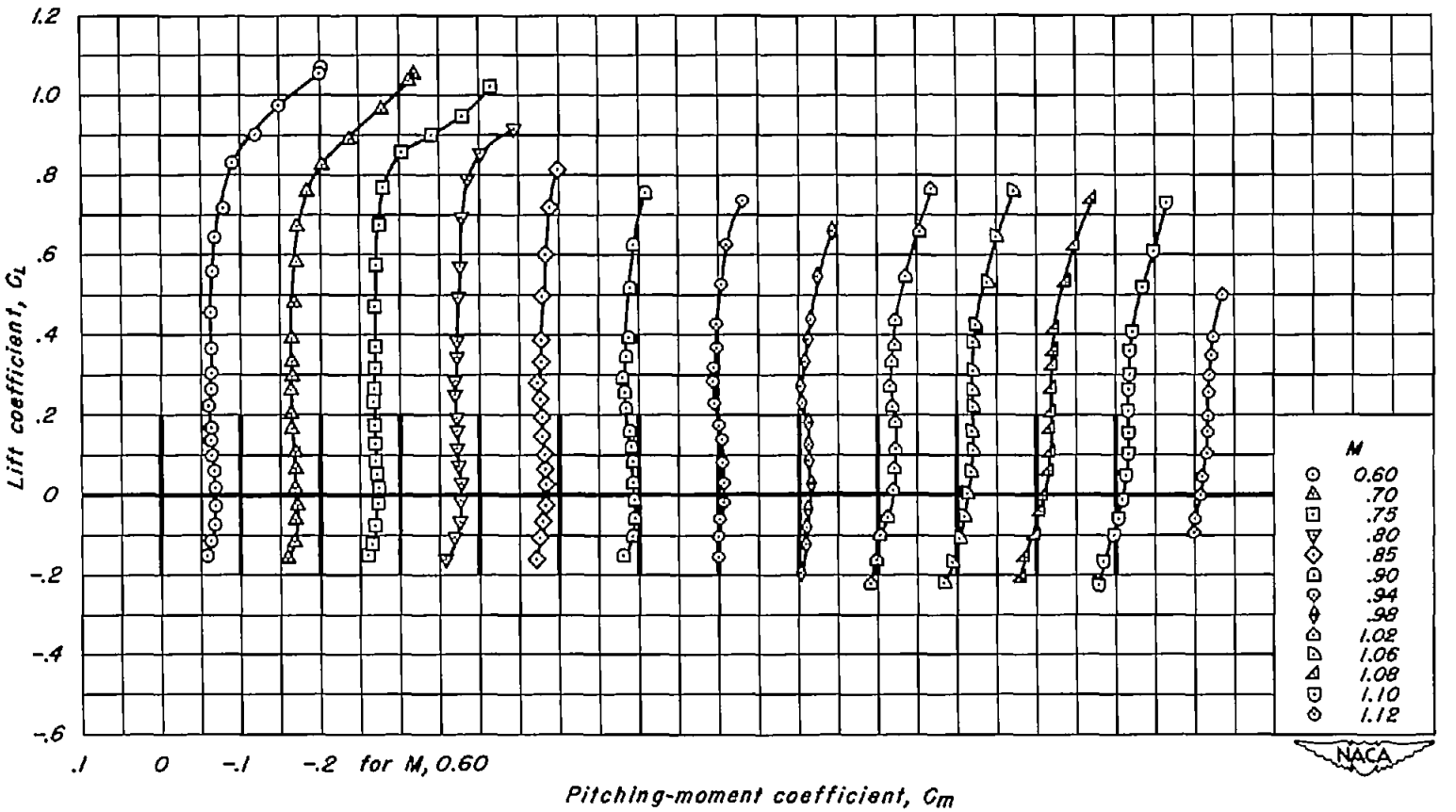

(n) A,1.5; t/c, 0.02

Figure 11.- Continued.

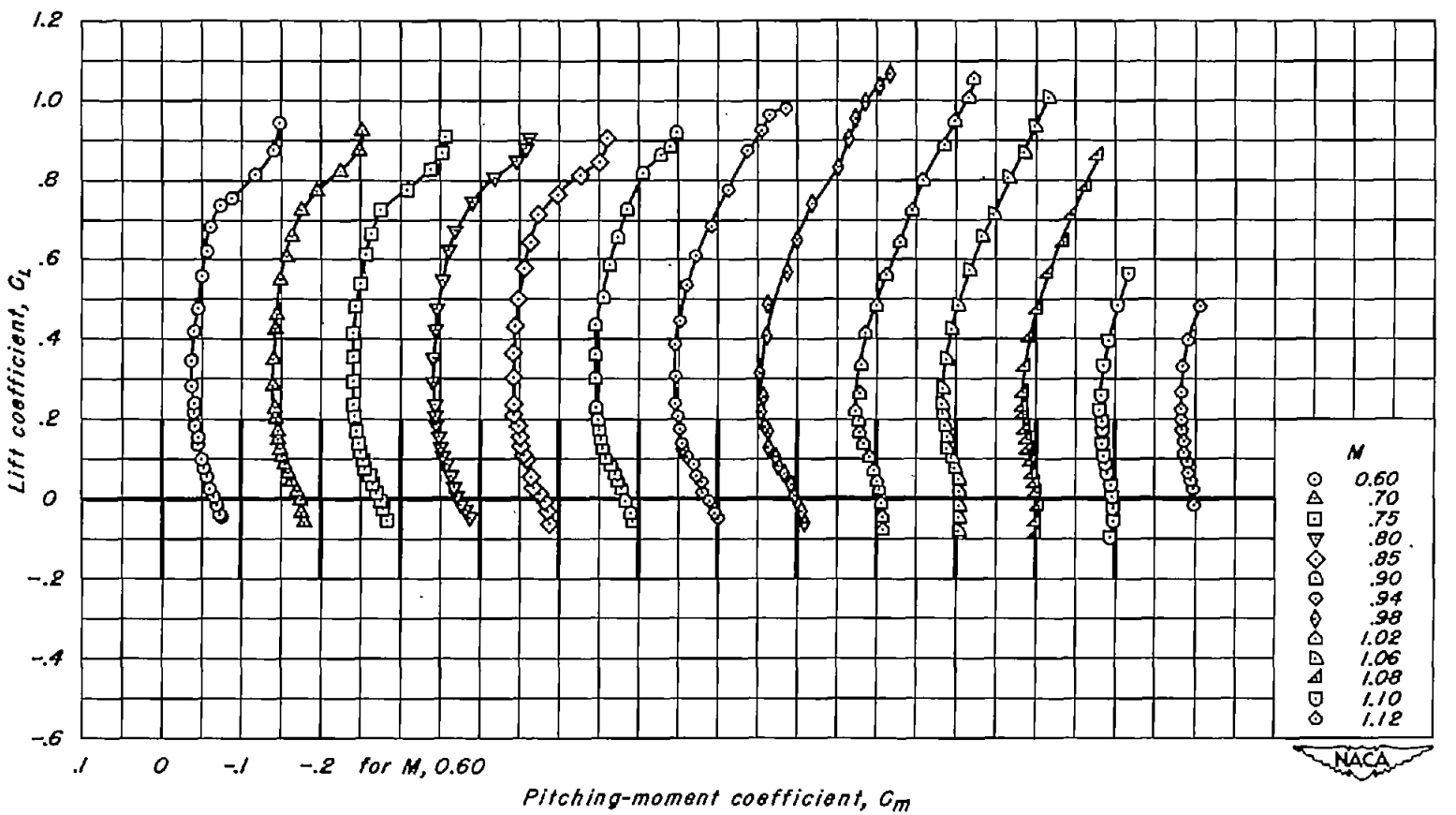

(o) A, 1, t/c, 0.10

Figure 11.- Continued.

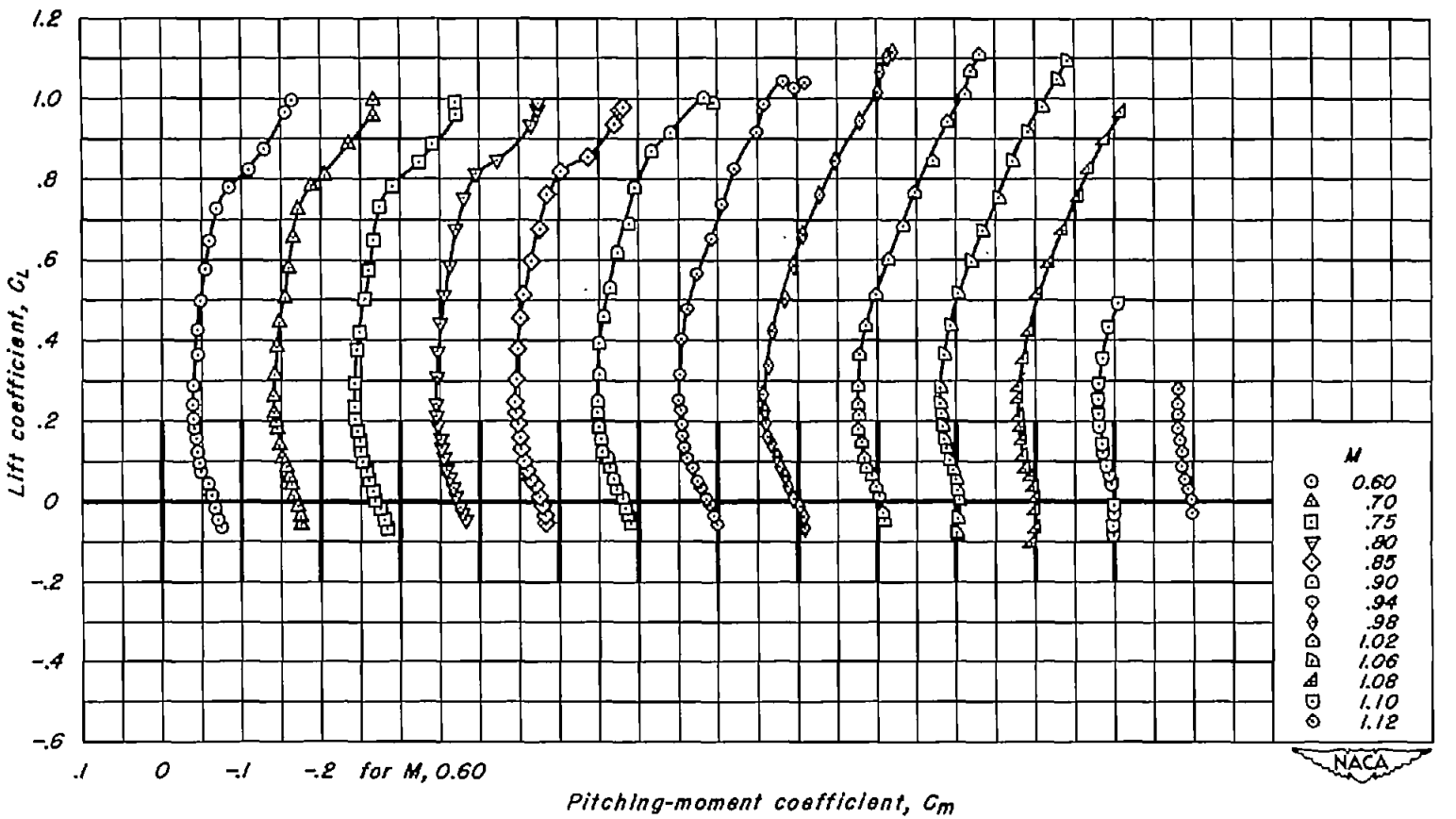

(p) A, 1; t/c, 0.08

Figure 11.- Continued.

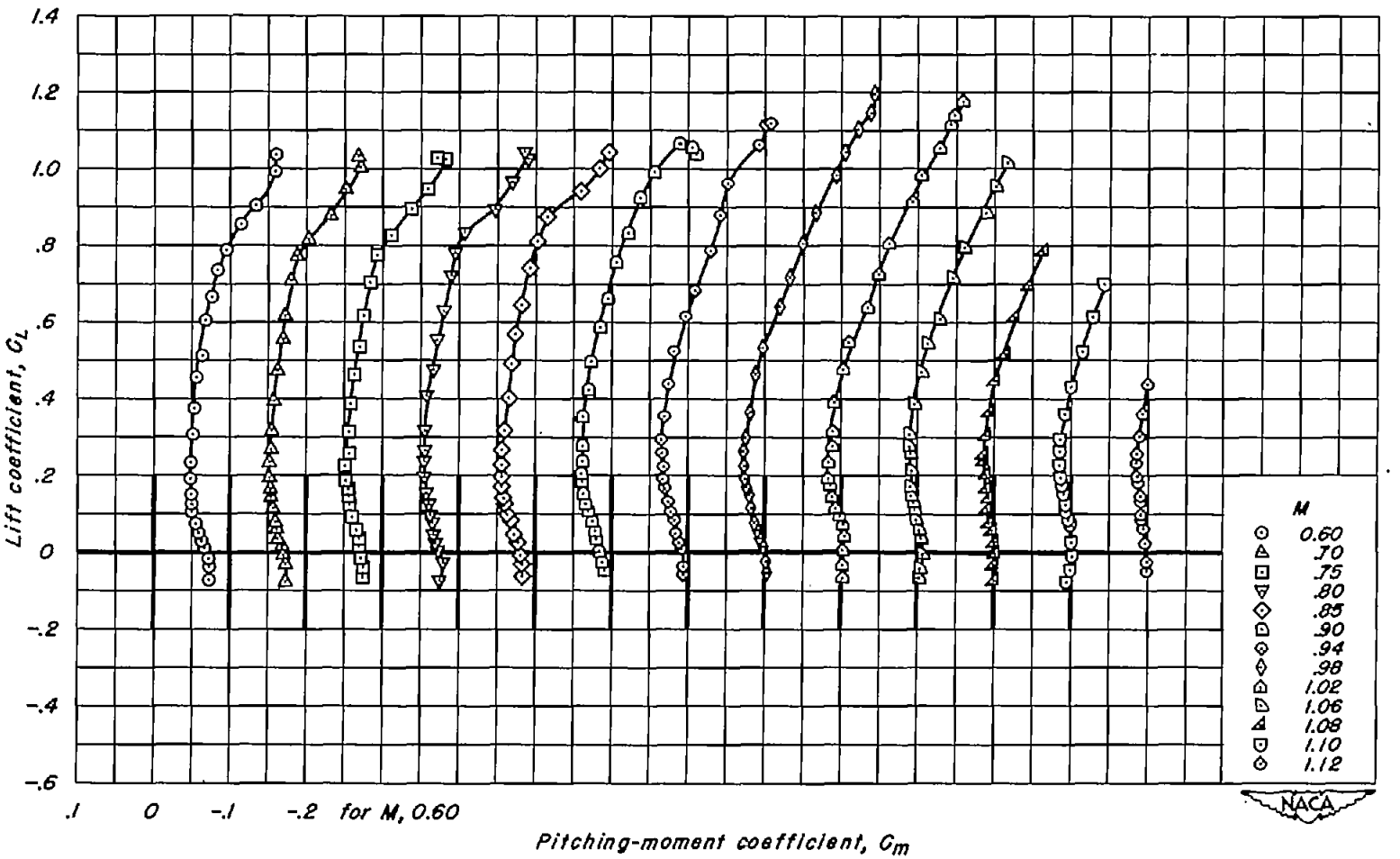

(q) A, 1; t/c, 0.06

Figure 11.- Continued.

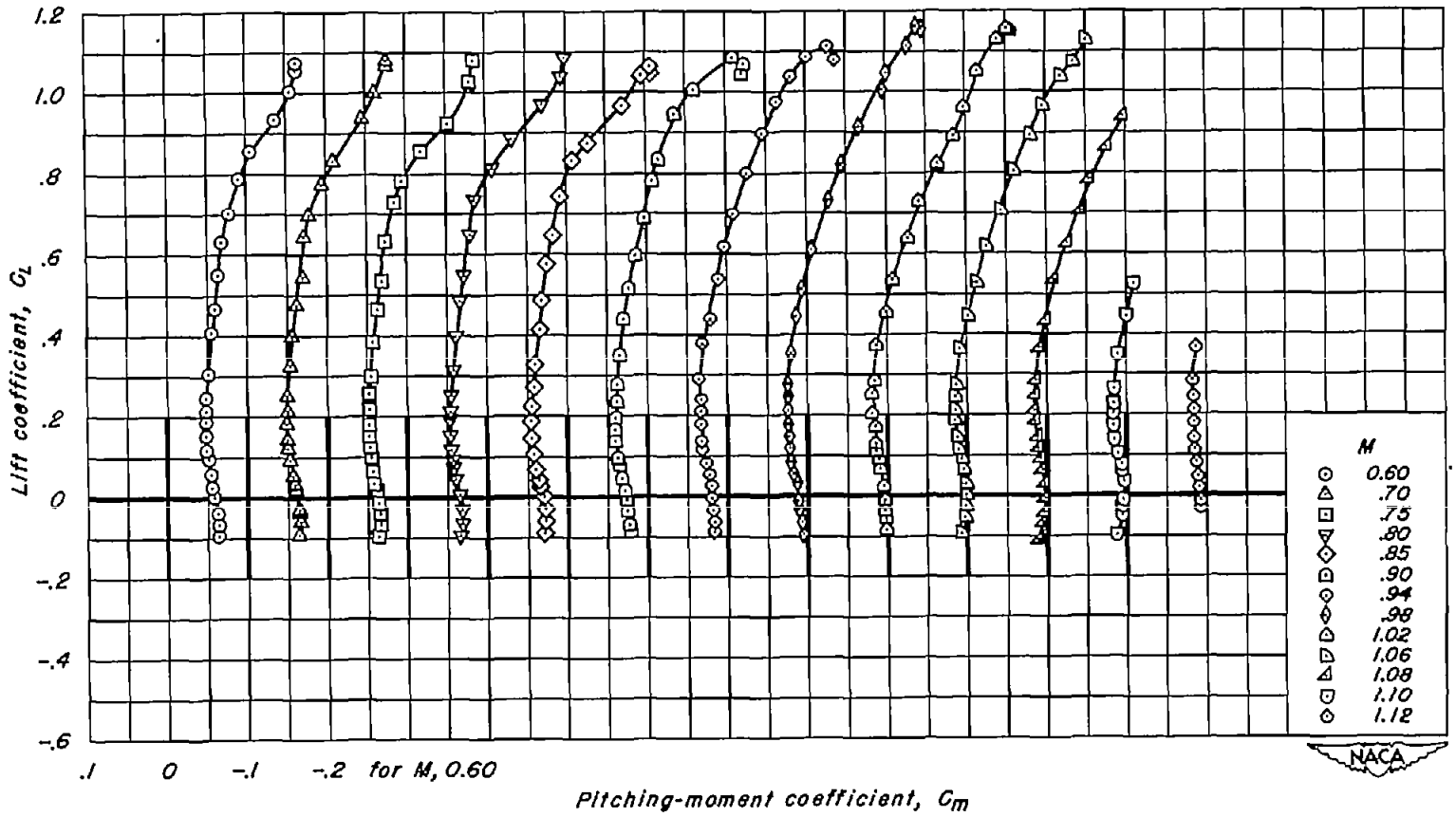

(r) A, 1; t/c, 0.04

Figure 11.- Continued.

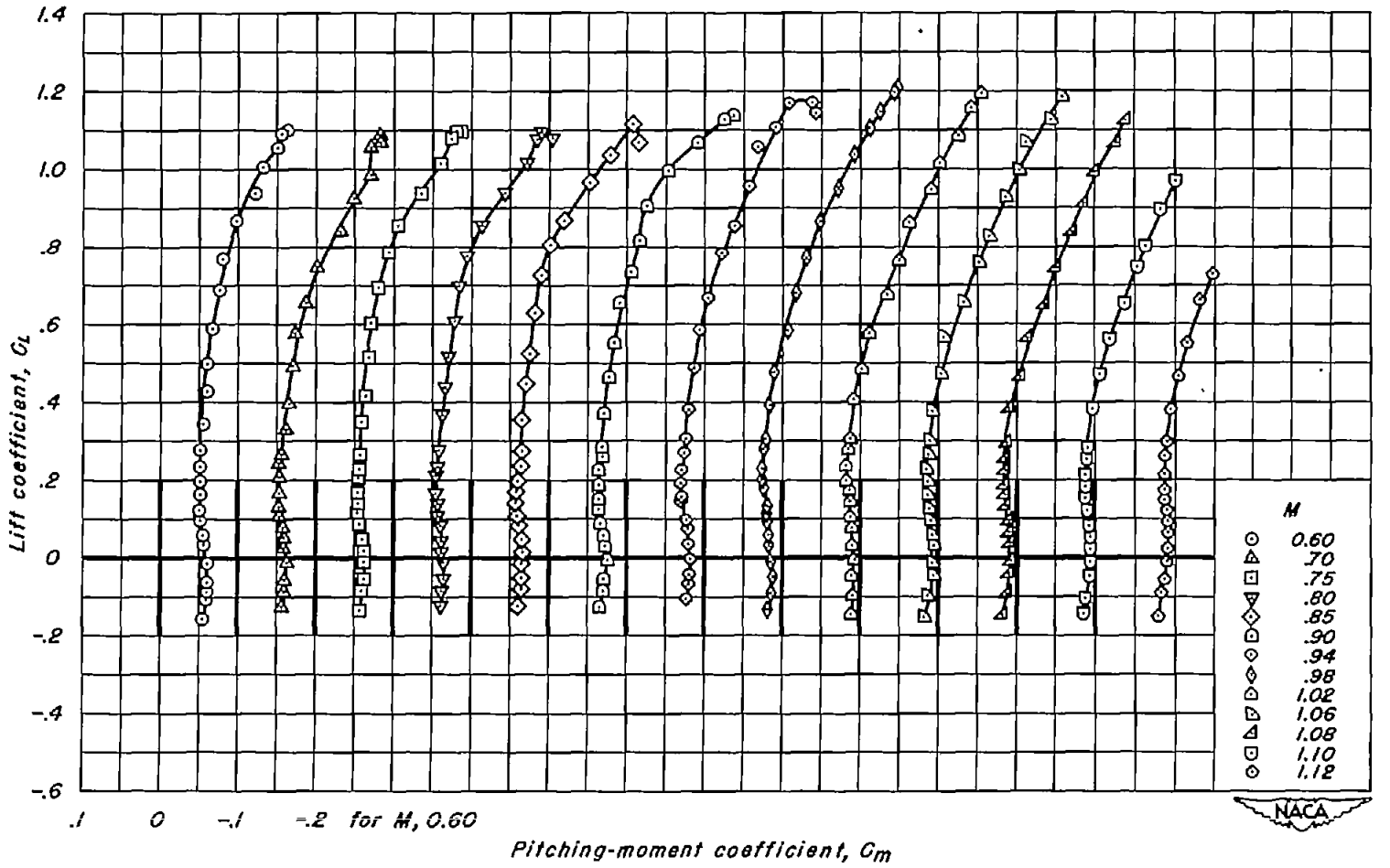

(s) A, 1; t/c, 0.02

Figure 11.- Concluded.

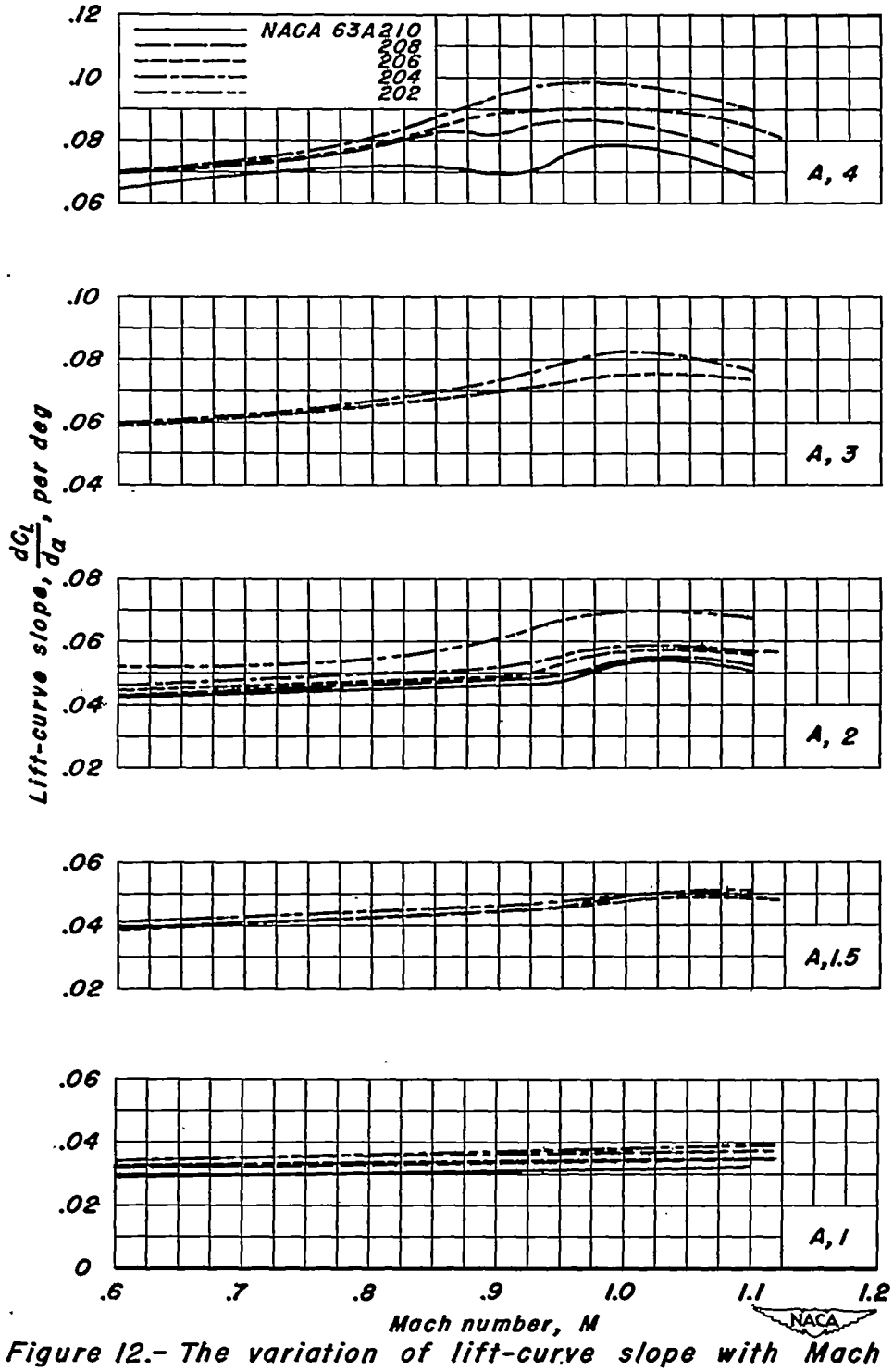

Figure 12.- The variation of lift-curve slope with Mach number for the wings with NACA 63A2XX sections at the design lift coefficient.

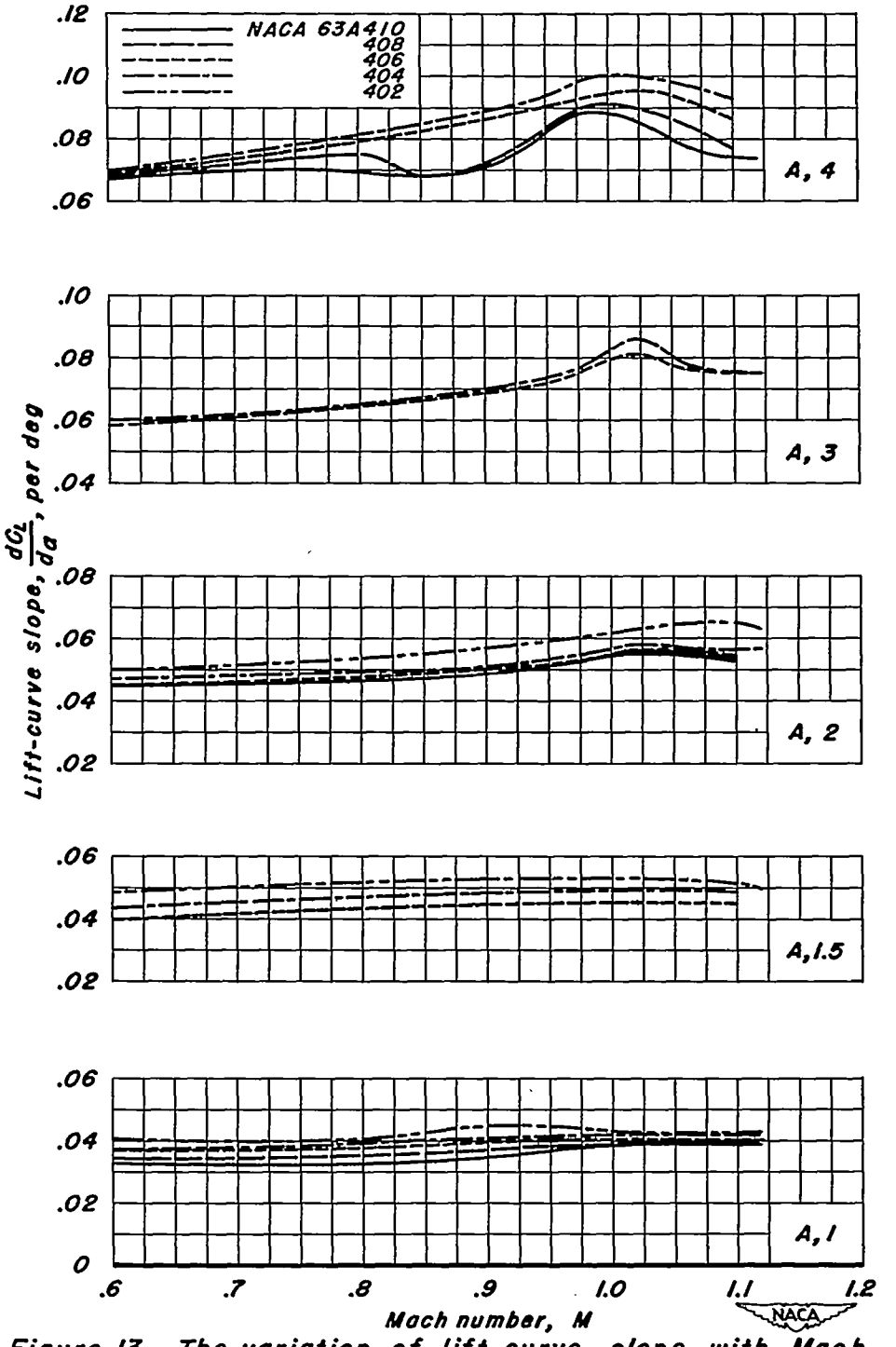

Figure 13.- The variation of lift-curve slope with Mach number for the wings with NACA 63A4XX sections at the design lift coefficient.

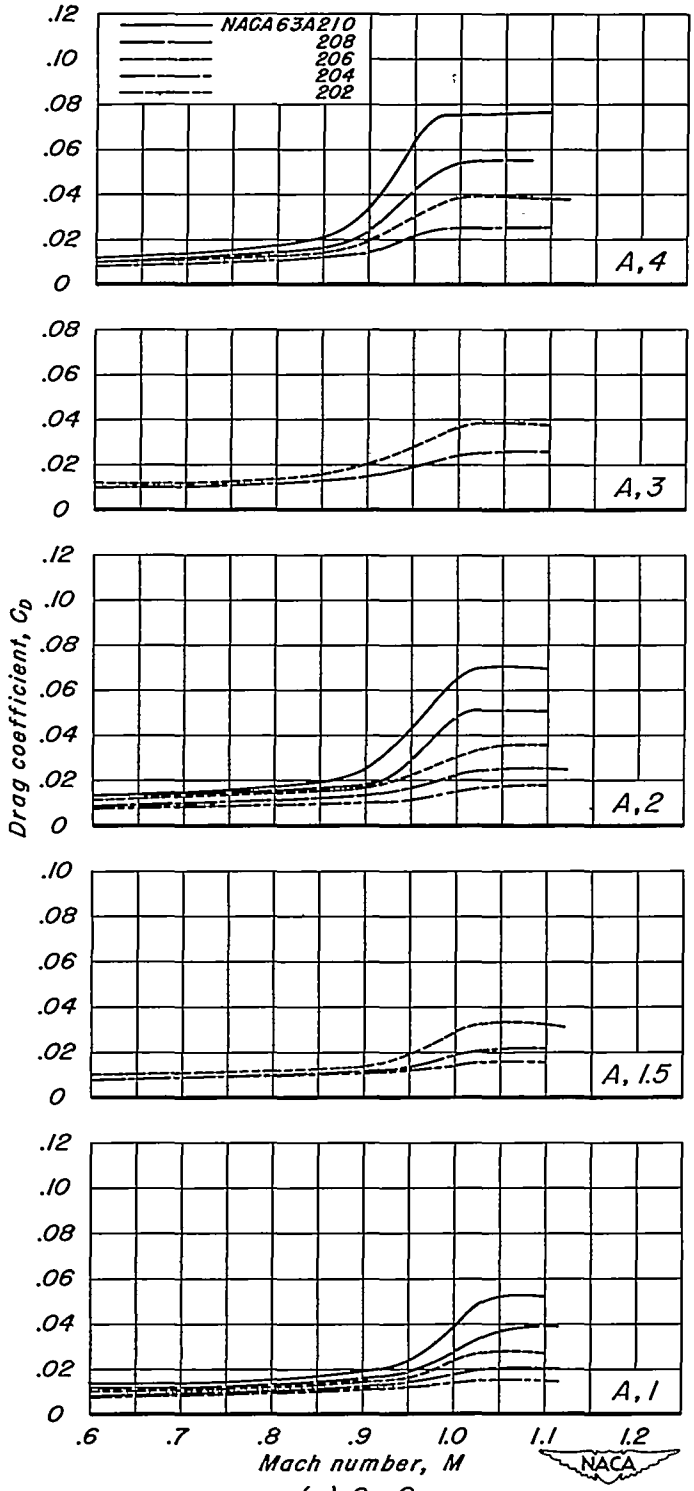

(a) C_L, 0

Figure 14.—The variation of drag coefficient with Mach number for the wings with NACA 63A2xx sections.

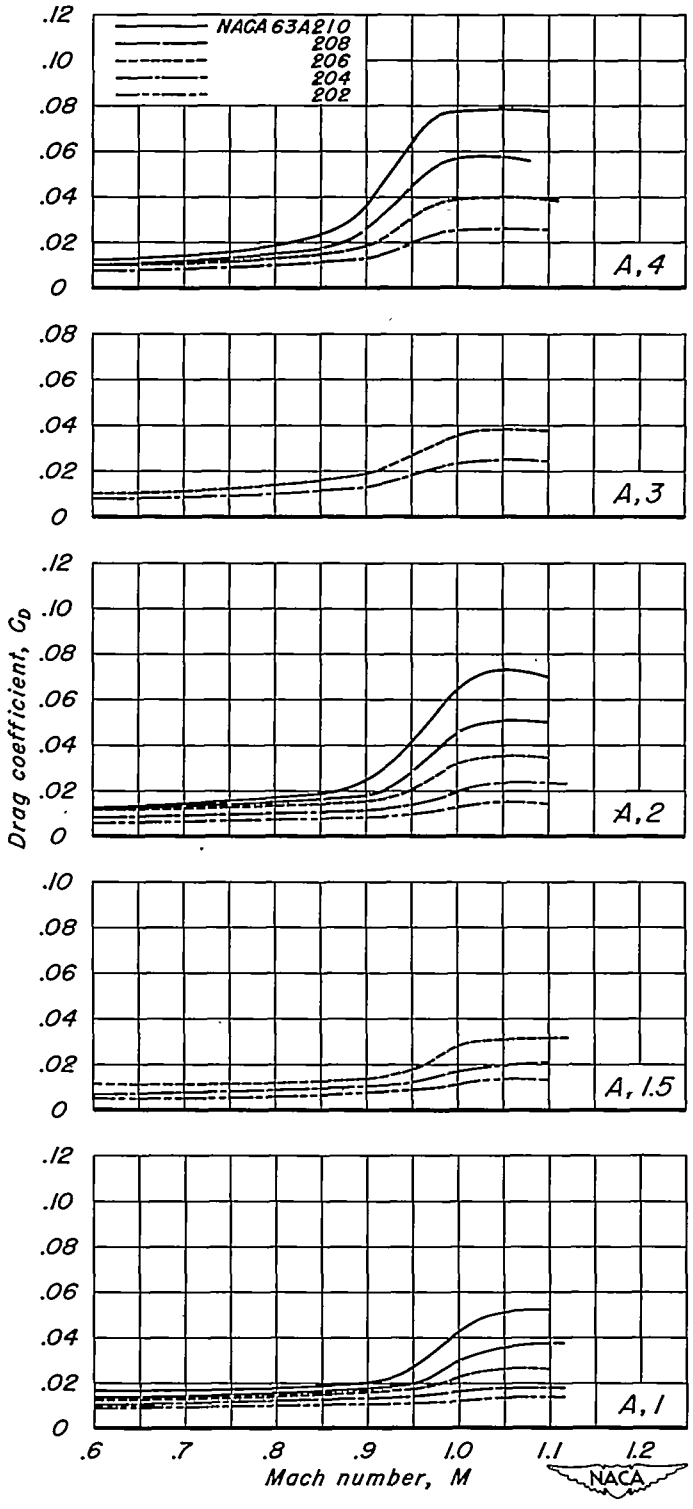

(b) C_L, 0.1

Figure 14.—Continued.

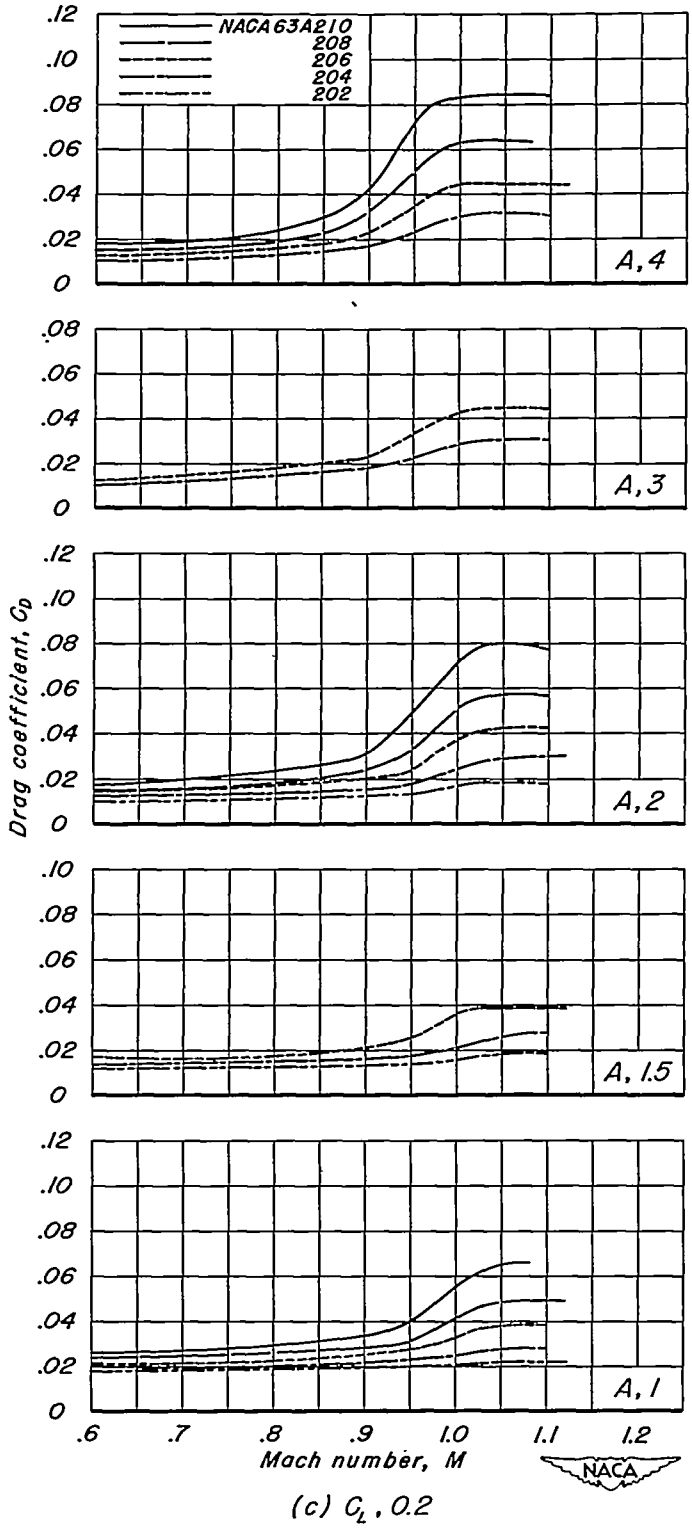

(c) C_L, 0.2

Figure 14.—Continued.

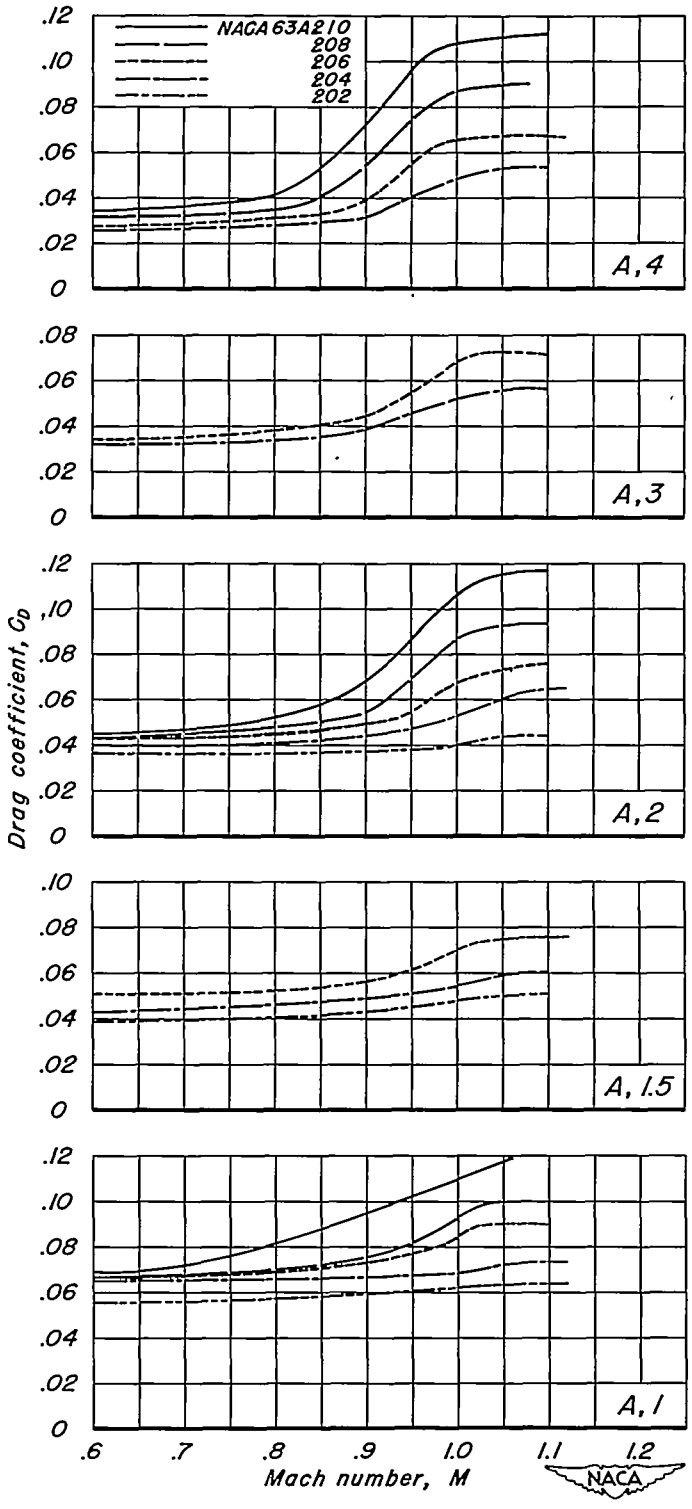

(d) C_L, 0.4

Figure 14.—Concluded.

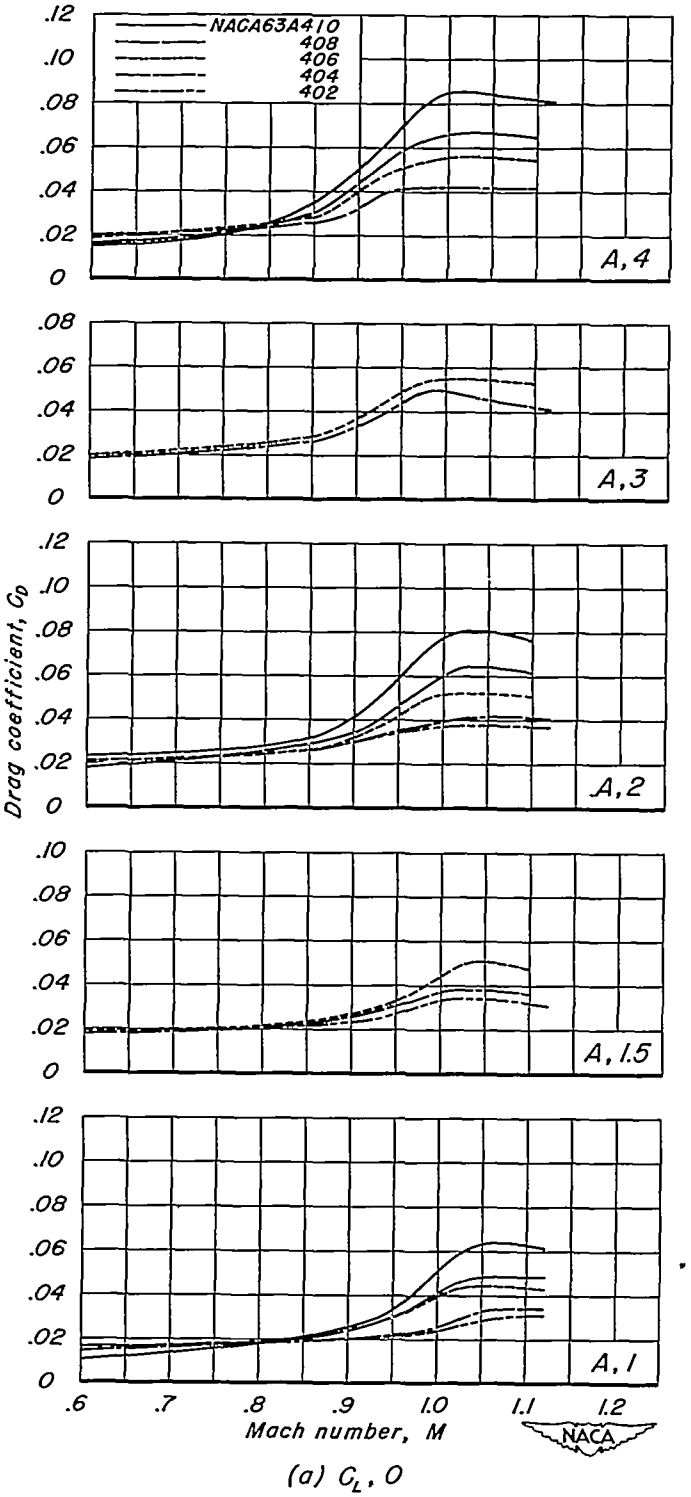

(a) C_L, 0

Figure 15.–The variation of drag coefficient with Mach number for the wings with NACA 63A4xx sections.

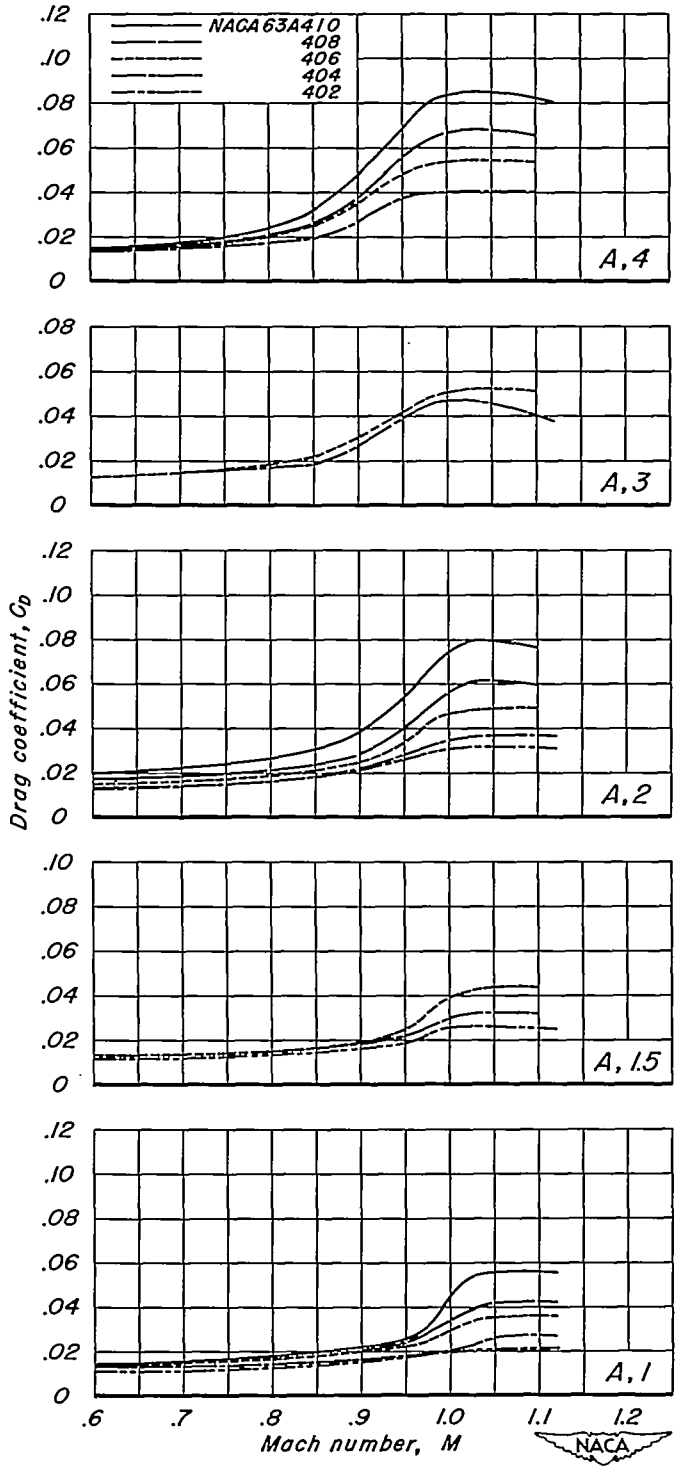

(b) C_L, 0.1

Figure 15.—Continued.

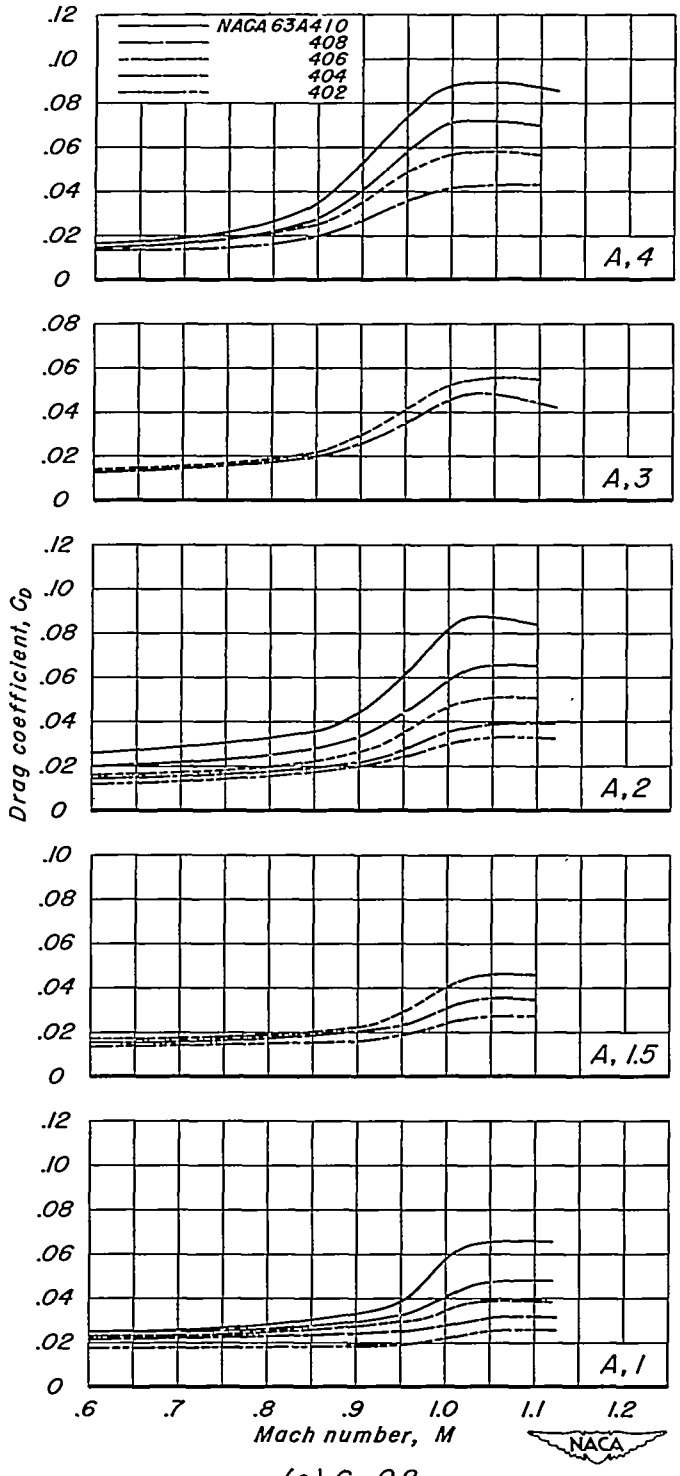

(c) C_L, 0.2

Figure 15.— Continued.

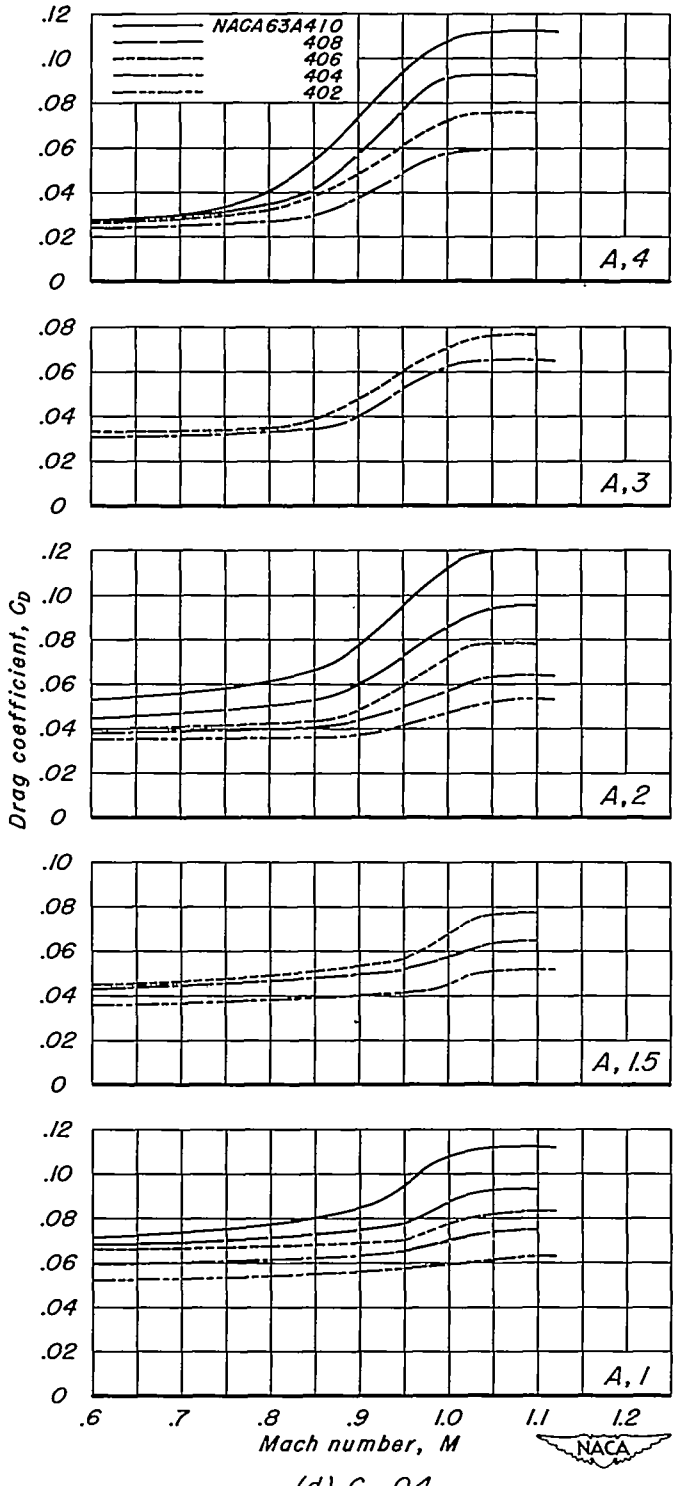

(d) C_L, 0.4

Figure 15.—Concluded.

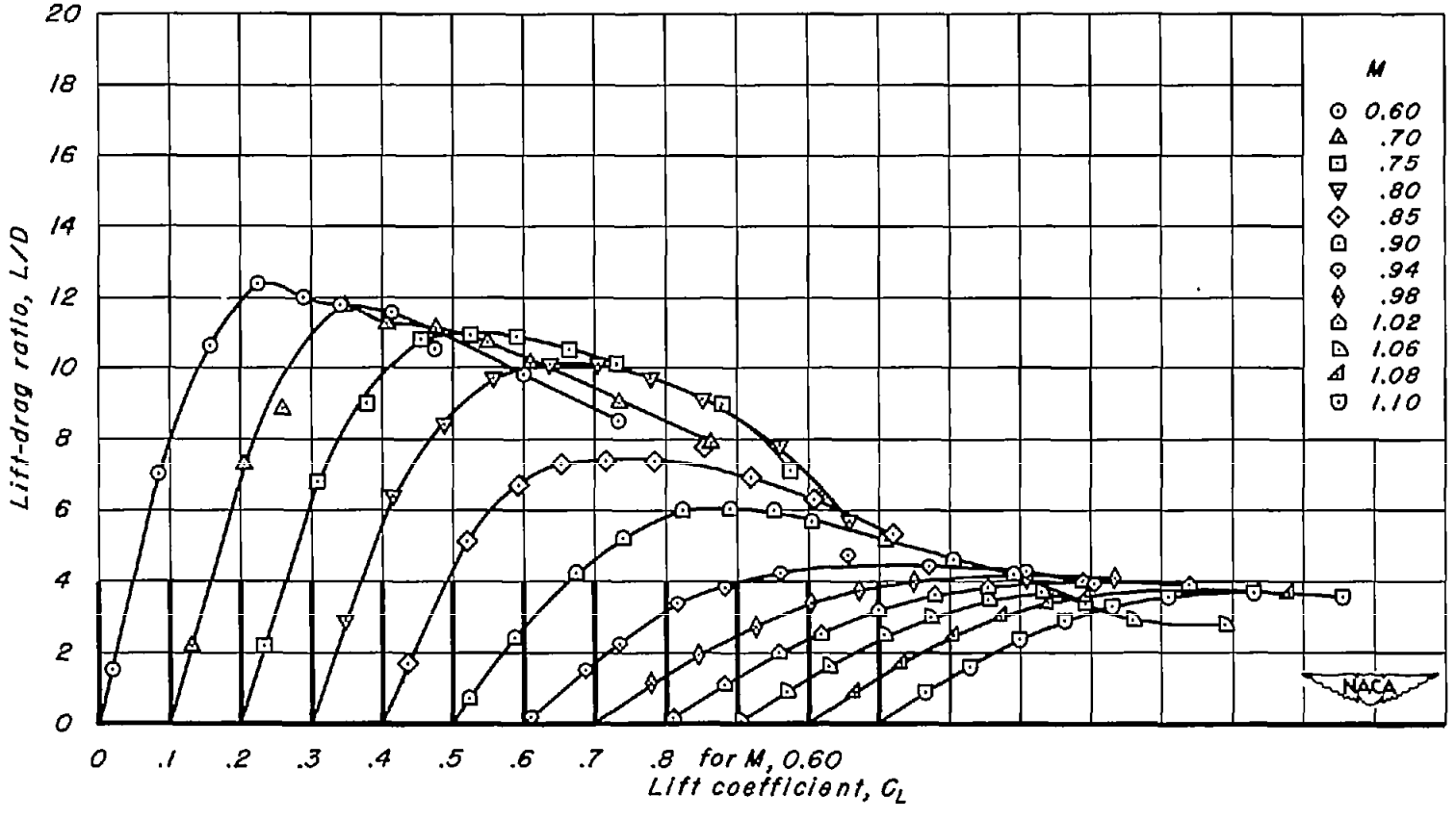

(a) A, 4; t/c, 0.10

Figure 16.—The variation of lift-drag ratio with lift coefficient for the wings with the NACA 63A2xx sections.

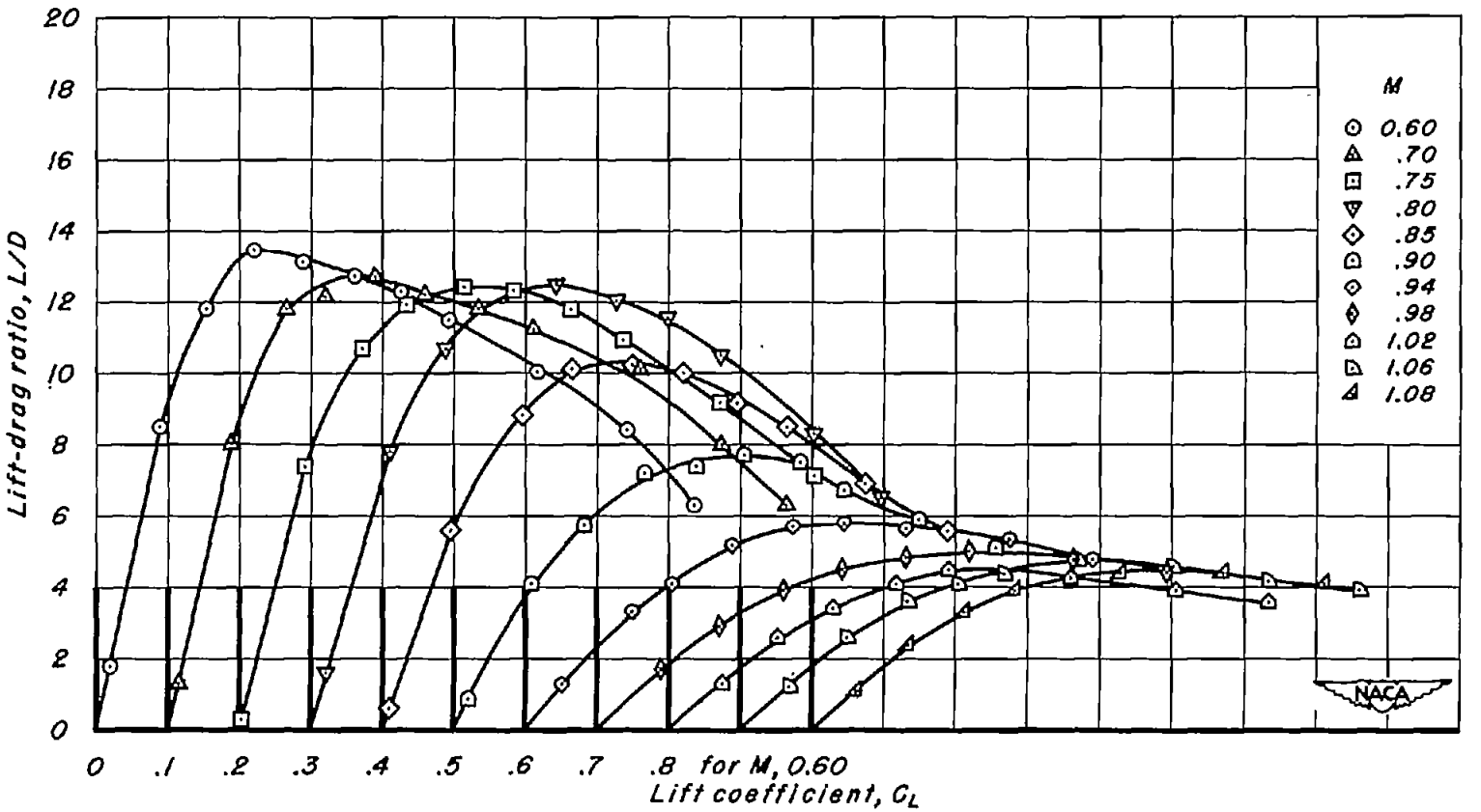

(b) A, 4, t/c, 0.08

Figure 16.- Continued.

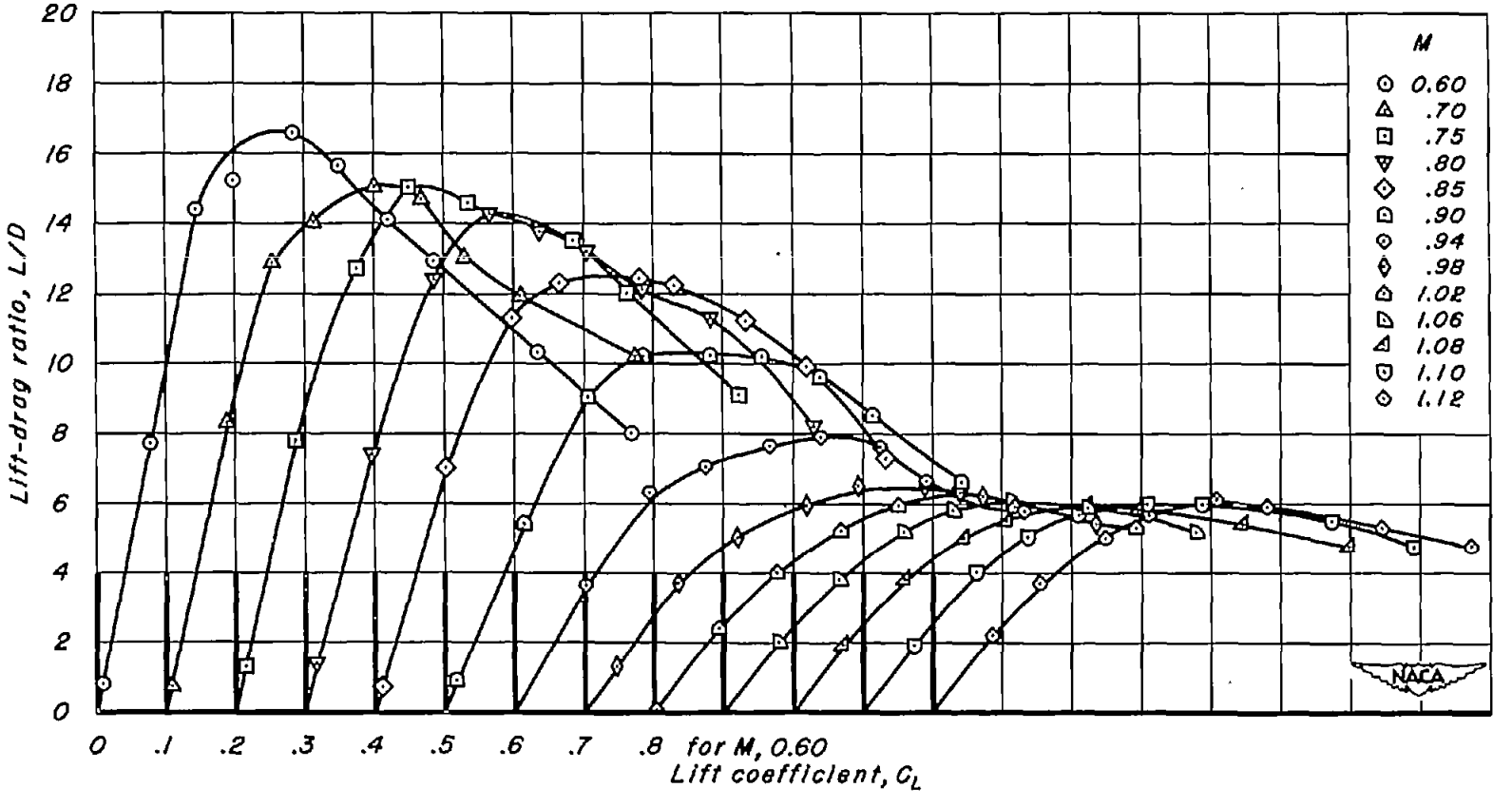

(c) A, 4; t/c, 0.06

Figure 16.- Continued.

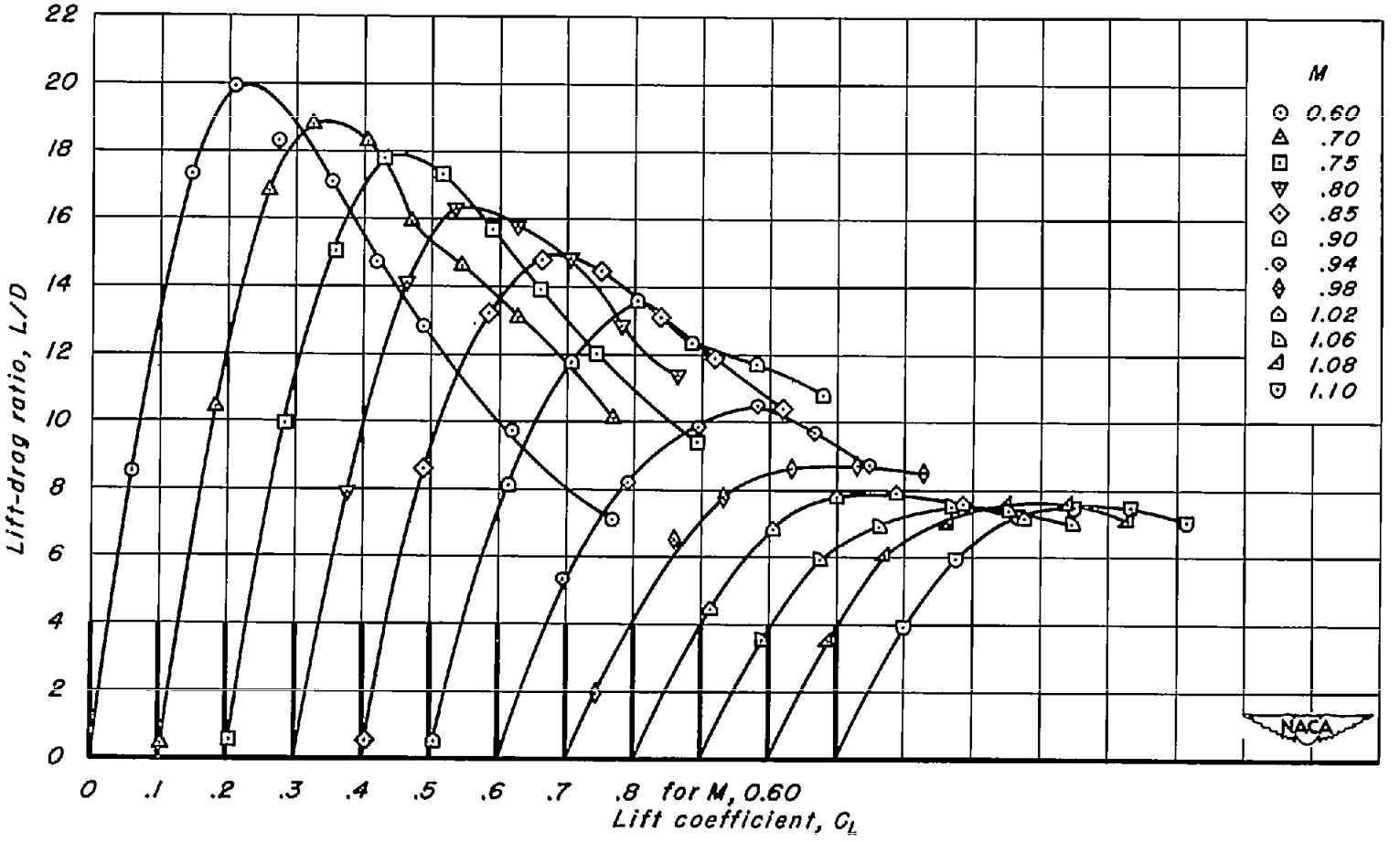

(d) A, 4; t/c, 0.04

Figure 16.- Continued.

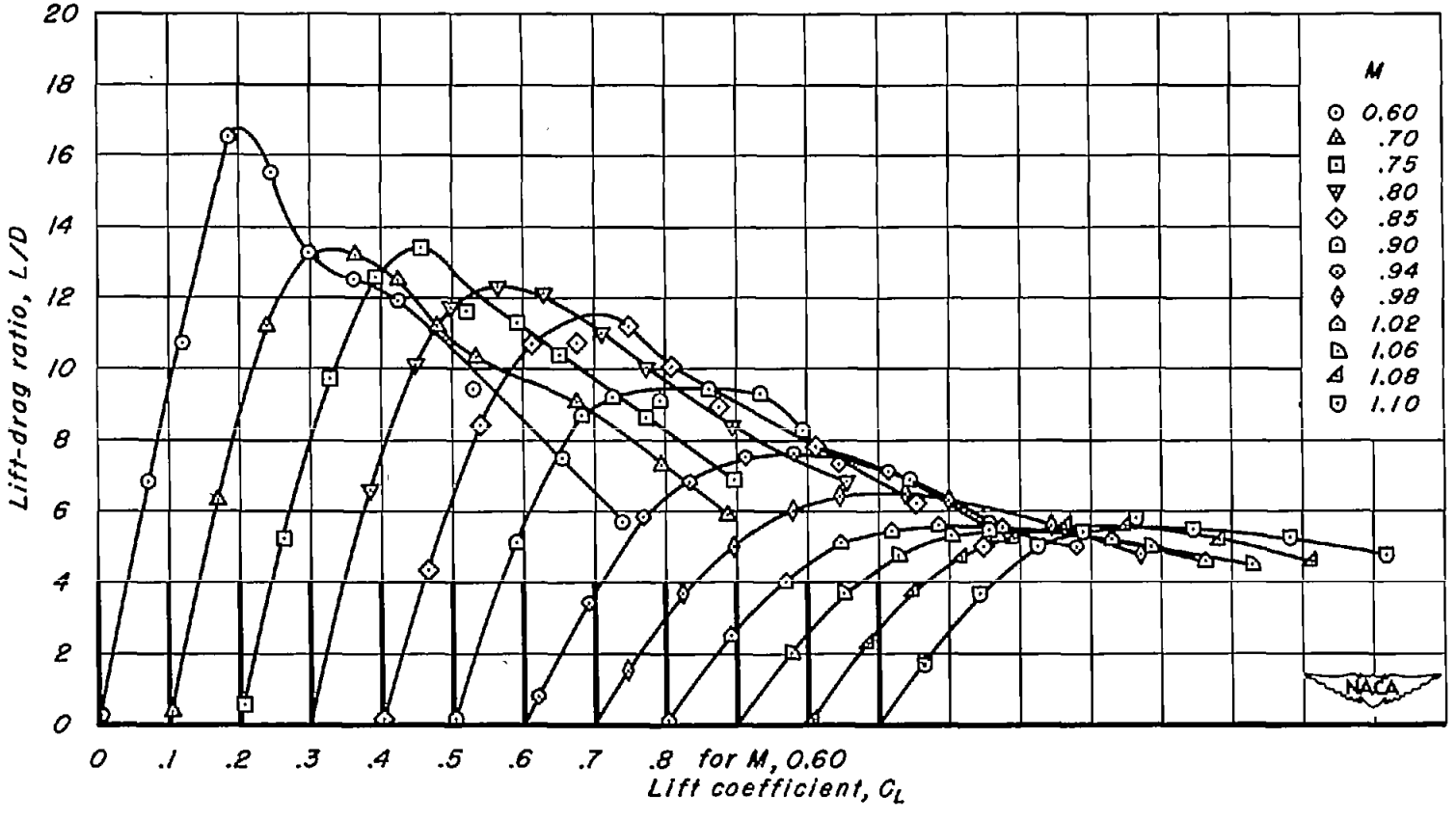

(e) A, 3; t/c, 0.06

Figure 16.- Continued.

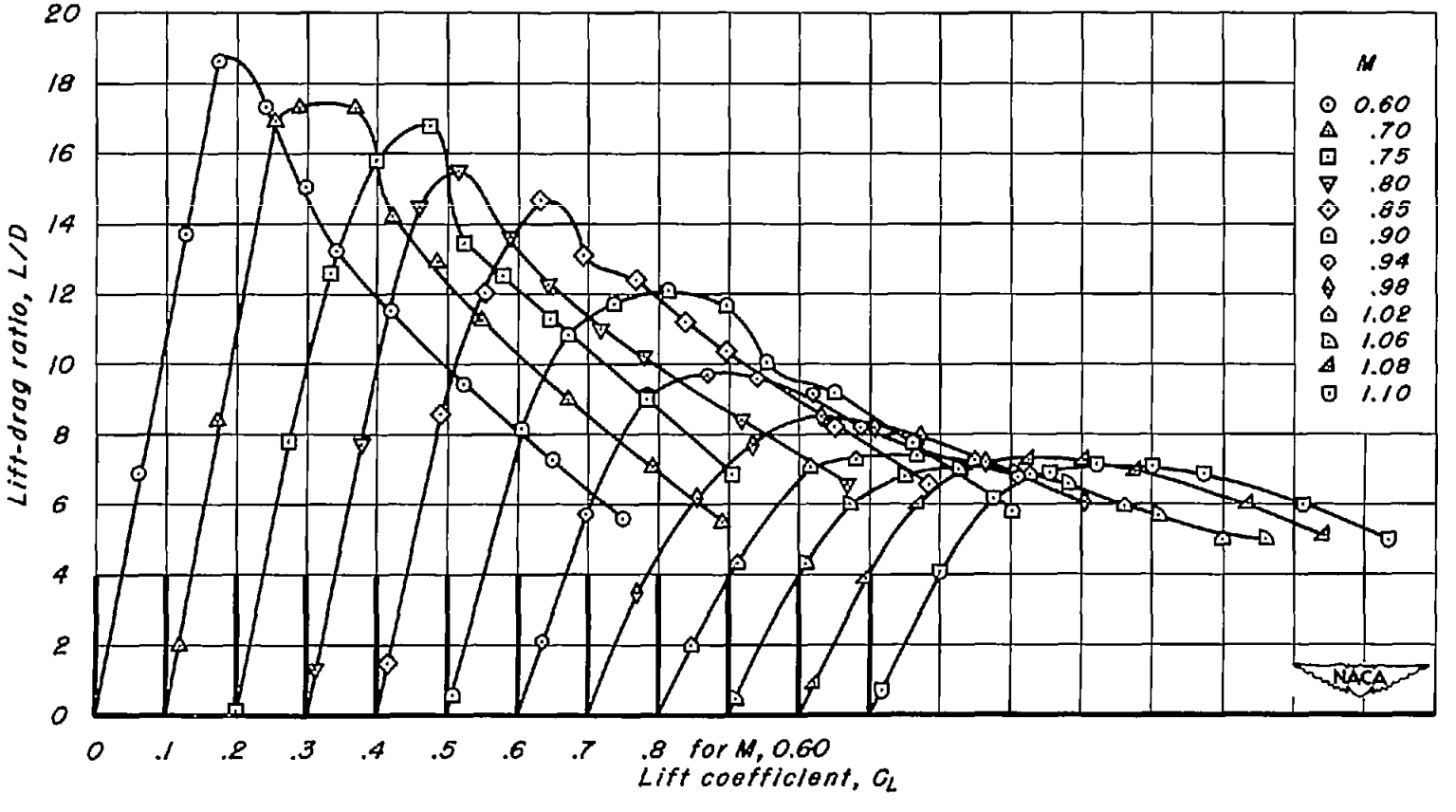

(f) A, 3; t/c, 0.04

Figure 16.- Continued.

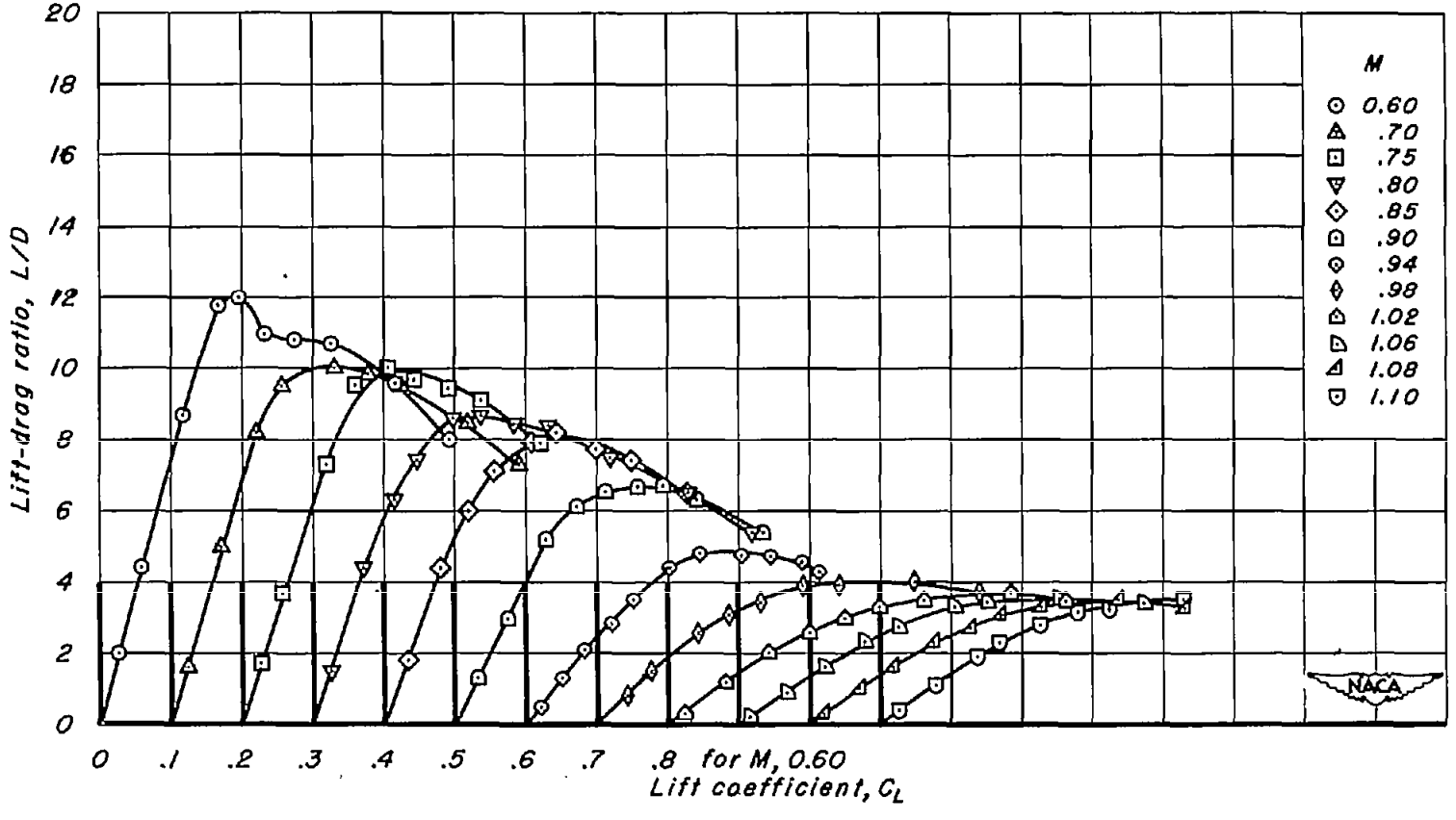

(g) A, 2; t/c, 0.10.

Figure 16.- Continued.

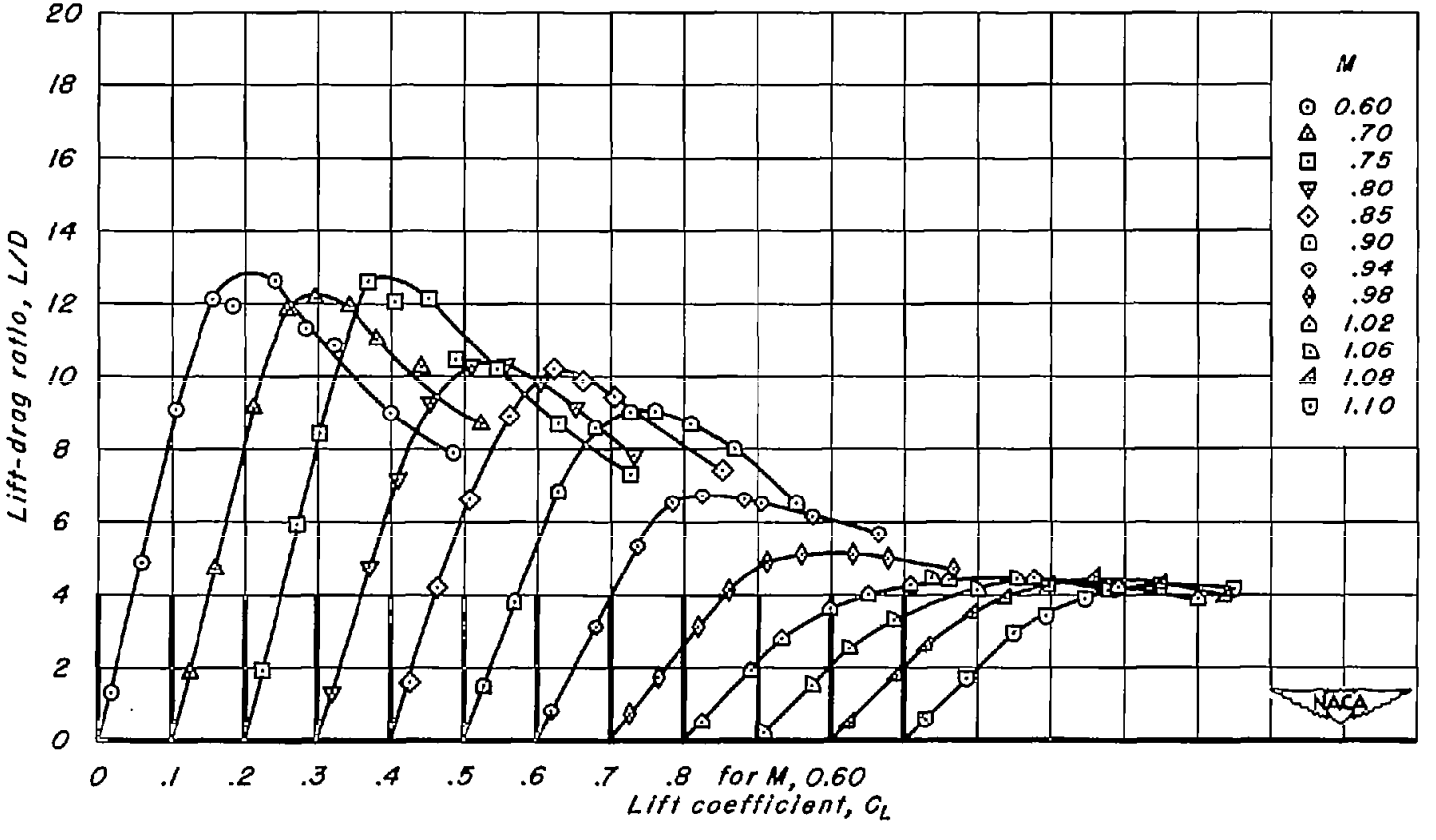

(h) A, 2; t/c, 0.08

Figure 16.- Continued.

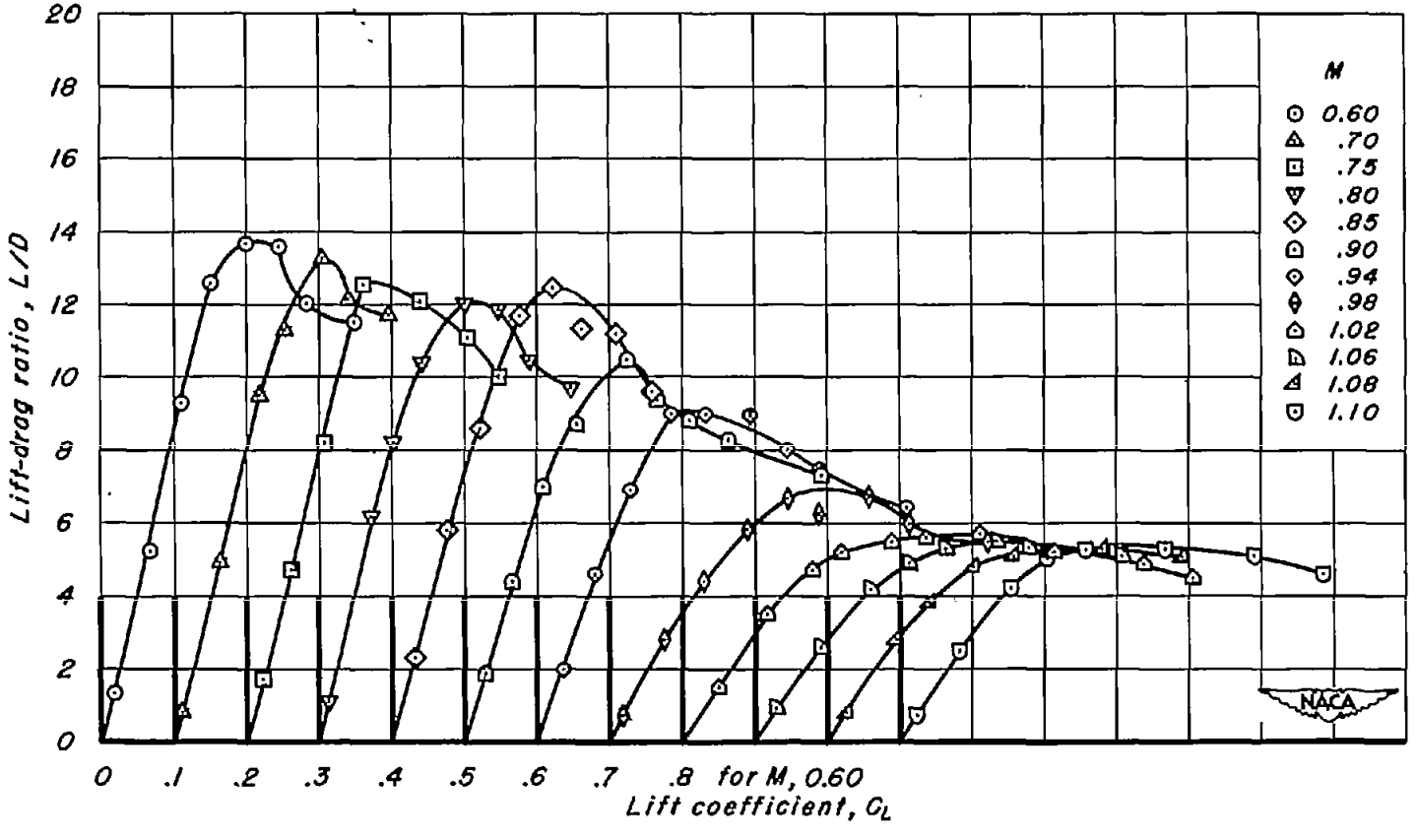

(i) A, 2; t/c, 0.06

Figure 16.- Continued.

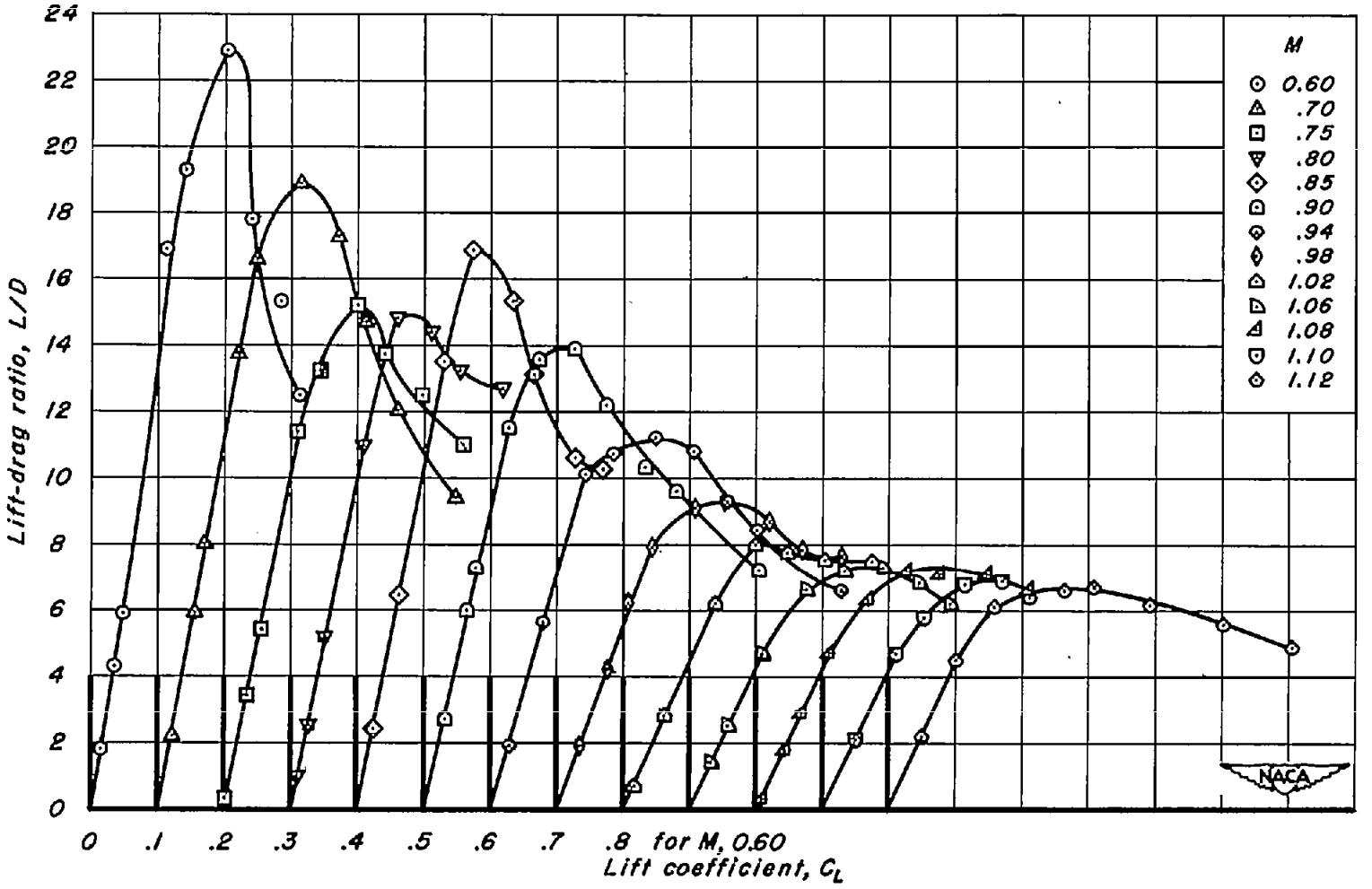

(j) A, 2; t/c, 0.04

Figure 16.- Continued.

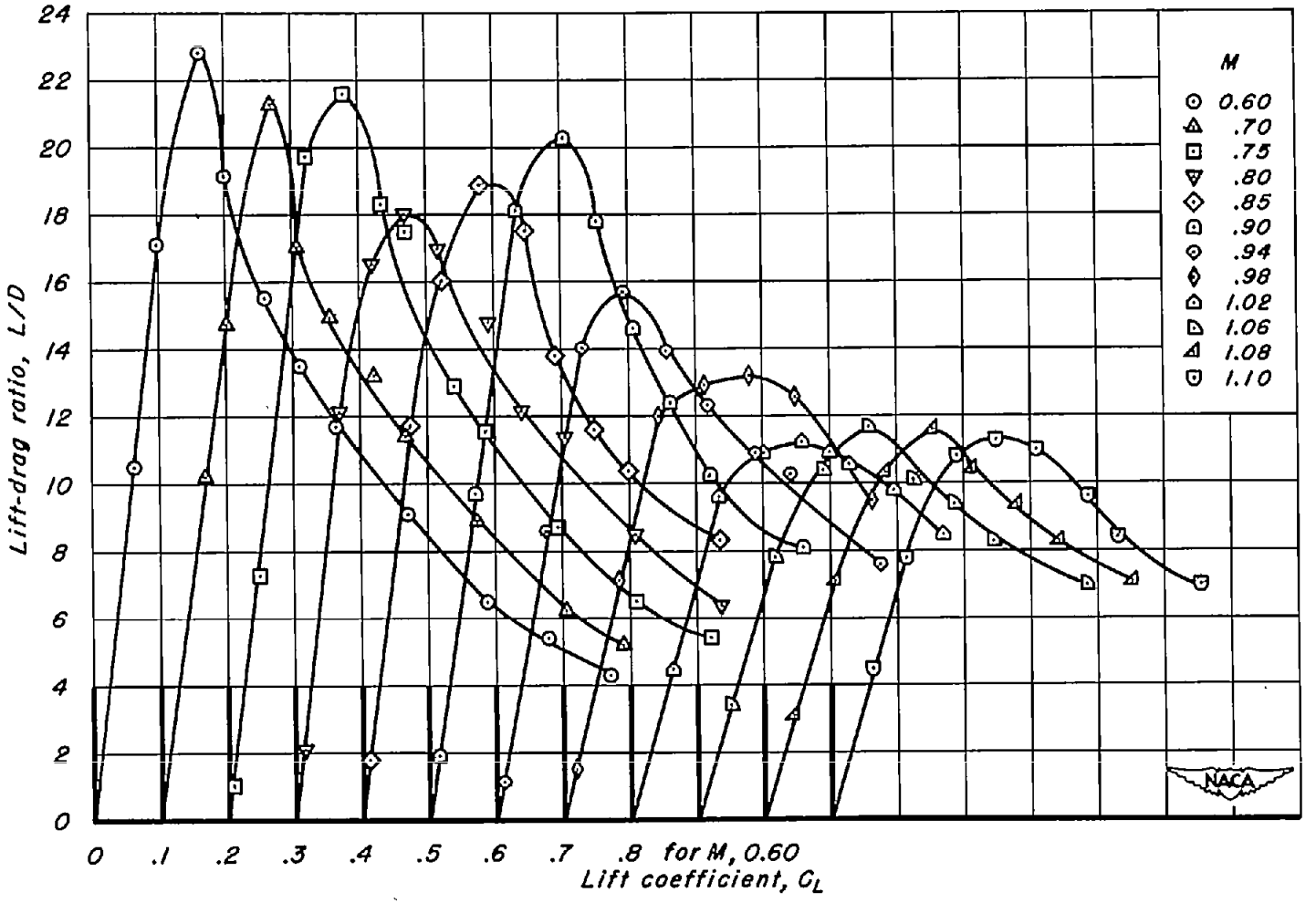

(k) A, 2; t/c, 0.02

Figure 16.- Continued.

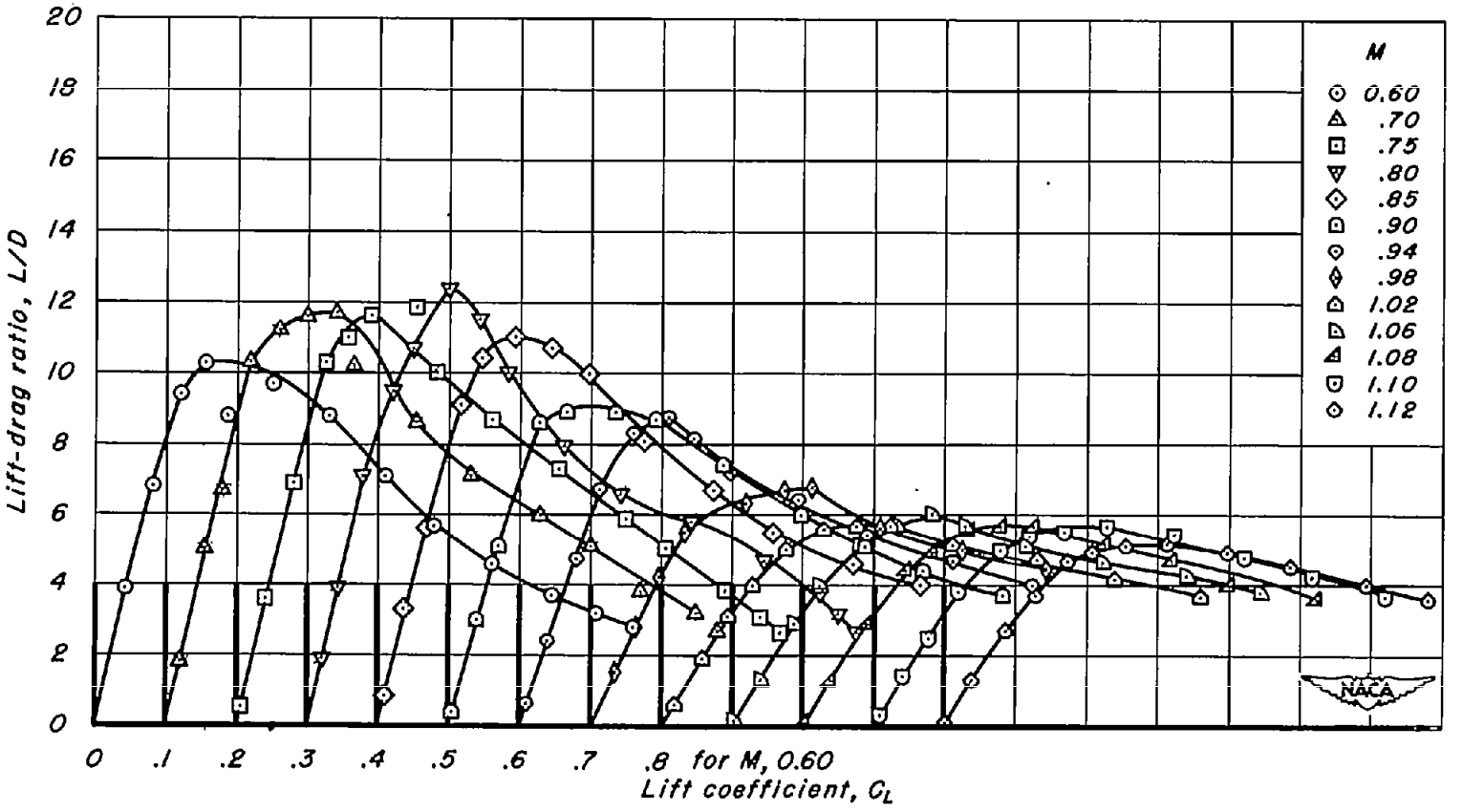

(1) A,1.5; t/c, 0.06

Figure 16.- Continued.

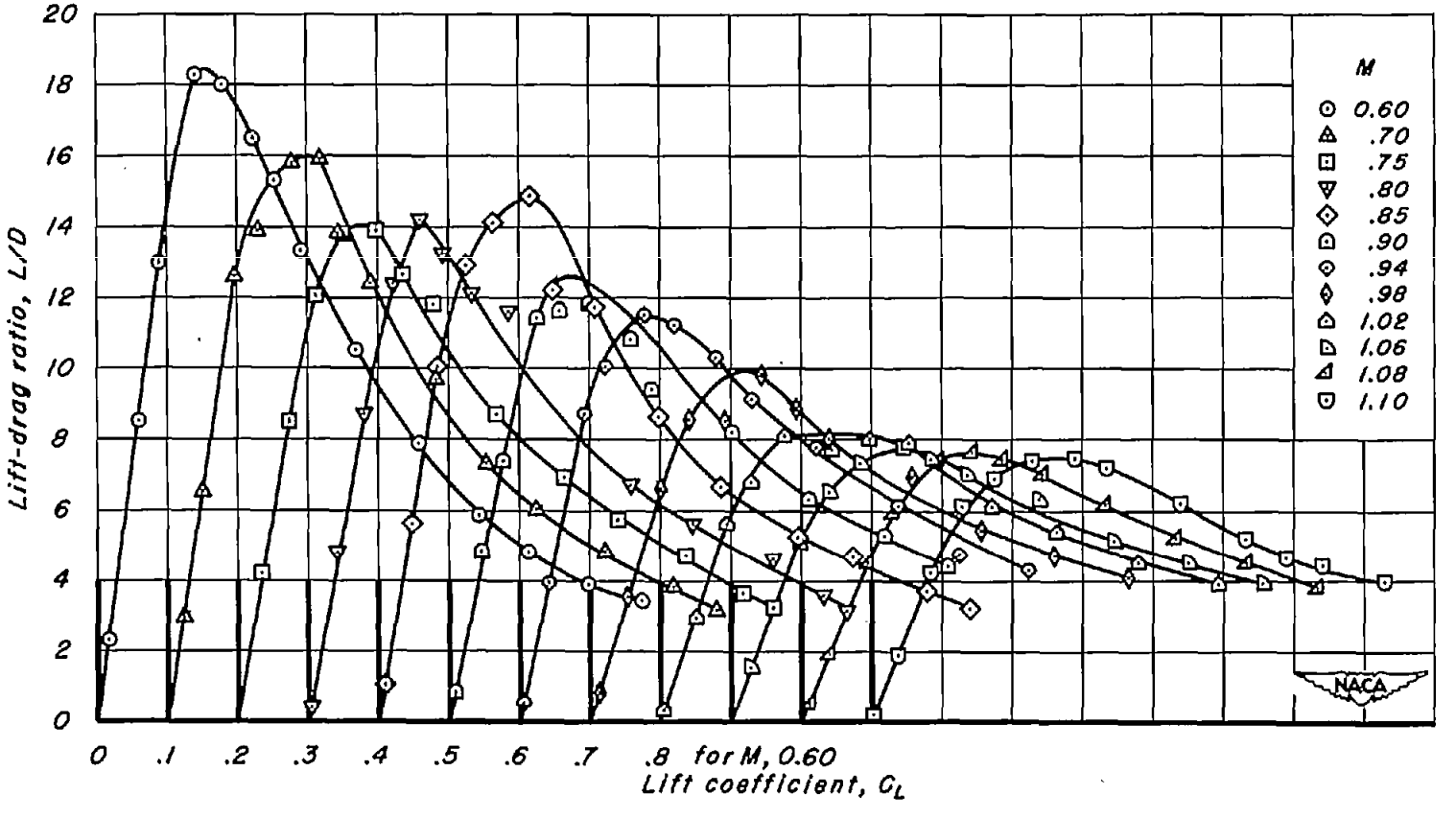

(m) A, 1.5; t/c, 0.04

Figure 16.- Continued.

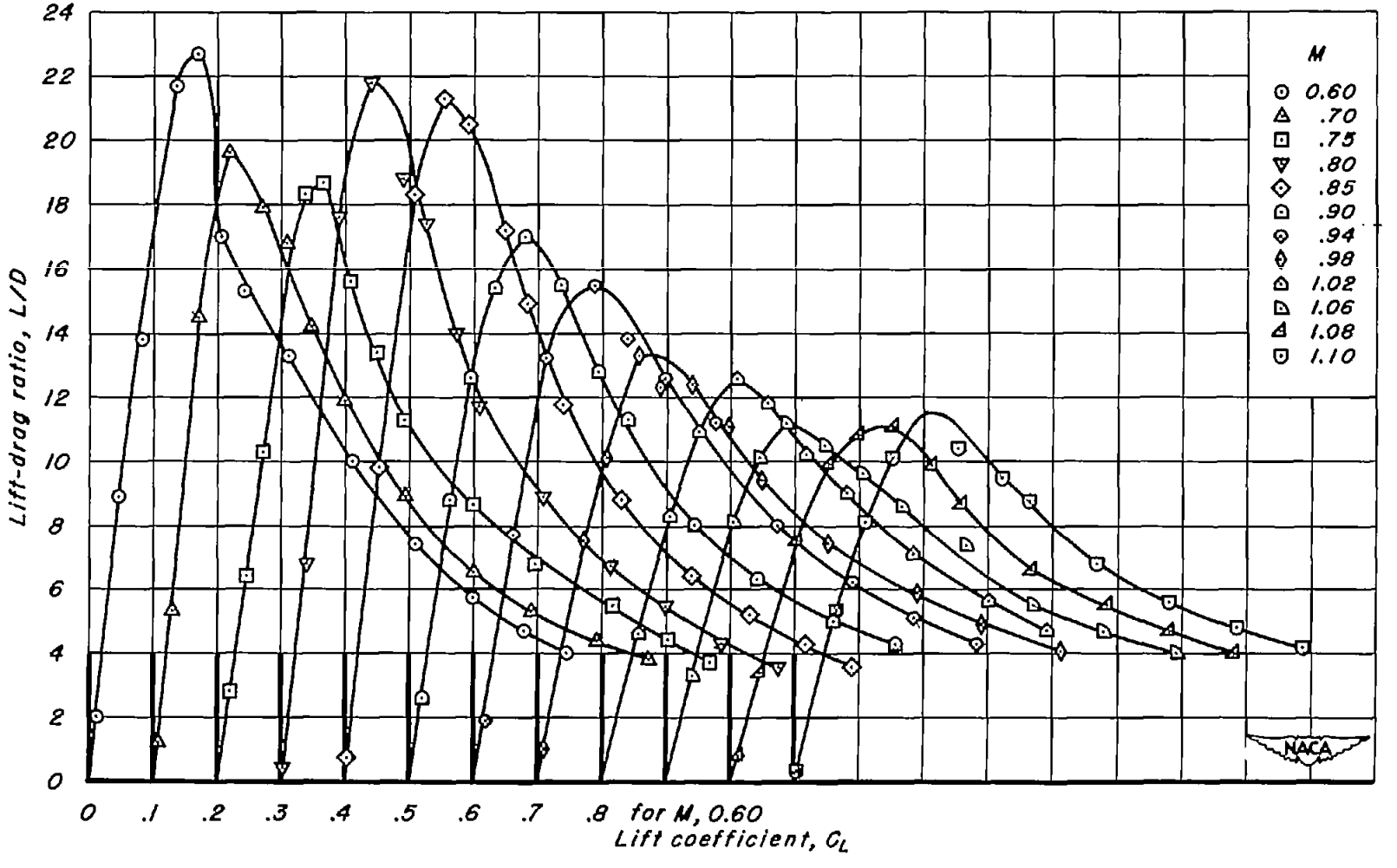

(n) A,1.5; t/c, 0.02

Figure 16.- Continued.

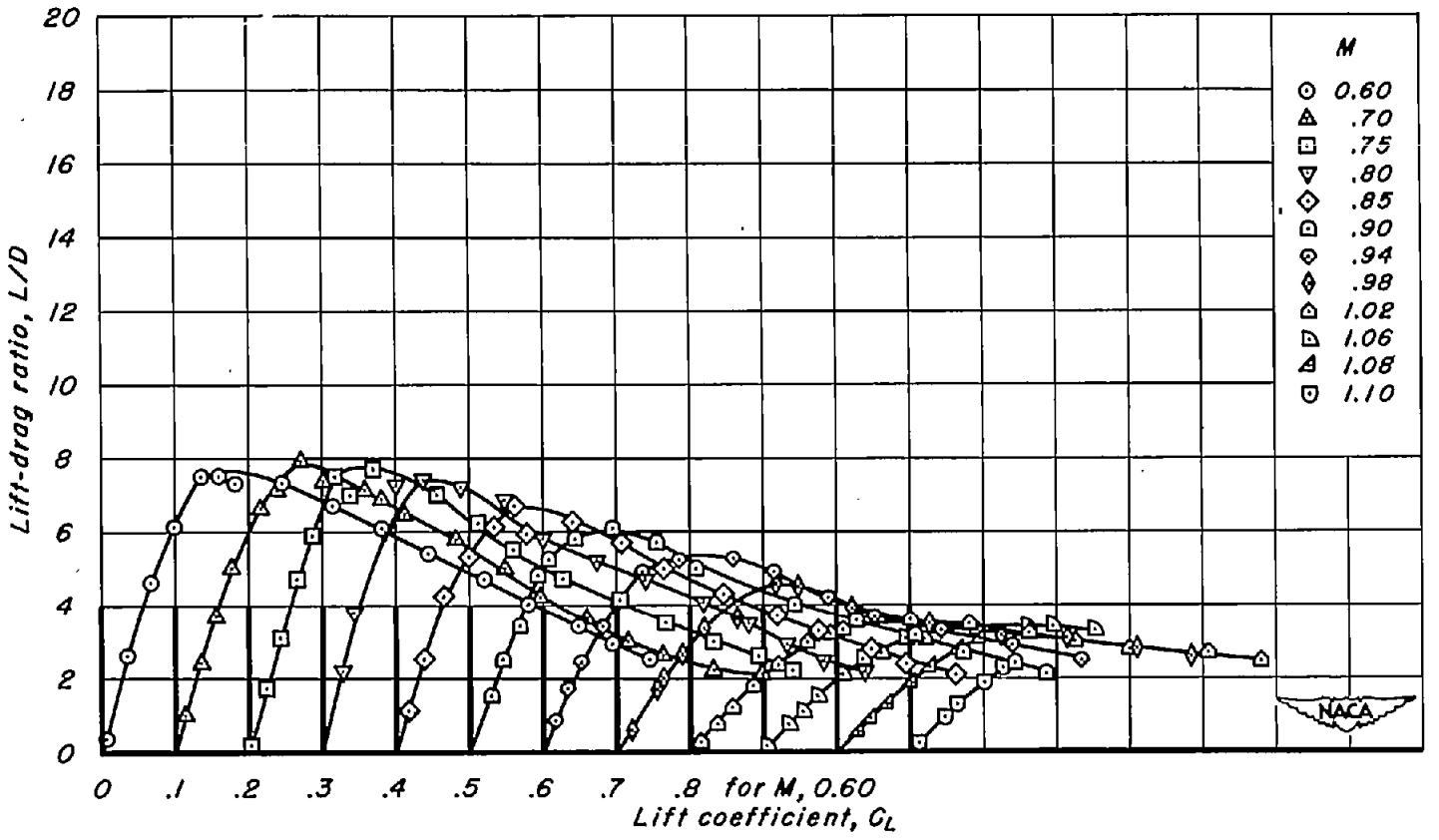

(o) A, 1; t/c, 0.10

Figure 16.- Continued.

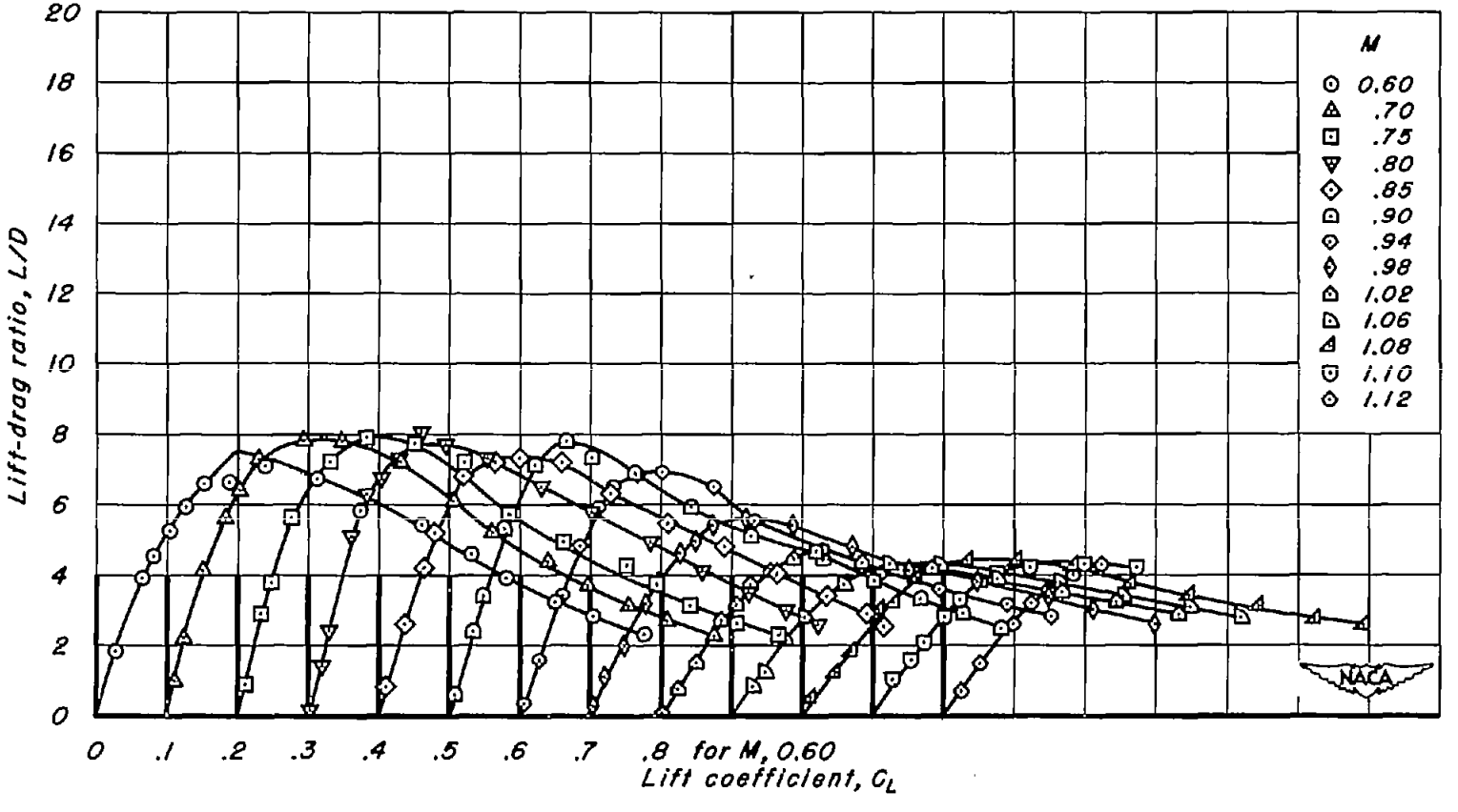

(p) A, 1; t/c, 0.08

Figure 16.- Continued.

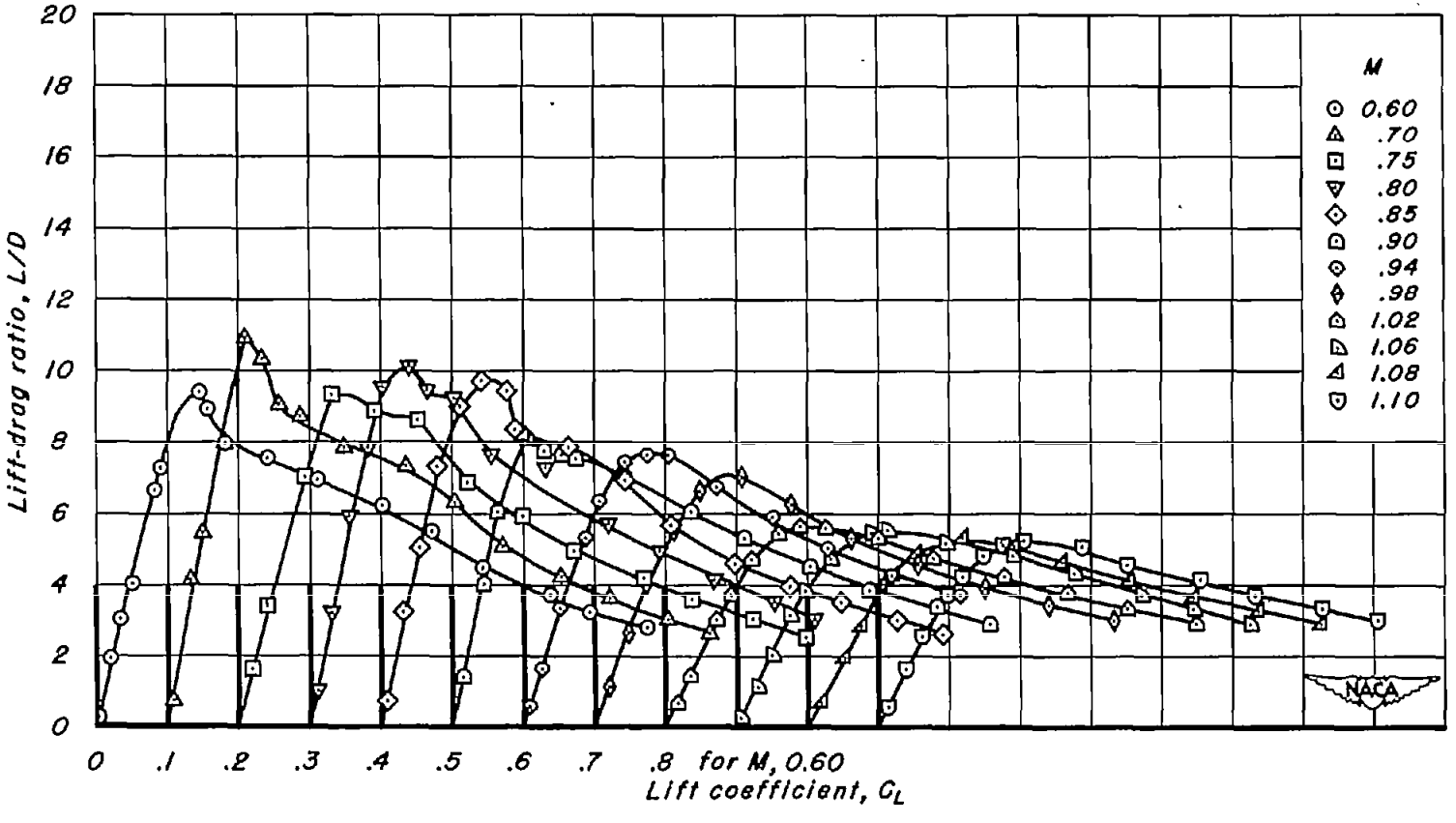

(q) A, 1; t/c, 0.06

Figure 16.- Continued.

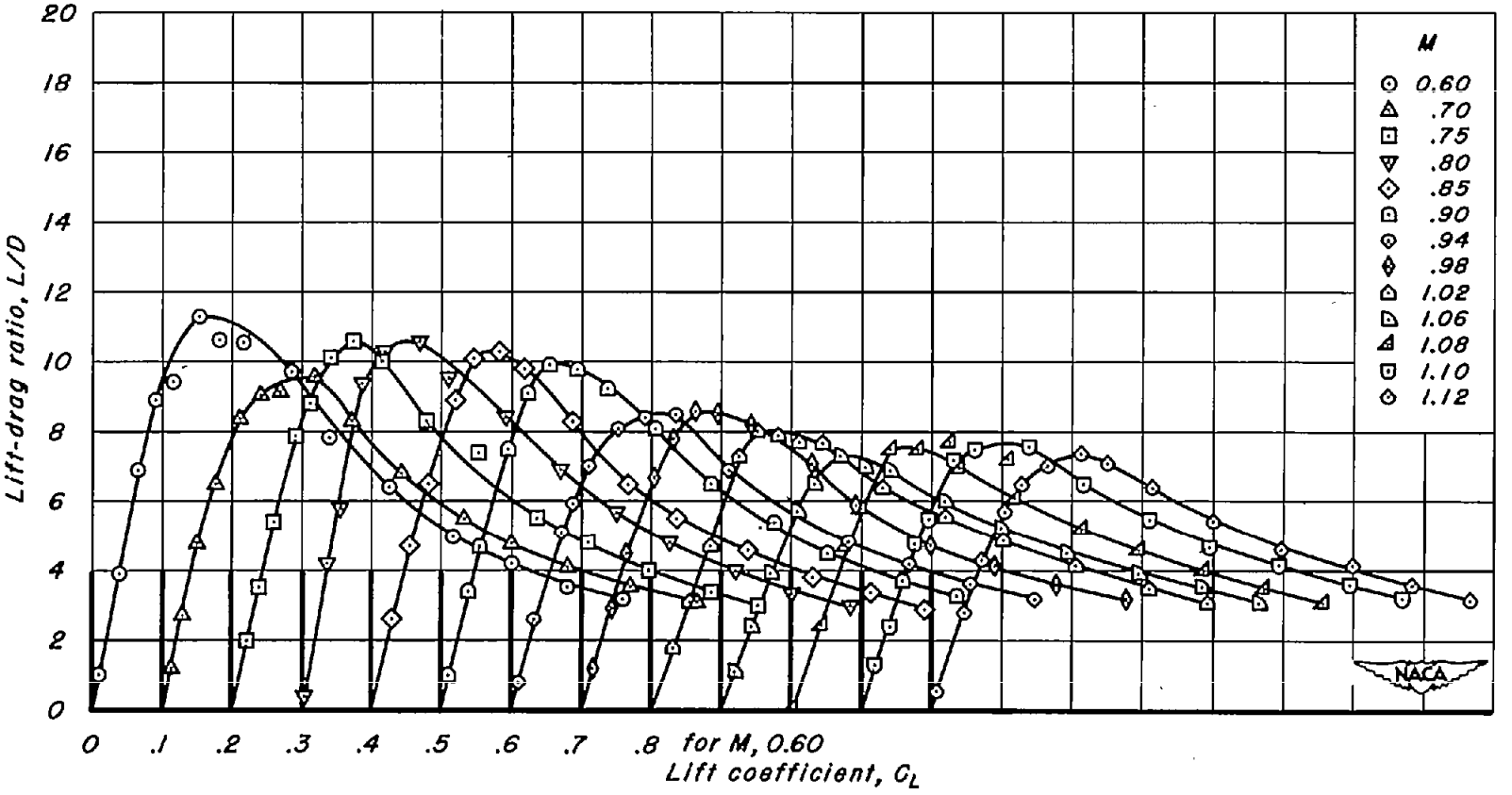

(r) A, 1; t/c, 0.04

Figure 16.- Continued.

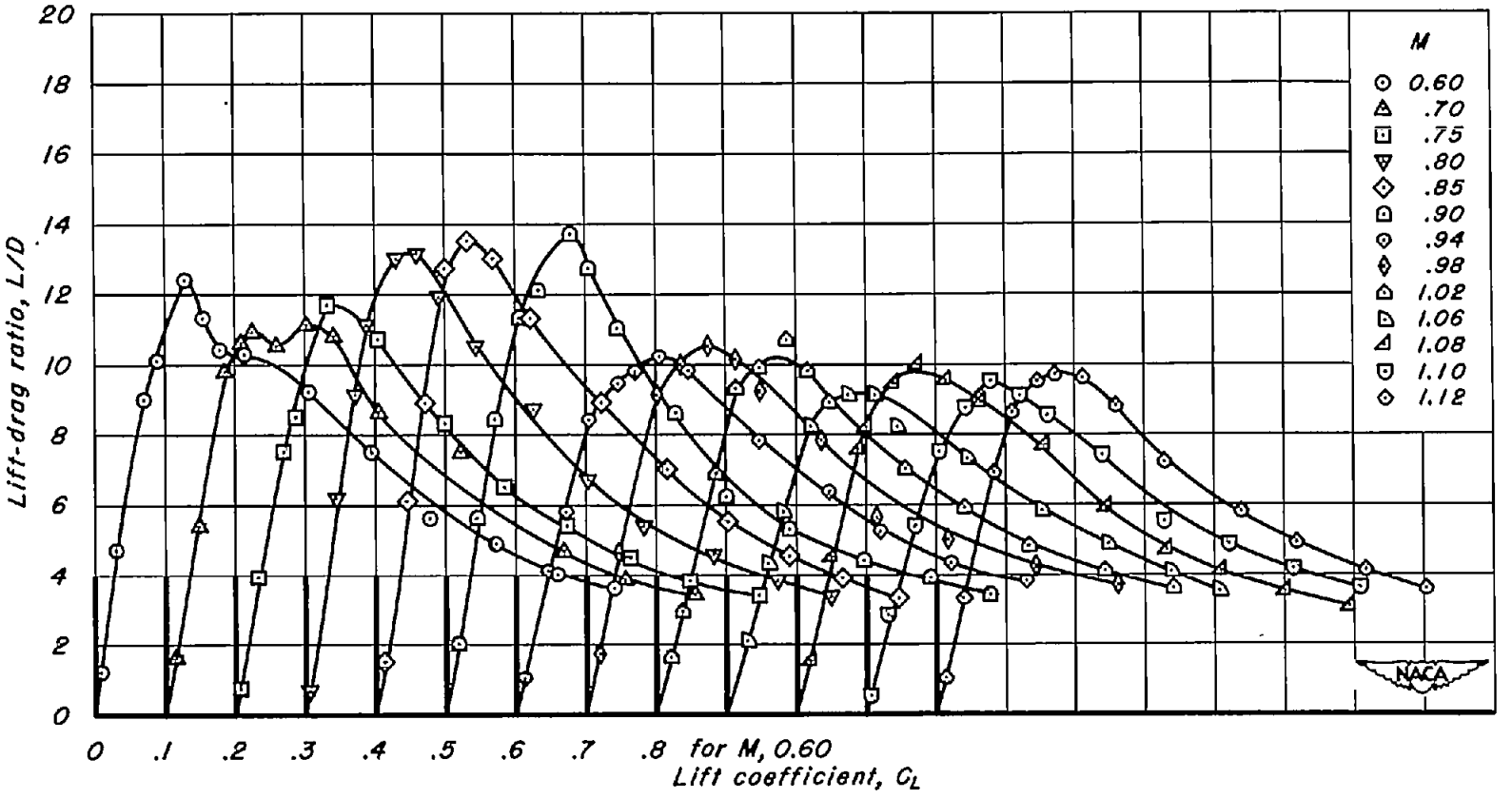

(s) A, 1; t/c, 0.02

Figure 16.- Concluded.

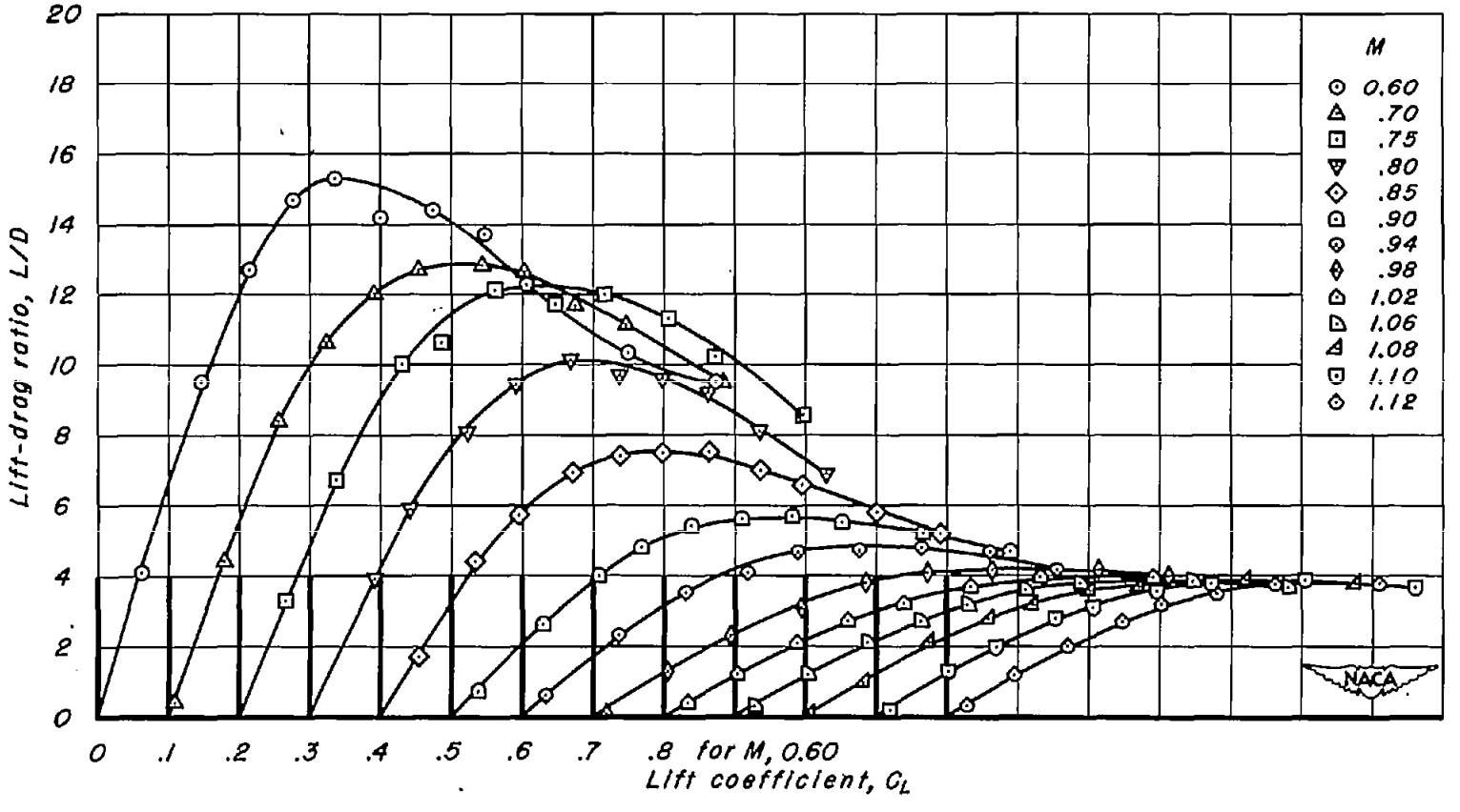

(a) A, 4; t/c, 0.10

Figure 17.—The variation of lift-drag ratio with lift coefficient for the wings with the NACA 63A4xx sections.

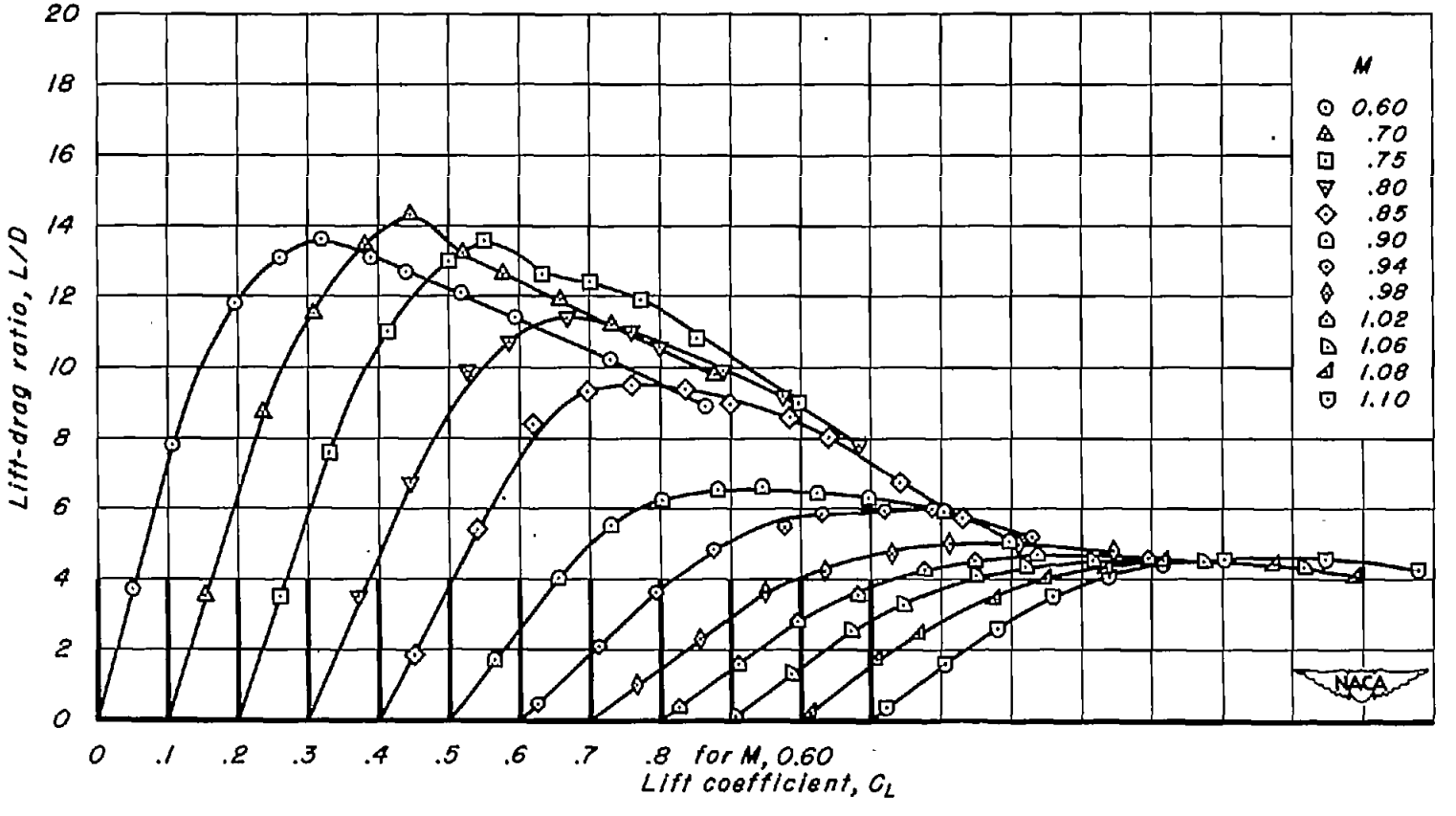

(b) A, 4; t/c, 0.08

Figure 17.- Continued.

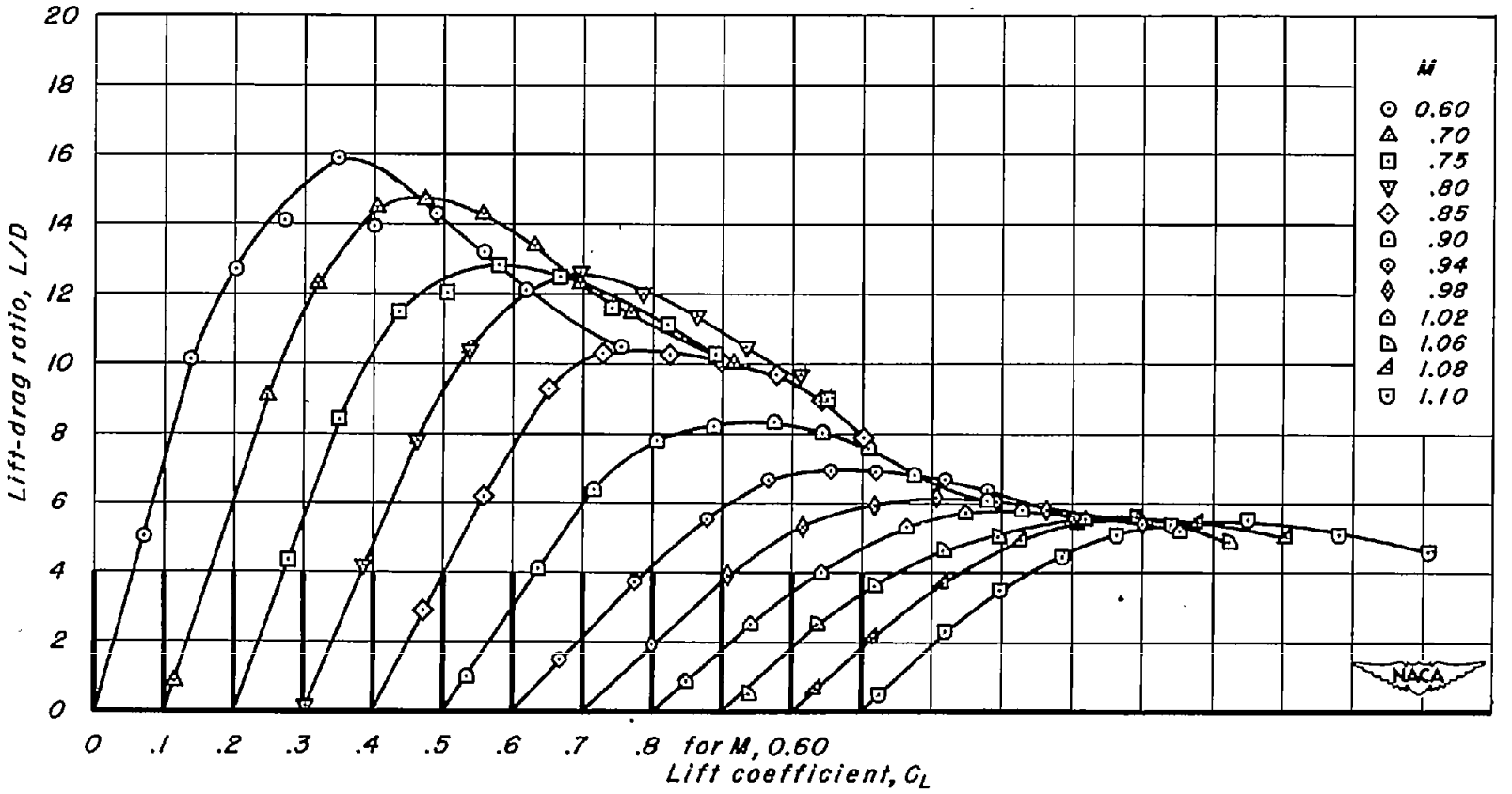

(c) A, 4; t/c, 0.06

Figure 17.- Continued.

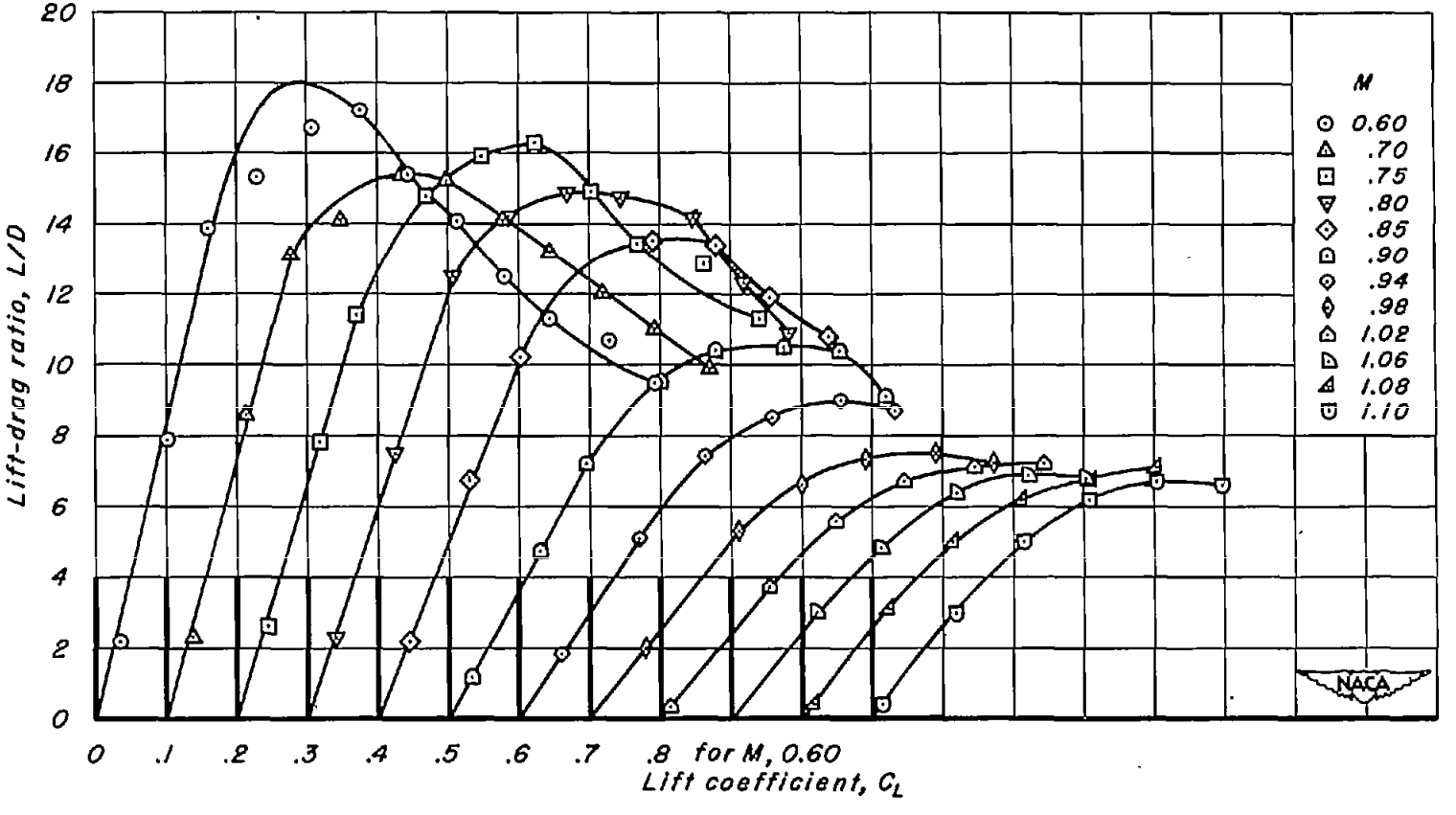

(d) A, 4; t/c, 0.04

Figure 17.- Continued.

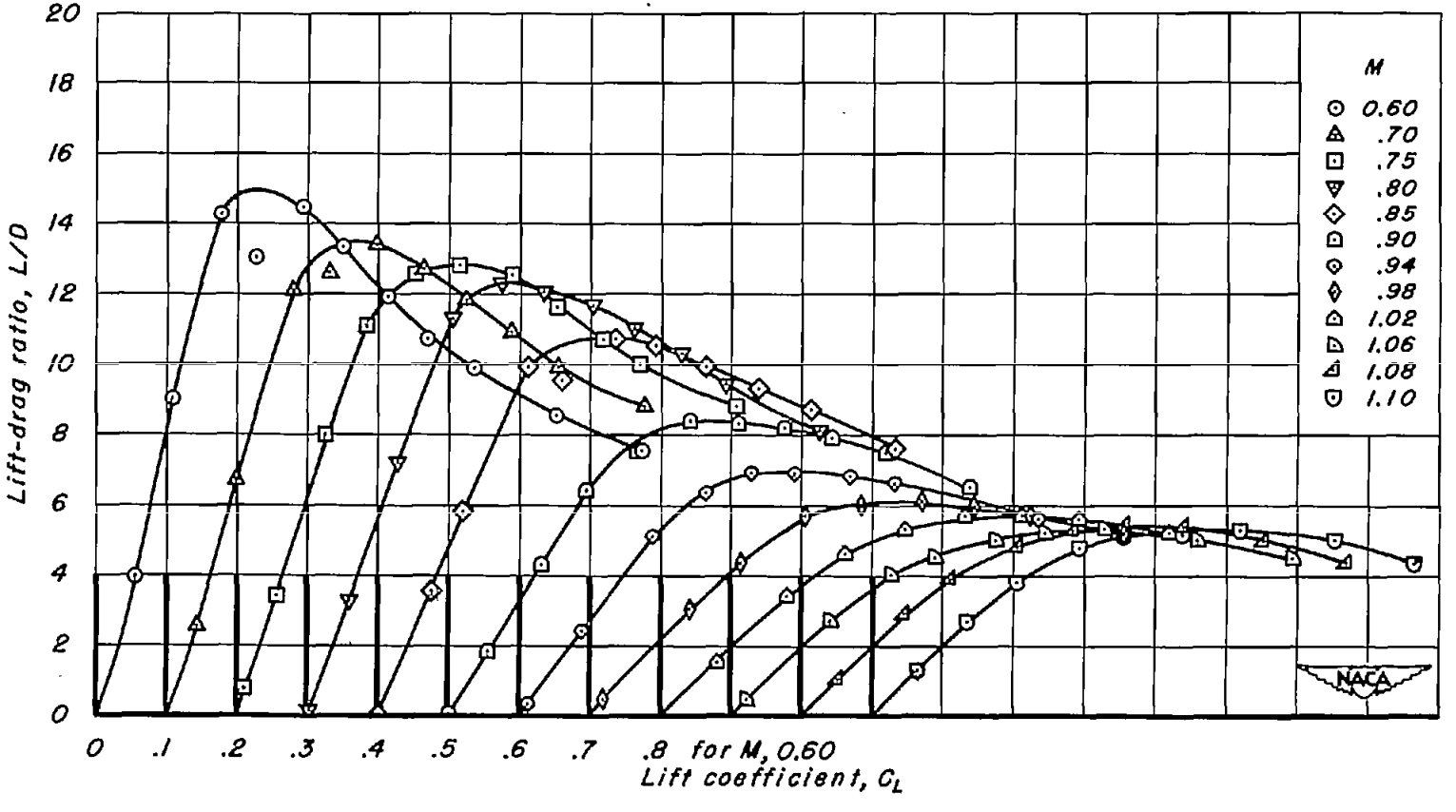

(e) A, 3; t/c, 0.06

Figure 17.- Continued.

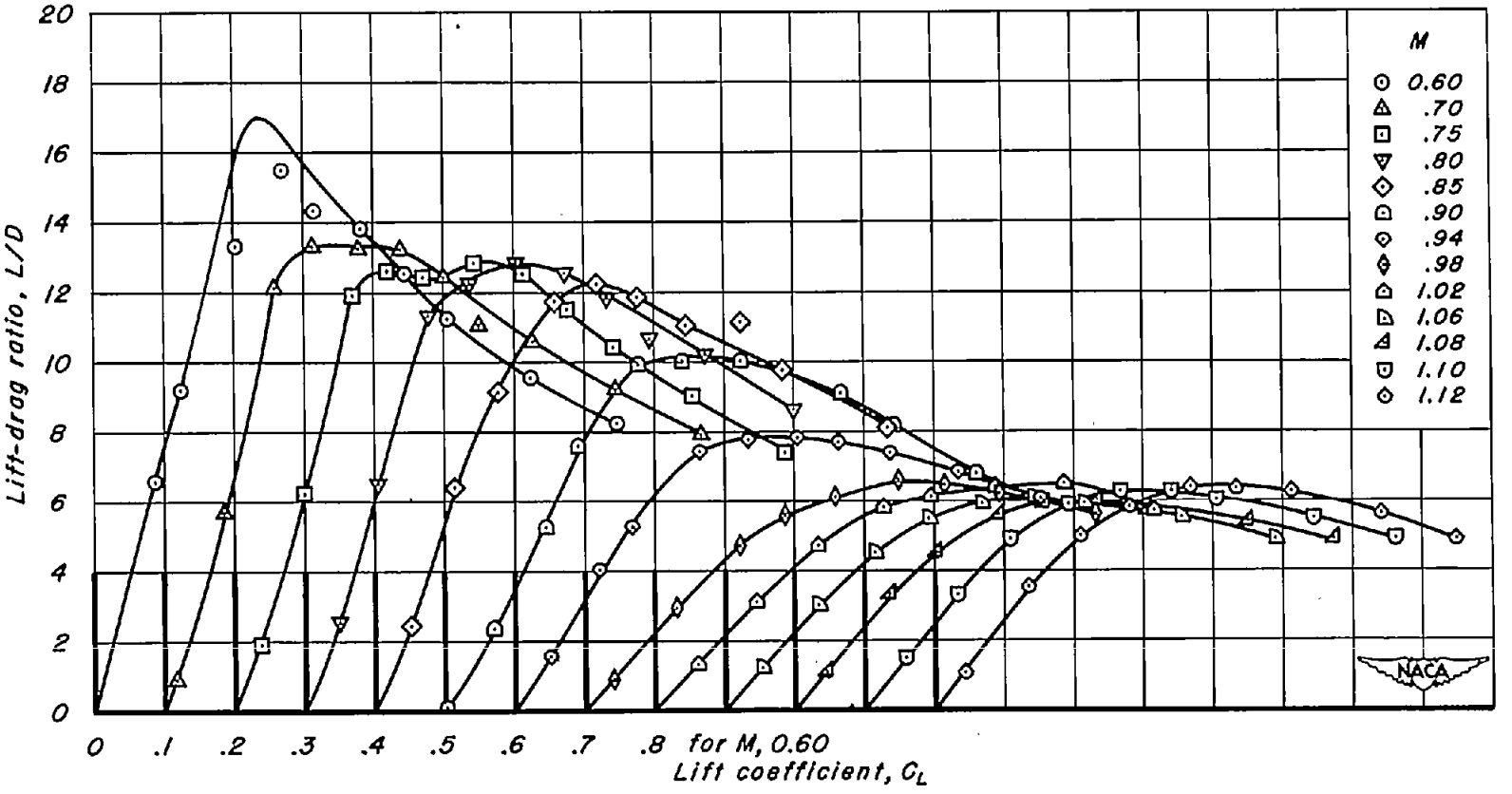

(f) A, 3; t/c, 0.04

Figure 17.- Continued.

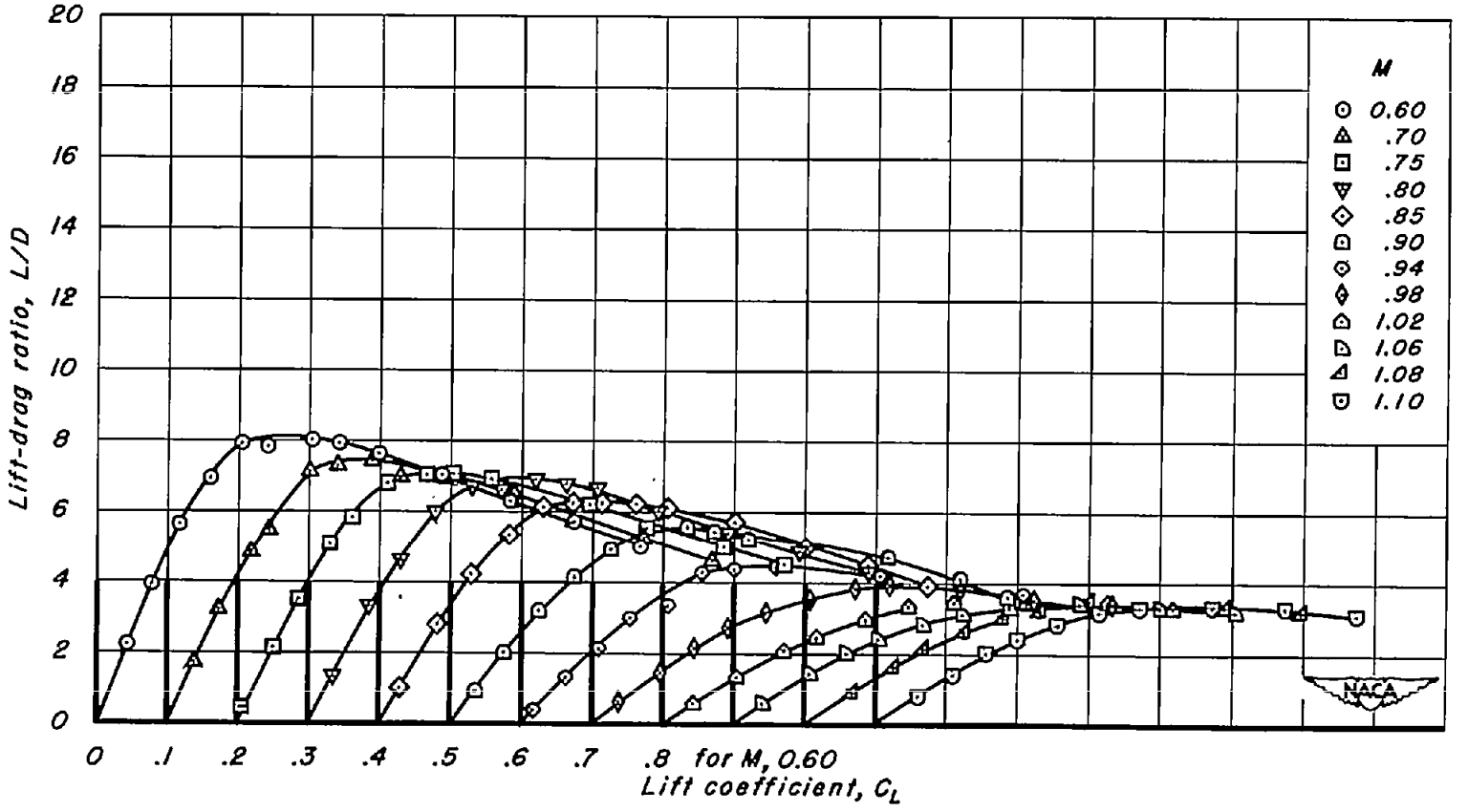

(g) A, 2, t/c, 0.10

Figure 17.- Continued.

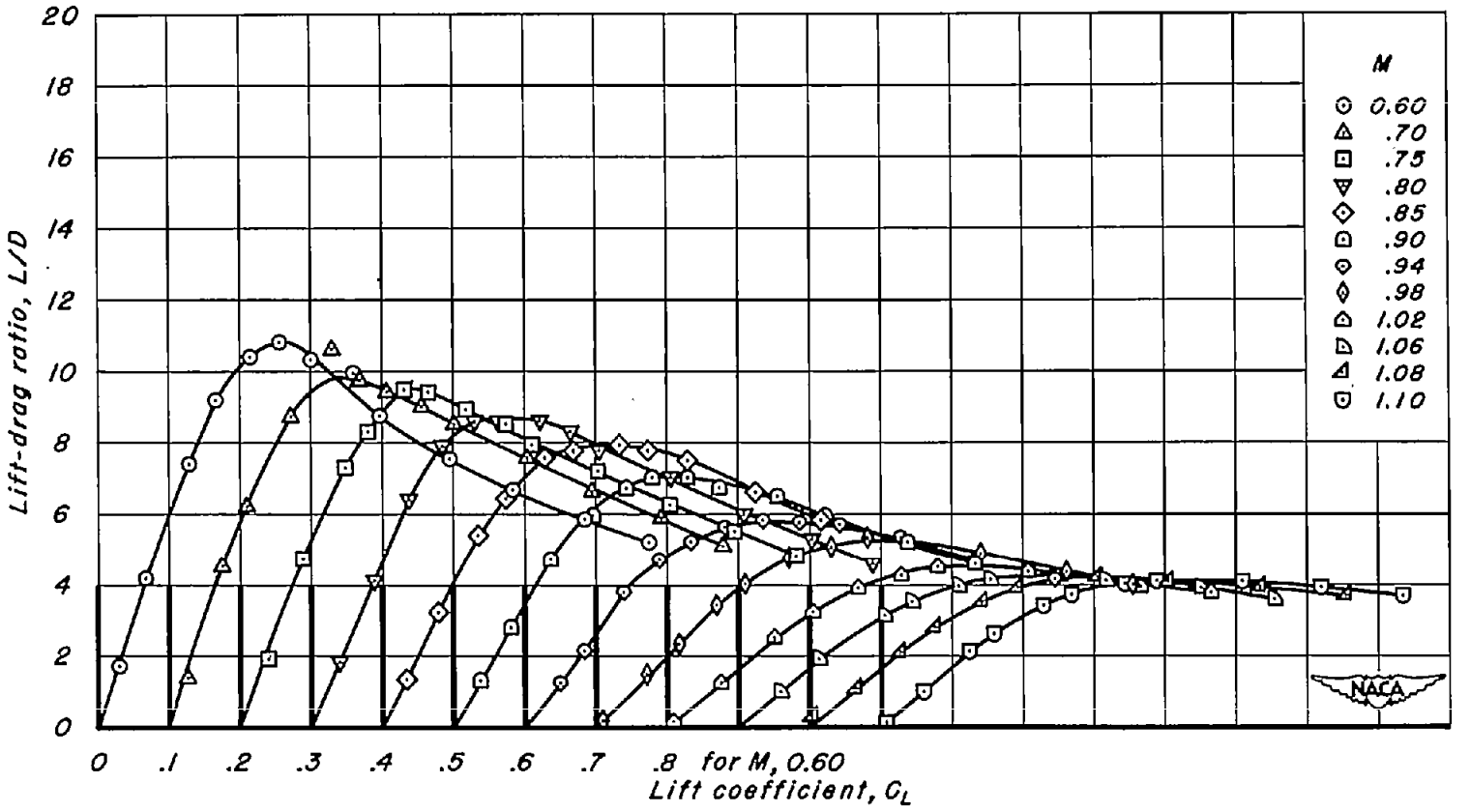

(h) A, 2; t/c, 0.08

Figure 17.- Continued.

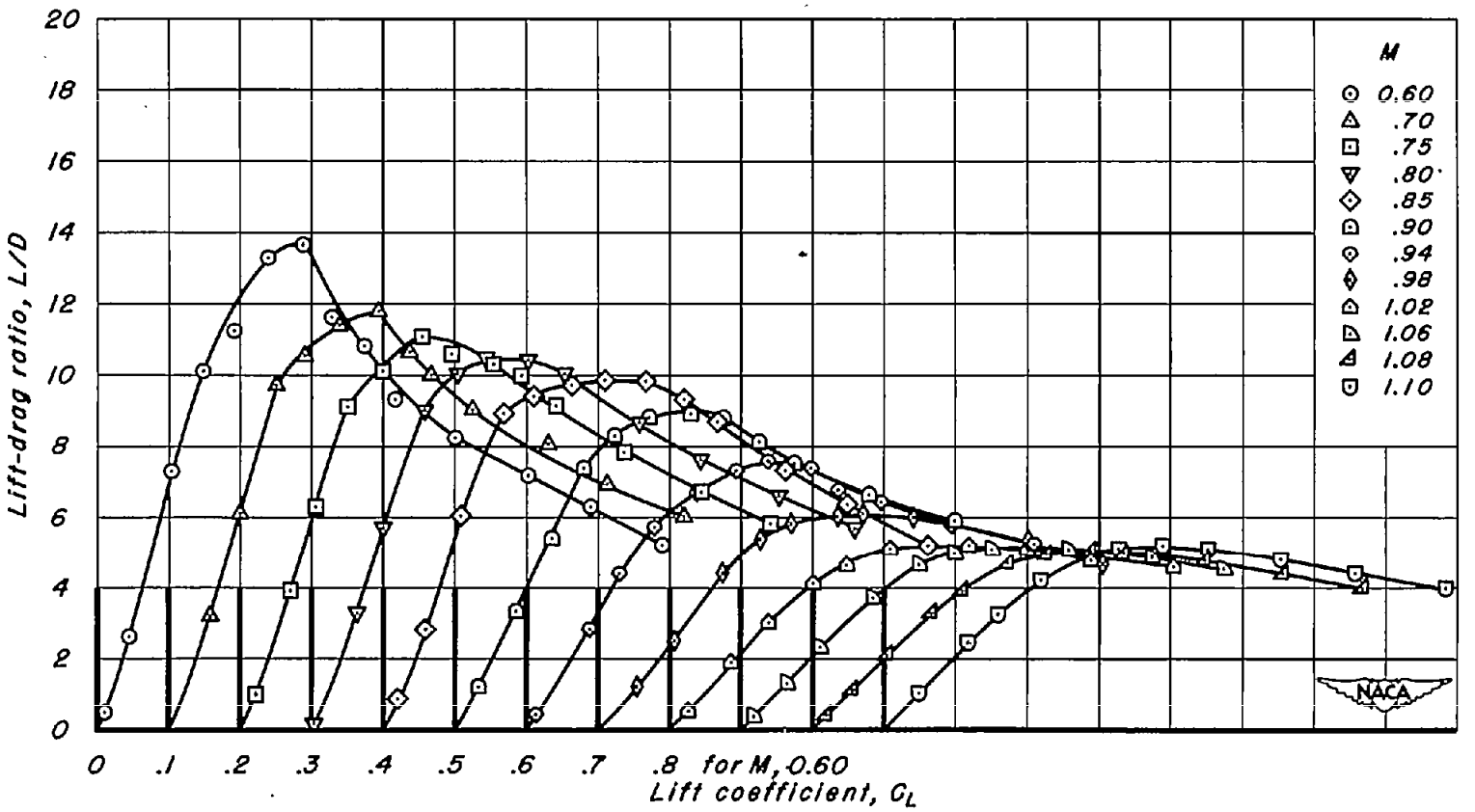

(i) A, 2; t/c, 0.06

Figure 17.- Continued.

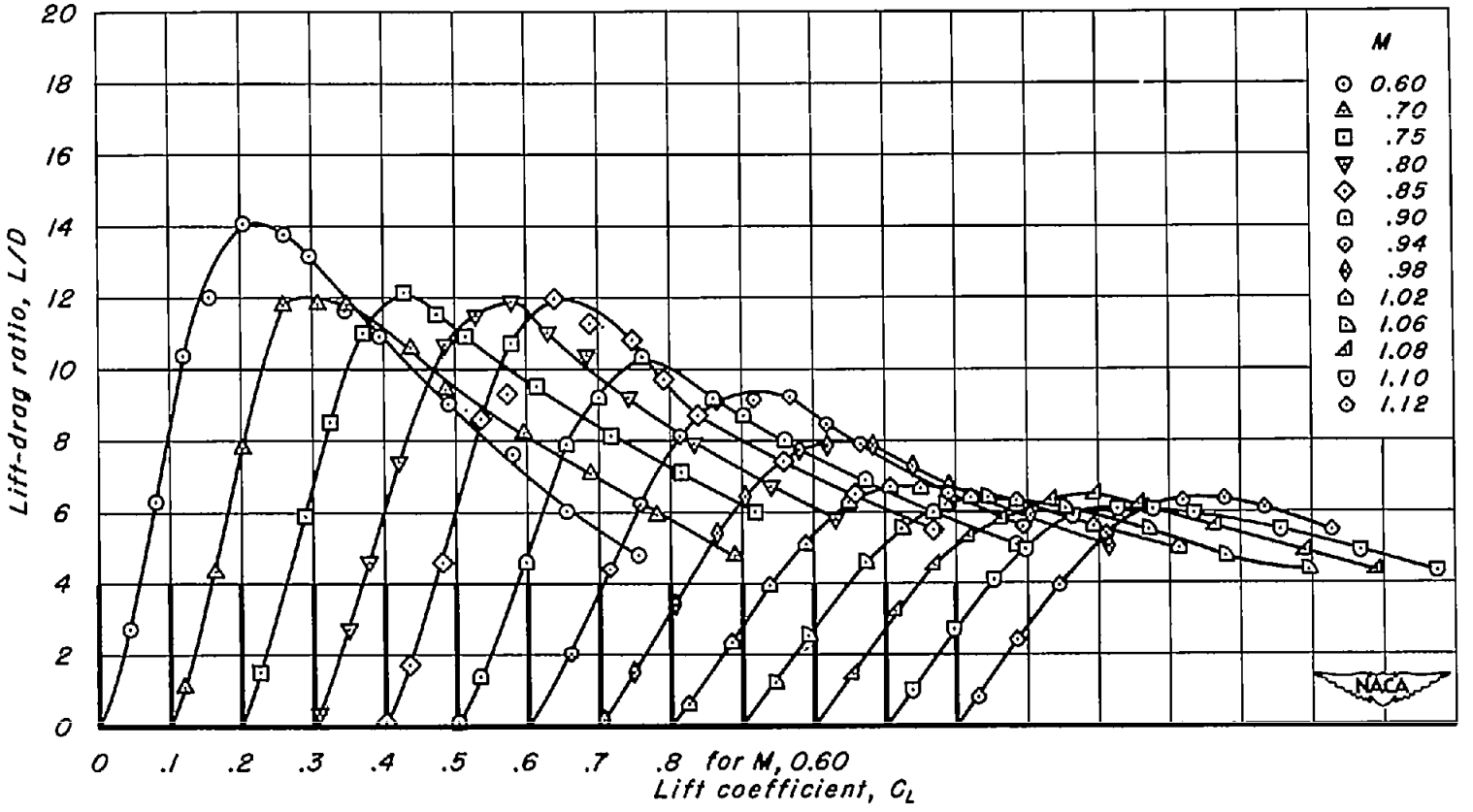

(j) A, 2; t/c, 0.04

Figure 17.- Continued.

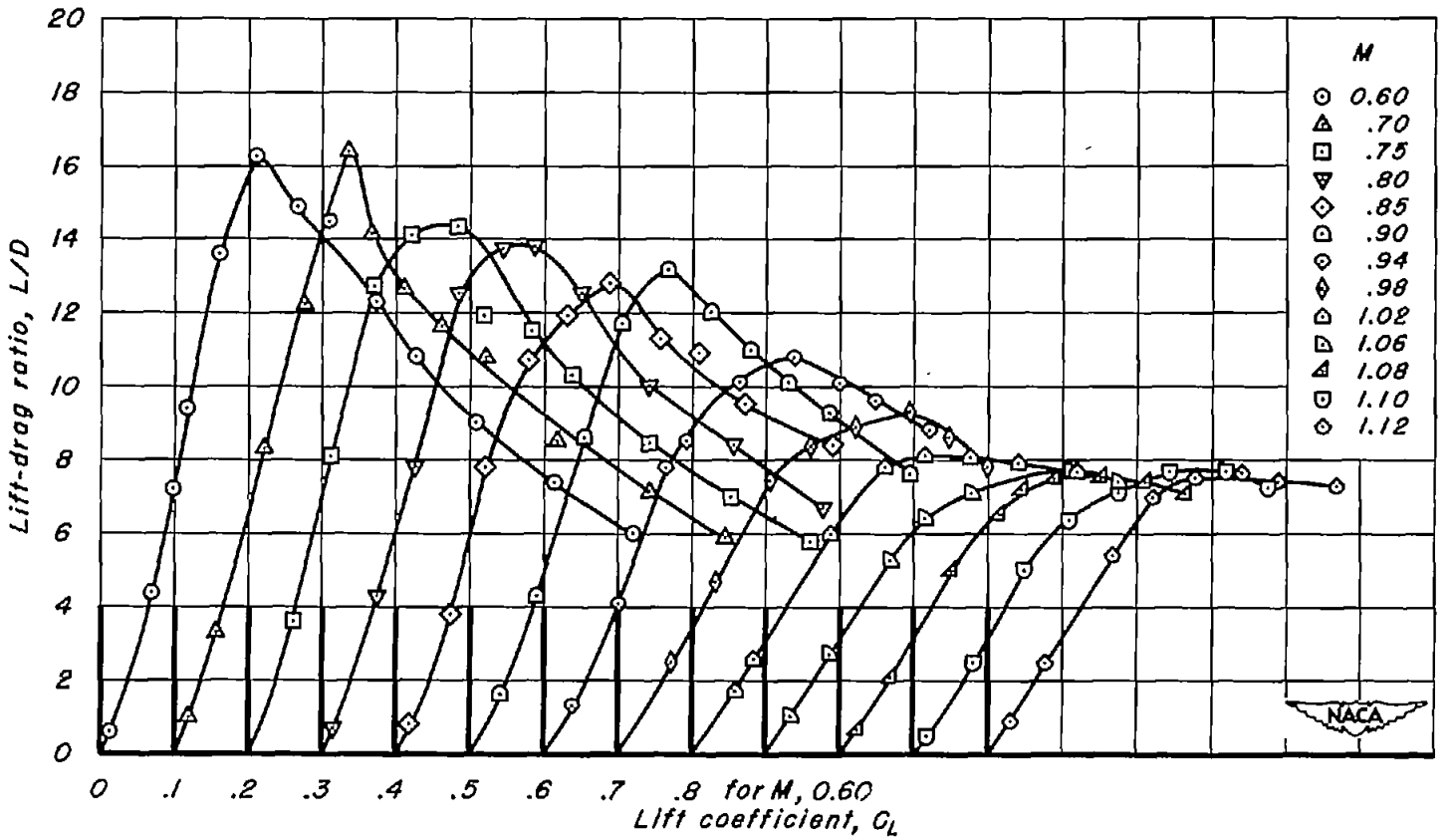

(k) A, 2; t/c, 0.02

Figure 17.- Continued.

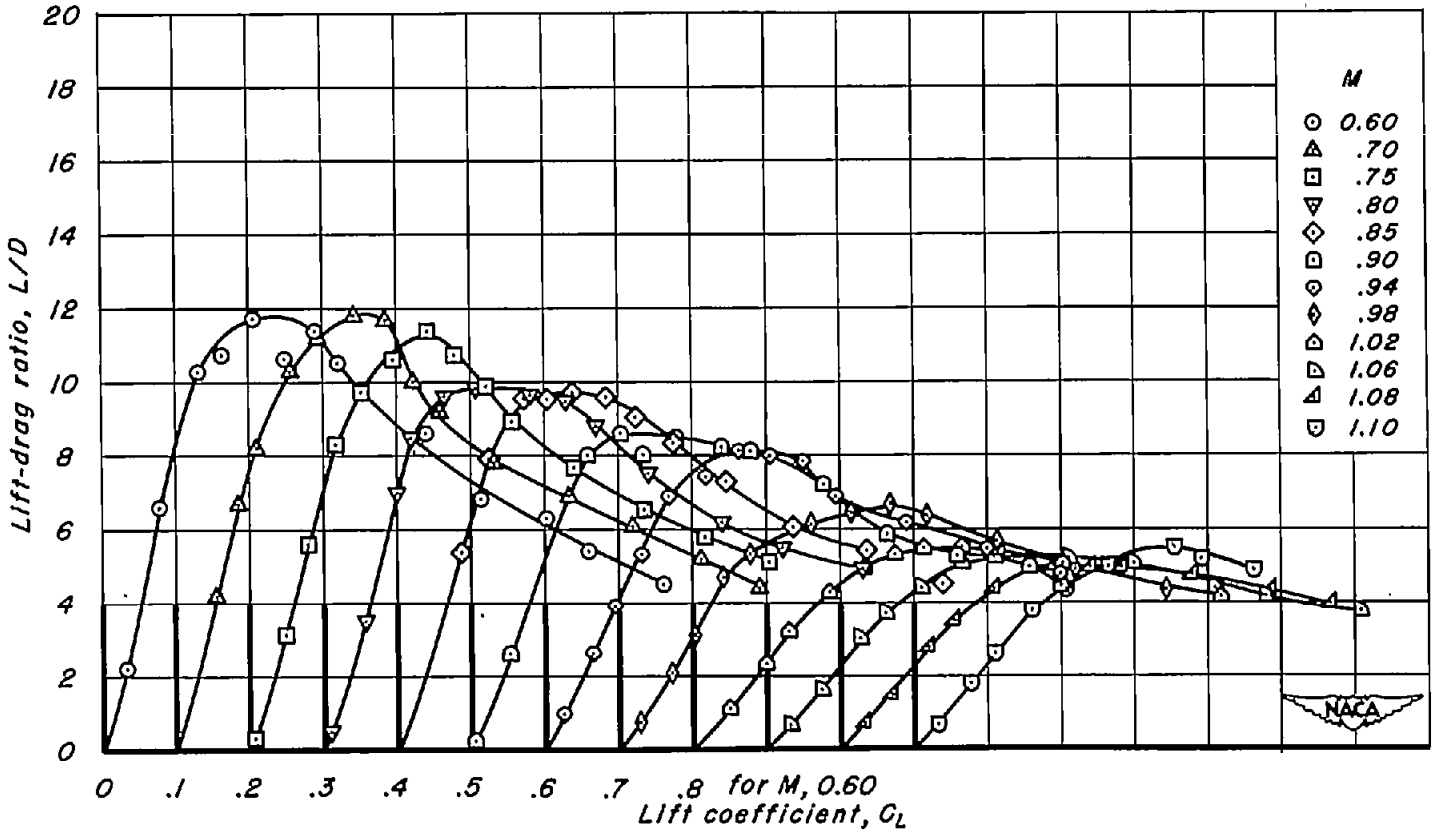

(l) A,1.5; t/c, 0.06

Figure 17.- Continued.

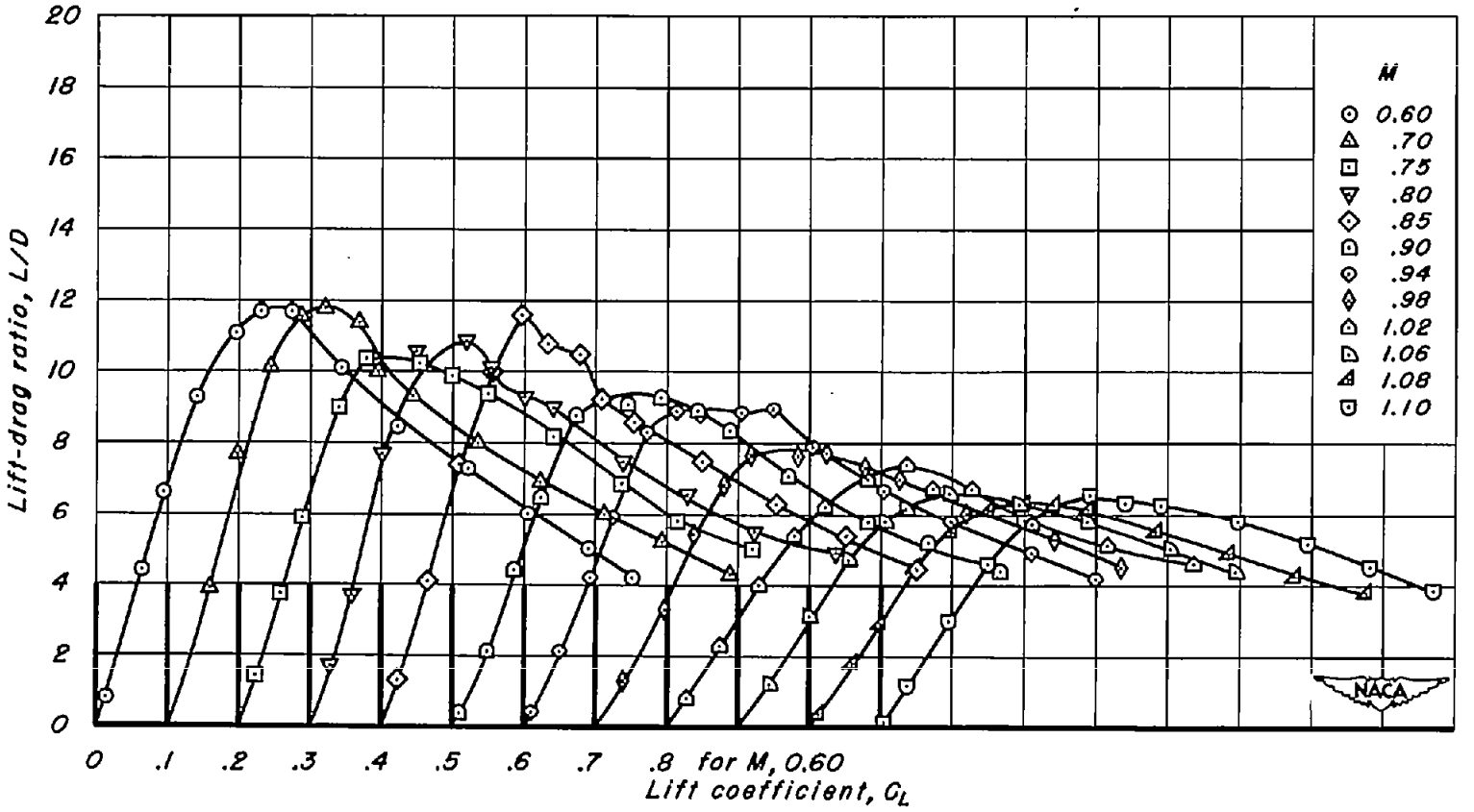

(m) A,1.5; t/c, 0.04

Figure 17.- Continued.

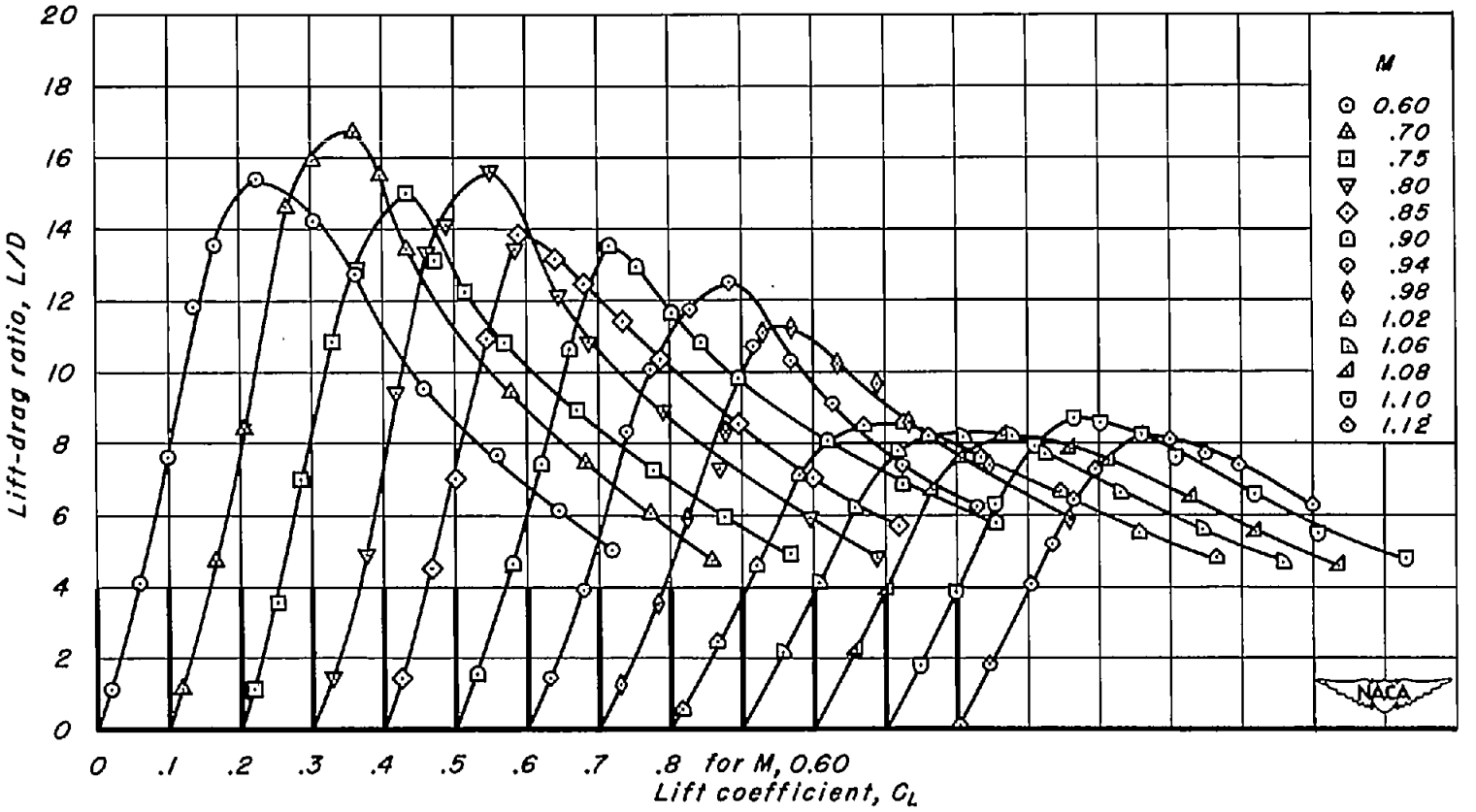

(n) A,1.5; t/c, 0.02

Figure 17.- Continued.

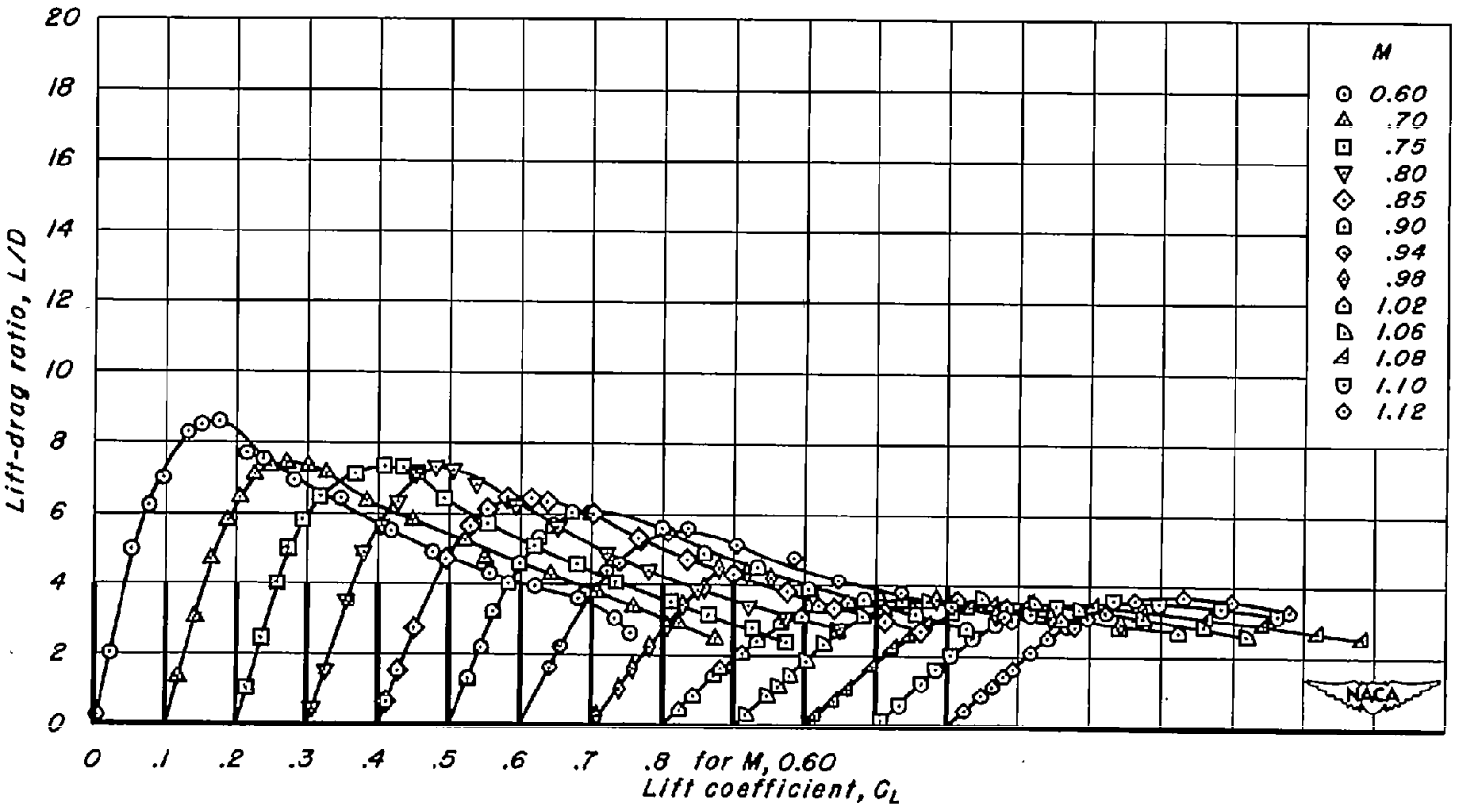

(o) A, 1; t/c, 0.10

Figure 17.- Continued.

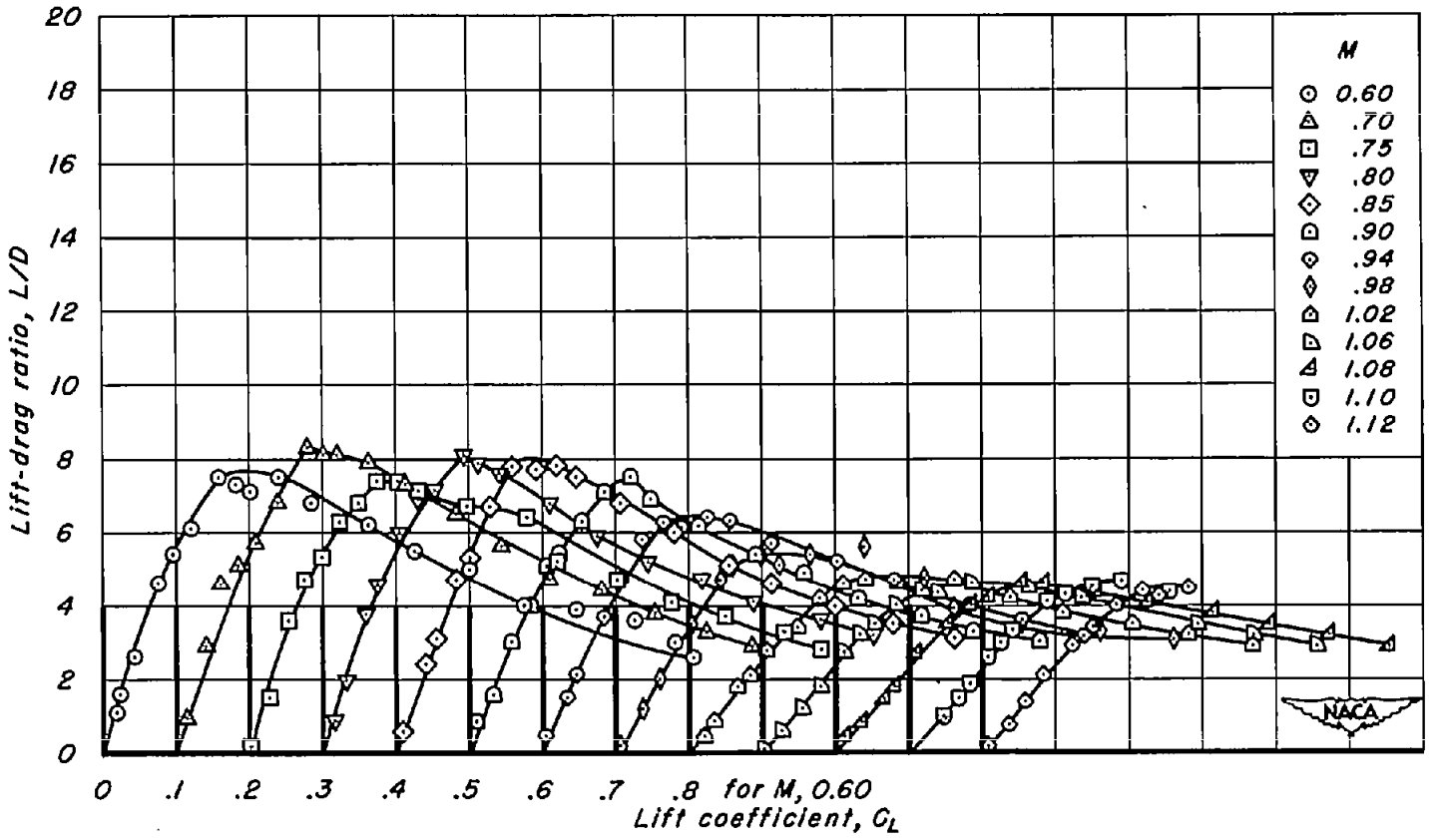

(p) A, I; t/c, 0.08

Figure 17.- Continued.

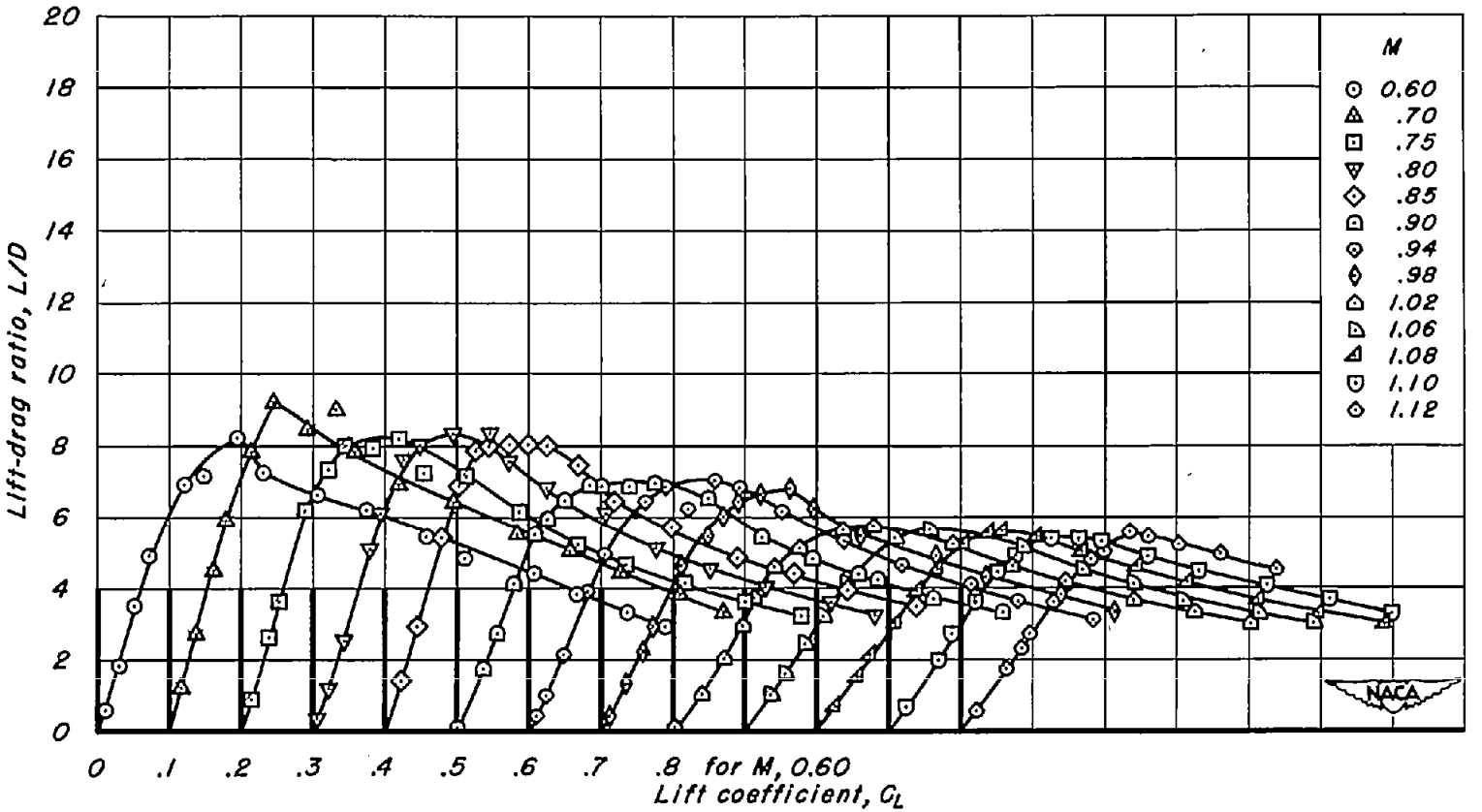

(q) A, 1; t/c, 0.06

Figure 17.- Continued.

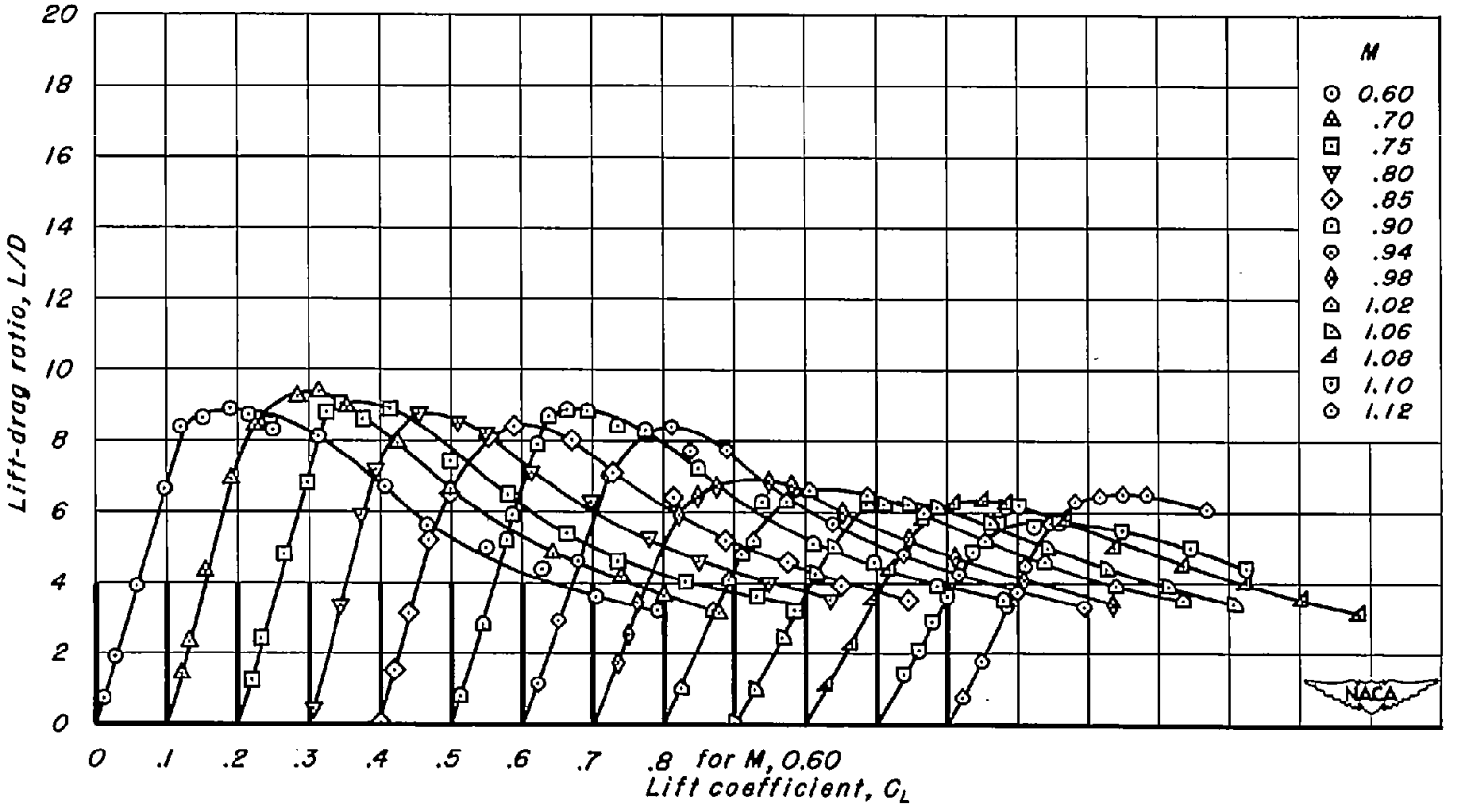

(r) A, 1; t/c, 0.04

Figure 17.- Continued.

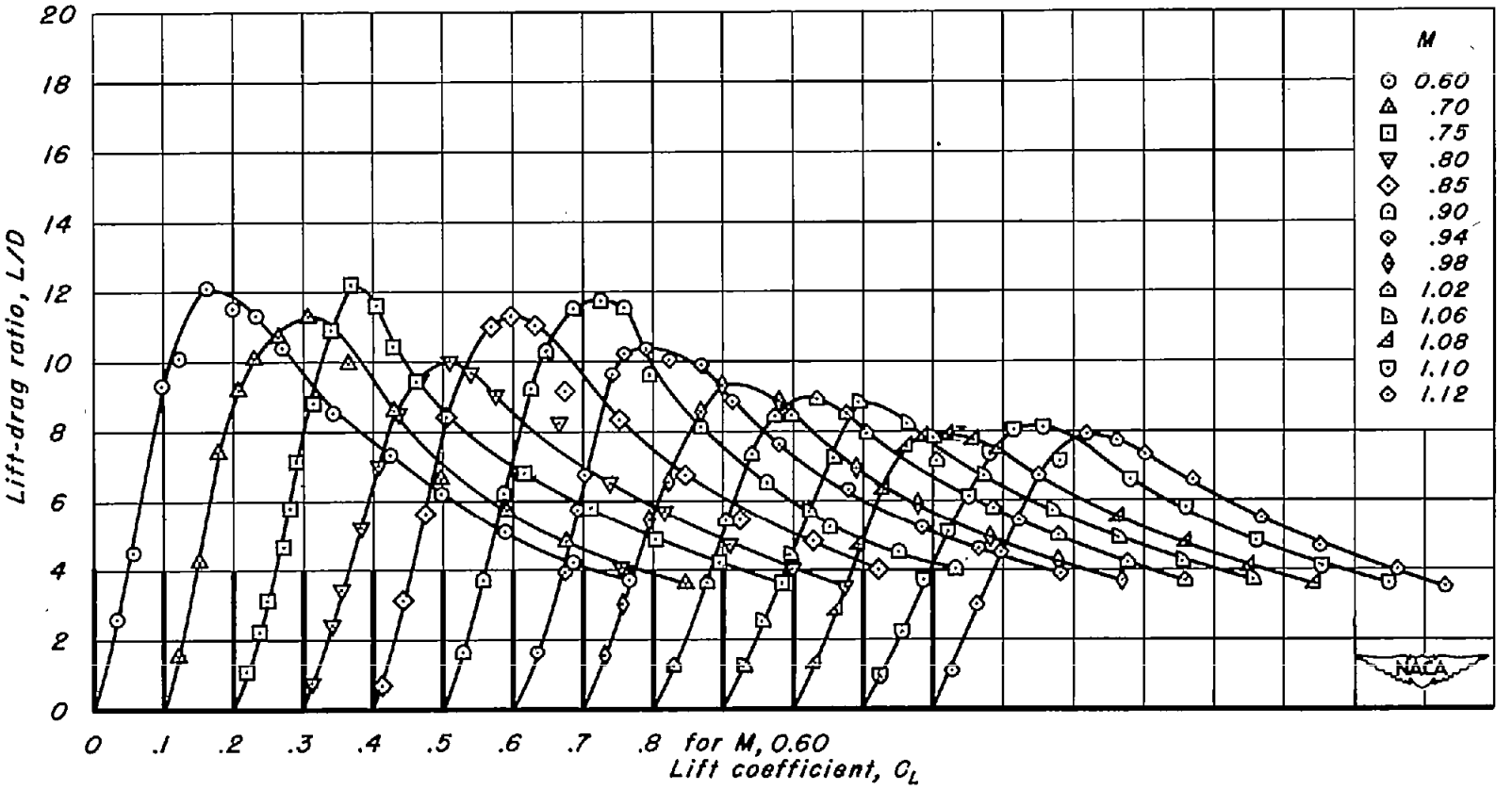

(s) A, 1; t/c, 0.02

Figure 17.- Concluded.

NACA-Langley - 6-8-56 - 1000